Interactions between the Orange Carotenoid Protein and the phycobilisomes in cyanobacterial photoprotection

Denis Jallet

UNIVERSITE PARIS-SUD

ÉCOLE DOCTORALE : SCIENCES DU VÉGÉTAL
Laboratoire des Mécanismes Fondamentaux de la Bioénergétique
UMR8221, CNRS/CEA

DISCIPLINE : BIOLOGIE

THÈSE DE DOCTORAT

Soutenance prévue le 29/11/2013

par

Denis JALLET

Interactions between the Orange Carotenoid Protein and the phycobilisomes in cyanobacterial photoprotection

Composition du jury :

Directeur de thèse **:**	Diana KIRILOVSKY	DR CNRS, CEA Saclay
Rapporteurs :	Cécile BERNARD	Professeur, Muséum national d'Histoire Naturelle
	Michel HAVAUX	DR CEA, CEA Cadarache
Examinateurs :	Ondrej PRASIL	Professeur, Academy of Sciences of the Czech Republic
	Anne-Soisig STEUNOU	CR CNRS, CGM Gif-sur-Yvette
Président :	Michel DRON	Professeur, Université Paris-Sud 11

LA DÉPÊCHE DU MIDI

TÉMOIGNAGE EXCLUSIF:

« COMMENT J'AI PU FIXER L'OCP SANS ApcD NI ApcF, OU MÊME AVEC UN ApcE DÉFECTUEUX »

Les habitants de la ville de Cauterets n'en sont toujours pas revenus et beaucoup restent incrédules. C'est à la suite d'un pèlerinage effectué dans la ville proche de Lourdes qu'un chercheur de renommée internationale a révélé [illegible]

Mgr BROUWET:

«ATTENDONS LES CONCLUSIONS DE LA COMMISSION DES MIRACLES»

Pour l'évêque de Tarbes et de Lourdes, la prudence est de mise. Selon lui, avant de conclure au miracle, il faut attendre le verdict de la commission des miracles qui se réunira le 29 novembre [illegible]

LE PAPE FRANÇOIS AURAIT DEMANDÉ A ÊTRE REÇU PAR L'ÉMINENT SAVANT

Rome (envoyé spécial) – On murmure au Vatican que le souverain pontife aurait sollicité une audition [illegible]

POUR EN SAVOIR PLUS:

DENIS JALLET vous invite à sa soutenance de thèse:

« INTERACTION BETWEEN THE ORANGE CAROTENOID PROTEIN AND THE PHYCOBILISOMES IN CYANOBACTERIAL PHOTOPROTECTION »

LE **29 NOVEMBRE** À 14 H, AMPHITHÉÂTRE DE L'IBP (bâtiment 630, rue de Noetzlin, Gif-sur-Yvette) ET ENSUITE AU **POT**

Acknowledgements

To my supervisor, Diana, thank you for letting me study such a fascinating topic. When I look back, you were always here to give good advices and to constructively discuss about the experimental results. It was a great pleasure to work with you over the last 3 years.

To all my coworkers – past and present – big thanks for everyday's good mood and for all the help provided. Adjélé, Sandrine, Michal, Rocio, Adrien and Céline (alias Poulpy), I will really miss our 3rd floor.

To Dr. Ryan L. Leverenz, Dr. Marcus Sutter, Dr. Cheryl A. Kerfeld, Dr. Radek Kana and Pr. Ondrej Prasil, thanks for all the fruitful collaborations we have had.

To Dr. Anja Krieger-Liszkay, Dr. Pierre Sétif, Dr. Ghada Ajlani, Dr. Hervé Bottin, Dr. Sun Un in CEA Saclay, thank you for having been always available and ready to share your knowledge with me.

I would also like to acknowledge Dr. Corinne Chauvat and Dr. Catherine de Vitry for participating in my "comité de these" and bringing interesting new ideas into the topic.

To Dr. Jacqui Shykoff, Dr. Marianne Delarue and Martine Fournier from "ED 145 Sciences du vegetal", thank you for creating a strong connection with Université Paris-Sud 11 and for easing so much the PhD students' administrative procedures.

To all the administrative staff in iBiTeC-S, particularly Karine, Josiane, Céline, Isabelle, Pascale, Dominique, Sophie, thanks for all your support over the time course of my thesis.

To Amin, Thomas, Sané, Denise, Liz, Margaux, Kathleen (alias Lena?), Mehdi Caherine, Eiri, Stéphanie, Hassina, Tiona, Qian and Eduardo thanks for all the good moments we spent together in Paris (and Brussels!) to relax after hard working.

Finally, thanks a lot to my family and friends from Pyrenees who always were there to encourage me.

This work was funded by the Université Paris-Sud 11, the CNRS, the CEA and the European Training Network Grant HARVEST (FP project n°238017).

TABLE OF CONTENTS

Introduction……1

1. Cyanobacteria 3

1.1. Overview of the cyanobacterial phylum 3

1.2. A model cyanobacterium: *Synechocystis* 5

2. Photosynthesis in cyanobacteria 7

2.1. The linear electron transport chain: PSII, cytb_6f and PSI. 7

2.2. Phycobilisomes: the cyanobacterial accessory light harvesting complexes 11

2.2.1. Composition and structure of the PBs 11

2.2.2. PBs function as antennae 17

2.2.3. PBs movement and possible implication in State Transitions 19

3. Drawbacks of photosystems functioning in an oxygenic medium and defensive strategies 22

3.1. Photoinhibition of PSII 22

3.2. Photoprotective mechanisms in cyanobacteria: an overview 23

3.3. Non-photochemical quenching of the excess light energy harvested. 25

4. The Orange Carotenoid Protein (OCP)-related non photochemical quenching of the energy harvested by PBs 27

4.1. Discovery 27

4.2. Distribution and regulation of the OCP 29

4.3. Crystal structure of the OCP isolated from *Arthrospira* 31

4.4. Photoactivity of the OCP and *Synechocystis* mutant studies 33

4.5. In vitro reconstitution of the OCP-related photoprotective mechanism 37

4.6. FRP allows rebooting the system. 39

5. Aims of the thesis 41

Chapitre 1: ApcD, ApcF and ApcE are not required for the OCP-related photoprotective mechanism inSynechocystis……53

Chapitre 2: Specificity of the cyanobacterial Orange Carotenoid Protein: Influences of OCP and phycobilisomes structures……89

Chapitre 3: Structural and functional modularity of the Orange Carotenoid Protein: Distinct roles for the N- and C- terminal domains in cyanobacterial photoprotection……135

ABBREVIATIONS EMPLOYED

ΔAB :	Allophycocyanin-deficient *Synechocystis* PCC 6803 mutant strain
α^{PC}/ β^{PC}/α^{APC}/β^{APC} :	α subunit of phycocyanin/β subunit of phycocyanin/α subunit of allophycocyanin/β subunit of allophycocyanin
A/**T**/**G**/**C** :	Adenine/Thymine/Cytosine/Guanine
Anabaena:	*Anabaena variabilis*
APC :	Allophycocyanin
ApcD, **ApcF**, **ApcE** :	Phycobilisome terminal emitters
Arthrospira:	*Arthrospira platensis* PCC 7345
ATP :	Adenosine triphosphate
Chl*a* :	Chlorophyll *a*
CK:	Phycocyanin-deficient *Synechocystis* PCC 6803 mutant strain
CrtO:	β-carotene ketolase (required for echinenone and 3'hydroxy-echinenone synthesis)
CrtR:	β-carotene hydroxylase (required for 3'hydroxy-echinenone and zeaxanthin synthesis)
Cytb_6f :	Cytochrome b_6f
DNA :	Deoxyribonucleic acid
ECN :	Echinenone
EM :	Electron microscopy
Fd:	Ferredoxin
FLIP:	Fluorescence Loss In Photobleaching
Flv:	Flavodiiron protein
F_m':	Maximal level of fluorescence measured using a PAM fluorometer
FRP:	Fluorescence Recovery Protein
FRAP:	Fluorescence Recovery After Photobleaching
hECN:	3'hydroxy-echinenone
HLIP:	High Light Induced Polypeptide
LHC:	Light Harvesting Complex
M:	Molar
Mb:	Mega-base
NADP:	Nicotinamide Adenine Dinucleotide Phosphate
NDH1:	NADH:ubiquinone oxidoreductase I
OCP^r/**OCP^o**:	Red form of the Orange Carotenoid Protein/orange form of the Orange Carotenoid Protein
ORF:	Open Reading Frame
P680/**P700**:	Special-pair chlorophyll of photosystem II/special-pair chlorophyll of photosystem I
PAM:	Pulse Amplitude Modulation
PB:	Phycobilisome
PC:	Phycocyanin
PCB:	Phycocyanobilin
PCC:	Pasteur Core Collection
PCy:	Plastocyanin

PDB: Protein Data Bank
PEB: Phycoerythrobilin
PQ/PQH_2: Plastoquinone/plastoquinol
psbA2: Photosystem II D1 protein encoding gene
PSI/PSII: Photosystem I/photosystem II
PTOX: Plastid Terminal Oxidase
PXB: Phycobiliviolin
Q_A/Q_B: Photosystem II-associated quinines
qE: Energy-dependent non-photochemical quenching
qP: Photochemical quenching
RCP: Red Carotenoid Protein
RNA: Ribonucleic Acid
ROS: Reactice Oxygen Species
Synechococcus: *Synechococcus* PCC 7942
Synechocystis: *Synechocystis* PCC 6803
Thermosynechococcus: *Thermosynechococcus elongatus*
TyrZ: Tyrozine Z of photosystem II
WOC : Water Oxidizing Complex
WT : Wild-type strain

Introduction

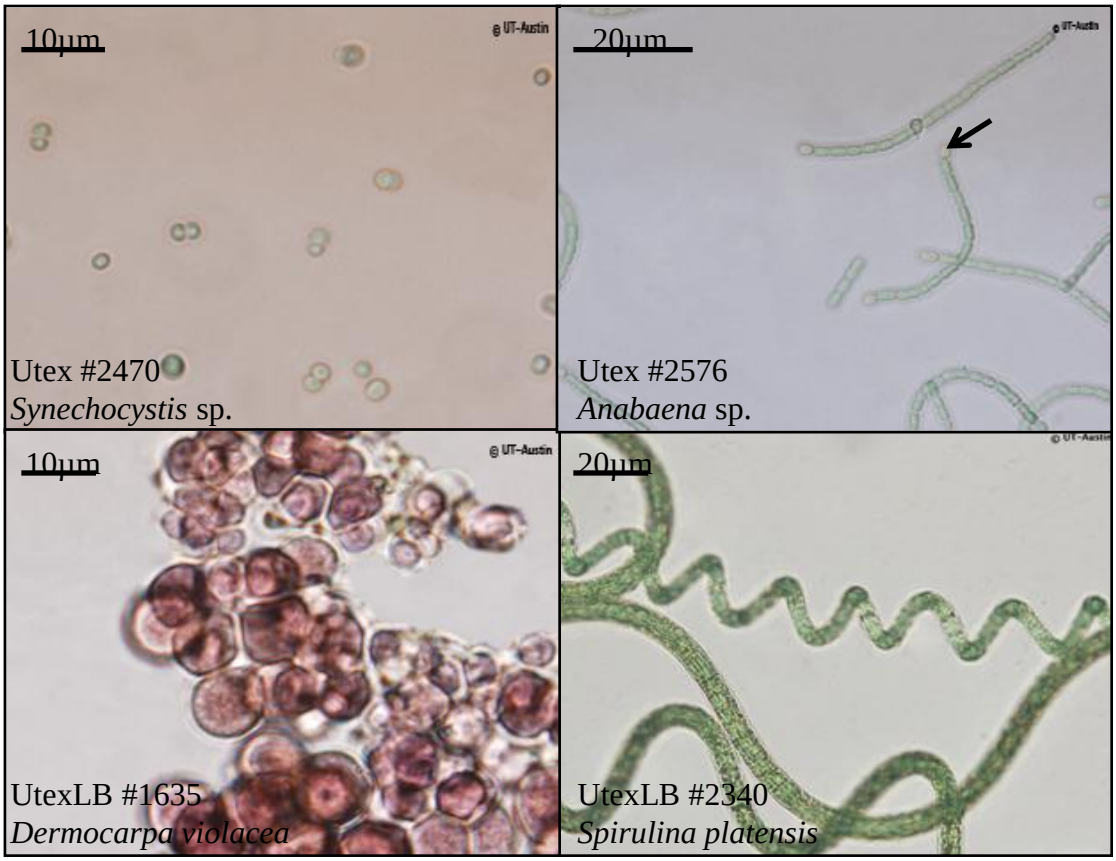

Figure 1. Optical microscopy observation of various cyanobacteria. A. The unicellular *Synechocystis* sp. *B.* The filamentous *Anabaena* sp., capable of forming heterocysts (indicated with an arrow) for nitrogen fixation C. *Dermocarpa violacea*, containing red pigments (phycoerythrin) belonging to the phycobiliprotein family D. The filamentous *Arthrospira platensis*. Copyright: UTEX - The Culture Collection of Algae at The University of Texas at Austin (used with permission)

Introduction

1. Cyanobacteria

1.1. Overview of the cyanobacterial phylum

Cyanobacteria are the only prokaryotic organisms able to perform oxygen evolving photosynthesis. It implies using light as a source of energy and water as a source of reducing power for converting inorganic carbon (CO_2) into hydrocarbons ($C_nH_{2n}O_n$), oxygen dioxide (O_2) and ATP being also produced. This ability, combined to the discovery of microfossils testifying their apparition more than 2.5 billion years ago, pointed out cyanobacteria as responsible for the Great Oxydation Event and subsequent life spreading on Earth (Rasmussen et al., 2008). The name blue-green algae was originally proposed because some early-discovered cyanobacterial strains displayed macroscopic, thallus-like structures, containing green (chlorophylls) plus blue (phycobiliproteins) pigments. However, no organelles such as nuclei, mitochondria, endoplasmic reticulum, Golgi apparatus and plastids were found in these organisms. This consequently designated them as prokaryotes unlike green, red and brown algae; the appellation cyanobacterium was suggested, cyano deriving from the greek κύανος (kyanos), blue (Stanier et al., 1978).

Cyanobacteria diverged since their apparition, becoming present in a great diversity of habitats like marine water, fresh water and soils. They have colonized extreme environments such as volcanic lakes (*Thermosynechococcus elongatus*: Yamaoka et al., 1978) or Antarctic mats (Taton et al., 2003). Some species act as symbionts, for example in lichens or in certain marine invertebrates (*Acaryochloris marina*: Miyashita et al., 1996); the endosymbiotic theory suggests that chloroplasts derive from cyanobacterial-like cells, originally symbiotically associated to protoeukaryotic hosts but now behaving semi-autonomously (reviewed in: McFadden, 2001). So far, the cyanobacterial phylum includes at least 7500 species distributed in 5 sections and more than 150 genera (NCBI taxonomy database: 11000 entries). The initial classification was built on differences observed among cyanobacteria considering cell diameters (10^{-7} to 10^{-5} m), division patterns, branching/non branching filaments formation and potential differentiations for nitrogen fixation (heterocysts) or survival under extreme drought conditions (akinetes) (Rippka et al., 1979) (Fig.1). More recently, 16S RNA sequencing partially confirmed the taxonomic groups previously established (reviewed in: Komárek, 2010). Many cyanobacterial genomes have been released, the amount of data available increasing faster and faster thanks to high-flow techniques

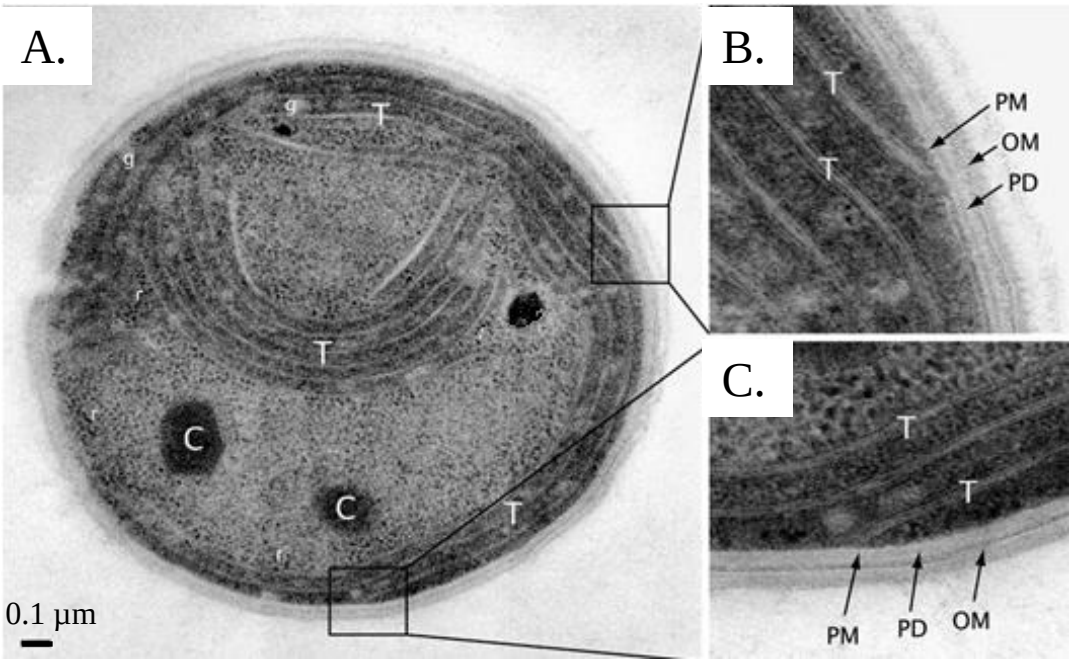

Figure 2. Electron micrograph of a thin section through a *Synechocystis* PCC 6803 cell A. Thin section of a *Synechocystis* cell revealing the various intracellular structures: ribosomes (r), glycogen granules (g), carboxysomes (C) and thylakoid membranes (T). B. and C.. Enlargments of the boxed areas in A., showing the plasma membrane (PM), the peptidoglycan layer (PD) and the outer membrane (OM). Adapted from Liberton et al., 2006.

propagation (deep-sequencing, see (Shih et al., 2013). A rapid survey indicates variable genome sizes (from 2Mb to 13Mb) as well as GC contents (30 to 75%), perfectly reflecting the enormous diversity in morphologies and habitats. Still, some common features exist across the phylum. First of all, even though classical organelles miss, sub-cellular compartments are clearly visible. Particularly, cyanobacterial cells contain membrane stacks that constitute the thylakoids where both photosynthesis and respiration take place (except for *Gloaeobacter violaceus*: Guglielmi et al., 1981) (Fig.2A). Also, hexagonal structures termed carboxysomes ensure Rubisco's optimal functioning by creating CO_2 enriched/O_2 depleted biochemical environments (reviewed in: Badger and Price, 2003; Price, 2011) (Fig.2A). Hydrocarbons stemming from photosynthesis are converted to glycogen for storage (Fig.2A). Finally a peptidoglycan layer and an outer membrane form the cell wall, which confers some mechanical resistance like in most gram-negative bacteria (see Fig.2B,C).

Certain species chosen to study cyanobacteria physiology and photosynthesis have been used for more than 40 years; among them, the cyanobacterium *Synechocystis* PCC 6803 (hereafter called *Synechocystis*) has been employed as a model species in this work.

1.2. A model cyanobacterium: *Synechocystis*

Synechocystis was isolated from a Californian freshwater lake (Stanier et al., 1971). The round-shaped cells, diameter approximately 2 µm, look greenish when observed using optical microscopy. Their thylakoid membranes form concentric stacks along the plasma membrane as revealed by electron microscopy (recent review: Liberton et al., 2006) (Fig.2A). *Synechocystis* cells can grow photoautotrophically in mineral media (Stanier et al., 1971). They naturally have the capacity to uptake exogenous DNA and to perform double-homologous recombination, which points them as perfectly suitable for genetic manipulations (Grigorieva and Shestakov, 1982). Moreover, they can grow heterotrophycally in glucose enriched media; under these conditions, mutations impairing the photosynthetic apparatus do not have a lethal effect (Rippka et al., 1979). *Synechocystis* genome was fully released in 1996, making it the first photosynthetic organism ever sequenced (3.5 Mb, 47.7% GC: Kaneko et al., 1996). Finally, transcriptomic data are also available (Hihara et al., 2001) and recently, RNAseq allowed Transcription Starting Sites mapping (Mitschke et al., 2011). All these points designate *Synechocystis* as a good model for photosynthesis study.

After giving a general overview about cyanobacteria, the mechanisms underlying cyanobacterial photosynthesis are now going to be addressed.

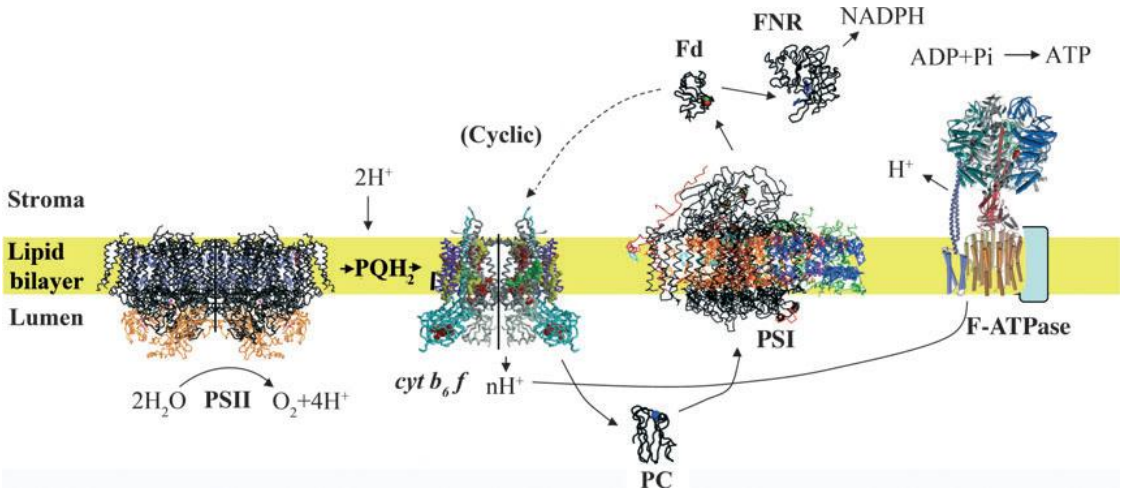

Figure 3. Components of the oxygenic photosynthesis inside of thylakoid membranes. This figure displays the various membrane-spanning complexes implied in oxygenic photosynthesis: Photosystem II (PSII), cytochrome b_6f and PSI. They are connected by mobile electron carriers such as plastoquinol (PQH_2), plastocyanin (PC) and ferredoxin (Fd). The linear electrons transport chains leads to NADPH accumulation and formation of a proton gradient across thylakoid membranes, used as a motive force for ATP synthesis. Under certain conditions, the cyclic electron transport chain leads to proton gradient formation without any concomitant NADPH production. Adapted from Nevo et al., 2012.

2. Photosynthesis in cyanobacteria

As said before, the cyanobacterial photosynthesis takes place inside of thylakoid membranes. It implies light energy harvesting and funneling towards special-pair chlorophylls (P680/P700), which upon excitation release low redox potential electrons then sequentially transferred from acceptor to acceptor (reviewed in: Witt, 1996). A proton gradient gets concomitantly created, allowing ATPase functioning; thus, photosynthesis provides NADPH (following $NADP^+$ reduction) and ATP necessary for the Calvin-Benson cycle.

Cyanobacteria, plants and algae actually have similar photosynthetic machinery comprising 2 photosystems (PSI/II), cytochrome b_6f ($cytb_6f$) and several mobile components (plastoquinone (PQ), plastocyanine (PCy), ferredoxin (Fd) working in series (Fig.3).

2.1. The linear electron transport chain: PSII, $cytb_6f$ and PSI.

Photosystems are pigment-protein complexes embedded in thylakoid membranes. They contain inner Chlorophyll *a* (Chl*a*)-binding antennae that harvest light and funnel the associated energy towards reaction centers where photochemistry takes place, i.e. where special-pair chlorophylls (P680/P700) realize charge separations upon excitation. The cofactors receiving electrons from P680/P700 form the acceptor side whereas the ones giving electrons to $P680^+/P700^+$ form the donor side; the peptide composition and the cofactors associated to acceptor/donor sides differ in both photosystems, PSII or PSI (Fig.4A,B).

PSII has been extensively studied over the last decades (reviewed in: Nelson and Yocum, 2006; Cardona et al., 2012). 35 Chl*a* molecules appear per monomer, mostly attached to the CP43/CP47 inner antennae. The reaction center comprises 2 proteins, D1/D2, where all cofactors required for photochemistry can be found; it also incorporates a cytochrome b559, absolutely necessary for its correct assembly. Upon excitation, P680 gives an electron to Pheophytin (D1 associated) that is then transferred to Q_A (D2-associated quinone) and Q_B (D1-associated quinone) (Fig.4A). Q_B can receive 2 electrons before getting protonated; it subsequently leaves PSII, in the plastoquinol (PQH_2) form, by diffusing inside of thylakoid membranes. On the donor side, Tyrozine Z (Tyr Z, D1 associated) reduces $P680^+$. Remarkably, the Water Oxidizing Complex (WOC) can finally retrieve electrons from water for $TyrZ^+$ reduction, with associated O_2 production (reviewed in: Vinyard et al., 2013). 4 successive P680 charge separations can lead to the formation of 1 O_2 and 2 PQH_2 molecules.4 protons are taken away from the cytoplasm, 4 protons accumulate

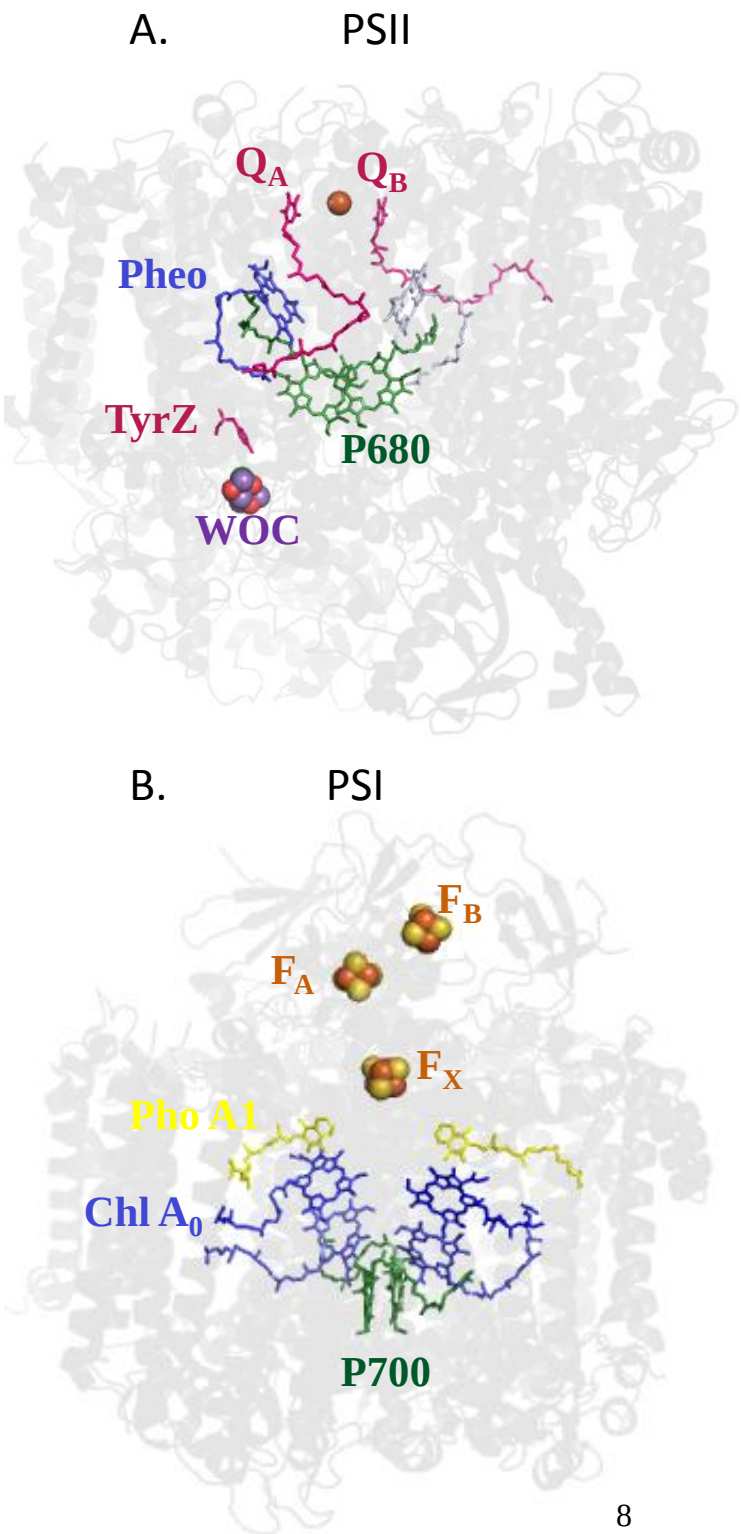

Figure 4. Cofactors associated to PSII and PSI for photosynthetic electron transport. A. Arrangement of the cofactors in PSII. Upon excitation, the special-pair chlorophyll (P680) gives an electron to the D1-protein associated Pheophytin (Pheo) then transferred sequentially to the D1-protein associated quinone (Q_A) and the D2-protein associated quinone (Q_B). Q_B receives 2 electrons before getting protonated and leaving the binding site as plastoquinol (PQH_2). The Water Oxidizing Complex (WOC) retrieves electrons from water and transfers it to P680+ through the Tyrosine Z (TyrZ), with associated O_2 emission. PDB file 3ARC (Umena et al., 2011) modified with PyMol. B. Arrangement of the cofactors in PSI. Upon excitation, the special-pair chlorphyll (P700) gives en electron to the Chlorophyll A_0 (Chl A_0, 2 branches possible: 1 on PsaA, the other on PsaB) then sequentially transferred to Phylloquinone A1 (Pho A_1) and to 3 iron-sulphur clusters (F_X, F_A, F_B) before reaching Ferredoxin. On the donor side, pastocyanin reduces $P700^+$. PDB file 1JB0 (Jordan et al., 2001) modified with PyMol.

inside of thylakoids. The first PSII structure ever resolved was obtained from *Synechococcu elongatus* with 3.8 Å resolution (PDB file 1FE1: Zouni et al., 2001); more recently, Umena et al. got a 1.9 Å structure of *Thermosynechococcus vulcanus* PSII allowing visualization of its WOC (PDB file 3ARC: Umena et al., 2011).

Cytochrome b_6f is another complex spanning thylakoid membranes that provides the electronic connection between PSII and PSI (3Å resolution crystal structure in Kurisu et al., 2003. PDB file: 1UM3). The Q_0 site of $cytb_6f$ binds PQH_2 and oxidizes it. One electron passes via a Rieske protein before reaching PCy; the other one follows a different route through 2 b-hemes, eventually reducing semiquinol in the Q_i site of $cytb_6f$ (reviewed in Osyczka et al., 2005). For 1 oxidized PQH_2, 2 protons accumulate inside of thylakoids and 1 proton is taken away from cytoplasm (semiquinol reduction/protonation).

Each PSI monomer attaches approximately 90 Chl*a* molecules (versus only 35 in PSII) (reviews about PSI: Brettel and Leibl, 2001; Grotjohann and Fromme, 2005). PsaA/PsaB heterodimers and PsaC constitute the reaction centers. On the donor side, PCy reduces $P700^+$ after charge separation . On the acceptor side, chlorophyll A_0, phylloquinone A_1 and 3 iron-sulphur clusters (F_X, F_A, F_B) successively accept the electrons which finally are transferred to the soluble Ferredoxin (Fd) (Fig.4B). An enzyme, the $NADP^+$-oxidoreductase, catalyzes NADPH formation using reduced Fd as substrate. 2 successive P700 charge separations potentially lead to the formation of 1 NADPH molecule, 1 proton being taken away from cytoplasm. Initially, PSI structure was determined in *Synechococcus elongatus* with 4 Å resolution; the resolution improved to 2.5 Å since that time (PDB file 1JB0: Jordan et al., 2001).

To summarize, electrons can flow from water to PQ via PSII, from PQH_2 to PCy via $cytb_6f$ and from PCy to Fd via PSI before reaching $NADP^+$ (Z-scheme of photosynthesis). During the electron migration a proton gradient is formed with low pH in the lumen and a high pH in the stroma (Fig.3). This constitutes the Linear Electron Transport (LET) chain, producing NADPH and a proton-motive force necessary for ATP synthesis. Interestingly, both the photosynthetic and the respiratory transport chains are situated in the thylakoid membranes when considering cyanobacteria; they share common components, like PQ, $cytb_6f$ and PCy.

A.

Biliprotein	Chromophore content of the (αβ) monomer	Preferential aggregation state	Absorption maximum (nm)	Fluorescence maximum (nm)
Allophycocyanin (APC)	2 PCB	$(\alpha\beta)_3$	650	660
C-phycocyanin (PC)	3 PCB	$(\alpha\beta)_6$	620	645
C-phycoerythrin (PE)	5-6 PEB	$(\alpha\beta)_6\gamma$	560	577
C-phycoerythrocyanin (PEC)	2 PCB, 1 PXB	$(\alpha\beta)_6$	570 to 595	625
ApcD	1 PCB	isolated protein	671	680
ApcE	1 PCB	isolated protein	670	676

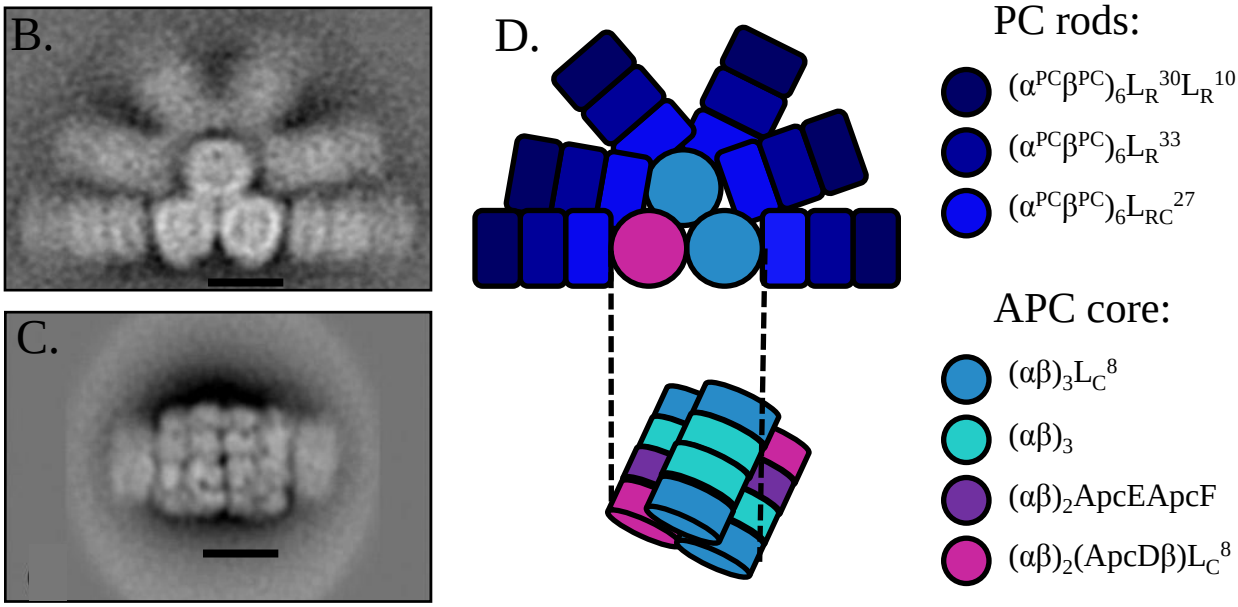

Figure 5. Phycobilisomes of the model cyanobacterium *Synechocystis* PCC 6803. A. Main features of the cyanobacterial phycobiliproteins. Table adapted and upgraded from Bryant, 1982. B and C. Single particle EM images showing a face view (B) or a top view (C) of *Synechocystis* phycobilisomes. The bar indicates 10 nm. (from Arteni et al., 2009). D. Schematic representation of the same phycobilisomes and orthogonal projection of their cores. PCB: phycocyanobilin; PEB: phycoerythrobilin; PXB: phycobiliviolin.

2.2. Phycobilisomes: the cyanobacterial accessory light harvesting complexes

Going deeper and deeper under water, light quality gets modified by a selective impoverishment in red photons. Since Chl*a* has major absorption bands on the red edge of the spectrum, it becomes less effective for light harvesting in deep water. Photosynthetic organisms living in aquatic media often have developed accessory antennae, containing different kind of pigments that allow using the whole wavelength range available. Most cyanobacteria (and also red algae, not included in this study) employ a special class of complexes called phycobilisomes for that purpose.

Early studies from the 19th century revealed that some cyanobacteria produce soluble pigments, blue or red in color, emitting strong pink fluorescence (review: Marsac, 2003). These pigments were shown to form gigantic granules visible by electron microscopy (EM) on thylakoid membranes and accordingly named phycobilisomes (PBs) (Gantt and Conti, 1966). High concentrations of phosphate (>0.5M) stabilize PBs, permitting to get them intact in a 2 steps process beginning with membrane solubilization using detergents and finishing with sucrose gradients for separation (Gantt et al., 1979).

2.2.1. Composition and structure of the PBs

PBs contain chromophorylated proteins called phycobiliproteins that represent up to 80% of their mass (Marsac and Cohen-bazire, 1977). These phycobiliproteins covalently bind open chain tetrapyrolles of the bilin family through thioether linkages implying one or several cysteines. They exist primarily as (αβ) monomers resulting from the association of 2 subunits, then tending to form $(\alpha\beta)_3$ trimers and sometimes $(\alpha\beta)_6$ hexamers. The number of cofactors per (αβ) monomer changes between phycobiliproteins, being for example of 2 in allophycocyanin (APC) and of 3 in phycocyanin (PC). This owes to the fact that α^{APC}, α^{PC} and β^{APC} subunits possess only 1 phycocyanibilin (PCB) binding cysteine whereas β^{PC} has 2 attachment sites for PCB. Phycobiliproteins are classified into 4 families according to the nature of their bilins, to their absorption profile and to their fluorescence emission properties summarized in Fig.5A (adapted from Bryant, 1982). PC and APC are common components of all cyanobacterial PBs, whereas Phycoerythrin and Phycoerythrocyanin production occurs only in certain species (for a review: MacColl, 1998).

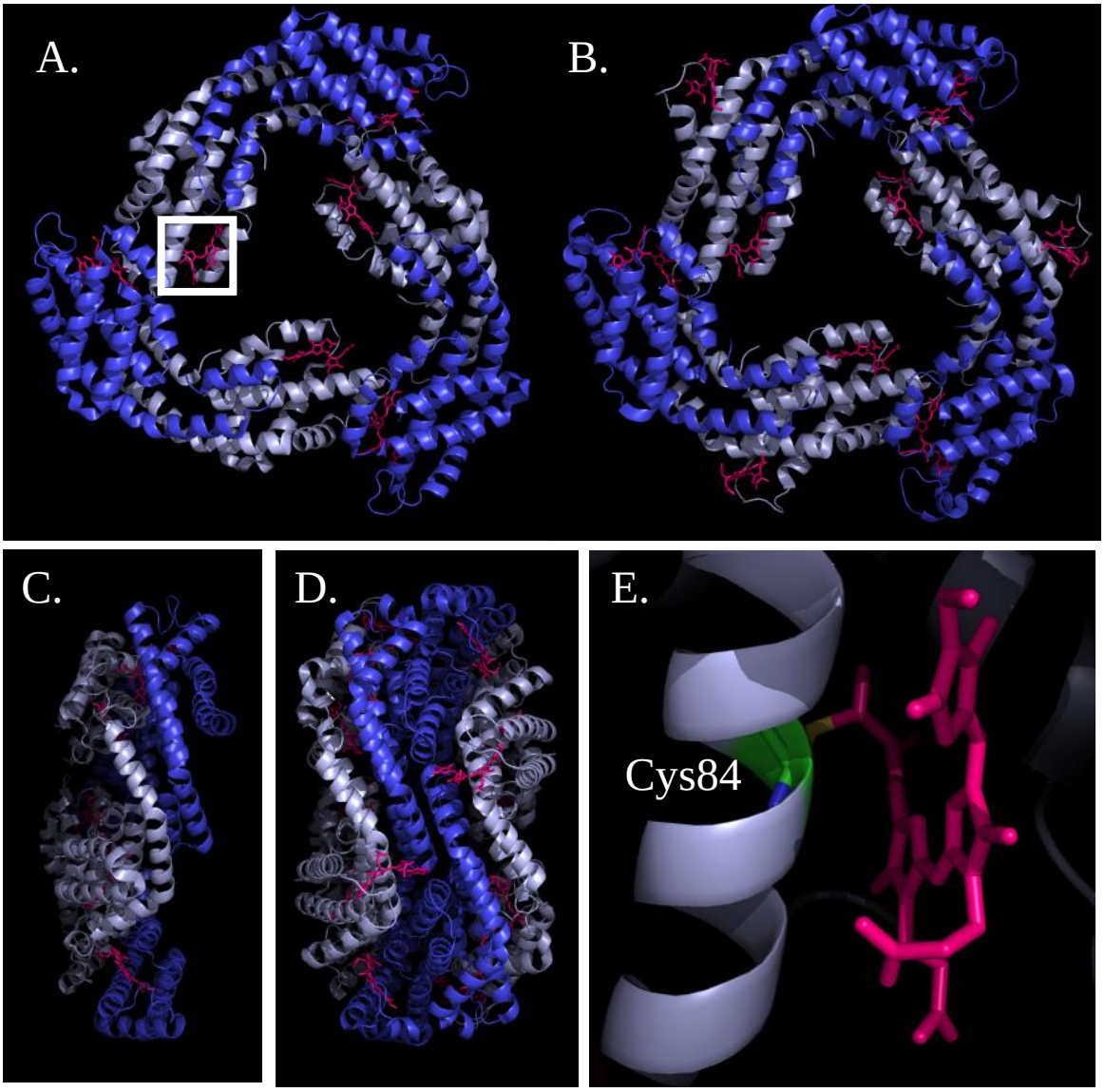

Figure 6. Crystal structures of the phycobiliproteins isolated from *Synechococcus elongatus PCC 7942*. A. Face view and C. side view of an APC trimer;. α^{APC} subunits are deep blue, β^{APC} subunits are light blue. B. Face view of a PC trimer and D. side view of a PC hexamer, showing 2 trimers associated back to back. α^{PC} subunits are deep blue, β^{PC} subunits are light blue. E. Close up of the white frame in A, showing the thioether bond between Cys84 of β^{APC} and phycocyanobilin (PCB). PCBs are shown as purple sticks. PDB files 4F0U and 4H0M (Marx et al., 2013) modified with PyMol.

In the introduction I will mainly focus on PBs of the cyanobacterium *Synechocystis* that was used as a model organism in this study. PBs with slightly different architectures and coming from other cyanobacterial strains will be presented in Chapter 2 of the present manuscript. When isolated and observed through EM, *Synechocystis* PBs appear as hemidiscoidal particles where PC rods (6 in general) radiate from an APC core laying on thylakoid membranes in vivo (Arteni et al., 2009) (Fig. 5B,C). Each rod is made of 2 or 3 PC hexamers. 4 APC trimers give a cylinder and 3 cylinders stack to form the core (Fig.5D). The complex is organized in a way that phycobiliproteins with the most blue-shifted absorption and fluorescence emission properties, namely PC (λ_{Amax}=620nm, λ_{Fmax}=650nm), surround phycobiliproteins with lower energetic levels (APC, λ_{Amax}=650nm, λ_{Fmax}=660nm). This allows funneling energy towards APC cores and directional energy transfer to Chl*a*.

Beyond that, no overall tri-dimensional structural picture of PBs is available so far. Isolated phycobiliproteins have been crystallized from diverse organisms in trimeric or hexameric aggregation states and their X-ray diffraction pattern was determined (reviewed in: Adir, 2005). They generally appear as disks of 100Å diameter with a central cavity of 30Å. The crystal structure of trimers or hexamers of *Synechocystis* PC was not resolved. Only the structure of a monomer of APC was published (PDB file 4F0T; Marx and Adir, 2013). However, crystal structures of PC hexamers and APC trimers of close organisms, for example *Synechococcus elongatus* PCC 7942 (PDB file 4H0M: Marx and Adir, 2013), are known (Fig.6).

Synechocystis PBs also incorporate colorless linker polypeptides that possibly get inserted into the central cavities of trimers and hexamers of phycobiliproteins (Yu and Glazer, 1982). L_{RC}^{27} (encoded by the *cpcg1* gene) enables the binding of PC rods to the APC core (Kondo et al., 2005). L_R^{33} (*cpcc1* gene) and L_R^{30} (*cpcc2* gene) are required for the elongation of PC rods (Ughy and Ajlani, 2004). L_R^{10} (*cpcd* gene) has been proposed to cap PC rods and terminate their elongation, similarly to L_C^8 (*apcc* gene) for APC cylinders in the core. Recently, whole PC rods have been crystallized (including L_{RC}^{27}, L_R^{30}, L_R^{33} and L_R^{10}) (David et al., 2011). Authors suggested that even though linkers could not be modeled in the subsequent structure due to symmetry problems, they increased the stability (quantified using the b-factor) of specific PC aminoacids situated on the inner cavity surface. Only one crystal structure exists so far showing linker-phycobiliprotein complexes: the L_C^8 was shown to be localized in the inner cavity of APC trimers from *Mastigocladus laminosus* and to interact

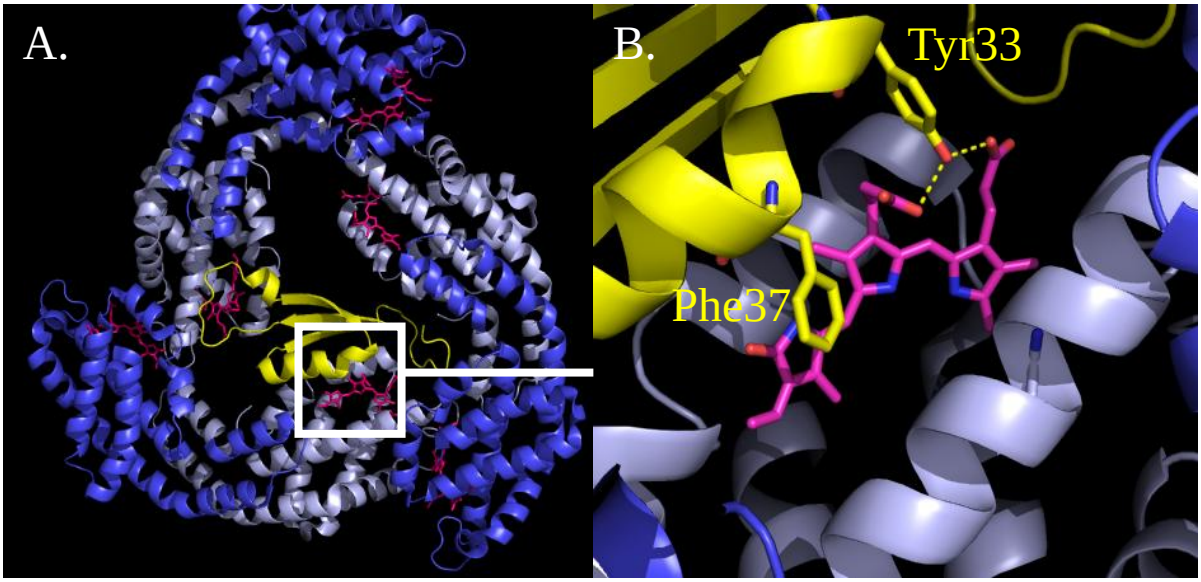

Figure 7. Crystal structure of the L_C^8-APC complex isolated from *Mastigocladus laminosus*. A. Face view of an APC trimer with incorporated linker. α^{APC} subunits are deep blue, β^{APC} subunits are light blue. The L_C^8 linker-polypeptide is represented in yellow. B. Close up of the white frame in A. showing interactions between L_C^8 and a β^{APC} bond PCB. The contacts have a hydrophobic (bling ring and Phe37 of LC8) or polar (bilin side groups and Tyr33) nature. PCBs are shown as purple sticks. PDB file 1B33 (Reuter et al., 1999) modified with PyMol.

with 2 out of 3 β^{APC} bond PCBs (Reuter et al., 1999) (Fig.7). This agrees well with the idea that linkers are not only necessary for PB assembly but also for tuning phycobiliprotein spectral properties, allowing an optimized polar energy transfer (Lundell et al., 1981a). When purified, PC has its maximum absorbance at 620 nm and fluorescence emission at 645nm (hexameric state). L_R^{33} (res. L_{RC}^{27}) shifts the maximum of absorbance to 623nm (res. 628nm) and of fluorescence to 648nm (res. 650nm). L_C^8 containing APC trimers have a red-shifted emission compared to normal APC trimers (Maxson et al., 1989). Linkers actually change the biochemical environment around PCBs (Fig.7B).

The APC core has a quite intricate organization. It was first described in *Synechococcus* PCC 6301, thanks to partial dissociation of PBs allowing isolation of "subcore particles" (Yamanaka et al., 1982). The proposed model was then extended to other species after confirmation in *Anabaena* PCC 7120 (Ducret et al., 1998). Fig.5D shows the tricylindrical APC core of *Synechocystis* where most trimers contain major APC forms (αβ) that absorb light at 650nm and emit fluorescence at 660nm (see Fig.5A). Differences in spectral properties between PC and APC come from diverging aminoacids surrounding the PCBs (McGregor et al., 2008). α^{APC} subunits have a more hydrophobic PCB binding pocket than α^{PC} subunits, responsible for the APC trimers bathochromic shift. The 2 basal cylinders of the core also include trimers with minor APC forms (ApcD, ApcF, ApcE). Purified ApcD (Glazer and Bryant, 1975) and ApcE (Lundell et al., 1981b) have a pronounced red-shift, absorbing light around 670nm then emitting fluorescence at 680nm. They are the lowest energy phycobiliproteins and play the role of PB terminal emitters (Gindt et al., 1994). The differences in the spectral properties are also due to more hydrophobic environments surrounding the bilins (McGregor et al., 2008). ApcE has actually several functions. Its N-terminal part shows some homology with α^{APC} subunits, binding 1 PCB thanks to Cys190. Its C-terminal part contains linker-like domains (called REP) separated by spacers (called arms); it acts as a scaffold for APC core assembly and probably fine-tunes APC spectral properties (Houmard et al., 1990). Finally, PB attachment to thylakoid membranes involves polar contacts between ApcE residues and charged lipid head groups, which explains why ApcE is sometimes called L_{CM} (core-membrane linker) (Ajlani and Vernotte, 1998).

We saw that PBs are highly organized complexes. Phycobiliproteins tend to aggregate, forming rows. Colorless linker polypeptides allow the apparition of 2 well defined zones, corresponding to PC rods and to the central APC cores. Spectral properties of

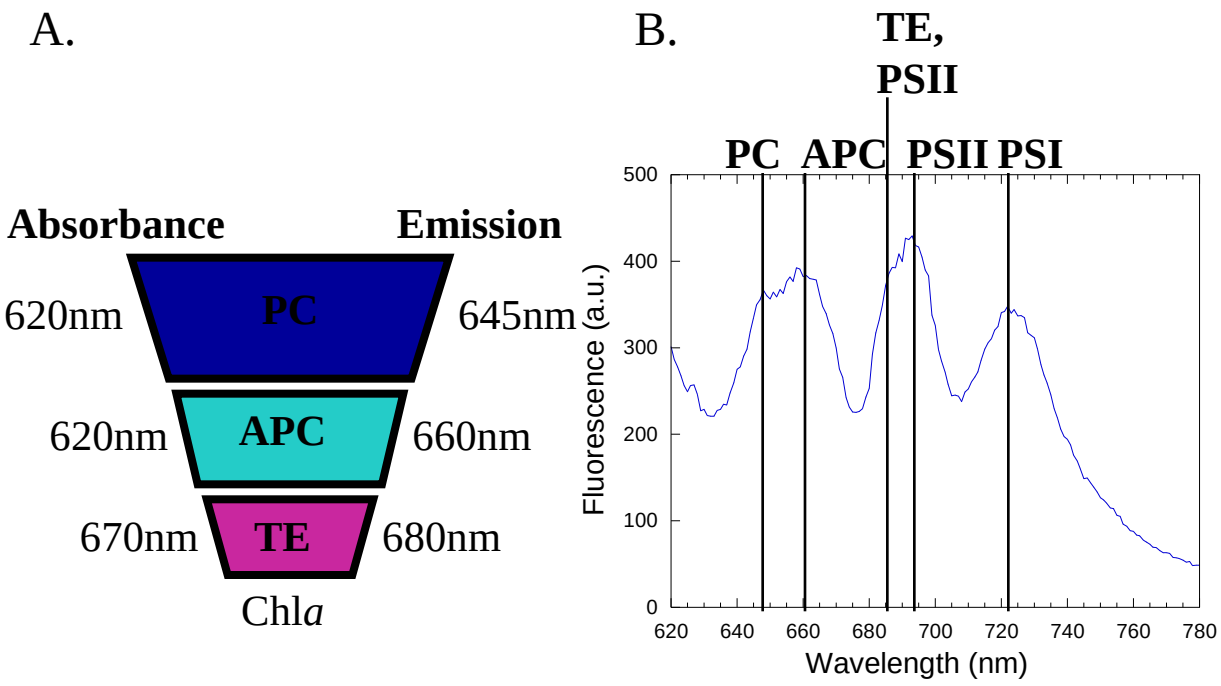

Figure 8. Energy transfer from phycobilisomes to photosystems in *Synechocystis*. A. Schematic representation of the energy transport pathway in *Synechocystis* phycobilisomes. B. 77K fluorescence emission spectrum of *Synechocystis* cells kept in the dark for 10' then excited using low intensity orange light (590nm) absorbed preferentially by PC.

phycobiliproteins are fine tuned for efficient energy transfer from PC to APC and finally terminal emitters (ApcD, ApcE, ApcF) (Fig.8A).

2.2.2. PBs function as antennae

PBs funnel light energy to the terminal emitters that in turn equilibrate with Chl*a* from both reaction centers (Fig.8A). When applying an excitation light absorbed preferentially by PC (around 600nm), the fluorescence spectra of cyanobacterial cells at 77K show distinct bands associated with PB components (PC 650 nm, APC 665 nm, TE 683 nm), PSII Chl*a* (CP43 685 nm, CP47 695 nm) and PSI Chl*a* (720 nm) (Campbell et al., 1998) (Fig.8B). In many articles, the ratios between these bands were used as a measure of energy transfer from the PBs to the photosystems (for example Ashby and Mullineaux, 1999). Getting a real quantitative estimate is more complicated. Based on target analysis of spectrally-resolved picosecond fluorescence data, Tian and coworkers (Tian et al., 2011) suggested that 50% of the energy collected by PBs goes to PSI and 50% to PSII in *Synechocystis* cells grown under their laboratory conditions. Combining fluorescence emission and excitation spectra interpretations, it was proposed that up to 80% of the energy harvested by PBs reaches PSI in *Arthrospira platensis* cells (Rakhimberdieva et al., 2001). Energy transfer from PBs to PSI could be achieved through a direct interaction between them (Mullineaux, 1992; Mullineaux, 1994) and/or through energy spillover between PSII Chl*a* and PSI Chl*a* (McConnell et al., 2002). Some reports also indicate a possible connection between regular PC rods (Li et al., 2003) or CpcG2-incorporating PC rods (Kondo et al., 2007) and PSI.

There are several terminal emitters per PB (ApcD, ApcF, ApcE) and each of them could create specific routes for energy transfer towards PSI or PSII. ApcD deficient *Synechococcus* PCC 7002 mutant cells were shown to have impaired energy transfer from PBs to PSI, resulting in a slowed down PSI photoxidation upon orange light illumination (Dong et al., 2009). 77K fluorescence emission spectra of *Synechocystis* cells lacking ApcD and/or ApcF strongly suggested that in this strain energy flow from PBs to PSI and PSII passes mainly by ApcF (or the associated ApcE) and not by ApcD (Ashby and Mullineaux, 1999). Further investigations are required for determining exactly the role of each of the terminal emitters.

2.2.3. PBs movement and possible implication in State Transitions

Strikingly, associations between PBs and PSs are extremely transient (for a review: Mullineaux, 2008). On one hand, FRAP combined to FLIP measurements revealed a very fast diffusion of PBs on thylakoid membranes' surface (Mullineaux et al., 1997; Sarcina et al., 2001; Yang et al., 2007). On the other hand, PSII complexes are immobile. It is impossible to say whether PSI is mobile or not because it has a low room temperature fluorescence yield making it hardly detectable using confocal microscopy. Anyway, this shows a very dynamic environment where PBs seem to continuously switch from reaction center to reaction center.

It was proposed that light quality is a determining factor that drives variations in the affinity between PBs and PSs through multiple ways. Any light absorbed predominantly by Chl*a* (blue/far red) tends to excite PSI specifically in cyanobacterial cells. Any light absorbed predominantly by phycobiliproteins (green/orange) excites relatively more PSII, at least at low intensities. This can set on an over-oxidation or over-reduction of inter-systems electron transporters and a situation where PSI or PSII becomes rate limiting for photosynthesis (reviewed in: Mullineaux and Emlyn-Jones, 2005). Cyanobacteria, like plants and algae, have developed a mechanism named "state transitions" to cope with the unbalanced PSs' functioning.

PQ reduction drives transition from State I to State II and a concomitant decrease in PSII fluorescence emission as assessed by 77K spectra and room temperature Pulse Amplitude Modulation (PAM) traces (illustrated in McConnell et al., 2002). PAM fluorometry allows measuring fluorescence yield over time (see Schreiber et al., 1986). A non-actinic modulated detection light (around 650 nm) excites Chl and phycobiliproteins; the emitted fluorescence, after passing through cutoff filters (selecting wavelengths higher than 700 nm), is detected by a synchronous photo-multiplicator. Application of a non-modulated actinic light does not have any impact on signal intensity but can have physiological effects that modify the sample's fluorescence yield. Several fluorescence levels can be recorded that way: minimum level F_0 (no actinic light ON), maximum level F_m (saturating actinic flash ON), steady-state level F_s' (continuous, sub-saturating actinic light ON) and maximum level under actinic illumination F_m' (see also El Bissati et al., 2000). Transition from State II to State I increases the $F_{m'}$ level (reviewed in: Allen and Mullineaux, 2004).

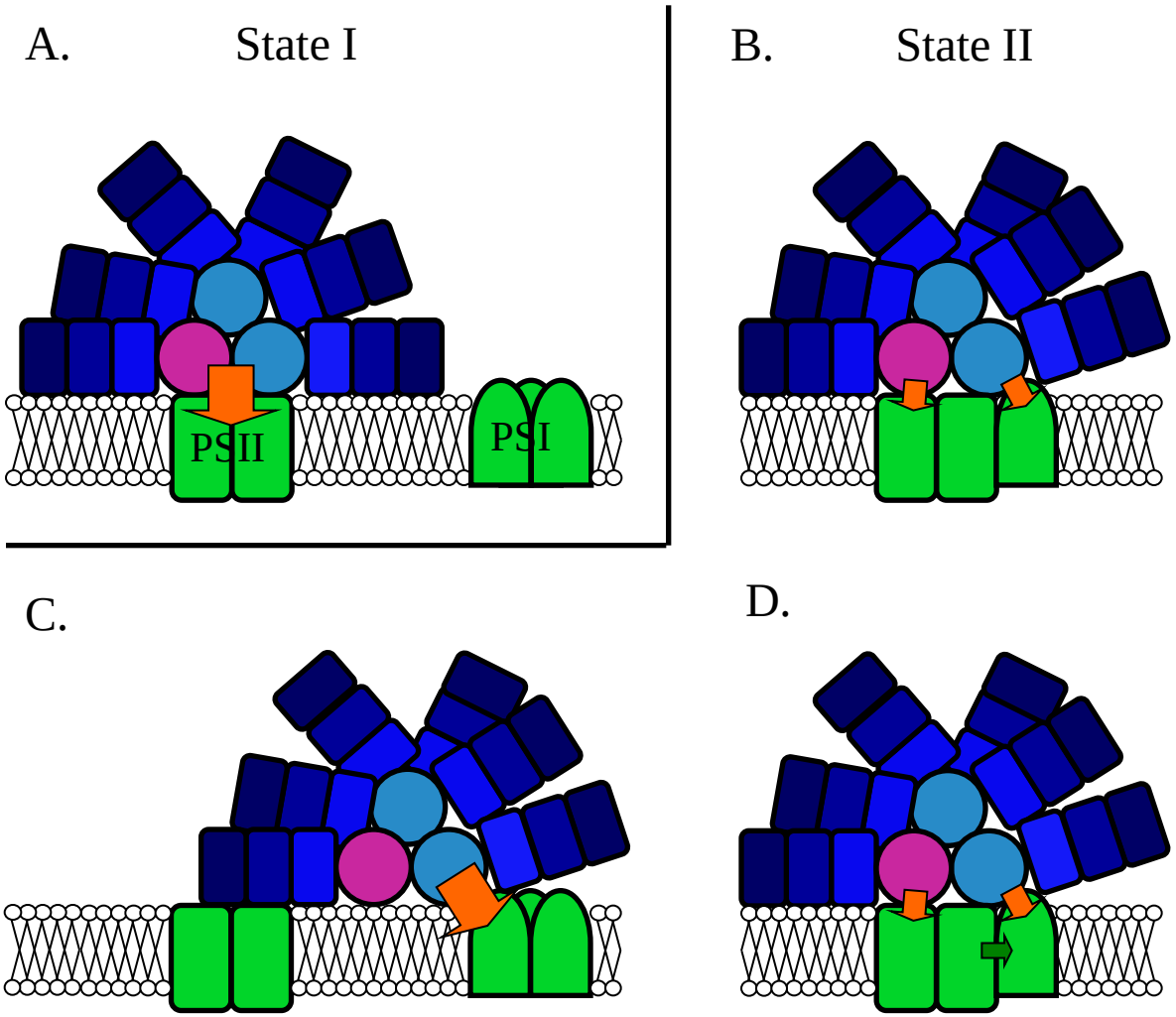

Figure 9. Alternative models for state transitions in *Synechocystis*. A. In State I, light preferentially excites PSI and triggers the association of phycobilisomes with PSII. Most of the energy harvested by phycobilisomes then arrives to PSII reaction centers (orange arrow). B. to C. Alternative models for State II. B. Upon State II transition, PSI trimers dissociate into monomers and move for a closer association with PSII. A slight translation of phycobilisomes allows their interaction with PSI, but they remain partly connected to PSII (orange arrows). C. Upon State II transition, phycobilisomes diffuse towards PSI and associate with it (orange arrows). They are no more connected to PSII. D. Similar model to B., adding energy spillover from PSII Chl a to PSI Chl a (drak green arrow).

It is probable that like in plants and algae the Qo site of cytochrome b_6f is involved in this mechanism (Mao et al., 2002; Huang et al., 2003). According to the mobile antennae model, the changes in PSII fluorescence are related to the movement of PBs from PSII to PSI (or contrary) and the associated diminution (or increase) of the PSII effective antenna size (Joshua and Mullineaux, 2004) (Fig.9) . It is not known how the signal goes from the PQ pool and/or the cyt b_6f to the PBs or photosystems. In plants and algae a kinase and a phosphatase are involved in the signal translation (reviewed in: Ruban and Johnson, 2009). In the past it was suggested that phosphorylation events were also involved in cyanobacterial state transitions (Allen et al., 1985) but these results were not confirmed and the discussion remains open.

The mobile antennae model is largely based on FRAP measurements. In 2004, Joshua and Mullineaux showed that there is a correlation between states transition and PB mobility: in cells treated with high molarity potassium-phosphate buffer or sucrose solution, both processes were inhibited (Joshua and Mullineaux, 2004). Published data about thylakoid membrane organization in *Synechocystis* WT cells shows colocalization between PSI and PSII; no massive PSI or PSII enriched clumps appear (Folea et al., 2008; Collins et al., 2012). Consequently, if PBs mobility is required for state transitions induction in *Synechocystis*, local rearrangements or tilting are more probably implied than long range diffusion (Fig.9). In contrast, ultrastructural studies of the thylakoid membranes using EM revealed that there are PSI and PSII enriched domains in *Synechococcus* PCC 7942 cells (Sherman et al., 1994). Thus, whether or not a long range movement of PBs is required for state transitions could depend on the species considered (see alternative model, Fig.9C).

Suppression of ApcD or ApcF in *Synechococcus* PCC 7002 (Gindt et al., 1994) and *Synechocystis* cells (Ashby and Mullineaux, 1999) led to the conclusion that both proteins are required for state transitions. 77K fluorescence emission spectra of ΔApcD (respectively ΔApcF) mutant cells suggest that they are locked in State I (respectively State II). PBs terminal emitters, beyond their functional role, could also act as physical bridges that are required for a correct association between PBs and reaction centers. A reverse genetics approach allowed identifying another protein called Regulation of PBs Association C (RpacC) which suppression impairs state transitions (Emlyn-Jones et al., 1999). RpaC is thought to permit the dynamic association between PBs and PSII (Joshua and Mullineaux, 2005). The absence of similar proteins in organisms other than cyanobacteria and RpaC's unique predicted folding constitute barriers to understand its exact biochemical role. The mobile

antennae model alone does not fully explain state transitions, also observed in mutants lacking assembled PBs (Olive et al., 1997; El Bissati et al., 2000). Movement of photosystems could also be involved in state transitions. PSII forms dimeric rows, particularly visible in State I and tending to disappear in State II (Olive et al., 1997). When present, these rows could prevent PBs attachment to PSI through steric hindrance effects (Bald et al., 1996). PSI exists as a mixture of monomers and trimers (Kruip et al., 1994) arranged more or less randomly on border of the PSII arrays. PSI monomerization increases PBs diffusion rates (Aspinwall et al., 2004) and accelerates state transition kinetics. It has been proposed that spillover from PSII Chl*a* to PSI Chl*a* is partially responsible for PSII fluorescence decrease and concomitant cross-section diminution upon State I-to-II transition (For review: Biggins and Bruce, 1989). This suggests that part of the light energy received by PSII Chl antennae gets transferred to PSI. Very close vicinity between PSII and PSI is required for spillover to occur, probably achieved when PSII dimeric rows disassemble in State II. An extended model has been proposed by McConnell and coworkers (McConnell et al., 2002) which suggests that state transitions are actually due to bot direct changes in PBs energy distribution and spillover from PSII to PSI (fig.9D).

This section aimed at emphasizing that cyanobacteria possess accessory antennae with unique features. The gigantic, soluble, highly organized PBs are designed for harvesting light in the gap form by Chl*a* absorption bands. They are optimized for a very efficient energy transfer towards terminal emitters. They can distribute energy to PSI or PSII, in a very dynamic manner controlled by other cellular processes.

3. Drawbacks of photosystems functioning in an oxygenic medium and defensive strategies

3.1. Photoinhibition of PSII

High light intensities trigger a decrease of PSII activity, irreversible when de novo protein synthesis gets chemically inhibited (lincomycin, chloramphenicol addition), referred to as photoinhibition. The underlying mechanisms are still debated but reactive oxygen species (ROS) generation (particularly singlet oxygen, $^1O_2$) and subsequent oxidative damages presumably play a central role (reviewed in: Krieger-Liszkay, 2005; Vass, 2012). Under strong illumination or any condition driving PQ over-reduction – like anaerobiosis, CO_2 deprivation and low temperatures – PSII acceptor side gets reduced because the Q_A-to-Q_B electron transfer step becomes rate-limiting (closed center). The Q_B pocket remains empty

if there is no oxidized PQ to fill it; as a consequence, forward electron flow gets interrupted and the probability for charge recombination increases. Spontaneous spin conversion of the primary radical pair [$P680^{+\bullet}Pheo^{-\bullet}$] occurs, going from singlet to triplet state, followed by a possible charge recombination leading to triplet Chl ($^3P680$) formation. $^3P680$ reacts fast with O_2 and the extremely reactive singlet oxygen ($^1O_2$) appears, as confirmed by chemical trapping in *Synechocystis* cells (Rehman et al., 2013). $^1O_2$ irreversibly damages the D1 protein then the whole PSII before of eventually impairing the translational and transcriptional machineries required for damaged proteins replacement. Other ROS can participate in photosynthetic apparatus degradation, such as superoxide ($O_2^{-\cdot}$) obtained when Q_A^- reacts with O_2. Donor side effects are observed as well: disruption of the WOC – for example by UV light – triggers oxidizing radicals ($P680^+$ or $TyrZ^+$) stabilization, which destroy their protein environment. Some groups suggest that visible light absorption by Mn also triggers a dose-dependent degradation of the WOC, directly impairing PSII functioning (reviewed in: Tyystjärvi, 2008).

3.2. Photoprotective mechanisms in cyanobacteria: an overview

Reestablishing a functional photosynthetic apparatus in photoinhibited cyanobacterial cells requires degrading the damaged D1/D2 proteins then assembling new PSII reaction centers, which consumes a lot of ATP. Some cost-effective photoprotective strategies have been developed aimed at limiting ROS production under high light and at preventing their deleterious effects. First of all, cyanobacterial cells possess a ROS scavenging machinery that allows controlling $O_2^{-\cdot}$ and H_2O_2 concentrations in vivo (reviewed in: Latifi et al., 2009); they also synthesize non-enzymatic antioxidants, such as carotenoids or α-tocopherol, able to quench $^1O_2$ (and lipid peroxides for the second one). Secondly, some alternative transport routes exist that can remove electrons from PSII acceptor side when the PQ pool is totally reduced: Flv2/Flv4 at the Q_B site (Zhang et al., 2012), PTOX at the PQH_2 level in certain cyanobacterial strains (reviewed in McDonald et al., 2011). Similarly, Cyclic Electron Transfer around PSI passing by the NDH1 complex then PQ permits ATP production without any associated $NADP^+$ reduction (for a review: Battchikova et al., 2011). Finally, strong irradiances cause changes in the expression levels of many genes (Hihara et al., 2001): this includes an upregulation of the ones encoding for D1 protein paralogues with modified Q_A

redox potential and less prone to perform charge recombination (reviewed in Mulo et al., 2009) or a downregulation of the ones encoding for enzymes implied in photosynthetic pigments synthesis.

In response to high light intensities, cyanobacteria also accumulate High Light Inducible Polypeptides (HLIPs) that show similarities to the Chl*a*/*b*-binding Light Harvesting Complexes of plants; they attach Chl*a*, possibly carotenoids, and form a single transmembrane α-helix (Dolganov et al., 1995). *Synechocystis* mutant cells depleted in their HLIPs grow normally under weak illumination but clearly have modified pigment content under strong illumination, accumulating more myxoxantophyll but less Chl than WT *Synechocystis* cells (Havaux et al., 2003; Xu et al., 2004). HLIPs are thought to stabilize other Chl-containing proteins or to play a role in Chl mobilization under light stress. IsiA constitutes another example of Chl*a*-binding protein induced in response to iron starvation (Havaux et al., 2005) but also to various other abiotic stresses (high light, hyperosmotic medium). 18 IsiA proteins can associate intro a ring that surrounds PSI and acts as an accessory antenna (Melkozernov et al., 2003). Empty IsiA rings also exist, dissipating as heat the light energy they collect and playing a photoprotective role (Ihalainen et al., 2005).

3.3. Non-photochemical quenching of the excess light energy harvested.

An excited photosynthetic pigment can be deactivated by transmitting its exciton to another pigment (until photochemistry occurs, photochemical quenching noted qP), by emitting a photon of fluorescence or by producing heat. The light harvesting antennae associated to photosystems perform very efficient energy transfer to reaction centers, approximately 90% (quantum efficiency) of the collected energy reaching the special-pair chlorophylls under non-saturating illumination. In plants and algae, a photoprotective mechanism increases heat dissipation at the level of Light Harvesting Complexes (LHCs, chl*a*/*b*-binding antennae) and concomitantly decreases fluorescence emission plus energy transfer to reaction centers under high light conditions (energy-dependent non-photochemical quenching, noted qE. Reviewed in: Müller et al., 2001). qE is induced by the ΔpH formation across thylakoid membranes; it requires the protonation of PsbS (LHC-like protein) and the xantophyll cycle activation (zeaxanthin converted into violaxanthin). Besides that, the exact mechanism underlying heat dissipation remains unsolved. Cyanobacteria do not possess any LHC but harvest light mainly thanks to their PBs. The work presented in this

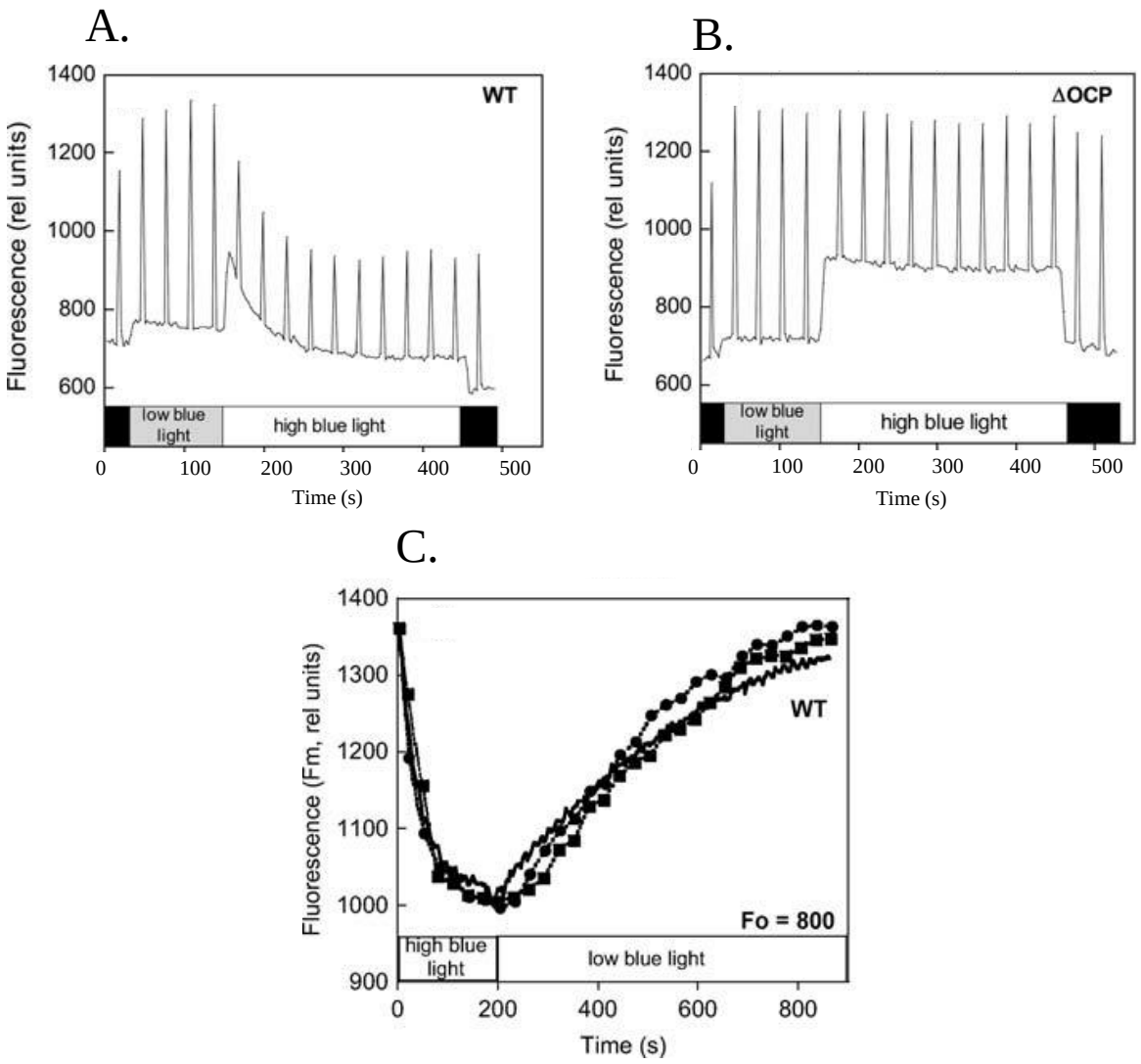

Figure 10. Blue-light induced OCP-related fluorescence quenching in *Synechocystis* cells. A. and B. Measurements of the fluorescence yield using a PAM fluorometer in dark-adapted wild-type (A) and ΔOCP (B) cells illuminated successively with low-intensity blue-green light (400 to 550 nm, 80 µmol.m^{-2}.s^{-1}) and high-intensity blue-green light (740 µmol.m^{-2}.s^{-1}). C. Similar experiments in WT cells showing the fluorescence recovery without any additions (circle) and in the presence of nigericin (squares) or DCMU (solid line), the F_m' level only being displayed. Adapted from Wilson et al., 2006.

manuscript focuses on a photoprotective mechanism enabling heat dissipation at the level of PBs under high irradiances.

4. The Orange Carotenoid Protein (OCP)-related non photochemical quenching of the energy harvested by PBs

4.1. Discovery

Illuminating *Synechocystis* cells with strong blue-green light was initially shown to trigger a 30% decrease in the maximal fluorescence level (Fm') on PAM traces (El Bissati et al., 2000). As soon as illumination stopped, fluorescence started recovering and finished by reaching its initial level (Fig. 10). Strikingly, this phenomenon kept occurring even below the thylakoid membrane phase transition point (25°C) in mutant cells lacking polyunsaturated fatty acids; thus, it was not related to state transitions that were completely blocked in these conditions (El Bissati et al., 2000). The addition of protein synthesis inhibitors had no impact on fluorescence quenching and recovery, which then could not originate from photoinhibition and subsequent photodamage repair (El Bissati et al., 2000). The addition of nigericin, a chemical decoupler, demonstrated there was no correlation between the transthylakoidal ΔpH formation and the fluorescence decrease induction (Wilson et al., 2006) (Fig.10). Taken together, these observations suggested the existence of an unknown cyanobacterial mechanism involving the antennae and diverting energy away from PSII under strong blue-green illumination.

The study of PSII-deficient *Synechocystis* mutant cells indicated that blue-green light is sensitized by a carotenoid-containing component and actually drives PBs fluorescence quenching (Rakhimberdieva et al., 2004). No fluorescence decrease was observed in PB deficient (PAL) or APC core deficient (ΔAB) *Synechocystis* mutant cells whereas it was retained in a strain lacking PC rods only (CK) (Wilson et al., 2006). Based on whole cells emission and decay associated spectra, Scott and coworkers arrived to the conclusion that blue-green light has an impact on APC (including red-shifted forms) but not on PC fluorescence emission and decay kinetics (Scott et al., 2006). Thus, the newly described mechanism is associated to APC cores fluorescence quenching.

It requires the presence of the soluble carotenoid-bearing Orange Carotenoid Protein (OCP) as blue-green light does not trigger any fluorescence quenching in OCP deficient *Synechocystis* mutant cells (Wilson et al., 2006) (see Fig. 10 and next sections for more details).

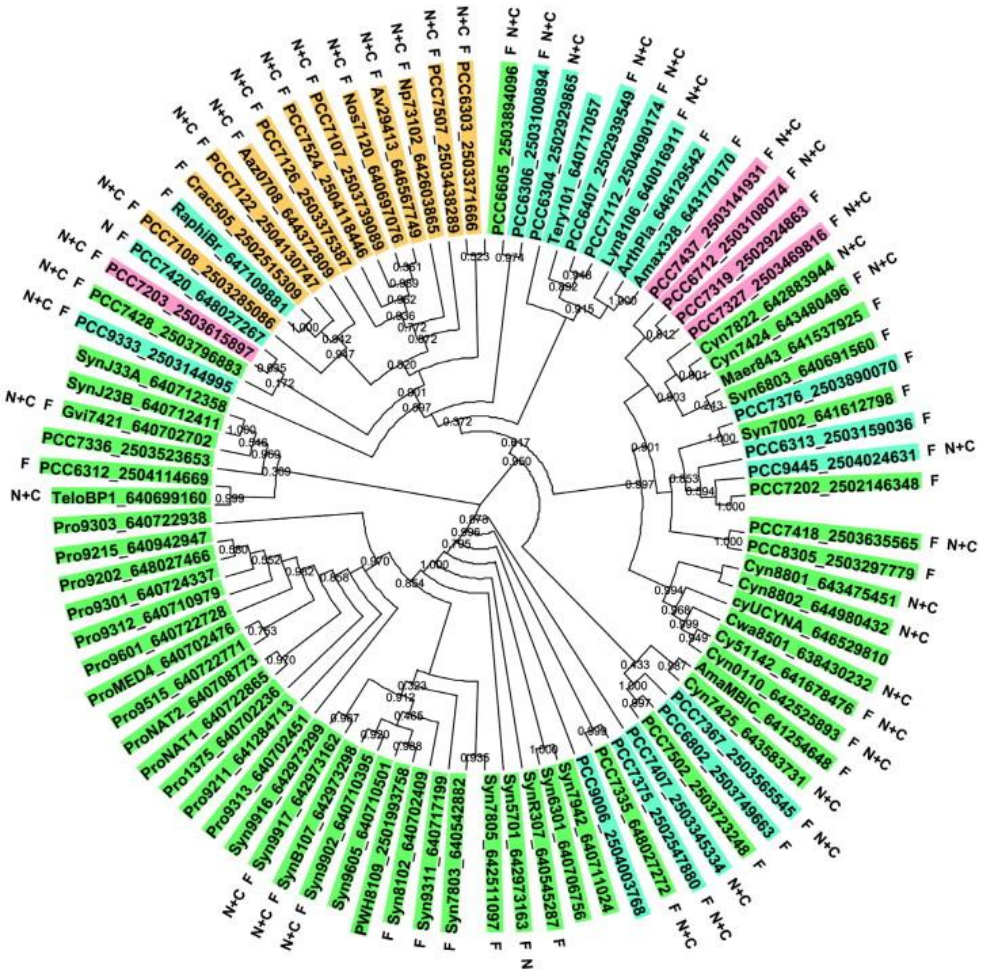

Gvi7421, Gloeobacter violaceus PCC 7421; Cwa8501, Crocosphaera watsonii WH 8501; PCC7202, Cyanobacterium stanieri PCC 7202; PCC7502, Synechococcus sp. PCC 7502; PCC7001, Cyanobium sp. PCC 7001; PCC6307, Cyanobium gracile PCC 6307; Cy51142, Cyanothece sp. ATCC 51142; Cyn0110, Cyanothece sp. CCY 0110; Cyn7424, Cyanothece sp. PCC 7424; Cyn7425, Cyanothece sp. PCC 7425; Cyn7822, Cyanothece sp. PCC 7822; Cyn8801, Cyanothece sp. PCC 8801; Cyn8802, Cyanothece sp. PCC 8802; PCC8305, Dactylococcopsis salina PCC 8305; PCC7418, Halothece sp. PCC 7418; Maer843, Microcystis aeruginosa NIES-843; Syn6301, Synechococcus elongatus PCC 6301; Syn7942, Synechococcus elongatus PCC 7942; SynB107, Synechococcus sp. BL107; Syn9311, Synechococcus sp. CC9311; Syn9605, Synechococcus sp. CC9605; Syn9902, Synechococcus sp. CC9902; SynJ23B, Synechococcus sp. JA-2-3Ba(2-13); SynJ33A, Synechococcus sp. JA-3-3Ab; Syn7002, Synechococcus sp. PCC 7002; PCC7335, Synechococcus sp. PCC 7335; SynR307, Synechococcus sp. RCC307; Syn9916, Synechococcus sp. RS9916; Syn9917, Synechococcus sp. RS9917; Syn5701, Synechococcus sp. WH 5701; Syn7803, Synechococcus sp. WH 7803; Syn7805, Synechococcus sp. WH 7805; Syn8102, Synechococcus sp. WH 8102; PWH8109, Synechococcus sp. WH 8109; PCC7336, Synechococcus sp. PCC 7336; Syn6803, Synechocystis sp. PCC 6803; TeloBP1, Thermosynechococcus elongatus BP-1; cyUCYNA, cyanobacterium UCYN-A; PC10605, Cyanobacterium sp. PCC 10605; PCC7428, Gloeocapsa sp. PCC 7428; PCC7126, Microchaete sp. PCC 7126; Aaz0708, Anabaena azollae 0708; Av29413, Anabaena variabilis ATCC 29413; PCC7122, Anabaena cylindrica PCC 7122; PCC7108, Anabaena sp. PCC 7108; Crac505, Cylindrospermopsis raciborskii CS-505; Nsp9414, Nodularia spumigena CCY9414; Np73102, Nostoc punctiforme PCC 73102; Nos7120, Nostoc sp. PCC 7120; PCC7107, Nostoc sp. PCC 7107; RaphiBr, Raphidiopsis brookii D9; PCC6303, Calothrix sp. PCC 6303; PCC7507, Calothrix sp. PCC 7507; Amax328, Arthrospira maxima CS-328; ArthPla, Arthrospira platensis str. Paraca; PCC9333, Crinalium epipsammum PCC 9333; PCC7407, Geitlerinema sp. PCC 7407; PCC6306, Leptolyngbya sp. PCC 6306; PCC7375, Leptolyngbya sp. PCC 7375; PCC7376, Leptolyngbya sp. PCC 7376; Lyn8106, Lyngbya sp. PCC 8106; PCC7420, Microcoleus chthonoplastes PCC 7420; PCC6304, Oscillatoria acuminata PCC 6304; PCC6407, Oscillatoria sp. PCC 6407; PCC7112, Oscillatoria sp. PCC 7112; PCC6802, Pseudanabaena sp. PCC 6802; PCC7367, Pseudanabaena sp. PCC 7367; PCC6313, Spirulina major PCC 6313; Tery101, Trichodesmium erythraeum IMS101; PCC6712, Chroococcidiopsis sp. PCC 6712; PCC7203, Chroococcidiopsis thermalis PCC 7203; PCC7319, Pleurocapsa sp. PCC 7319; PCC7327, Pleurocapsa sp. PCC 7327; PCC7437, Stanieria cyanosphaera PCC 7437; Pro9601, Prochlorococcus marinus AS9601; Pro9202, Prochlorococcus marinus str. MIT 9202; Pro9211, Prochlorococcus marinus MIT 9211; Pro9215, Prochlorococcus marinus MIT 9215; Pro9301, Prochlorococcus marinus MIT 9301; Pro9303, Prochlorococcus marinus MIT 9303; Pro9312, Prochlorococcus marinus MIT 9312; Pro9313, Prochlorococcus marinus MIT 9313; Pro9515, Prochlorococcus marinus MIT 9515; ProNAT1, Prochlorococcus marinus NATL1A; ProNAT2, Prochlorococcus marinus NATL2A; Pro1375, Prochlorococcus marinus marinus CCMP1375; ProMED4, Prochlorococcus marinus pastoris CCMP1986; AmaMBIC, Acaryochloris marina MBIC11017; uncyPop, uncultivated cyanobacterium (Poplar biomass community MLE1-like); PCC6605, Chamaesiphon sp. PCC 6605; PCC9006, Prochlorothrix hollandica PCC 9006; PCC9445, Spirulina sp. PCC 9445; PCC6312, Synechococcus sp. PCC 6312; PCC7524, Nostoc sp. PCC 7524

Figure 11. Distribution of the OCP among cyanobacteria. A 16S species tree of cyanobacteria with sequenced genomes (including the ones published in Shih et al., 2013). Organism IDs are colored by section (green, Section I; red, Section II; blue, Section III; yellow, Section IV). F = full-length *ocp* gene, N, C correspond to genes encoding the N- and C-terminal domain, respectively. Adapted from Kirilovsky and Kerfeld, 2012.

Importantly, oxygen evolution dropped faster and to a more important extent under saturating white light illumination (3000µmol.m^{-2}.s^{-1}) in ΔOCP cells than in WT *Synechocystis* cells (Wilson et al., 2006). This is due to a decrease of the effective antenna size induced by the OCP related mechanism (Wilson et al., 2006). When this photoprotective mechanism is absent, under high irradiance, more light energy arrives to PSII, which leads to reactive oxygen species formation and to photoinhibition. It was envisioned that OCP sensitizes strong blue-green illuminations then inducing, directly or not, a non-photochemical quenching of the excess light energy harvested by PBs. As a result, energy flow to PSII and fluorescence yield both decrease (Wilson et al., 2006). Measuring P700 oxidation kinetics in PSII deficient cells and fluorescence induction kinetics in PSI deficient cells, Rakhimberdieva and coworkers (Rakhimberdieva et al., 2010) estimated that a 60% decrease in PB fluorescence correlates to a 30-40% drop in quantum efficiency of one or the other photoreaction. Even if the heat dissipation process takes place in APC cores, Chl*a* fluorescence can partly be quenched as uphill energy transfer sometimes occurs (Rakhimberdieva et al., 2007b).

The OCP-related quenching is reversible, fluorescence starting to recover as soon as light source gets turned off (El Bissati et al., 2000). This owes to another actor called the Fluorescence Recovery Protein (Boulay et al., 2010; see also section 4.6.). A better understanding of the OCP related photoprotective mechanism required isolation of the different proteins implied and their subsequent characterization in vitro.

4.2. Distribution and regulation of the OCP

OCP had been detected in *Arthrospira maxima*, *Microcystis aeruginosa* and *Anabaena flos-aquae* long before the discovery of its actual photoprotective role (Holt and Krogmann, 1981). It is encoded by a single gene in *Synechocystis* (*slr1963*: Wilson et al., 2006) that has orthologues in most of the PBs-containing cyanobacterial strains sequenced so far (for review: Kirilovsky and Kerfeld, 2012) (Fig.11). The predicted primary structures for OCP homologues show between 62% and 82% identity to that of *Synechocystis* OCP, certain absolutely conserved aminoacids probably playing key functional roles. Sometimes, short *slr1963*-like genes also appear, putatively encoding for truncated OCP with a yet to determine function (Fig.11). Cyanobacteria naturally lacking an *ocp* encoding gene - for example *Thermosynechococcus elongatus* and *Synechococcus elongatus* PCC 7942) - are more susceptible to PSII photodamage under high irradiance (Boulay et al., 2008); illumination

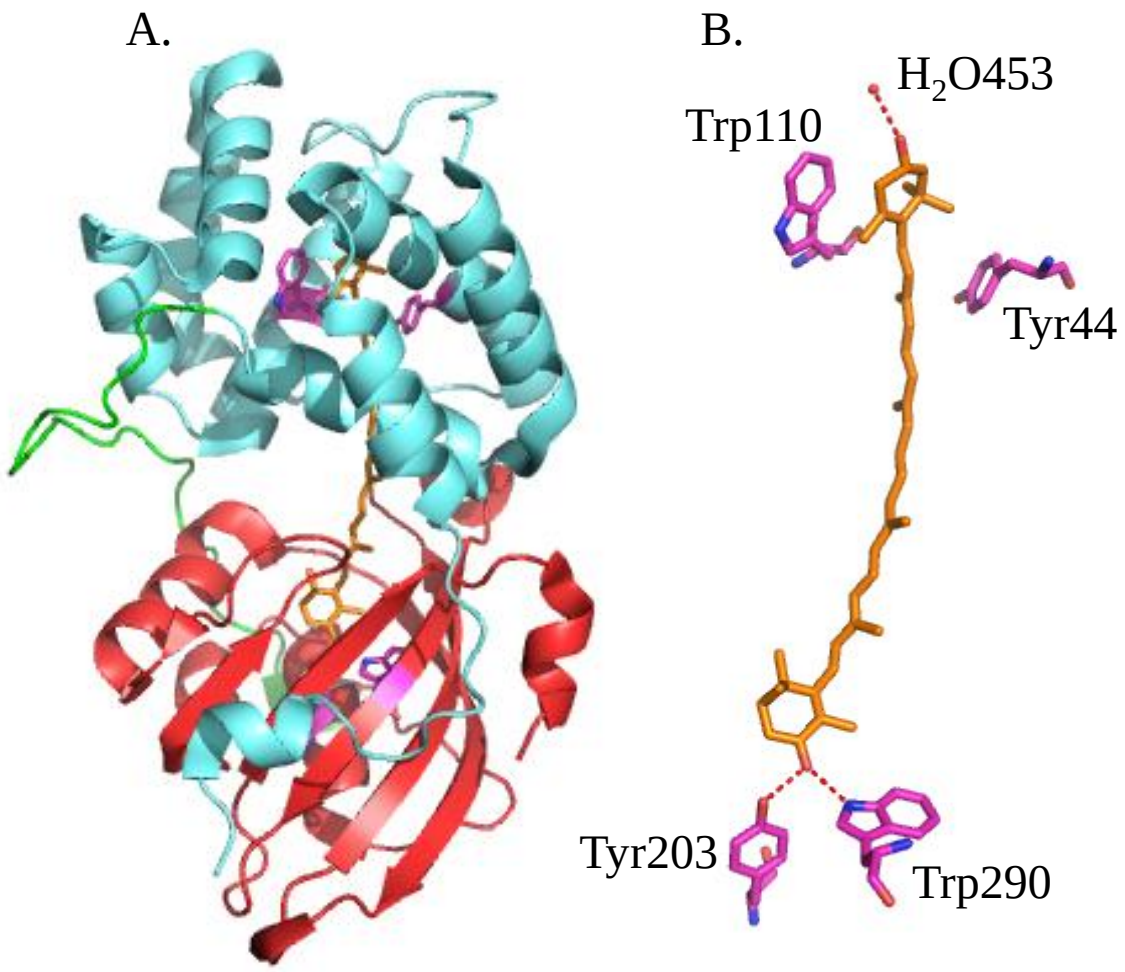

Figure 12. Structure of the OCP isolated from *Arthrospira maxima*. A. View of an OCP monomer showing the N-terminal domain (residues 1-165) in cyan, the C-terminal domain (residues 186-317) in red and the flexible linker in green. hECN appears as orange sticks, its hydroxyl ring lying in the N-terminal domain and its carbonyl ring in the C-terminal domain. B.Close up showing some conserved OCP aminoacids interacting with hECN and presented with purple sticks. Potential hydrogen bonds are indicated using dashed red lines. PDB file 1M98 modified with PyMol.

with saturating white light (2500 µmolphotons.m^{-2}.s^{-1}) for 3 min triggered a non-reversible fluorescence decrease (15-20%) associated to photoinhibition in both strains, less visible when considering *Arthrospira* or *Synechocystis* cells producing OCP. Transcriptomic data indicates that *slr1963* expression, which is constitutive, gets upregulated upon high light treatment (Hihara et al., 2001). Iron depletion also leads to OCP over-accumulation in various cyanobacterial strains (Wilson et al., 2007; Boulay et al., 2008). This over-accumulation correlates with an increased amount of blue-green light triggered PB fluorescence quenching; the F_m' drops by 60% instead of only 30% when considering iron starved *Synechocystis* cells (Wilson et al., 2007). OCP acts well as a switch for the non-photochemical fluorescence quenching, in a dose dependent manner.

Non-stressful growth conditions (90µmol.m^{-2}.s^{-1} white light plus CO_2 enriched atmosphere) lead to the production of 1 OCP for 2-3 PBs in *Synechocystis*, as revealed by Western Blot analysis (Wilson et al., 2006). OCP is situated on the stromal side of thylakoid membranes as demonstrated by cell fractionation experiments and immunogold labeling (Wilson et al., 2006), thus lying in close vicinity to PBs.

4.3. Crystal structure of the OCP isolated from *Arthrospira*

The structure of OCP was resolved before the understanding of its function. Following isolation from *Arthrospira maxima* cells, OCP appeared as a soluble orange protein with 35 kDa molecular mass (Wu and Krogmann, 1997). Its absorption spectrum exhibited a shoulder at 440 nm plus peaks at 467 nm and 496 nm indicating the presence of a bound carotenoid, identified as 3'-hydroxyechinenone (hECN) (Wu and Krogmann, 1997). The protein environment modifies hECN spectral properties, which normally has a yellowish color when solubilized with organic solvents (Polívka et al., 2005). A 2.1 Å crystal structure was released in 2003 (PDB file: 1M98. Kerfeld et al., 2003) revealing that OCP consists of 2 domains separated by a flexible linker region (Fig.12). The N-terminal domain (residues 1 – 165), made of 2 α-helices bundles (4 helices each, PFAM 09150), is unique to OCP and exists only in cyanobacteria. The C-terminal domain (residues 190 - 317) displays 2 α-helices and a 5 fold β-sheet, reminiscent of the Nuclear Transport Factor 2 family (PFAM 02136). hECN (1 per OCP) spans these domains, its hydroxyl ring getting inserted between the N-terminal α-helices bundles and its keto ring lying in a hydrophobic cleft formed on the C-terminal β-

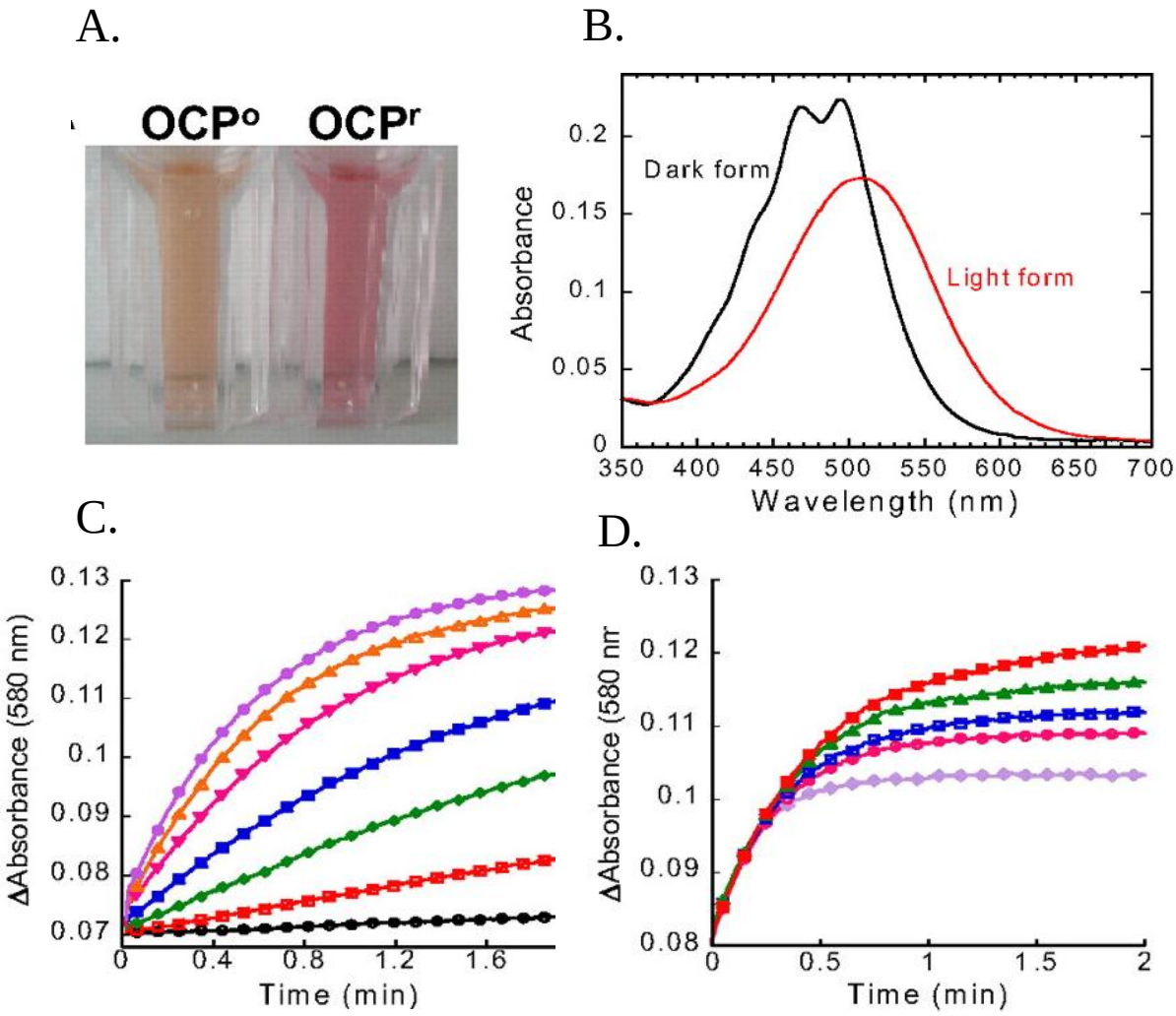

Figure 13. Isolated *Synechocystis* OCP responsivity to light. A. Photograph of isolated OCP^o and OCP^r. To obtain OCP^r the protein was illuminated with blue-green light at 740 µmol photons.m^{-2}.s^{-1} at 12°C for 2 min. B. Absorbance spectra of the dark orange form (OCP^o; black) and the light red form (OCP^r; red). C. OCP^r accumulation at 11°C and different light intensities: 20 (black), 50 (red), 120 (green),210 (blue), 350 (rose), 740 (orange), and 1,200 (violet) µmolphotons.m^{-2}.s^{-1} of blue-green light. D. photoconversion from the OCP^o to the OCP^r form using a 350 µmol photons.m^{-2}.s^{-1} blue-green light intensity at different temperatures: 32°C (violet), 28°C (rose), 24°C (blue), 19°C (green), 15°C (red). The protein concentration was OD 0.2 at 495 nm. Adapted from Wilson et al., 2008.

sheet. It was found that several absolutely conserved aminoacids among OCP orthologues are situated in close vicinity to hECN and potentially interact with it (Kerfeld et al., 2003) (Fig.12). In the N-terminal domain, Tyr44 and Trp110 possibly establish hydrophobic contacts with the hydroxyl ring. In the C-terminal domain, Tyr203 and Trp290 form hydrogen bonds with the keto-group through their side chains. Also, conserved water molecules can connect hECN hydroxyl-group to the protein backbone through hydrogen bonds. All these interactions are potentially responsible for the fine tuned hECN spectral properties or allow for carotenoid selectivity (Kerfeld et al., 2003).

4.4. Photoactivity of the OCP and *Synechocystis* mutant studies

Arthrospira maxima cannot be genetically manipulated. Thus, it is impossible to modify *Arthrospira* OCP to facilitate its isolation via affinity chromatography or to investigate the role of specific aminoacids through targeted mutagenesis. Thus, *Synechocystis* mutants producing OCP with a C-terminal His-tag for facilitated purification were constructed. Isolated *Synechocystis* OCP appears orange under dark conditions (OCP^o), has a very similar absorption spectrum to that of *Arthrospira maxima* OCP and binds hECN mainly (Wilson et al., 2008).

Strong blue-green illumination induces OCP^o photoconversion to a red from (OCP^r) with maximum absorbance at 500 nm (Wilson et al., 2008) (Fig.13A, B). The OCP^r accumulation gets fastened and its final amount increases when actinic light intensity rises (Fig.13C). Lowering temperature (16°C to 32°C frame) does not much affect the rate of photoconversion but leads to higher OCP^r concentrations at equilibrium. This comes from the fact that OCP^r spontaneously reconverts to OCP^o, and that low temperatures largely hinder such a recovery (Wilson et al., 2008). The quantum yield of OCP photoactivation was evaluated to approximately 0.03 based on transient absorption spectroscopy, which is quite low and explains why only high intensity blue-green light triggers significant OCP^r formation. The metastable OCP^r was then proposed to act as a molecular switch turning on the mechanism that leads to PB fluorescence quenching.

Resonance Raman spectroscopy revealed that hECN, which is slightly twisted in OCP^o, gets unbent in OCP^r resulting in an increased apparent conjugation length (Wilson et al., 2008). The secondary structure of OCP also gets modified upon photoactivation as

revealed by Fourier Transform Infrared spectroscopy, showing less rigid α-helices and a more compact β-sheet in OCP^r than OCP^o (Wilson et al., 2008). Calculations of the OCP-related photoprotective mechanism activation energies at different temperatures suggested that soluble protein folding/unfolding occurs following blue-green illumination (Rakhimberdieva et al., 2007a). Gorbunov and coworkers, based on similar calculations, proposed that proline isomerisations may also be involved (Pro224, Pro225) (Gorbunov et al., 2011).
So far, nobody was able to crystallize OCP^r and to obtain direct structural data about it.

However, during the period of my thesis, 2 studies realized in our laboratory in collaboration with the group of Cheryl Kerfeld indicated that OCP^r has an opened structure while OCP^o has a closed structure. I am involved in one of these studies (see results chapter 3).

For further studies on *Synechocystis* OCP, a plasmid was constructed containing the *slr1963* open reading frame surrounded by the *psbA2* flanking regions (Wilson et al., 2010). After transfection of WT *Synechocystis* cells using this plasmid, double homologous recombination allowed placing *slr1963* under control of the strong *psbA2* promoter. The resulting mutant overaccumulated OCP as shown by Western Blots analysis on whole cells extracts (Wilson et al., 2010). A 60% decrease in the F_m' level could be observed upon strong blue-green illumination, phenotype reminding that of iron depleted cells and indicating important quantities of active OCP. His-tagged OCP purified from this mutant at repeated occasions had a very changing carotenoid content, echinenone (ECN) being mainly attached with various amounts of hECN and zeaxanthin. Nevertheless, it formed crystals that allowed determining *Synechocystis* OCP^o structure with a resolution of 1.65 Å (PDB file 3MG1: Wilson et al., 2010). This structure superimposes well with that of *Arthrospira maxima* OCP^o, even though differences exist that have functional impacts and are discussed in chapter 2 of the present manuscript. Both OCPs appeared as dimers in the crystal lattices, with an important area (>1000 $Å^2$) buried at the monomer-monomer interface. The dimerization process could then be physiologically relevant, even if gel filtration did not help concluding because giving opposite results when considering solutions of isolated *Arthrospira* OCP (dimers mainly: (Kerfeld et al., 2003) or *Synechocystis* OCP (monomers mainly: Wilson et al., 2010). Whether OCP exists in cells as monomers, or dimers, or both still remains to be determined. OCP^o and OCP^r could have different oligomerization behaviors.

Synechocystis OCP was also placed under control of the strong *psba2* promoter in *Synechocystis* mutant strains with modified carotenoid biosynthesis pathways (Punginelli et

al., 2009; Wilson et al., 2011). When a strain lacking the β-carotene ketolase (CrtO) was used, which is unable to produce ECN or hECN, OCP mainly attached zeaxanthin (Punginelli et al., 2009). The isolated OCP, which appeared yellowish, completely lost its photoactivity. In addition, no blue-light induced PB fluorescence quenching could be recorded in vivo. Zeaxanthin lacks the keto group then it cannot establish hydrogen bonds with Tyr201/Trp288 (*Synechocystis* numbering), pointing out that these bonds are essential for photoactivity. When a strain lacking the β-carotene hydroxylase (CrtR) and unable to produce hECN or zeaxanthin was used instead, OCP homogeneously attached ECN (Wilson et al., 2011). This neither modified its photoactivity nor its ability to induce PBs fluorescence quenching in vivo. The hydrogen bonds that the hydroxyl ring of hECN can establish with water molecules lack in ECN-binding OCP but this does not have any functional impact in *Synechocystis* OCP.

Work on *Synechocystis* permitted to elucidate the role of specific aminoacids through targeted mutagenesis. After replacing Tyr44 by a serine in an over-accumulating strain, OCP kept binding ECN preferentially and no noticeable changes were observed looking at its dark absorption spectrum or crystal structure (PDB file 3MG2: Wilson et al., 2010). Strikingly though, no conversion to the red form was noticed upon illumination revealing Tyr44's importance in the photoactivation process. Similar approaches allowed confirming that Trp110, Tyr201 and Trp288 are also required for photoactivation (Wilson et al., 2010; (Wilson et al., 2011). Moreover, their substitution can lead to very changed carotenoid contents that suggest these residues' implication in carotenoid selectivity. The non-photoactive OCPs were all unable to induce PB fluorescence quenching upon strong blue-green illumination in vivo.

A different phenotype was observed after replacing Arg155, situated at the N-to-C terminal domains interface, by a lysine (Wilson et al., 2010). The isolated OCP had normal carotenoid content and photoactivity but no fluorescence quenching could be monitored in vivo. Photoactivation is then required but not sufficient for the OCP-related photoprotective mechanism induction.

Study of isolated OCP gave insights into the biochemical mechanism allowing photoactivation upon blue-green light illumination. The next important point was to understand which steps follow OCP^r formation, finally driving the effective photoprotective mechanism.

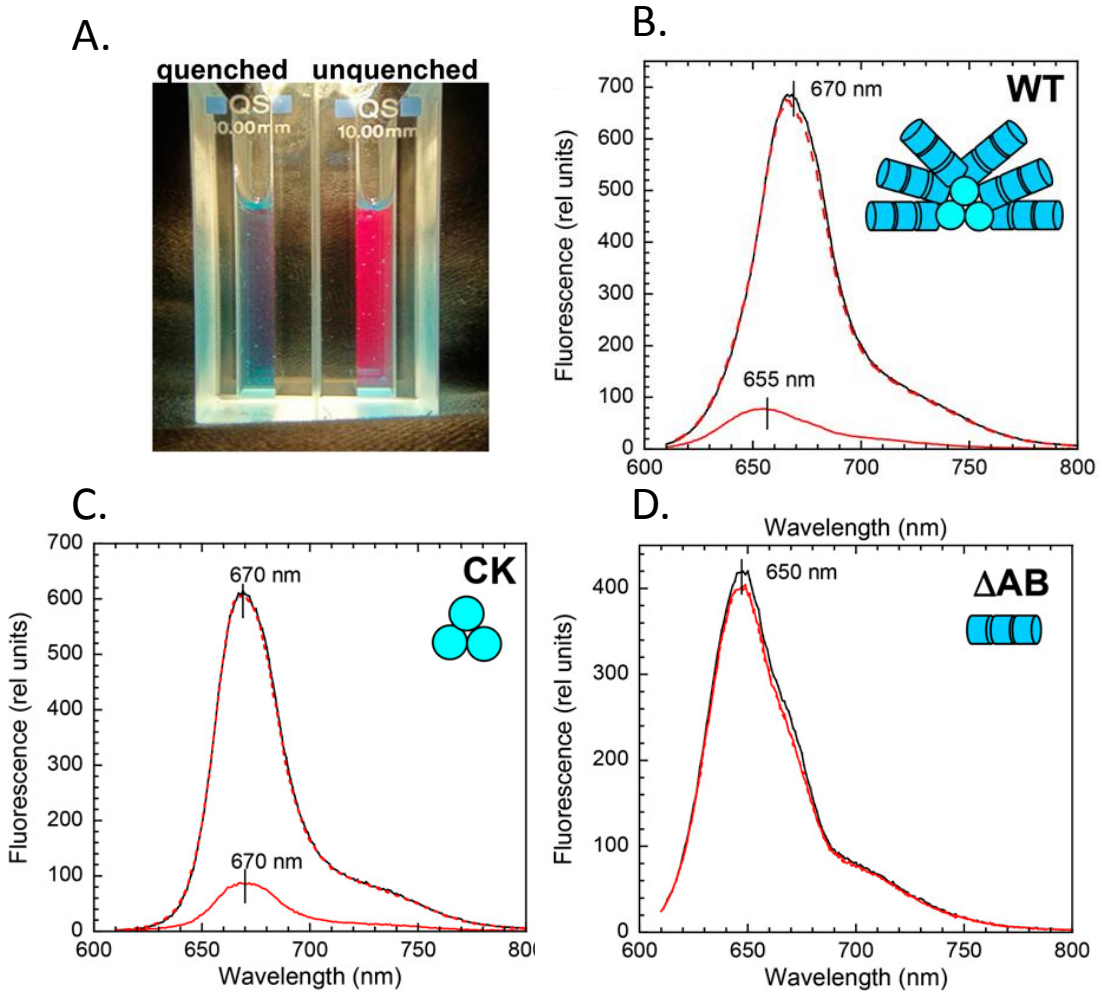

Figure 14. Fluorescence quenching induced by illumination of phycobilisomes in the presence of OCP in vitro. A. Photograph of the quenched (left) and unquenched (right) phycobilisomes illuminated by white light showing the fluorescence emitted by the samples. The color of the unquenched phycobilisomes is a result of the red fluorescence of PC and APC. B. to D. The room temperature fluorescence spectra of dark unquenched (solid black line), light unquenched (dashed red line), and light quenched PBs (solid red line) isolated from B. wild-type, C. PC deficient (CK) and D. APC deficient (ΔAB) Synechocystis strains. The PBs (0.013 mM) were illuminated 5 min with white light (5000 µmol photons.m^{-2}.s^{-1}) in the absence (light unquenched) or in the presence of OCP (0.53 mM) (light quenched). Adapted from Gwizdala et al., 2011.

4.5. In vitro reconstitution of the OCP-related photoprotective mechanism

Just before I arrived in our laboratory, Michal Gwizdala developed an in vitro system that allows reconstituting PB fluorescence quenching (Gwizdala et al., 2011). Details can be found about it looking at chapters 1 and 2 of the present manuscript. Briefly, PBs were retrieved from *Synechocystis* cells in solution containing high phosphate concentration (0.5M or more) to maintain their integrity. A large excess of OCP^o (at least 4
OCP per PB) was then added under dark conditions without any impact on PB fluorescence emission. When illumination with blue-green light started, partial photoconversion of OCP^o to OCP^r occurred that correlated with a progressive PB fluorescence quenching (Gwizdala et al., 2011) (Fig.14A,B). For the first time, it was demonstrated that OCP not only senses strong blue-green illuminations but that its interaction with PBs directly triggers the photoprotective mechanism. At 0.8M phosphate the fluorescence decrease upon blue-green illumination was very important (90%) and appeared completely irreversible; re-isolation of quenched PBs became possible through sucrose gradients ultracentrifugation (Gwizdala et al., 2011). Subsequent SDS-PAGE electrophoresis combined to Western Blot analysis revealed the attachment of 1 or 2 OCP per quenched PB. No such attachment could be detected after carrying out similar experiments under complete dark conditions. This proved that OCP^o needs to be photoconverted before being able to bind PBs. OCP^r could attach to PBs isolated from PC deficient mutant (CK) and WT *Synechocystis* cells but not to the ones coming from APC deficient (ΔAB) mutant cells (Fig14C,D); OCP, once photoactivated, interacts with the APC core of PBs.

A completed model was then emitted, where OCP^r attachment to the core of the PB triggers heat dissipation of the light energy harvested by PBs. Whether OCP acts directly as a quencher, through its bound carotenoid, or whether it turns one of the APC bilins into an energy quencher through local changes in the environment remained to be determined at the beginning of my thesis. Also, it was not known the role of the different components of the core and the site of quenching. During my thesis, I participated in the elucidation of these important points (see chapter 1).

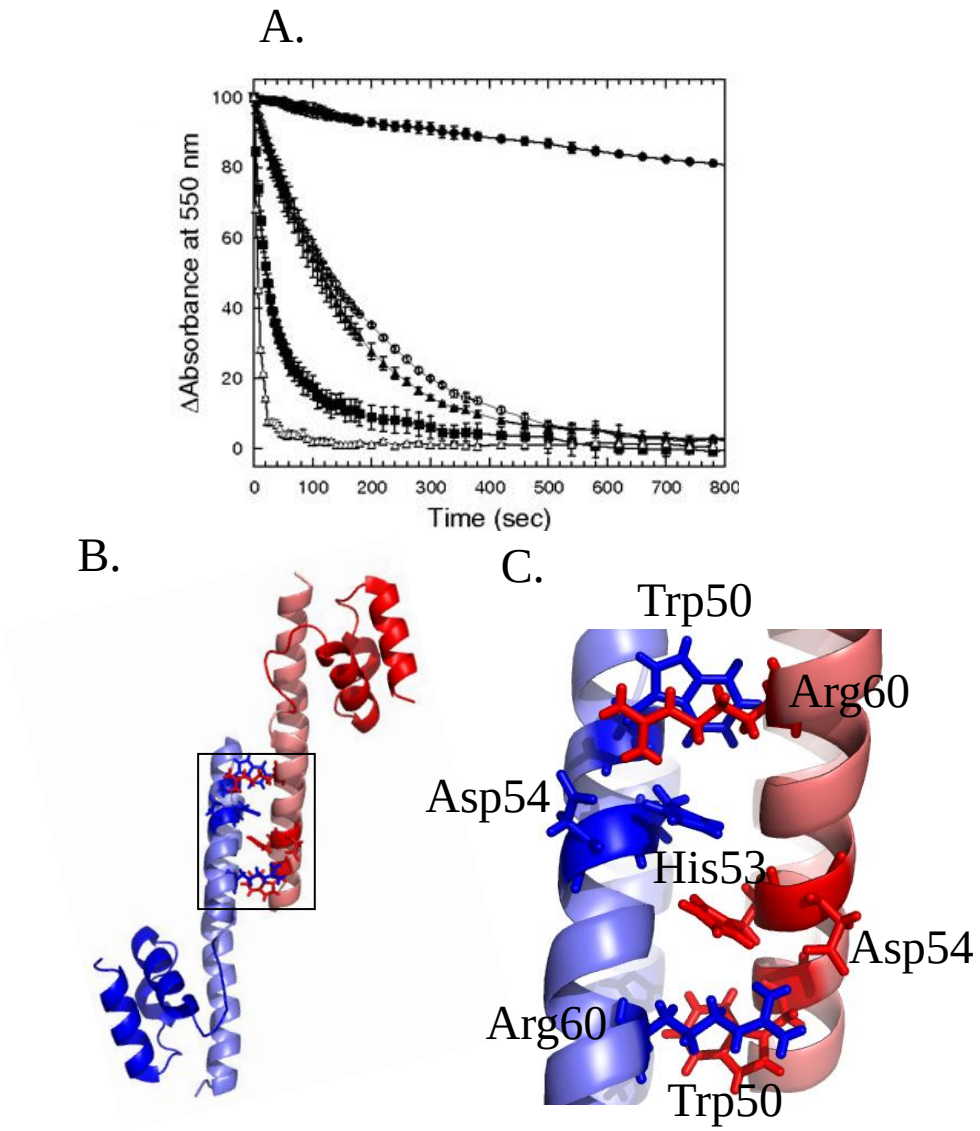

Figure 15. **FRP interacts with OCP^r and reconverts it to OCP^o.** A. Darkness OCP^r to OCP^o (isolated protein, 2.3 μM) conversion in the absence (circle) or in the presence of 2.3 μM FRP (square) or 1.15 μM FRP (triangle) at 8 °C (closed symbols) or at 18 °C (open symbols). Average of three independent experiments is shown. Taken from Boulay et al., 2010. B. Crystal structure of the FRP dimer, showing one monomer in blue and the other in red (light colors for N-terminal part, dark colors for C-terminal part). Some of the absolutely conserved aminoacids among FRP orthologues, thought to form a part of the active site, are presented as sticks. C. Close up of the black frame in B. PyMol file 4JDX (from Sutter et al., 2013) modified with PyMol.

4.6. FRP allows rebooting the system.

In *Synechocystis* and most OCP-containing cyanobacterial strains, a second gene is found downstream of the *ocp* one that encodes for a protein with putative function named Fluorescence Recovery Protein (FRP) (*slr1964*: Boulay et al., 2010). *Synechocystis* mutant cells in which *slr1964* was interrupted by an antibiotic resistance cassette displayed normal or even slightly increased PB fluorescence quenching upon strong blue-green illumination (Boulay et al., 2010). However, almost no subsequent low light/dark recovery could be observed and much time was required for fluorescence to reach its initial level. The whole *slr1964* ORF (according to Cyanobase annotations) was overexpressed in *Synechocystis* cells for N-terminal His-tagged FRP purification. The protein had a 14kDa molecular mass and appeared colorless strongly suggesting the absence of any bound chromophore (Boulay et al., 2010). Surprisingly, FRP interacted strongly with membranes whereas no trans-membrane α-helix could be predicted looking at its primary structure. Comparing *slr1964* nucleotide sequence to that of its orthologues from other cyanobacterial strains, it was noticed that most *frp* genes start at the codon encoding for Met26 in *slr1964*. When a corresponding shorter version of the *slr1964* ORF was overexpressed in *Escherichia coli* cells, important amounts of FRP could be obtained from the soluble fraction. This FRP was shown to interact with isolated *Synechocystis* OCP^r but not with OCP^o based on co-immunoprecipitation experiments (Boulay et al., 2010). It was strikingly able to trigger a very fast reconversion of OCP^r to OCP^o, even at temperatures normally blocking this phenomenon (Fig.15A). Added to the in vitro reconstitution system after quenching induction, it was associated to a strong increase in fluorescence recovery rate (Gwizdala et al., 2011). Altogether, this data indicated that FRP is responsible for the reversibility of the OCP-related photoprotective mechanism. FRP acts on isolated OCP^r by reconverting it to OCP^o and probably does the same on PB-bound OCP, causing its detachment. During the years of my thesis it was confirmed that only "short" FRP (starting Met26, hereafter simply designed as FRP) accumulates in WT *Synechocystis* cells under our growth conditions; N-terminal his-tagged FRP was then isolated from an overaccumulating *Synechocystis* mutant strain and shown to behave similarly to FRP retrieved from *E.coli* (Gwizdala et al., 2013).

Synechocystis FRP structure was determined in Cheryl Kerfeld's laboratory in collaboration with our group, giving many insights into the protein's mechanism of action (2.5Å resolution,

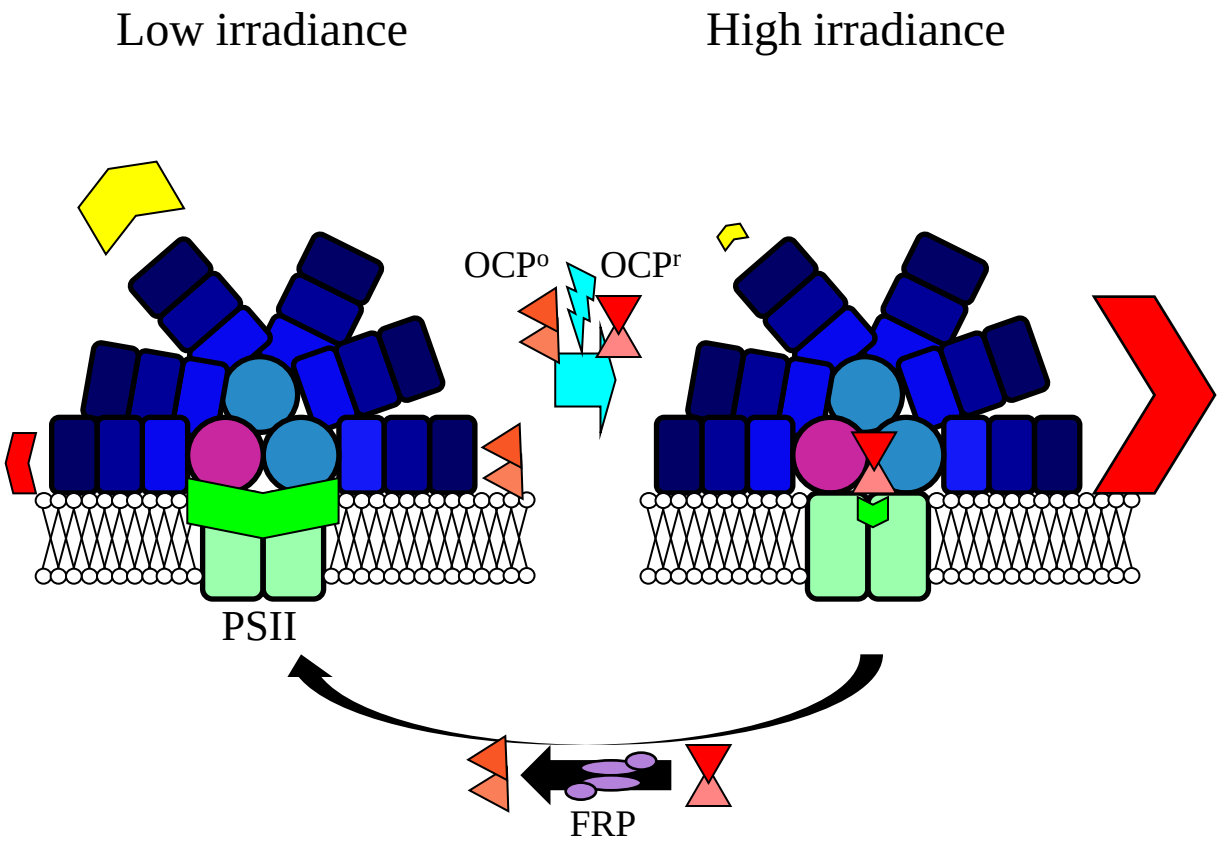

Figure 16. Schematic model of the OCP-related photoprotective mechanism in cyanobacteria. Under low light conditions (left), most of the light energy absorbed by phycobilisomes is transferred to reaction centers where photochemistry takes place (green arrow); few losses occur as heat dissipation (red arrow) or fluorescence emission (yellow arrow). Under strong white or blue-green illumination (right), OCP^o is photoconverted to OCP^r that interacts with phycobilisome cores and increases heat dissipation, triggering a decrease in both fluorescence emission and energy transfer to reaction centers. Finally, FRP induces OCP^r reconversion to OCP^o and allows resetting the system (bottom).

PDB file 4JDX: Sutter et al., 2013). FRP is made up with an elongated α-helical N-terminal domain (residues 1-65) followed by a more globular C-terminal part (residues 66-109) (Fig.15B). It formed both dimers and tetramers in the crystal lattice, displaying very different chain conformations; estimation of the buried area at monomers interface plus the associated free enthalpies designated dimers as the most stable aggregation state. Tetramers could barely be observed in solution after FRP isolation as revealed by gel filtration assays, which does not completely rule out their possible existence in vivo under certain conditions (Sutter et al., 2013). A huge patch of very well conserved aminoacids (containing particularly Trp50, His53, Asp54 and Arg60), exposed on one side of FRP dimers, gets completely buried in tetramers with possible functional consequences (Fig.15C). Targeted mutagenesis of Asp54, Trp50 and His53 partially impaired FRP's ability to trigger OCP^r reconversion to OCP^o (Sutter et al., 2013). Even more drastic effects were observed after Arg60 replacement, which led to a complete loss of FRP function even when lysine (positively charged) was employed for substitution. It was then proposed that Arg60 plays a central role in OCP^r attachment. Cation-π interactions between the Arg60 and Trp50 and subsequent salt-bridging with Asp54 permit its correct orientation towards OCP. The conserved patch is thought to be FRP's active site.

Based on co-immuno precipitation experiments, it was proved that FRP interacts specifically with the C-terminal (but not with the N-terminal) domain of OCP and a docking model was built in silico (Sutter et al., 2013). Beyond giving a hint of the contacts underlying FRP-OCP interactions, this data also points out that both OCP domains may have different roles related to the photoprotective mechanism.

5. Aims of the thesis

The model presented in Fig.16 summarizes what was known about OCP's photoprotective role when this project started. Thanks to its attached carotenoid, OCP^o absorbs blue-green light then getting converted to OCP^r. OCP^r binds PB cores, where it induces an increase in heat dissipation associated with a drop in fluorescence emission and energy transfer to both photosystems. Under dark conditions, FRP triggers OCP^r detachment from PBs plus its concomitant reconversion to OCP^o. The whole process allows for very dynamic responses to changing light regimes (Fig.16). Thus, we already had a good overview of OCP's function at that time even if several molecular aspects remained unclear.

Particularly, we had no clue about how OCP^r interacts with PB cores. For a better characterization of the OCP-PB complex, my work focused on 3 main questions.

What is the binding site for OCP in PB cores? It was found that only 1 or 2 OCP^r bind(s) per quenched PB (Gwizdala et al., 2011). The core includes major APC subunits (α^{APC}, β^{APC}) and minor ones, called terminal emitters (ApcD, ApcF, ApcE). I employed a mutant approach in *Synechocystis* to check whether these terminal emitters are required for the OCP-related photoprotection onset (see chapter 1; from Jallet et al., 2012).

How does the PB core architecture influence OCP binding? The PB core in *Synechocystis* contains 3 APC cylinders. I isolated PBs from other cyanobacterial strains containing either 2, 3 or 5 APC cylinders and tested their interaction with *Synechocystis* OCP in vitro (see chapter 2; from Jallet et al., 2013). My aim was to check whether a smaller (respectively bigger) number of APC cylinders would lead to a diminished (respectively increased) affinity for OCP.

Which kind(s) of interactions underlie the OCP-PB complex formation? I compared the ability of OCPs coming from 2 different cyanobacterial strains to induce fluorescence quenching in vitro (see chapter 2; from Jallet et al., 2013). This allowed identifying charged aminoacids potentially important for PBs binding. Moreover, I worked in collaboration with Pr. C.Kerfeld's group (Michigan State University) to study the respective roles of OCP N-terminal and C-terminal domains (see chapter 3; from Leverenz et al., in press).

Adir N (2005) Elucidation of the molecular structures of components of the phycobilisome: reconstructing a giant. Photosynth Res **85**: 15–32

Ajlani G, Vernotte C (1998) Deletion of the PB-loop in the L(CM) subunit does not affect phycobilisome assembly or energy transfer functions in the cyanobacterium Synechocystis sp. PCC6714. Eur J Biochem FEBS **257**: 154–159

Allen JF, Mullineaux CW (2004) Probing the Mechanism of State Transitions in Oxygenic Photosynthesis by Chlorophyll Fluorescence Spectroscopy, Kinetics and Imaging. *In* GC Papageorgiou, Govindjee, eds, Chlorophyll Fluoresc. Springer Netherlands, pp 447–461

Allen JF, Sanders CE, Holmes NG (1985) Correlation of membrane protein phosphorylation with excitation energy distribution in the cyanobacterium Synechococcus 6301. FEBS Lett **193**: 271–275

Arteni AA, Ajlani G, Boekema EJ (2009) Structural organisation of phycobilisomes from Synechocystis sp. strain PCC6803 and their interaction with the membrane. Biochim Biophys Acta BBA - Bioenerg **1787**: 272–279

Ashby MK, Mullineaux CW (1999) The role of ApcD and ApcF in energy transfer from phycobilisomes to PS I and PS II in a cyanobacterium. Photosynth Res **61**: 169–179

Aspinwall CL, Sarcina M, Mullineaux CW (2004) Phycobilisome Mobility in the Cyanobacterium Synechococcus sp. PCC7942 is Influenced by the Trimerisation of Photosystem I. Photosynth Res **79**: 179–187

Badger MR, Price GD (2003) CO2 concentrating mechanisms in cyanobacteria: molecular components, their diversity and evolution. J Exp Bot **54**: 609–622

Bald D, Kruip J, Rögner M (1996) Supramolecular architecture of cyanobacterial thylakoid membranes: How is the phycobilisome connected with the photosystems? Photosynth Res **49**: 103–118

Battchikova N, Eisenhut M, Aro E-M (2011) Cyanobacterial NDH-1 complexes: Novel insights and remaining puzzles. Biochim Biophys Acta BBA - Bioenerg **1807**: 935–944

Biggins J, Bruce D (1989) Regulation of excitation energy transfer in organisms containing phycobilins. Photosynth Res **20**: 1–34

Boulay C, Abasova L, Six C, Vass I, Kirilovsky D (2008) Occurrence and function of the orange carotenoid protein in photoprotective mechanisms in various cyanobacteria. Biochim Biophys Acta BBA - Bioenerg **1777**: 1344–1354

Boulay C, Wilson A, D'Haene S, Kirilovsky D (2010) Identification of a protein required for recovery of full antenna capacity in OCP-related photoprotective mechanism in cyanobacteria. Proc Natl Acad Sci **107**: 11620–11625

Brettel K, Leibl W (2001) Electron transfer in photosystem I. Biochim Biophys Acta BBA - Bioenerg **1507**: 100–114

Campbell D, Hurry V, Clarke AK, Gustafsson P, Öquist G (1998) Chlorophyll Fluorescence Analysis of Cyanobacterial Photosynthesis and Acclimation. Microbiol Mol Biol Rev **62**: 667–683

Cardona T, Sedoud A, Cox N, Rutherford AW (2012) Charge separation in Photosystem II: A comparative and evolutionary overview. Biochim Biophys Acta BBA - Bioenerg **1817**: 26–43

Collins AM, Liberton M, Jones HDT, Garcia OF, Pakrasi HB, Timlin JA (2012) Photosynthetic Pigment Localization and Thylakoid Membrane Morphology Are Altered in Synechocystis 6803 Phycobilisome Mutants. Plant Physiol **158**: 1600–1609

David L, Marx A, Adir N (2011) High-Resolution Crystal Structures of Trimeric and Rod Phycocyanin. J Mol Biol **405**: 201–213

Dolganov NA, Bhaya D, Grossman AR (1995) Cyanobacterial protein with similarity to the chlorophyll a/b binding proteins of higher plants: evolution and regulation. Proc Natl Acad Sci **92**: 636–640

Dong C, Tang A, Zhao J, Mullineaux CW, Shen G, Bryant DA (2009) ApcD is necessary for efficient energy transfer from phycobilisomes to photosystem I and helps to prevent photoinhibition in the cyanobacterium Synechococcus sp. PCC 7002. Biochim Biophys Acta BBA - Bioenerg **1787**: 1122–1128

Ducret A, Müller SA, Goldie KN, Hefti A, Sidler WA, Zuber H, Engel A (1998) Reconstitution, characterisation and mass analysis of the pentacylindrical allophycocyanin core complex from the cyanobacterium Anabaena sp. PCC 7120. J Mol Biol **278**: 369–388

El Bissati K, Delphin E, Murata N, Etienne A-L, Kirilovsky D (2000) Photosystem II fluorescence quenching in the cyanobacterium Synechocystis PCC 6803: involvement of two different mechanisms. Biochim Biophys Acta BBA - Bioenerg **1457**: 229–242

Emlyn-Jones D, Ashby MK, Mullineaux CW (1999) A gene required for the regulation of photosynthetic light harvesting in the cyanobacterium Synechocystis 6803. Mol Microbiol **33**: 1050–1058

Folea IM, Zhang P, Aro E-M, Boekema EJ (2008) Domain organization of photosystem II in membranes of the cyanobacterium Synechocystis PCC6803 investigated by electron microscopy. FEBS Lett **582**: 1749–1754

Gantt E, Conti SF (1966) Granules Associated with the Chloroplast Lamellae of Porphyridium Cruentum. J Cell Biol **29**: 423–434

Gantt E, Lipschultz CA, Grabowski J, Zimmerman BK (1979) Phycobilisomes from Blue-Green and Red Algae Isolation Criteria and Dissociation Characteristics. Plant Physiol **63**: 615–620

Gindt YM, Zhou J, Bryant DA, Sauer K (1994) Spectroscopic studies of phycobilisome subcore preparations lacking key core chromophores: assignment of excited state energies to the Lcm, beta 18 and alpha AP-B chromophores. Biochim Biophys Acta **1186**: 153–162

Glazer AN, Bryant DA (1975) Allophycocyanin B (lambdamax 671, 618 nm): a new cyanobacterial phycobiliprotein. Arch Microbiol **104**: 15–22

Gorbunov MY, Kuzminov FI, Fadeev VV, Kim JD, Falkowski PG (2011) A kinetic model of non-photochemical quenching in cyanobacteria. Biochim Biophys Acta BBA - Bioenerg **1807**: 1591–1599

Grigorieva G, Shestakov S (1982) Transformation in the cyanobacterium Synechocystis sp. 6803. FEMS Microbiol Lett **13**: 367–370

Grotjohann I, Fromme P (2005) Structure of cyanobacterial Photosystem I. Photosynth Res **85**: 51–72

Guglielmi G, Cohen-Bazire G, Bryant DA (1981) The structure of Gloeobacter violaceus and its phycobilisomes. Arch Microbiol **129**: 181–189

Gwizdala M, Wilson A, Kirilovsky D (2011) In Vitro Reconstitution of the Cyanobacterial Photoprotective Mechanism Mediated by the Orange Carotenoid Protein in Synechocystis PCC 6803. Plant Cell Online **23**: 2631–2643

Gwizdala M, Wilson A, Omairi-Nasser A, Kirilovsky D (2013) Characterization of the Synechocystis PCC 6803 Fluorescence Recovery Protein involved in photoprotection. Biochim Biophys Acta BBA - Bioenerg **1827**: 348–354

Havaux M, Guedeney G, Hagemann M, Yeremenko N, Matthijs HCP, Jeanjean R (2005) The chlorophyll-binding protein IsiA is inducible by high light and protects the cyanobacterium Synechocystis PCC6803 from photooxidative stress. FEBS Lett **579**: 2289–2293

Havaux M, Guedeney G, He Q, Grossman AR (2003) Elimination of high-light-inducible polypeptides related to eukaryotic chlorophyll a/b-binding proteins results in aberrant photoacclimation in Synechocystis PCC6803. Biochim Biophys Acta BBA - Bioenerg **1557**: 21–33

Hihara Y, Kamei A, Kanehisa M, Kaplan A, Ikeuchi M (2001) DNA Microarray Analysis of Cyanobacterial Gene Expression during Acclimation to High Light. Plant Cell Online **13**: 793–806

Houmard J, Capuano V, Colombano MV, Coursin T, Marsac NT de (1990) Molecular characterization of the terminal energy acceptor of cyanobacterial phycobilisomes. Proc Natl Acad Sci **87**: 2152–2156

Huang C, Yuan X, Zhao J, Bryant DA (2003) Kinetic analyses of state transitions of the cyanobacterium Synechococcus sp. PCC 7002 and its mutant strains impaired in electron transport. Biochim Biophys Acta BBA - Bioenerg **1607**: 121–130

Ihalainen JA, D'Haene S, Yeremenko N, van Roon H, Arteni AA, Boekema EJ, van Grondelle R, Matthijs HCP, Dekker JP (2005) Aggregates of the Chlorophyll-Binding Protein IsiA (CP43′) Dissipate Energy in Cyanobacteria†. Biochemistry (Mosc) **44**: 10846–10853

Jallet D, Gwizdala M, Kirilovsky D (2012) ApcD, ApcF and ApcE are not required for the Orange Carotenoid Protein related phycobilisome fluorescence quenching in the cyanobacterium Synechocystis PCC 6803. Biochim Biophys Acta **1817**: 1418–1427

Jallet D, Thurotte A, Leverenz RL, Perreau F, Kerfeld CA, Kirilovsky D (2013) Specificity of the cyanobacterial Orange Carotenoid Protein: Influences of OCP and phycobilisome structures. Plant Physiol pp.113.229997

Jordan P, Fromme P, Witt HT, Klukas O, Saenger W, Krauß N (2001) Three-dimensional structure of cyanobacterial photosystem I at 2.5 |[angst]| resolution. Nature **411**: 909–917

Joshua S, Mullineaux CW (2004) Phycobilisome Diffusion Is Required for Light-State Transitions in Cyanobacteria. Plant Physiol **135**: 2112–2119

Joshua S, Mullineaux CW (2005) The rpaC gene product regulates phycobilisome–photosystem II interaction in cyanobacteria. Biochim Biophys Acta BBA - Bioenerg **1709**: 58–68

Kaneko T, Sato S, Kotani H, Tanaka A, Asamizu E, Nakamura Y, Miyajima N, Hirosawa M, Sugiura M, Sasamoto S, et al (1996) Sequence analysis of the genome of the unicellular cyanobacterium Synechocystis sp. strain PCC6803. II. Sequence determination of the entire genome and assignment of potential protein-coding regions (supplement). DNA Res Int J Rapid Publ Rep Genes Genomes **3**: 185–209

Kay Holt T, Krogmann DW (1981) A carotenoid-protein from cyanobacteria. Biochim Biophys Acta BBA - Bioenerg **637**: 408–414

Kerfeld CA, Sawaya MR, Brahmandam V, Cascio D, Ho KK, Trevithick-Sutton CC, Krogmann DW, Yeates TO (2003) The Crystal Structure of a Cyanobacterial Water-Soluble Carotenoid Binding Protein. Structure **11**: 55–65

Kirilovsky D, Kerfeld CA (2012) The orange carotenoid protein in photoprotection of photosystem II in cyanobacteria. Biochim Biophys Acta BBA - Bioenerg **1817**: 158–166

Komárek J (2010) Recent changes (2008) in cyanobacteria taxonomy based on a combination of molecular background with phenotype and ecological consequences (genus and species concept). Hydrobiologia **639**: 245–259

Kondo K, Geng XX, Katayama M, Ikeuchi M (2005) Distinct roles of CpcG1 and CpcG2 in phycobilisome assembly in the cyanobacterium Synechocystis sp. PCC 6803. Photosynth Res **84**: 269–273

Kondo K, Ochiai Y, Katayama M, Ikeuchi M (2007) The Membrane-Associated CpcG2-Phycobilisome in Synechocystis: A New Photosystem I Antenna. Plant Physiol **144**: 1200–1210

Krieger-Liszkay A (2005) Singlet oxygen production in photosynthesis. J Exp Bot **56**: 337–346

Kruip J, Bald D, Boekema E, Rögner M (1994) Evidence for the existence of trimeric and monomeric Photosystem I complexes in thylakoid membranes from cyanobacteria. Photosynth Res **40**: 279–286

Kurisu G, Zhang H, Smith JL, Cramer WA (2003) Structure of the Cytochrome b6f Complex of Oxygenic Photosynthesis: Tuning the Cavity. Science **302**: 1009–1014

Latifi A, Ruiz M, Zhang C-C (2009) Oxidative stress in cyanobacteria. FEMS Microbiol Rev **33**: 258–278

Li D, Xie J, Zhao Y, Zhao J (2003) Probing connection of PBS with the photosystems in intact cells of Spirulina platensis by temperature-induced fluorescence fluctuation. Biochim Biophys Acta BBA - Bioenerg **1557**: 35–40

Liberton M, Howard Berg R, Heuser J, Roth R, Pakrasi HB (2006) Ultrastructure of the membrane systems in the unicellular cyanobacterium Synechocystis sp. strain PCC 6803. Protoplasma **227**: 129–138

Lundell DJ, Williams RC, Glazer AN (1981a) Molecular architecture of a light-harvesting antenna. In vitro assembly of the rod substructures of Synechococcus 6301 phycobilisomes. J Biol Chem **256**: 3580–3592

Lundell DJ, Yamanaka G, Glazer AN (1981b) A terminal energy acceptor of the phycobilisome: the 75,000-dalton polypeptide of Synechococcus 6301 phycobilisomes--a new biliprotein. J Cell Biol **91**: 315–319

MacColl R (1998) Cyanobacterial Phycobilisomes. J Struct Biol **124**: 311–334

Mao H-B, Li G-F, Ruan X, Wu Q-Y, Gong Y-D, Zhang X-F, Zhao N-M (2002) The redox state of plastoquinone pool regulates state transitions via cytochrome b6f complex in Synechocystis sp. PCC 6803. FEBS Lett **519**: 82–86

Marsac NT de (2003) Phycobiliproteins and phycobilisomes: the early observations. Photosynth Res **76**: 193–205

Marsac NT de, Cohen-bazire G (1977) Molecular composition of cyanobacterial phycobilisomes. Proc Natl Acad Sci **74**: 1635–1639

Marx A, Adir N (2013) Allophycocyanin and phycocyanin crystal structures reveal facets of phycobilisome assembly. Biochim Biophys Acta BBA - Bioenerg **1827**: 311–318

Maxson P, Sauer K, Zhou JH, Bryant DA, Glazer AN (1989) Spectroscopic studies of cyanobacterial phycobilisomes lacking core polypeptides. Biochim Biophys Acta **977**: 40–51

McConnell MD, Koop R, Vasil'ev S, Bruce D (2002) Regulation of the Distribution of Chlorophyll and Phycobilin-Absorbed Excitation Energy in Cyanobacteria. A Structure-Based Model for the Light State Transition. Plant Physiol **130**: 1201–1212

McDonald AE, Ivanov AG, Bode R, Maxwell DP, Rodermel SR, Hüner NPA (2011) Flexibility in photosynthetic electron transport: The physiological role of plastoquinol terminal oxidase (PTOX). Biochim Biophys Acta BBA - Bioenerg **1807**: 954–967

McFadden GI (2001) Primary and Secondary Endosymbiosis and the Origin of Plastids. J Phycol **37**: 951–959

McGregor A, Klartag M, David L, Adir N (2008) Allophycocyanin trimer stability and functionality are primarily due to polar enhanced hydrophobicity of the phycocyanobilin binding pocket. J Mol Biol **384**: 406–421

Melkozernov AN, Bibby TS, Lin S, Barber J, Blankenship RE (2003) Time-Resolved Absorption and Emission Show that the CP43' Antenna Ring of Iron-Stressed Synechocystis sp. PCC6803 Is Efficiently Coupled to the Photosystem I Reaction Center Core†,‡. Biochemistry (Mosc) **42**: 3893–3903

Mitschke J, Georg J, Scholz I, Sharma CM, Dienst D, Bantscheff J, Voss B, Steglich C, Wilde A, Vogel J, et al (2011) An experimentally anchored map of transcriptional start sites in the model cyanobacterium Synechocystis sp. PCC6803. Proc Natl Acad Sci U S A **108**: 2124–2129

Miyashita H, Ikemoto H, Kurano N, Adachi K, Chihara M, Miyachi S (1996) Chlorophyll d as a major pigment. Nature **383**: 402–402

Müller P, Li X-P, Niyogi KK (2001) Non-Photochemical Quenching. A Response to Excess Light Energy. Plant Physiol **125**: 1558–1566

Mullineaux CW (1992) Excitation energy transfer from phycobilisomes to Photosystem I in a cyanobacterium. Biochim Biophys Acta BBA - Bioenerg **1100**: 285–292

Mullineaux CW (1994) Excitation energy transfer from phycobilisomes to Photosystem I in a cyanobacterial mutant lacking Photosystem II. Biochim Biophys Acta BBA - Bioenerg **1184**: 71–77

Mullineaux CW (2008) Phycobilisome-reaction centre interaction in cyanobacteria. Photosynth Res **95**: 175–182

Mullineaux CW, Emlyn-Jones D (2005) State transitions: an example of acclimation to low-light stress. J Exp Bot **56**: 389–393

Mullineaux CW, Tobin MJ, Jones GR (1997) Mobility of photosynthetic complexes in thylakoid membranes. Nature **390**: 421–424

Mulo P, Sicora C, Aro E-M (2009) Cyanobacterial psbA gene family: optimization of oxygenic photosynthesis. Cell Mol Life Sci **66**: 3697–3710

Nelson N, Yocum CF (2006) Structure and Function of Photosystems I and Ii. Annu Rev Plant Biol **57**: 521–565

Olive J, Ajlani G, Astier C, Recouvreur M, Vernotte C (1997) Ultrastructure and light adaptation of phycobilisome mutants of Synechocystis PCC 6803. Biochim Biophys Acta BBA - Bioenerg **1319**: 275–282

Osyczka A, Moser CC, Dutton PL (2005) Fixing the Q cycle. Trends Biochem Sci **30**: 176–182

Polívka T, Kerfeld CA, Pascher T, Sundström V (2005) Spectroscopic Properties of the Carotenoid 3′-Hydroxyechinenone in the Orange Carotenoid Protein from the Cyanobacterium Arthrospira maxima†. Biochemistry (Mosc) **44**: 3994–4003

Price GD (2011) Inorganic carbon transporters of the cyanobacterial CO2 concentrating mechanism. Photosynth Res **109**: 47–57

Punginelli C, Wilson A, Routaboul J-M, Kirilovsky D (2009) Influence of zeaxanthin and echinenone binding on the activity of the Orange Carotenoid Protein. Biochim Biophys Acta BBA - Bioenerg **1787**: 280–288

Rakhimberdieva MG, Boichenko VA, Karapetyan NV, Stadnichuk IN (2001) Interaction of Phycobilisomes with Photosystem II Dimers and Photosystem I Monomers and Trimers in the Cyanobacterium Spirulina platensis†. Biochemistry (Mosc) **40**: 15780–15788

Rakhimberdieva MG, Bolychevtseva YV, Elanskaya IV, Karapetyan NV (2007a) Protein–protein interactions in carotenoid triggered quenching of phycobilisome fluorescence in Synechocystis sp. PCC 6803. FEBS Lett **581**: 2429–2433

Rakhimberdieva MG, Elanskaya IV, Vermaas WFJ, Karapetyan NV (2010) Carotenoid-triggered energy dissipation in phycobilisomes of Synechocystis sp. PCC 6803 diverts excitation away

from reaction centers of both photosystems. Biochim Biophys Acta BBA - Bioenerg **1797**: 241–249

Rakhimberdieva MG, Stadnichuk IN, Elanskaya IV, Karapetyan NV (2004) Carotenoid-induced quenching of the phycobilisome fluorescence in photosystem II-deficient mutant of Synechocystis sp. FEBS Lett **574**: 85–88

Rakhimberdieva MG, Vavilin DV, Vermaas WFJ, Elanskaya IV, Karapetyan NV (2007b) Phycobilin/chlorophyll excitation equilibration upon carotenoid-induced non-photochemical fluorescence quenching in phycobilisomes of the cyanobacterium Synechocystis sp. PCC 6803. Biochim Biophys Acta BBA - Bioenerg **1767**: 757–765

Rasmussen B, Fletcher IR, Brocks JJ, Kilburn MR (2008) Reassessing the first appearance of eukaryotes and cyanobacteria. Nature **455**: 1101–1104

Reuter W, Wiegand G, Huber R, Than ME (1999) Structural analysis at 2.2 A of orthorhombic crystals presents the asymmetry of the allophycocyanin-linker complex, AP.LC7.8, from phycobilisomes of Mastigocladus laminosus. Proc Natl Acad Sci U S A **96**: 1363–1368

Rippka R, Deruelles J, Waterbury JB, Herdman M, Stanier RY (1979) Generic Assignments, Strain Histories and Properties of Pure Cultures of Cyanobacteria. J Gen Microbiol **111**: 1–61

Ruban AV, Johnson MP (2009) Dynamics of higher plant photosystem cross-section associated with state transitions. Photosynth Res **99**: 173–183

Sarcina M, Tobin MJ, Mullineaux CW (2001) Diffusion of Phycobilisomes on the Thylakoid Membranes of the Cyanobacterium Synechococcus 7942 EFFECTS OF PHYCOBILISOME SIZE, TEMPERATURE, AND MEMBRANE LIPID COMPOSITION. J Biol Chem **276**: 46830–46834

Schreiber U, Schliwa U, Bilger W (1986) Continuous recording of photochemical and non-photochemical chlorophyll fluorescence quenching with a new type of modulation fluorometer. Photosynth Res **10**: 51–62

Scott M, McCollum C, Vasil'ev S, Crozier C, Espie GS, Krol M, Huner NPA, Bruce D (2006) Mechanism of the Down Regulation of Photosynthesis by Blue Light in the Cyanobacterium Synechocystis sp. PCC 6803†. Biochemistry (Mosc) **45**: 8952–8958

Sherman DM, Troyan TA, Sherman LA (1994) Localization of Membrane Proteins in the Cyanobacterium Synechococcus sp. PCC7942 (Radial Asymmetry in the Photosynthetic Complexes). Plant Physiol **106**: 251–262

Shih PM, Wu D, Latifi A, Axen SD, Fewer DP, Talla E, Calteau A, Cai F, Tandeau de Marsac N, Rippka R, et al (2013) Improving the coverage of the cyanobacterial phylum using diversity-driven genome sequencing. Proc Natl Acad Sci U S A **110**: 1053–1058

Stanier RY, Kunisawa R, Mandel M, Cohen-Bazire G (1971) Purification and properties of unicellular blue-green algae (order Chroococcales). Bacteriol Rev **35**: 171–205

Stanier RY, Sistrom WR, Hansen TA, Whitton BA, Castenholz RW, Pfennig N, Gorlenko VN, Kondratieva EN, Eimhjellen KE, Whittenbury R, et al (1978) Proposal to Place the Nomenclature of the Cyanobacteria (Blue-Green Algae) Under the Rules of the International Code of Nomenclature of Bacteria. Int J Syst Bacteriol **28**: 335–336

Sutter M, Wilson A, Leverenz RL, Lopez-Igual R, Thurotte A, Salmeen AE, Kirilovsky D, Kerfeld CA (2013) Crystal structure of the FRP and identification of the active site for modulation of OCP-mediated photoprotection in cyanobacteria. Proc Natl Acad Sci **110**: 10022–10027

Taton A, Grubisic S, Brambilla E, Wit RD, Wilmotte A (2003) Cyanobacterial Diversity in Natural and Artificial Microbial Mats of Lake Fryxell (McMurdo Dry Valleys, Antarctica): a Morphological and Molecular Approach. Appl Environ Microbiol **69**: 5157–5169

Tian L, van Stokkum IHM, Koehorst RBM, Jongerius A, Kirilovsky D, van Amerongen H (2011) Site, Rate, and Mechanism of Photoprotective Quenching in Cyanobacteria. J Am Chem Soc **133**: 18304–18311

Tyystjärvi E (2008) Photoinhibition of Photosystem II and photodamage of the oxygen evolving manganese cluster. Coord Chem Rev **252**: 361–376

Ughy B, Ajlani G (2004) Phycobilisome rod mutants in Synechocystis sp. strain PCC6803. Microbiology **150**: 4147–4156

Umena Y, Kawakami K, Shen J-R, Kamiya N (2011) Crystal structure of oxygen-evolving photosystem II at a resolution of 1.9 Å. Nature **473**: 55–60

Vass I (2012) Molecular mechanisms of photodamage in the Photosystem II complex. Biochim Biophys Acta BBA - Bioenerg **1817**: 209–217

Vinyard DJ, Ananyev GM, Dismukes GC (2013) Photosystem II: the reaction center of oxygenic photosynthesis. Annu Rev Biochem **82**: 577–606

Wilson A, Ajlani G, Verbavatz J-M, Vass I, Kerfeld CA, Kirilovsky D (2006) A Soluble Carotenoid Protein Involved in Phycobilisome-Related Energy Dissipation in Cyanobacteria. Plant Cell Online **18**: 992–1007

Wilson A, Boulay C, Wilde A, Kerfeld CA, Kirilovsky D (2007) Light-Induced Energy Dissipation in Iron-Starved Cyanobacteria: Roles of OCP and IsiA Proteins. Plant Cell Online **19**: 656–672

Wilson A, Kinney JN, Zwart PH, Punginelli C, D'Haene S, Perreau F, Klein MG, Kirilovsky D, Kerfeld CA (2010) Structural Determinants Underlying Photoprotection in the Photoactive Orange Carotenoid Protein of Cyanobacteria. J Biol Chem **285**: 18364–18375

Wilson A, Punginelli C, Couturier M, Perreau F, Kirilovsky D (2011) Essential role of two tyrosines and two tryptophans on the photoprotection activity of the Orange Carotenoid Protein. Biochim Biophys Acta BBA - Bioenerg **1807**: 293–301

Wilson A, Punginelli C, Gall A, Bonetti C, Alexandre M, Routaboul J-M, Kerfeld CA, Grondelle R van, Robert B, Kennis JTM, et al (2008) A photoactive carotenoid protein acting as light intensity sensor. Proc Natl Acad Sci **105**: 12075–12080

Witt HT (1996) Primary reactions of oxygenic photosynthesis. Berichte Bunsenges Für Phys Chem **100**: 1923–1942

Wu YP, Krogmann DW (1997) The orange carotenoid protein of Synechocystis PCC 6803. Biochim Biophys Acta BBA - Bioenerg **1322**: 1–7

Xu H, Vavilin D, Funk C, Vermaas W (2004) Multiple Deletions of Small Cab-like Proteins in the Cyanobacterium Synechocystis sp. PCC 6803 CONSEQUENCES FOR PIGMENT BIOSYNTHESIS AND ACCUMULATION. J Biol Chem **279**: 27971–27979

Yamanaka G, Lundell DJ, Glazer AN (1982) Molecular architecture of a light-harvesting antenna. Isolation and characterization of phycobilisome subassembly particles. J Biol Chem **257**: 4077–4086

Yamaoka T, Satoh K, Katoh S (1978) Photosynthetic activities of a thermophilic blue-green alga. Plant Cell Physiol **19**: 943–954

Yang S, Su Z, Li H, Feng J, Xie J, Xia A, Gong Y, Zhao J (2007) Demonstration of phycobilisome mobility by the time- and space-correlated fluorescence imaging of a cyanobacterial cell. Biochim Biophys Acta BBA - Bioenerg **1767**: 15–21

Yu MH, Glazer AN (1982) Cyanobacterial phycobilisomes. Role of the linker polypeptides in the assembly of phycocyanin. J Biol Chem **257**: 3429–3433

Zhang P, Eisenhut M, Brandt A-M, Carmel D, Silén HM, Vass I, Allahverdiyeva Y, Salminen TA, Aro E-M (2012) Operon flv4-flv2 Provides Cyanobacterial Photosystem II with Flexibility of Electron Transfer. Plant Cell Online **24**: 1952–1971

Zouni A, Witt HT, Kern J, Fromme P, Krauss N, Saenger W, Orth P (2001) Crystal structure of photosystem II from Synechococcus elongatus at 3.8 A resolution. Nature **409**: 739–743

Chapter 1

ApcD, ApcF and ApcE are not required for the Orange Carotenoid Protein related phycobilisome fluorescence quenching in the cyanobacterium *Synechocystis* PCC 6803

Summary of work

When the project started, it was already known that OCP and phycobilisomes isolated from *Synechocystis* can directly interact under strong blue-green illumination and trigger fluorescence quenching (Gwizdala et al., 2011). This was proved using an in vitro reconstitution system, which allowed drawing several other conclusions: 1 or 2 OCP^r (not OCP^o) bind(s) per phycobilisome in a light independent process, at the level of the allophycocyanin (APC) core (Gwizdala et al., 2011). Given the complexity of the core, containing 72 APC subunits, several questions arose: which components are able to bind OCP^r? Where exactly does the quenching take place?

We built *Synechocystis* mutants affected in their phycobilisome terminal emitters (ApcD, ApcF, ApcE). Firstly assessing the effect of strong blue-green light on whole cells thanks to a PAM fluorometer, we also looked for subtle differences by isolating intact phycobilisomes from all these strains and testing their interaction with OCP in vitro.

Our results demonstrated that none of the terminal emitters is absolutely required for the OCP-related photoprotective mechanism. By elimination, OCP probably binds to a basal APC form (α^{APC} or β^{APC}) upon photoactivation.

Contribution to this work

M.Gwizdala constructed the ΔApcD and ΔApcF plasmids. I performed all subsequent molecular biology, biochemistry and spectroscopy work.

This chapter is based on:

Jallet D, Gwizdala M, Kirilovsky D (2012) ApcD, ApcF and ApcE are not required for the Orange Carotenoid Protein related phycobilisome fluorescence quenching in the cyanobacterium Synechocystis PCC 6803. Biochim Biophys Acta **1817**: 1418–1427

ApcD, ApcF and ApcE are not required for the Orange Carotenoid Protein related phycobilisome fluorescence quenching in the cyanobacterium *Synechocystis* PCC 6803

Denis Jallet [1,2] , Michal Gwizdala[1,2] and Diana Kirilovsky [1,2]

[1]Commissariat à l'Energie Atomique (CEA), Institut de Biologie et Technologies de Saclay (iBiTec-S), 91191 Gif sur Yvette and

[2]Centre National de la Recherche Scientifique (CNRS), URA 2096, 91191 Gif sur Yvette, France.

Corresponding author:

Diana Kirilovsky, iBiTec-S, Bât 532, CEA Saclay, 91191 Gif sur Yvette, FRANCE;

E-mail: diana.kirilovsky@cea.fr

Abstract

In cyanobacteria, strong blue-green light induces a photoprotective mechanism involving an increase of energy thermal dissipation at the level of phycobilisome (PB), the cyanobacterial antenna. This leads to a decrease of the energy arriving to the reaction centers. The photoactive Orange Carotenoid Protein (OCP) has an essential role in this mechanism. The binding of the red photoactivated OCP to the core of the PB triggers energy and PB fluorescence quenching. The core of PBs is constituted of allophycocyanin trimers emitting at 660 or 680 nm. ApcD, ApcF and ApcE are the responsible of the 680 nm emission. In this work, the role of these terminal emitters in the photoprotective mechanism was studied. Single and double *Synechocystis* PCC 6803 mutants, in which the *apcD* or/and *apcF* genes were absent, were constructed. The Cys190 of ApcE which binds the phycocyanobilin was replaced by a Ser. The mutated ApcE attached an unusual chromophore emitting at 710 nm. The activated OCP was able to induce the photoprotective mechanism in all the mutants. Moreover, *in vitro* reconstitution experiments showed similar amplitude and rates of fluorescence quenching. Our results demonstrated that ApcD, ApcF and ApcE are not required for the OCP-related fluorescence quenching and they strongly suggested that the site of quenching is one of the APC trimers emitting at 660 nm.

Keywords: cyanobacteria**,** orange carotenoid protein, photoprotection, phycobilisome, *Synechocystis*

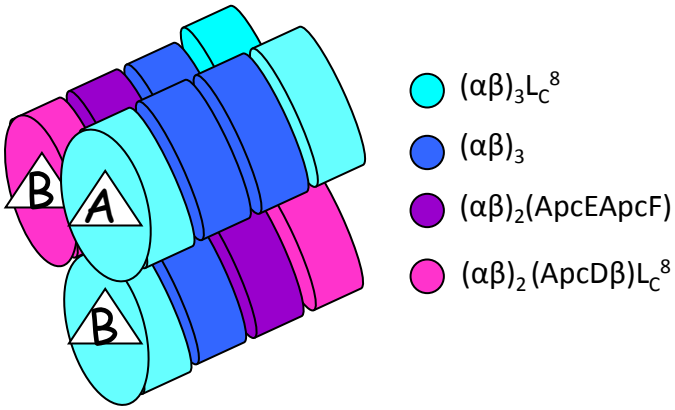

Figure 1. Schematic orthogonal projection of the tri-cylindrical core of *Synechocystis.* The figure is based on the model presented in [10].The top cylinder (noted A) contains only ApcA-ApcB trimers emitting at 660 nm. Each of the basal cylinders (noted B), adjacent to the membrane, contains two trimers emitting at 660 nm ($ApcA_3$ $ApcB_3$) and two trimers emitting at 683 nm: $ApcA_2$ ApcD $ApcB_3$ and $ApcA_2$ $ApcB_2$ ApcF ApcE. In each cylinder the 2 external trimers contain a 8.7 kDa linker protein (ApcC).

Introduction

Light, which is essential for photosynthesis, could become a major source of stress for photosynthetic organisms like plants, algae and cyanobacteria. Under low and medium irradiance, most of the light energy absorbed by the antennae and directed to the reaction centers is used for the photochemical reactions. Less than 10% of this energy is dissipated as heat or comes back as fluorescence. However, under high light conditions, the photosynthetic electron transport chain becomes reduced and only a small portion of the energy absorbed is then used for photosynthesis. The excess energy induces the formation of dangerous reactive oxygen species at the level of both photosystems causing the damage of Photosystem II and of the translational and transcriptional machinery (for reviews see [1, 2]). In order to diminish the formation of these species, oxygenic photosynthetic organisms have developed a photoprotective mechanism that decreases the energy arriving to the reaction centers by increasing the energy dissipation via heat at the level of the antenna (reviews [3-5]).

In cyanobacteria light is principally collected by the phycobilisome, a large extramembrane complex covalently binding red and blue chromophores (phycobilins). The phycobilisome (PB), which is built of phycobiliproteins and linker proteins, consists of a core from which radiate rods (reviews [6-9]). In *Synechocystis* PCC 6803 [10], the strain used in this work, the rods are formed by 3 hexamers of the blue phycocyanin (PC). The PC, a heterodimer αPC-βPC, binds 3 phycocyanobilins, 2 to the α subunit and one to the β subunit. The rods and the hexamers are stabilized by non-chromophored linker proteins (L_R^{10}, L_R^{30}, L_R^{33} and L_{RC}). L_{RC} also stabilizes the binding of the rods to the core. The core consists of 3 cylinders, each one formed by 4 trimers of allophycocyanin (APC) (Fig. 1). Two third of these trimers contain 3 APC formed by a heterodimer αAPC-βAPC which binds 2 phycocyanobilins, one in each subunit. These trimers have a maximal emission at 660 nm (APC_{660}). The upper cylinder contains only APC_{660} trimers. In contrast, each basal cylinder contains 2 APC_{660} trimers, one trimer in which one αAPC subunit is replaced by a special αAPC-like subunit called ApcD and a last trimer in which one β subunit is replaced by ApcF, a βAPC-like subunit, and one α subunit is replaced by the N-terminal domain of ApcE, a αAPC-like domain (Fig 1). Each of these special APC-like subunits binds a single phycocyanobilin and the trimers containing one or two of these special subunits have a maximal emission at 680 nm (APC_{680}). It was proposed that the red shift of the absorbance and emission of these subunits is related to an additional polarity around the bilin [11]. The

trimer containing ApcD is one of the external trimers, in contrast the exact position of the trimer containing ApcF and ApcE remains to be elucidated (see review [7]). It is not clear if these two trimers are in contact. In each cylinder the 2 external trimers are stabilized by a 8.7 kDa linker protein [7].

The ApcE subunit, also called Lcm, is essential for the stabilization of the core of the PB [12-15]. The C-terminal part of *Synechocystis* ApcE contains 3 repeated domains of about 120 residues (Rep) which are similar to the conserved domains of rod linkers and most probably are involved in the interaction between the APC trimers [16-18]. Lcm is also involved in the interaction between the PB and the thylakoids. First, it was suggested that a loop of about 50 aminoacids that interrupts the N-terminal APC-like domain is involved in the attachment of PBs to the thylakoids [16-18]. However, Ajlani and Vernotte (1998) demonstrated that deletion of this loop does neither affect the integrity of the PB nor its binding to the membranes. They proposed that the region between Rep 2 and 3, called arm 2, is the one that participates in the PB-membrane interaction [12].

In most of the PB-containing cyanobacteria strains, light activates a 35 kDa soluble protein attaching a ketocarotenoid, the Orange Carotenoid Protein (OCP) [19]. The activated OCP binds to the PBs [20] and induces an increase of thermal dissipation of excess energy thereby decreasing the energy arriving to both reaction centers (RCII and RCI) [19, 21, 22]. As a consequence also the yield of fluorescence decreases. This characteristic is very useful to follow the induction of the photoprotective mechanism known as the OCP-dependent nonphotochemical (NPQ) mechanism. Since the activation of the OCP has a very low quantum yield, the concentration of activated protein is zero or very low in darkness and under low light conditions [23]. Thus, the photoprotective mechanism functions only under high light conditions. OCP-like genes are absent in about 20% of the already sequenced cyanobacteria strains (ex: *Synechococcus elongatus* PCC 7942; *Termosynechococcus elongatus*) [24, 25]. These strains lacking the photoprotective mechanism are more sensitive to high irradiance [24]. In *Synechocystis* PCC 6803 (hereafter referred to as *Synechocystis*), OCP is constitutively expressed but stress conditions like high light, iron starvation or high salt increases its transcription [26-29]. Since there is a direct relationship between the concentration of OCP and the strength of the photoprotective mechanism [20], under stress conditions the importance of this OCP-related mechanism in photoprotection is higher than in laboratory normal growth conditions (30-90 µmol photons m^{-2} s^{-1}).

The discovery of the OCP [30], its first isolation [30, 31] and the resolution of its structure [32] were realized long time before its role in photoprotection was elucidated [19].

The soluble apo-protein binds one carotenoid molecule, the ketocarotenoid 3'-hydroxyechinenone (hECN). It is largely buried in the OCP and spans the all α-helical N-terminal domain and the α/β C-terminal domain [32, 33]. The OCP is a photoactive protein [23]. Absorption of blue-green light by its bound hECN induces conformational changes in the carotenoid and the apo-protein, converting the stable dark orange OCP form into an activated metastable red OCP form. The carbonyl group of the carotenoid is essential for the photoactivity [34]. Only the red activated OCP form is able to bind to the PBs [20]. Thus, mutated OCPs, which are not converted to the red form upon light absorption, are unable to induce fluorescence quenching [33-35]. *In vitro* reconstitution experiments demonstrated that while the red OCP accumulates more and more with an increasing light intensity, its binding to the PBs is light independent [20]. This light independent binding of the activated OCP to PBs was also observed in *in vivo* experiments [36, 37].

The recovery of the full antenna capacity and fluorescence after exposure to a high irradiance needs another protein, the Fluorescence Recovery Protein (FRP) [38]. This soluble 13 kDa protein interacts as a trimer only with the activated red OCP [38]. It accelerates the red to orange OCP conversion and helps the OCP to detach from the PB [20, 38].

The study of the OCP-related NPQ mechanism in *Synechocystis* mutant strains containing PBs formed only by the core or only by the rods strongly suggested that OCP interacts with the core of the PB [19]. This was recently demonstrated by *in vitro* reconstitution experiments in which phycobilisome fluorescence quenching was induced upon illumination of isolated PB cores [20]. In contrast, OCP was unable to bind and quench the fluorescence of PBs containing only PC rods [20]. However we were unable to demonstrate to which type of trimer, APC_{660} or APC_{680}, the OCP binds. The site of binding must be very specific since only one OCP bound to the PB is sufficient to quench its fluorescence [20]. The structures of ApcD, ApcF and the N-terminal region of ApcE are rather similar to the α and β APC subunits but not identical [11]. Also the exposed charges of the proteins differ [11]. These differences could determine that OCP interacts only with APC_{660} or only with APC_{680} trimers.

The site of quenching in the WT PB core remains one of the important questions to be elucidated. To answer this question, we have constructed single and double phycobilisome *Synechocystis* mutants and studied the OCP-related NPQ mechanism in these strains. *In vitro* reconstitution experiments using isolated PBs and OCP clearly showed that none of the subunits emitting at 680 nm is essential for fluorescence and energy quenching.

2-Materials and Methods

2.1 Culture conditions

The mesophylic freshwater cyanobacteria *Synechocystis* PCC 6803 wild-type and mutants were grown photoautotrophically in a modified BG11 medium [39] containing a double amount of sodium nitrate and appropriate quantities of antibiotics. Cells were kept in a rotary shaker (120 rpm) at 30°C, illuminated by fluorescent white lamps giving a total intensity of about 30–40 μmol photons m^{-2} s^{-1} under a CO_2-enriched atmosphere. Cells were maintained in their logarithmic phase of growth. For PBS isolation, cells were grown in 3L Erlenmeyers in a rotary shaker under a light intensity of 90–100 μmol photons m^{-2} s^{-1}. They were harvested at OD_{800}=1.0.

2.2 Plasmid constructions

ΔApcD plasmid

A 1-kb DNA region surrounding the *sll0928* gene encoding for ApcD was amplified by PCR using genomic DNA of *Synechocystis* as template. Two synthesized restriction sites- creating oligonucleotides were used as primers: FD_NotI and RD_XhoI (Table SI and fig.S1A). The resulting PCR product was cloned in the polylinker *Not*I-*Xho*I restriction sites of pBluescriptSK$^+$ plasmid (Stratagene) thanks to the *Not*I and *Xho*I sites engineered by the amplifying primers. The *sll0928* gene was interrupted by inserting a 1-kb DNA fragment containing a gene conferring resistance to chloramphenicol in the unique *Bam*HI restriction site.

ΔApcF plasmid

A 1kb DNA region surrounding the *slr1459 Synechocystis* gene encoding for ApcF was amplified by PCR using the oligonucleotides FF_NotI and RF_XhoI (Table SI and fig. S1B). The resulting PCR product was digested by *Not*I and *Xho*I restriction enzymes and cloned in the polylinker *Not*I-*Xho*I restriction sites of pBluescript SK$^+$ plasmid. The *slr1459* gene was inactivated by insertion of a 2.2-kb DNA fragment containing the *aadA* gene from Tn7, giving resistance to Spectinomycin/Streptomycin (Sp/Sm), in the unique *Pst*I site.

ApcE-C190S plasmid

A 3.4-kb DNA region containing the *slr0335* gene of *Synechocystis*, encoding for ApcE, was amplified by PCR using the oligonucleotides FE_NotI and RE_XhoI (Table SI and fig. S1C). The PCR product was digested with the *Not*I and *Xho*I restriction enzymes then cloned in the

polylinker *NotI-XhoI* restriction sites of pBluescript SK^+ plasmid. A *Pml*I restriction site was created 151-pb downstream of the *slr0335* stop-codon to insert a cassette conferring resistance to Sp/Sm in the obtained plasmid. The point mutation was created by site directed mutagenesis using the Quickchange XL kit of Stratagene and synthetic mutagenic oligonucleotides FE_PmlI and RE_PmlI (Table SI and fig.S1C). The C190S point mutation in ApcE was obtained using primers FE_C190S and RE_C190S (Table SI and fig.S1C). These oligonucleotides introduced a second mutation that suppresses a unique *Cla*I restriction site present in *slr0335*. The presence of the mutations was checked through digestion with the *Cla*I restriction enzyme and confirmed by sequencing.

2.3 Transformation, selection, genetic analysis of mutants.

The ΔApcD, ΔApcF, apcE-C190S plasmid constructs were used to transform WT *Synechocystis* cells. Selection was made at 33°C, under dim light (30 μmol photons m^{-2} s^{-1}) on plates containing the modified BG11 medium supplemented with 1% agarose and different antibiotics: 25μg/mL spectinomycin and 12μg/mL streptomycin, 40μg/mL kanamycin or 27 μg/mL chloramphenicol. Genomic DNA was isolated from *Synechocystis* cells as described in [40]. To confirm the homoplasmicity and complete segregation of the different mutants, PCR analysis and specific digestions by restriction enzymes were performed. To obtain the ΔApcDF double mutant, ΔApcD cells were transformed with the ΔApcF plasmid.

2.4 Isolation of PBs, OCP and FRP

The purification of PBs was performed according to the procedure applied in [13], with some modifications described in [20]. Briefly, harvested cells were washed twice with 0.8 M potassium phosphate buffer (pH=7.5) and concentrated to 1 mg of chlorophyll per mL. Cells were then broken by vortexing in the presence of glass beads, 1mM EDTA, 1mM caproic acid, 1mM phenylmethylsulfonyl gluoride, 1mM benzamidine and 50μg/mL DNase. After 2 hours of incubation with Triton X-100 (2% v/v), debris were removed by centrifugation at 20000g for 20 min at 23°C. The supernatant was loaded in a sucrose gradient as described in [20] and spun at 150000g, 23°C for 5 hours. The different layers were collected and their absorbance spectra were recorded.

OCP was isolated from the over-expressing C-terminal His-tagged ΔCrtR strain as described in [23]. FRP was purified from an *Escherichia coli* strain over-expressing the short FRP from *Synechocystis*, using the procedure described in [38].

2.5 Fluorescence measurements

PAM fluoremeter

Fluorescence quenching and recovery were monitored using a pulse amplitude modulated fluoremeter (101/102/103-PAM; Walz). Measurements were made in 1 cm diameter stirred cuvettes. All experiments carried on whole cells were performed at a chlorophyll concentration of 3µg/mL, at 33°C. *In vitro* reconstitutions were handled at a phycobilisome concentration of 0.012 µM in 0.8 M (or 0.5 M) phosphate buffer, at 23°C. Fluorescence quenching was induced *in vivo* by 1400 $\mu mol.m^{-2}.s^{-1}$ of blue-green light (Halogen white light filtered by a Corion cut-off 550-nm filter; 400 to 550 nm). *In vitro* blue-green light of 900 $\mu mol.m^{-2}.s^{-1}$ was used for quenching, whereas recovery was recorded in the darkness.

Emission spectra

Fluorescence emission spectra were monitored in a CARY Eclipse spectrophotometer (Varian). For studies at room temperature, samples were placed in a 1 cm diameter stirred cuvette. For 77 K measurements, samples were collected in Pasteur pipettes then frozen by immersion in liquid nitrogen. Excitation was made at 590 nm.

3 Results and Discussion

3.1 The mutated PBs:

In order to elucidate whether one of the phycobiliproteins emitting at 680 nm is essential to the OCP-related fluorescence quenching, single and double PB mutants were constructed. The *apcD* and/or the *apcF* gene of *Synechocystis* were interrupted by antibiotic resistance cassettes leading to strains lacking one or both of the proteins encoded by these genes. Mutants of *Synechocystis* and *Synechococcus* PCC 7002 lacking these subunits were previously constructed and their phenotype described by two other research groups [41, 42]. In the PBs of these mutants the ApcD subunit is replaced by an αAPC subunit and the ApcF subunit is replaced by a βAPC subunit [41, 42]. Thus, in the double mutant, the only 680 nm emitter is ApcE (or Lcm). The ApcE subunit cannot be deleted. Its absence leads to the lack of phycobilisome core assembly [12-15]. Instead we have constructed a *Synechocystis* ApcE mutant in which the Cys 190, normally binding the phycocyanobilin, was changed to a Ser. In a similar mutant, previously constructed in *Synechococcus* PCC 7002, ApcE binds non-covalently an unusual chromophore, probably 3(Z)-phycocyanobilin which emits at 710 nm [42, 43]. The details of the construction of the different mutants are described in Materials and Methods.

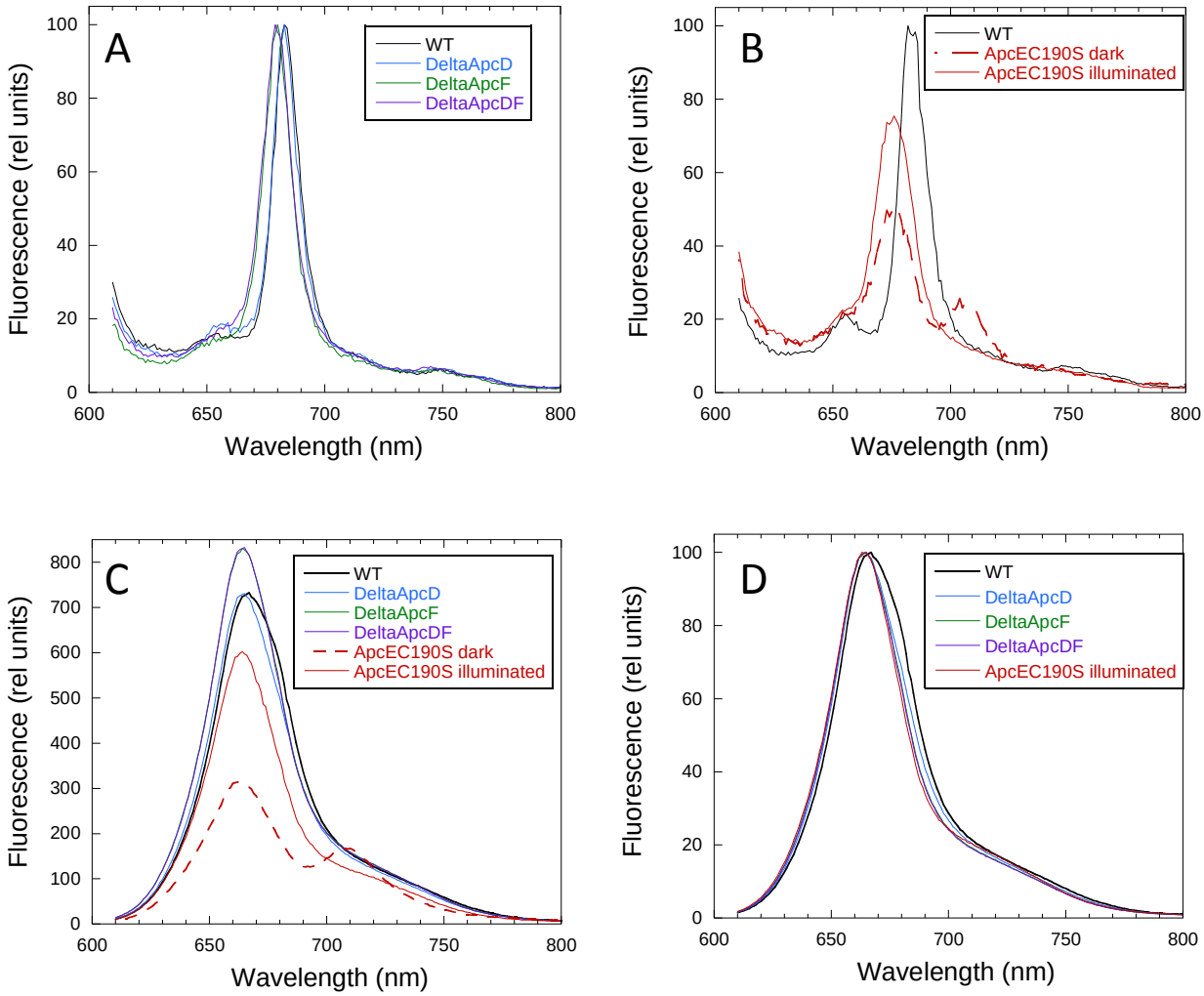

Figure 2. Fluorescence emission spectra of isolated phycobilisomes. (A) 77 K spectra of WT (black), ΔApcD (blue), ΔApcF (green) and ΔApcDF (violet) PBs. (B) 77 K spectra of WT PBs (black) and ApcE-C190S PBs kept in the dark (red, dashed line) or after a 3'illumination with 5000 µmol photons m^{-2} s^{-1} white light (red, solid line). (C) Room temperature fluorescence spectra of WT, ΔApcD, ΔApcF, ΔApcDF, dark and pre-illuminated ApcEC190S PBs. Same colors as in (A) (D) Room temperature fluorescence spectra of WT, ΔApcD, ΔApcF, ΔApcDF and pre-illuminated ApcE-C190S PBs. Same colors as in (A). Spectra in A and D were normalized at their maximum of emission; spectra in B were normalized at 800 nm. All the spectra were realized at the same PB concentration: 0.012 µM. Excitation was made at 590 nm.

Figures 2 A and B show the 77 K fluorescence spectra of PBs isolated from *Synechocystis* WT and PB mutants. WT, ΔApcD, ΔApcF and ΔApcDF PBs presented a major fluorescence emission at around 674-684 nm, related to the terminal PB emitters, with a small peak or shoulder at 655-665 nm related to PC and APC (Fig 2A). The spectra were normalized at the maximum of the emission in the 674-684 nm region to better visualize possible shifts in the maximum position. The maximum of fluorescence was at 682-684 nm in the WT and ΔApcD PBs containing ApcF and ApcE. The emission was blue-shifted in the two other mutants lacking ApcF. This result suggested that the lack of ApcF and its replacement by a βAPC subunit modified the emission of the chromophore attached to ApcE. It is also possible that the blue-shifted emission of the trimer is related to the fact that it contains only one 680 nm emitter in ΔApcF PBs whereas it contains two of them in the WT PBs .The absence of ApcF also seemed to modify the emission of ApcD even though they are present in different trimers. Another explanation could be that the emission of ApcD is always blue-shifted compared to ApcE in *Synechocystis*. The ApcE-C190S mutated PBs presented a third fluorescence peak with a maximum at 710 nm probably related to the unusual chromophore attached to ApcE (Fig 2B). The maximum of the peak of fluorescence related to ApcD and ApcF is at 674-676 nm. Thus, the emissions of these subunits are blue-shifted compared to ApcE or are largely modified by the lackof phycocyanobilin in the ApcE subunit. The strong 676 nm fluorescence emission in the dark spectra could be explained by a low efficiency in the energy transfer between the chromophores or most probably by the absence of the 710 nm emitting chromophore in around half of PBs. The emission at 710 nm was photo-labile. Illumination of ApcE-C190S PBs bleached the emission at 710 nm and largely increased the emission at 674-676 nm indicating that the energy transfer from ApcD and/or ApcF to the chromophore emitting at 710 nm was completely disrupted.

The fluorescence spectra at room temperature of WT and mutated PBs showed a typical maximum at 665 nm largely related to APC_{660} (Fig 2C and D). Only WT PBs presented a clear shoulder at 680 nm related to terminal emitters (Fig 2C). This could be explained by the blue-shift of the emission of the terminal emitters in the other mutants and/or a weaker energy transfer from APC_{660} to APC_{680} especially in ΔApcDF PBs which presented a slightly stronger emission at 665 nm (Fig 2C). In ApcE-C190S PBs, the emission at 665nm was weaker than in the other PBs and a peak with maximum at 710 nm was visible. As already observed in the 77K fluorescence spectra, after illumination, this peak disappeared and the 665 nm emission was doubled.

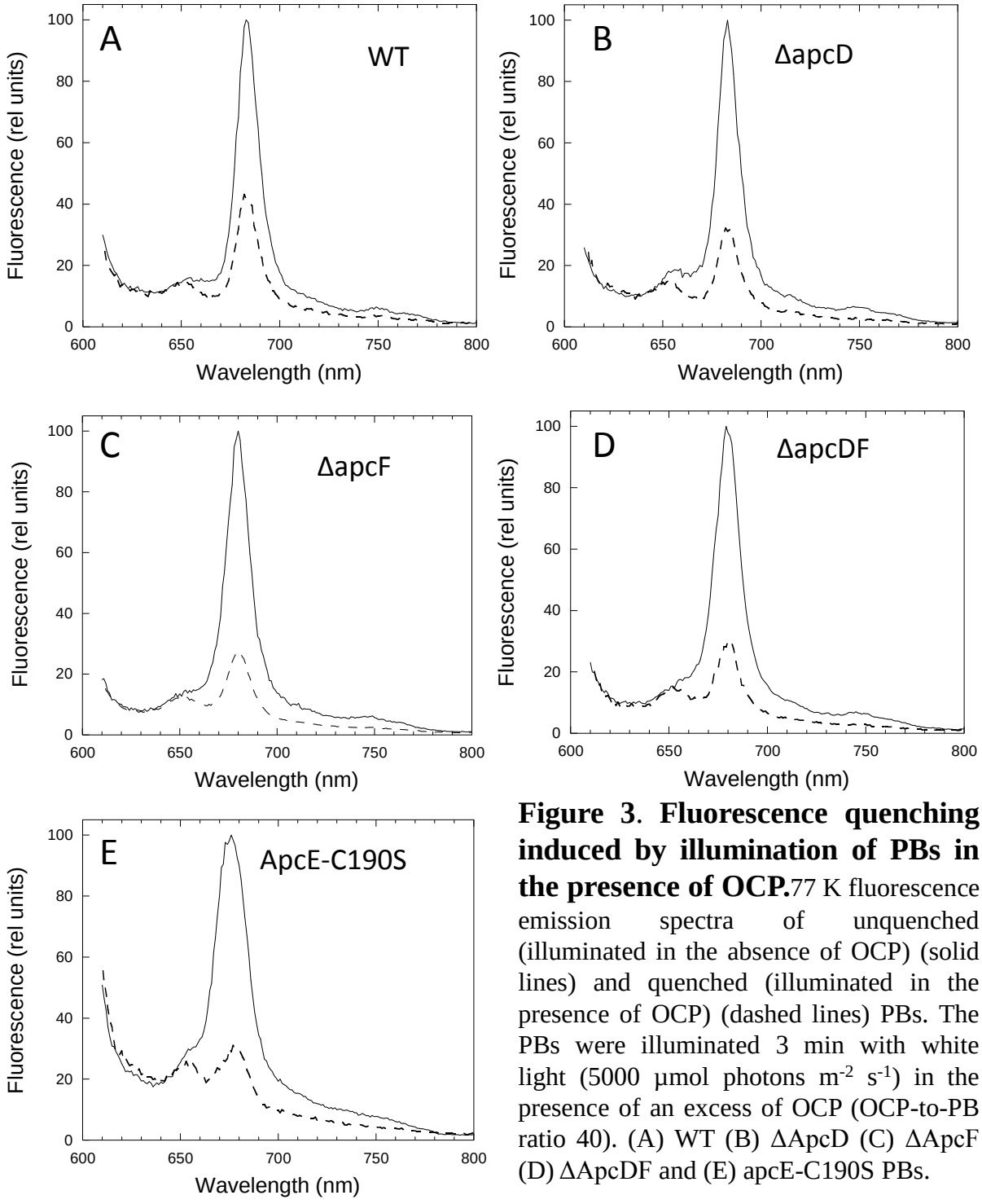

Figure 3. Fluorescence quenching induced by illumination of PBs in the presence of OCP. 77 K fluorescence emission spectra of unquenched (illuminated in the absence of OCP) (solid lines) and quenched (illuminated in the presence of OCP) (dashed lines) PBs. The PBs were illuminated 3 min with white light (5000 µmol photons m^{-2} s^{-1}) in the presence of an excess of OCP (OCP-to-PB ratio 40). (A) WT (B) ΔApcD (C) ΔApcF (D) ΔApcDF and (E) apcE-C190S PBs.

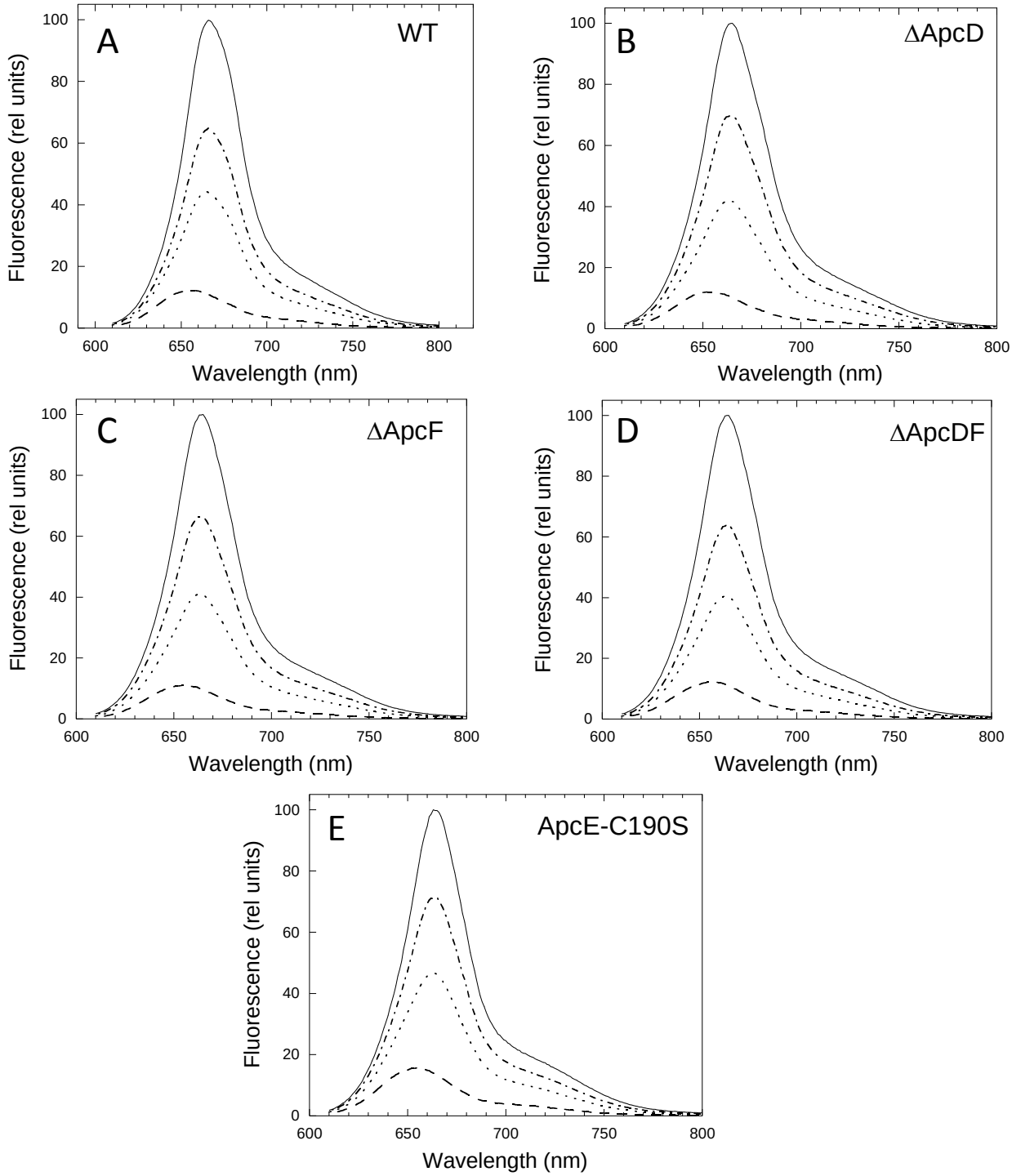

Figure 4. Influence of OCP-to-PB ratio on fluorescence quenching. Room temperature emission spectra of unquenched (illuminated in the absence of OCP) (solid lines) and quenched PBs illuminated in the presence of different OCP concentrations giving OCP-to-PB ratios of 40 (dashed), 8 (dotted) or 4 (dashed-dotted).(A) WT PBs (B) ΔApcD PBs (C) ΔApcF PBs (D) ΔApcDF PBs (E) ApcE-C190S PBs.

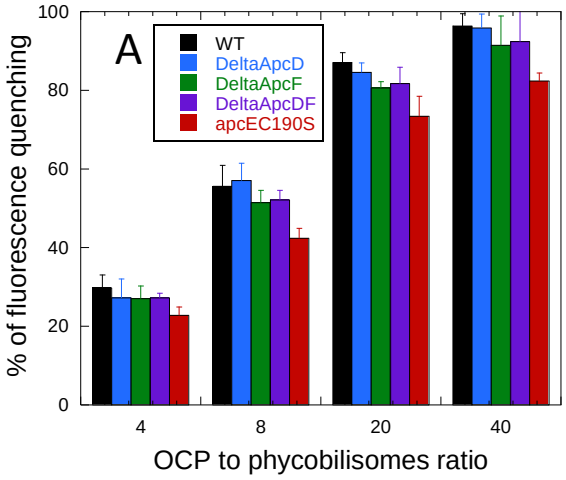

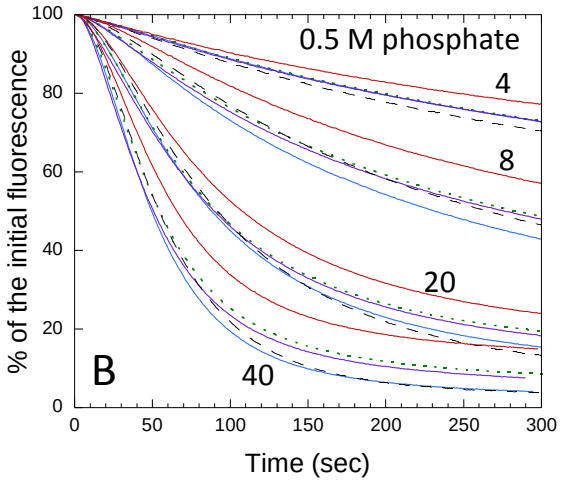

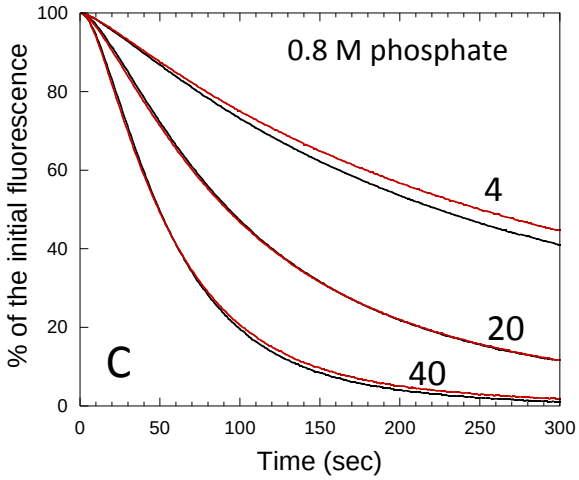

Figure 5. Kinetics of fluorescence decrease in the WT and mutated PBs illuminated in the presence of different OCP concentrations.
(A) Percentage of fluorescence quenching after 5 min of illumination with 900 µmol photons m^{-2} s^{-1} blue-green light for the WT (black), ΔApcD (blue), ΔApcF (green), ΔApcDF (violet) and pre-illuminated ApcE-C190S (red) PBs. Different OCP concentrations giving OCP-to-PB ratios of 40, 20, 8 and 4 were used. Data shows the mean (±SD) of three independent experiments.
(B) Kinetics of fluorescence decrease in WT, ΔApcD, ΔApcF, ΔApcDF and pre-illuminated ApcE-C190S PBs recorded with a PAM fluoremeter. Different OCP amounts giving an OCP-to-PB ratio of 40, 20, 8 or 4 were used with a phosphate buffer concentration of 0.5 M. Data shows the mean of three independent experiments. The colors are as in Fig 5A.
(C) Kinetics of fluorescence decrease in WT (black) and pre-illuminated ApcE-C190S PBs (red) in 0.8 M phosphate buffer with an OCP-to PB ratio of 40, 8 or 4. Data shows the mean of three independent experiments.

3.2 The OCP-related fluorescence quenching in isolated PBs: *in vitro* reconstitution

The WT and mutated PBs were illuminated in the presence of an excess of OCP. The 77 K fluorescence spectra of the PBs before and after illumination shown in Fig 3 clearly demonstrated that OCP was able to induce fluorescence quenching in all the mutated PBs. As already described in a previous article [20], the emission at 650 nm related to PC was not quenched by the OCP while 70-80% of the emission at 674-684 nm decreased. The ApcE-C190S PBs were pre-illuminated to bleach the 710 nm emission before illumination in the presence of OCP.

To further characterize the interaction between the OCP and the different mutated PBs and to look for differences in the strength of the OCP binding, the effect of OCP and phosphate concentrations were studied. The amplitude and the rate of fluorescence quenching depend on the OCP to PB ratio [20]. Lowering the phosphate concentration from 0.8 M to 0.5 M induces a decrease on the strength of OCP binding to the PBs [20]. Figure 4 shows room temperature fluorescence spectra of phycobilisomes illuminated without OCP or in the presence of 4 or 8 or 40 OCP per PB at 0.8 M phosphate. No significant differences in the amplitude of fluorescence quenching were detected between the different types of PBs.

At 0.5 M phosphate slight differences in the amplitude (Fig 5A) and the rates of fluorescence quenching were observed (Fig 5B). The most affected mutant was ApcE-C190S; the rate of fluorescence quenching was slower and the amplitude was smaller than in the WT and other mutants. This difference was not observed at 0.8 M phosphate (Fig 5C). Gwizdala et al (2011) clearly demonstrated that there is a direct relationship between the quenching extent and the OCP binding strength [20]. Thus, it seems that ApcE-C190S PBs bind OCP weakly compared to the other PBs. This hypothesis was confirmed by measurements of dark fluorescence recovery in the absence or presence of FRP. Fluorescence recovery was faster in the ApcE-C190S mutated PB than in the WT and all other mutated PBs in the absence or presence of FRP (Fig 6). As already shown in a previous publication [20], fluorescence recovery is faster in the presence of FRP, which helps the detachment of the OCP from the phycobilisome.

3.3 The blue-green light induced quenching in whole cells

Induction of fluorescence quenching by strong blue-green light was also monitored in whole WT and mutant cells using a PAM fluorometer (Fig 7). Dark adapted cells were transferred first to low intensities (30 $\mu mol.m^{-2}.s^{-1}$) and then to strong intensities (1400 $\mu mol.m^{-2}.s^{-1}$) of blue-green light. The ΔApcD, ΔApcF and ΔApcDF mutant cells presented a

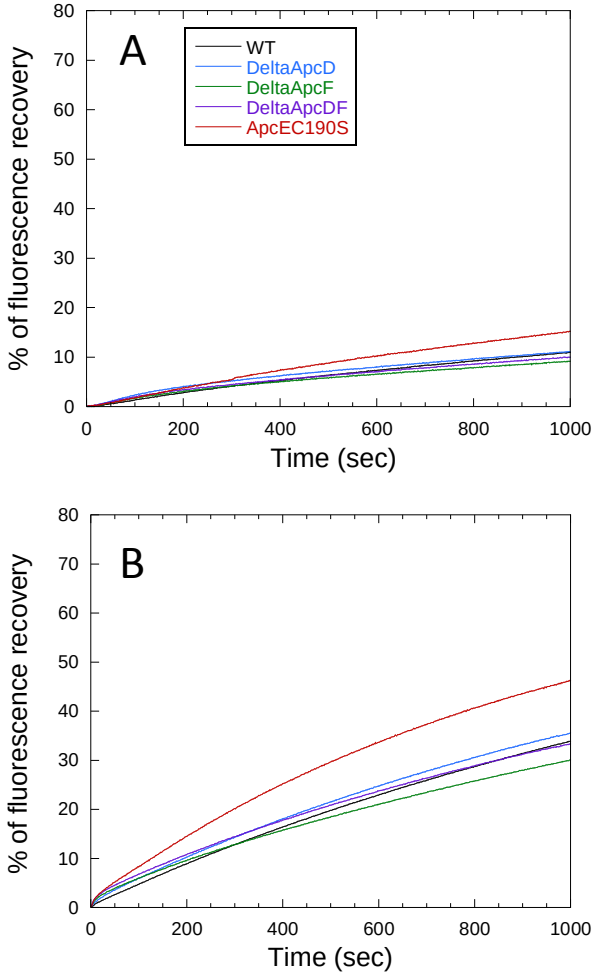

Figure 6. **Dark recovery of fluorescence in the WT and mutated PBs. Effect of FRP.** WT (black), ΔApcD (blue), ΔApcF (green), ΔApcDF (violet) and pre-illuminated ApcE-C190S (red) PBs were quenched in the presence of an excess of OCP (OCP-to-PB ratio 40). After switching off the light, the recovery of fluorescence in the absence (A) or in the presence of FRP (FRP-to-OCP ratio 40) (B) was recorded.

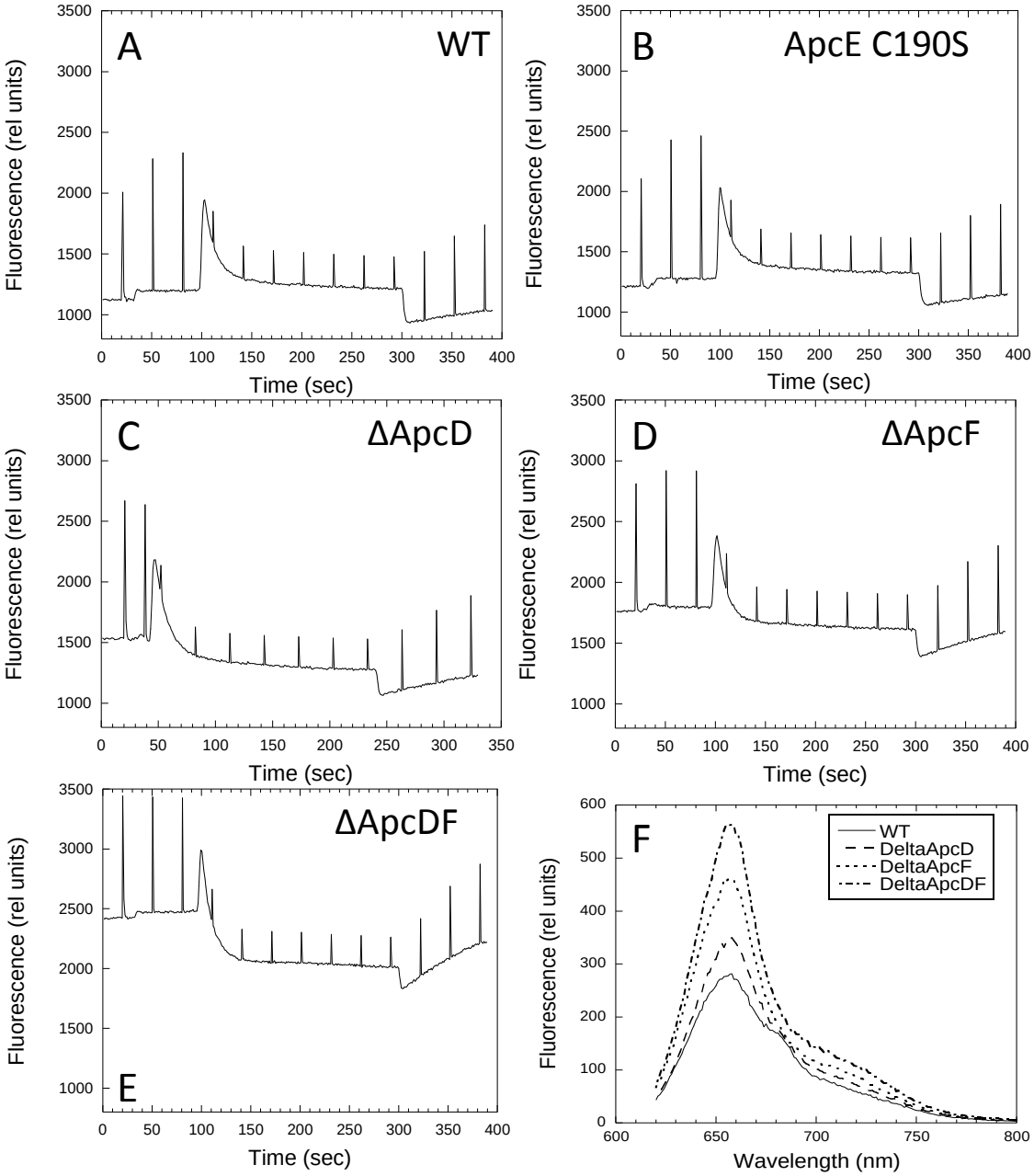

Figure 7. Changes of fluorescence levels induced by different intensities of blue-green light in WT and mutant cells. (A to E) Measurements of fluorescence yield by a PAM fluoremeter in dark adapted WT (A), ApcE-C190S (B), ΔApcD (C), ΔApcF (D) and ΔApcDF (E) cells illuminated successively with low intensity blue-green light (30 µmol photons m^{-2} s^{-1}) and strong blue-green light (1400 µmol photons m^{-2} s^{-1}). (F) Room temperature emission spectra (excitation at 590 nm) of whole cells. WT (black, solid), ΔApcD (blue, dashed), ΔApcF (green, dotted), ΔApcDF (violet, dashed-dotted).

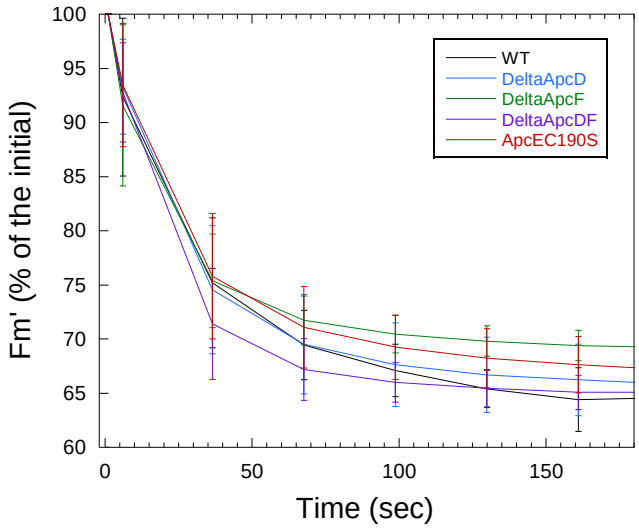

Figure 8. **OCP related fluorescence quenching in the WT and mutant cells.** Decrease of maximal fluorescence induced by illumination with strong blue-green light (1400 µmol photons m^{-2} s^{-1}) in WT (black), ΔApcD (blue), ΔApcF (green), ΔApcDF (violet) and ApcE-C190S (red) cells. Data shows the mean (± SD) of at least three independent experiments.

higher Fo level (minimal fluorescence level in dark-adapted cells). The Fo level of cyanobacteria measured in a PAM fluorometer depends on the cellular phycobiliprotein concentration and on the efficiency of energy transfer from the PBs to the reaction centers. The PAM Fluorometer uses a measuring light (650 nm) that is efficiently absorbed by the PBs [44]. Absorbance spectra showed that the ratio PC to Chl was similar in all the strains. In contrast, all these *Synechocystis* mutants are affected in energy transfer from the PBs to the reaction centers [41]. The most affected is the ΔApcDF mutant presenting the highest Fo level [41]. This was also observed in fluorescence spectra at room temperature of WT and mutant cells (Fig 7F). All spectra presented a maximum at 665 nm related to APC. However, the shoulder at 680 nm which is related to energy transfer to PSII chlorophyll was clearly visible only in WT cells. In the ΔApcD mutant, the shoulder was still visible but an increase of the 665 nm fluorescence was observed. This increase was larger in the ΔApcF and ΔApcDF mutants indicating a lower energy transfer from the PBs to the reaction centers.

In dark-adapted WT *Synechocystis* cells, the PQ pool is reduced and the cells are in the low PSII fluorescent State 2 [45, 46]. Upon illumination, a clear increase of the maximal fluorescence level (Fm') associated to a transition to State 1 was observed in WT and ApcE-C190S cells (Fig 7A and B). The transition to State 1 is induced by the oxidation of the pool of PQ that occurs in the dark to light transition. The fluorescence increase was very small in ΔApcF cells and null in ΔApcD and ΔApcDF cells (Fig 7). The lack of ApcD and ApcF largely inhibits the mechanism of state transitions [15, 41]. This was explained by the fact that in *Synechococcus* 7002, energy transfer from PBs to PSI needs ApcD while ApcF is needed to transfer energy to PSII. Thus in the *Synechococcus* PCC 7002 ΔApcD mutant, PBs always transfer the absorbed energy principally to PSII even in conditions inducing reduction of the PQ pool while in the ΔApcF mutant PBs transfer preferentially to PSI under all conditions [47]. Different results were obtained with *Synechocystis* cells, in which ApcD plays a minor role in energy transfer and ApcF is needed for energy transfer to both photosystems [41]. Energy transfer from PBs to photosystems and the causes for inhibition of state transition in ΔApcD and ΔApcF *Synechocystis* mutants are currently being re-studied in our laboratory.

Nevertheless, once the low light adapted WT and mutant cells were exposed to a strong blue-green light, fluorescence quenching was induced in all the strains (Fig 7). The amplitude and rates of quenching of maximal fluorescence were rather similar in all the strains (Fig 8). Thus, ApcD and ApcF are not required for the OCP-dependent fluorescence quenching to occur. Moreover, fluorescence quenching does not depend on the functional

connectivity of the phycobilisomes: WT and ΔApcDF phycobilisomes were similarly quenched even though the efficiency of the energy transfer from the latter PBs to the reaction centers was largely reduced. Also in *Anabaena* PCC 7120 cells, the absence of ApcD did not reduce the fluorescence quenching induced by strong blue-green light [48].

The lower and smaller fluorescence quenching observed with the isolated ApcE-C190S PBs was not detected in whole cells. *In vitro*, the non-covalent binding of the unusual chromophore and moreover the loss of this chromophore probably destabilized the conformation of the core, provoking a weaker binding of OCP. Illumination of cells even with strong intensities of white light did not induce the loss of the 710 nm emitting chromophore (Fig S3). Thus, the stability and conformation of the PB core must be less perturbed *in vivo* than *in vitro* allowing a better OCP binding. We can conclude that ApcE is not the site of fluorescence quenching.

4 Conclusions

Our results clearly demonstrated that ApcD and ApcF are not essential to the OCP-related phycobilisome fluorescence quenching. The fact that the ApcE-C190S PBs were quenched by strong blue-green light in the cells strongly suggested that the usual phycocyanobilin chromophore attached to ApcE and emitting at 680 nm is not directly involved in OCP induced quenching. This was confirmed by *in vitro* experiments, in which OCP is able to induce phycobilisome fluorescence quenching even in the absence of any chromophore attached to ApcE.

Recently spectrally-resolved picosecond fluorescence measurements on WT and OverOCP *Synechocystis* cells in the quenched and unquenched states were realized [49]. The global and target analysis of the obtained data strongly suggested that quenching takes place at the level of APC_{660} [49]. Since this conclusion depends on the model utilized and on the fitting of the data, they must be confirmed by other methods. Our results, with a completely different approach, also strongly suggest that OCP interacts with APC_{660} trimers and quenches their fluorescence.

5 Additional discussion elements (not included in the original paper)

Following this paper submission, some other groups released additional information about the quenching site in phycobilisomes. Tian and coworkers (in collaboration with our

laboratory) performed spectrally resolved picosecond fluorescence spectroscopy measurements on *Synechocystis* cells kept either under dark conditions or under strong blue-green illumination to trigger the OCP-related photoprotective mechanism. The WT, the OCP-overaccumulating strain and the OCP-deficient strain were compared [49]. A model placing the various photosynthetic pigment pools into separated compartments was built then completed through data target analysis, i.e. Species Associated Spectra (SAS) establishment, permitting to estimate the energy transfer rates between each compartment [49]. The OCP-associated trapping was integrated as an additional dissipation route and its position iteratively changed, giving satisfying fits only when placed in the APC_{660nm} pool [49]. Thus, these results confirmed that OCP^r interacts mainly with an APC_{660nm} trimer. The assessed molecular quenching rate ($(240\pm60\ fs)^{-1}$) appeared extremely fast, suggesting possible electron transfer from hECN to PCB upon quenching induction or a very rapid excitation energy transfer from PCB to the S1 state of hECN in OCP^r (Tian et al., 2011). The same approach applied to isolated phycobilisomes illuminated or not in the presence of OCP rose similar conclusions, indicating identical quenching mechanisms in vivo and in vitro (still, slightly slower quenching rate of $(500\pm50\ fs)^{-1}$ in vitro; [50]).

Submitting PSI/PSII-deficient *Synechocystis* mutant cells to non-linear laser fluorometry, Kuzminov and coworkers retrieved several parameters associated with the various phycobiliproteins – including relaxation times, effective excitation cross-sections – in a quenched versus non quenched state [51]. Their results demonstrated OCP's capacity to induce heat dissipation at the level of both APC_{660nm} and APC_{680nm}; however, the actual amount of energy diverted from each pigment type remained unquantified [51]. This globally agrees with our own findings designating no terminal emitter (APC_{680nm}) as absolutely required for the OCP-related photoprotective mechanism: in the absence of APC_{680nm}, OCP^r can still interact with APC_{660nm}. Tian and coworkers ([49]; [50])) have demonstrated that APC_{660nm} mainly gets quenched but could not completely rule out a small amount of heat dissipation at the level of APC_{680nm}.

Stadnichuk and coworkers isolated ApcE from *Synechocystis* phycobilisomes then tested its interaction with OCP in vitro. They showed a small fluorescence decrease when ApcE was illuminated in the presence of OCP ([52]; [53]). However, the very acidic solution employed for ApcE solubilization (63 mM formic acid pH 2.5) plus the addition of urea did not mimic physiological conditions and significantly modified OCP^o/OCP^r absorption spectra suggesting a partial denaturation of the OCP (see Fig.1 in [52]). Thus, whether the quenching observed also occurs in vivo seems questionable. In addition, APC_{660nm} trimers were purified then

illuminated in the presence of OCP at various phosphate concentrations without any visible effect; OCP appeared unable to interact with *isolated* APC trimers [52]. More than discarding the possibility of any contact between OCP and APC_{660nm}, this last result suggests that it can occur only in well assembled phycobilisome cores.

From all these experimental results, several conclusions can be drawn: 1) OCP^r induces quenching at the level of APC_{660nm} mainly ([49]; this chapter) and to a small extent at the ;level of APC_{680nm} ([51]; [52]; [53]) 2) the OCP^r -binding phycobilisome subunit does not necessarily corresponds to the quenching site (that could be a neighboring subunit); OCP attachment does not depend on ApcD and ApcF presence (this chapter; Stadnichuk [52]) 3) the specific interactions between OCP and phycobilisomes could need fully assembled APC cores 4) the extremely fast quenching rates observed ([49]; [50]) suggest either direct excitation energy transfer from a PCB to the OCP-bound hECN or electron transfer from this hECN to PCB upon strong blue-green illumination, which triggers heat dissipation.

Supplementary data

Primer name	Primer sequence
FD_NotI (+*Not*I)	5’-CATTGCGGCCGCCATTGTTGCTGCCGGTTTAG-3’
RD_XhoI (+*Xho*I)	5’-CCCGTACTCGAGGGCTGAGGATTATCGTGATC-3’
FF_NotI (+*Not*I)	5’-GTAAGCGGCCGCCCTAGCCATGAATTTAACCG-3’
RF_XhoI (+*Xho*I)	5’-CCCGATCTCGAGGGATAAACTCCGTCAGTTGC-3’
FE_NotI (+*Not*I)	5’-CAACGCGGCCGCGCCATTCAATCAAGTTCTCC-3’
RE_XhoI (+*Xho*I)	5’-CGGCAACTCGAGGCTTAACTTTTCCACTGGGC-3’
FE_PmlI (AGAAGT ->ACACGT) (+*Pml*I)	5’-CCAGCCGAAGATGGGACACGTGGACAAAACCTGACAAAAATTC-3’
RE_PmlI (ACTTCT ->ACGTGT) (+*Pml*I)	5’-GAATTTTTGTCAGGTTTTGTCCACGTGTCCCATCTTCGGCTGG-3’
FE_C190S (TGTTCCATCGAT ->TCTTCCATTGAT) (-*Cla*I)	5’-GTCATTGAAAATGCCT**C**TTCCATTGATGCCACC-3’
RE_C190S (ATCAATGGAACA -> ATCGATGGAAGA, (-*Cla*I)	GGTGGCATCAATGGAAGAGGCATTTTCAATGAC

Supplementary table 1. Oligonucleotides used for PCR. The point mutations introduced by mutagenesis are indicated in red. The restriction sites created are underlined.

A ΔapcD mutant construction.

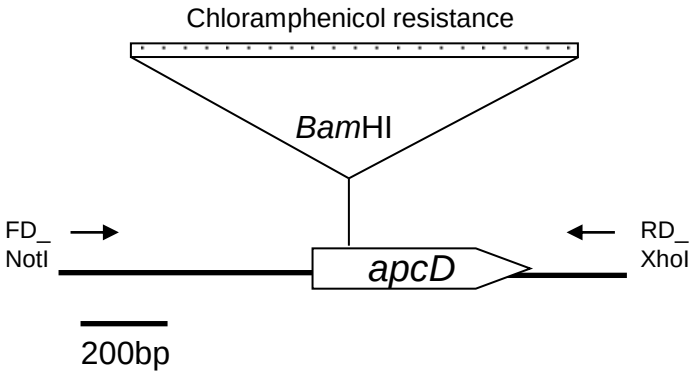

B ΔapcF mutant construction.

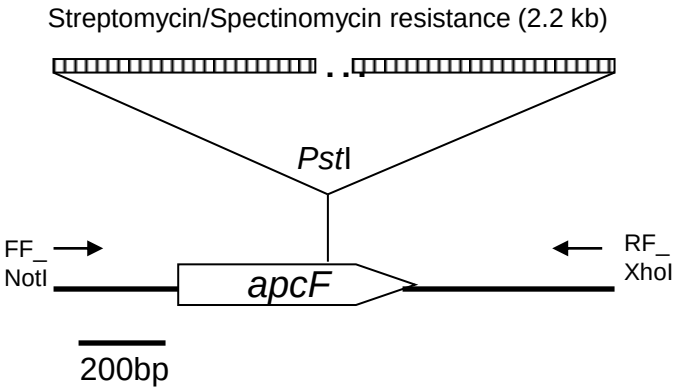

C apcEC190S mutant construction.

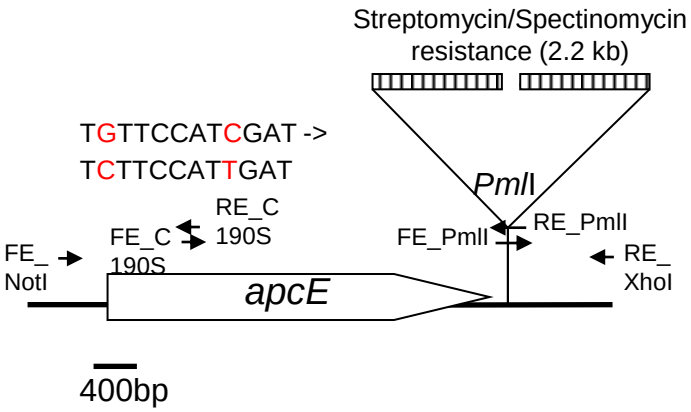

Supplemantary figure 1. Mutants construction in *Synechocystis* PCC 6803. The positions of the oligonucleotides, restriction sites and point mutations used are indicated. (A) ΔapcD mutant construction (B) ΔapcF mutant construction. The ΔapcDF double mutant combines both constructions. (B) apcEC190S mutant construction.

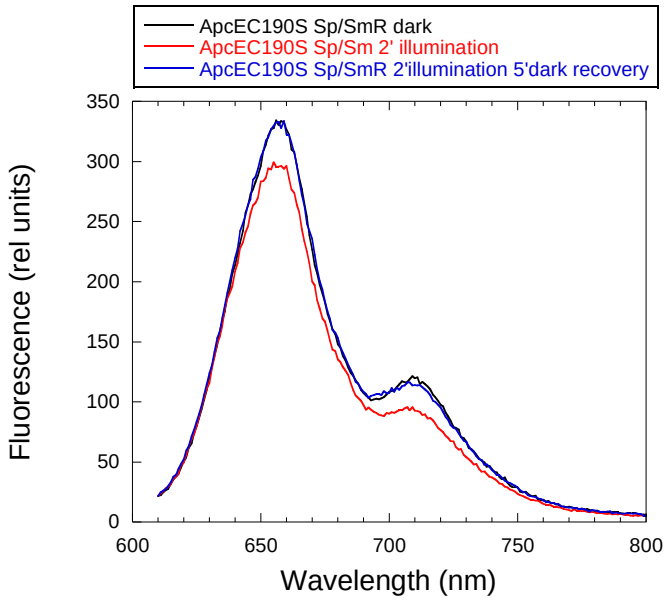

Supplemantary figure 2. Effect of strong white light on ApcEC190S cells fluorescence. Room temperature emission spectra represent dark adapted ApcEC190S cells (black), the same cells illuminated for 2 min with 5000 µmol m-2 s-1 white light to induce quenching (red) and after 5 min of dark recovery (blue). During illumination both 660 nm and 710 nm emissions decreased similarly and both recovered during the dark incubation. This result indicates that *in vivo* the chromophore emitting at 710 nm is not photobleached and remains attached to the phycobilisome.

Acknowledgements

We thank Adjélé Wilson for technical help and useful discussions. We thank Dr Ghada Ajlani for stimulating discussions. This work was supported by the CNRS, the CEA and the European Marie Curie Research Training Network Grant HARVEST (FP project n° 238017). MG has a fellowship from the HARVEST project. DJ has a fellowship from the French Research Ministry.

References

[1] Y. Nishiyama, S.I. Allakhverdiev, N. Murata, Protein synthesis is the primary target of reactive oxygen species in the photoinhibition of photosystem II, Physiol. Plant. 142 (2011) 35-46.

[2] I. Vass, Role of charge recombination processes in photodamage and photoprotection of the photosystem II complex, Physiol. Plant. 142 (2011) 6-16.

[3] P. Horton, A.V. Ruban, R.G. Walters, Regulation of light harvesting in green plants, Annu. Rev. Plant Physiol. Plant Mol. Biol. 47 (1996) 655-684.

[4] D. Kirilovsky, The photoactive orange carotenoid protein and photoprotection in cyanobacteria, Adv. Exp. Med. Biol. 675 (2010) 139-159.

[5] K.K. Niyogi, Photoprotection revisited: Genetic and molecular approaches, Annu. Rev. Plant Physiol. Plant Mol. Biol. 50 (1999) 333-359.

[6] N. Adir, Elucidation of the molecular structures of components of the phycobilisome: reconstructing a giant, Photosynth. Res. 85 (2005) 15-32.

[7] A.N. Glazer, Phycobilisome - a macromolecular complex optimized for light energy-transfer, Biochim. Biophys. Acta 768 (1984) 29-51.

[8] A.R. Grossman, M.R. Schaefer, G.G. Chiang, J.L. Collier, The phycobilisome, a light-harvesting complex responsive to environmental-conditions, Microbiol. Rev. 57 (1993) 725-749.

[9] R. MacColl, Cyanobacterial phycobilisomes, J. Struct. Biol. 124 (1998) 311-334.

[10] A.A. Arteni, G. Ajlani, E.J. Boekema, Structural organisation of phycobilisomes from *Synechocystis* sp. strain PCC6803 and their interaction with the membrane, Biochim. Biophys. Acta 1787 (2009) 272-279.

[11] A. McGregor, M. Klartag, L. David, N. Adir, Allophycocyanin trimer stability and functionality are primarily due to polar enhanced hydrophobicity of the phycocyanobilin binding pocket, J. Mol. Biol. 384 (2008) 406-421.

[12] G. Ajlani, C. Vernotte, Deletion of the PB-loop in the Lcm subunit does not affect phycobilisome assembly or energy transfer functions in the cyanobacterium *Synechocystis* sp. PCC 6714, Eur. J. Biochem. 257 (1998) 154-159.

[13] G. Ajlani, C. Vernotte, L. Dimagno, R. Haselkorn, Phycobilisome Core Mutants of *Synechocystis* PCC 6803, Biochim. Biophys. Acta 1231 (1995) 189-196.

[14] G. Shen, S. Boussiba, W.F. Vermaas, *Synechocystis* sp PCC 6803 strains lacking photosystem I and phycobilisome function, Plant Cell 5 (1993) 1853-1863.

[15] J.D. Zhao, J.H. Zhou, D.A. Bryant, Energy transfer processes in phycobilisomes as deduced from mutational analyses, Photosynth. Res. 34 (1992) 83-83.

[16] D.A. Bryant, Cyanobacterial phycobilisomes: progress towards a complete structural and functional analysis via molecular genetics, in: L. Bogorad, I.K. Vasil (Eds.), The molecular biology of plastids and mitochondria, Academic Press, New York, 1991, pp. 257-300.

[17] V. Capuano, A.S. Braux, N. Tandeau de Marsac, J. Houmard, The "anchor polypeptide" of cyanobacterial phycobilisomes. Molecular characterization of the *Synechococcus* sp. PCC 6301 *apcE* gene, J. Biol. Chem. 266 (1991) 7239-7247.

[18] V. Capuano, J.C. Thomas, N. Tandeau de Marsac, J. Houmard, An *in vivo* approach to define the role of the L_{CM}, the key polypeptide of cyanobacterial phycobilisomes, J. Biol. Chem. 268 (1993) 8277-8283.

[19] A. Wilson, G. Ajlani, J.M. Verbavatz, I. Vass, C.A. Kerfeld, D. Kirilovsky, A soluble carotenoid protein involved in phycobilisome-related energy dissipation in cyanobacteria, Plant Cell 18 (2006) 992-1007.

[20] M. Gwizdala, A. Wilson, D. Kirilovsky, In vitro reconstitution of the cyanobacterial photoprotective mechanism mediated by the Orange Carotenoid Protein in Synechocystis PCC 6803, Plant Cell 23 (2011) 2631-2643.

[21] M.G. Rakhimberdieva, I.V. Elanskaya, W.F.J. Vermaas, N.V. Karapetyan, Carotenoid-triggered energy dissipation in phycobilisomes of *Synechocystis* sp. PCC 6803 diverts excitation away from reaction centers of both photosystems, Biochim. Biophys. Acta 1797 (2010) 241-249.

[22] M. Scott, C. McCollum, S. Vasil'ev, C. Crozier, G.S. Espie, M. Krol, N.P. Huner, D. Bruce, Mechanism of the down regulation of photosynthesis by blue light in the Cyanobacterium *Synechocystis* sp. PCC 6803, Biochemistry 45 (2006) 8952-8958.

[23] A. Wilson, C. Punginelli, A. Gall, C. Bonetti, M. Alexandre, J.M. Routaboul, C.A. Kerfeld, R. van Grondelle, B. Robert, J.T. Kennis, D. Kirilovsky, A photoactive

carotenoid protein acting as light intensity sensor, Proc. Natl. Acad. Sci. U. S. A. 105 (2008) 12075-12080.

[24] C. Boulay, L. Abasova, C. Six, I. Vass, D. Kirilovsky, Occurrence and function of the orange carotenoid protein in photoprotective mechanisms in various cyanobacteria, Biochim. Biophys. Acta 1777 (2008) 1344-1354.

[25] D. Kirilovsky, C.A. Kerfeld, The orange carotenoid protein in photoprotection of photosystem II in cyanobacteria, Biochim. Biophys. Acta (2011).doi: 10.1016/j.bbabio.2011.04.013

[26] S. Fulda, S. Mikkat, F. Huang, J. Huckauf, K. Marin, B. Norling, M. Hagemann, Proteome analysis of salt stress response in the cyanobacterium *Synechocystis* sp. strain PCC 6803, Proteomics 6 (2006) 2733-2745.

[27] Y. Hihara, A. Kamei, M. Kanehisa, A. Kaplan, M. Ikeuchi, DNA microarray analysis of cyanobacterial gene expression during acclimation to high light, Plant Cell 13 (2001) 793-806.

[28] A.K. Singh, E. Thanura, M. Bhattacharyya-Pakrasi, R. Aurora, B. Ghosh, H.B. Pakrasi, Intergration of carbon and nitrogen metabolism with energy production is crucial to light acclimation in the cyanobacterium *Synechocystis*, Plant Physiol. 148 (2008) 467-478.

[29] A. Wilson, C. Boulay, A. Wilde, C.A. Kerfeld, D. Kirilovsky, Light-induced energy dissipation in iron-starved cyanobacteria: roles of OCP and IsiA proteins, Plant Cell 19 (2007) 656-672.

[30] T.K. Holt, D.W. Krogmann, A carotenoid-protein from cyanobacteria, Biochim. Biophys. Acta 637 (1981) 408-414.

[31] Y.P. Wu, D.W. Krogmann, The orange carotenoid protein of *Synechocystis* PCC 6803, Biochim. Biophys. Acta 1322 (1997) 1-7.

[32] C.A. Kerfeld, M.R. Sawaya, V. Brahmandam, D. Cascio, K.K. Ho, C.C. Trevithick-Sutton, D.W. Krogmann, T.O. Yeates, The crystal structure of a cyanobacterial water-soluble carotenoid binding protein, Structure 11 (2003) 55-65.

[33] A. Wilson, J.N. Kinney, P.H. Zwart, C. Punginelli, S. D'Haene, F. Perreau, M.G. Klein, D. Kirilovsky, C.A. Kerfeld, Structural determinants underlying photoprotection in the photoactive orange carotenoid protein of cyanobacteria, J. Biol. Chem. 285 (2010) 18364-18375.

[34] C. Punginelli, A. Wilson, J.M. Routaboul, D. Kirilovsky, Influence of zeaxanthin and echinenone binding on the activity of the Orange Carotenoid Protein, Biochim. Biophys. Acta 1787 (2009) 280-288.

[35] A. Wilson, C. Punginelli, M. Couturier, F. Perrau, D. Kirilovsky, Essential role of two tyrosines and two tryptophans on photoprotection activity of the Orange Carotenoid Protein, Biochim. Biophys. Acta 1807 (2011) 293-301.

[36] M.Y. Gorbunov, F.I. Kuzminov, V.V. Fadeev, J.D. Kim, P.G. Falkowski, A kinetic model of non-photochemical quenching in cyanobacteria, Biochim. Biophys. Acta (2011) doi: 10.1016/j.bbabio.2011.08.009

[37] M.G. Rakhimberdieva, F.I. Kuzminov, I.V. Elanskaya, N.V. Karapetyan, *Synechocystis* sp. PCC 6803 mutant lacking both photosystems exhibits strong carotenoid-induced quenching of phycobilisome fluorescence, FEBS Lett. 585 (2011) 585-589.

[38] C. Boulay, A. Wilson, S. D'Haene, D. Kirilovsky, Identification of a protein required for recovery of full antenna capacity in OCP-related photoprotective mechanism in cyanobacteria, Proc. Natl. Acad. Sci. U. S. A. 107 (2010) 11620-11625.

[39] M. Herdman, S.F. Delaney, N.G. Carr, A new medium for the isolation and growth of auxotrophic mutants of the blue-green alga *Anacystis nidulans,* J. Gen. Microbiol. 79 (1973) 233-237.

[40] Y.P. Cai, C.P. Wolk, Use of a conditionally lethal gene in *Anabaena* sp. strain PCC 7120 to select for double recombinants and to entrap insertion sequences, J. Bacteriol. 172 (1990) 3138-3145.

[41] M.K. Ashby, C.W. Mullineaux, The role of ApcD and ApcF in energy transfer from phycobilisomes to PSI and PSII in a cyanobacterium, Photosynth. Res. 61 (1999) 169-179.

[42] Y.M. Gindt, J. Zhou, D.A. Bryant, K. Sauer, Spectroscopic studies of phycobilisome subcore preparations lacking key core chromophores: assignment of excited state energies to the L_{cm}, β^{18} and $\alpha^{AP\text{-}B}$ chromophores, Biochim. Biophys. Acta 1186 (1994) 153-162.

[43] Y.M. Gindt, J. Zhou, D.A. Bryant, K. Sauer, Core mutations of Synechococcus sp. PCC 7002 phycobilisomes: a spectroscopic study, J Photochem. Photobiol. B 15 (1992) 75-89.

[44] D. Campbell, V. Hurry, A.K. Clarke, P. Gustafsson, G. Öquist, Chlorophyll fluorescence analysis of cyanobacterial photosynthesis and acclimation, Microbiol. Mol. Biol. Rev. 62 (1998) 667-683.

[45] P.J. Dominy, W.P. Williams, The role of respiratory electron flow in the control of excitation energy distribution in blue-green-algae, Biochim. Biophys. Acta 892 (1987) 264-274.

[46] C.W. Mullineaux, J.F. Allen, State 1 - State 2 transitions in the Cyanobacterium *Synechococcus* 6301 are controlled by the redox state of electron carriers between Photosystem I and Photosystem II, Photosynth. Res. 23 (1990) 297-311.

[47] C. Dong, A. Tang, J. Zhao, C.W. Mullineaux, G. Shen, D.A. Bryant, ApcD is necessary for efficient energy transfer from phycobilisomes to photosystem I and helps to prevent photoinhibition in the cyanobacterium *Synechococcus* sp. PCC 7002, Biochim. Biophys. Acta 1787 (2009) 1122-1128.

[48] C. Dong, J. Zhao, ApcD is required for state transition but not involved in blue-light induced quenching in the cyanobacterium *Anabaena* sp. PCC7120, Chi. Sci. Bull. 53 (2008) 3422-3424.

[49] L. Tian, I.H. van Stokkum, R.B. Koehorst, A. Jongerius, D.L. Kirilovsky, H. van Amerongen, Site, rate and mechanism of photoprotective quenching in cyanobacteria, J. Am. Chem. Soc. 133 (2011) 18304-18311.

[50] L. Tian, M. Gwizdala, I.H. van Stokkum, R.B. Koehorst, D. Kirilovsky, H. can Amerongen, Picosecond kinetics of light harvesting and photoprotective quenching in wild-type and mutant phycobilisomes isolated from the cyanobacterium *Synechocystis* PCC 6803, Biophys. J. 102 (2012) 1692-1700.

[51] F.I. Kuzminov, N.V. Karapetyan, M.G. Rakhimberdieve, I.V. Elanskaya, M.Y. Gorbunov, V.V. Fadeev, Investigation of OCP-triggered dissipation of excitation energy in PSI/PSII-less *Synechocystis* sp. PCC 6803 mutant using non-linear laser fluorometry, Biochim. Biophys. Acta 1817 (2012) 1012-1021.

[52] I.N. Stadnichuk, M.F. Yanyushin, E.G. Maksimov, E.P. Lukashev, S.K. Zharmukhamedov, I.V. Elanskaya, V.Z. Paschenko, Site of non-photochemical quenching of the phycobilisome by orange carotenoid protein in the cyanobacterium *Synechocystis* sp. PCC 6803, Biochim. Biophys. Acta 1817 (2012) 1436-1445.

[53] I.N. Stadnichuk, M.F. Yanyushin, G. Bernat, D.V. Zlenko, P.M. Krasilnikov, E.P. Lukashev, E.G. Maksimov, V.Z. Paschenko, Fluorescence quenching of the

phycobilisome terminal emitter LCM from the cyanobacterium *Synechocystis* sp. PCC 6803 detected *in vivo* and *in vitro*, J. of Photochem. Photobiol. B 125 (2013) 137-145

Chapter 2

Specificity of the cyanobacterial Orange Carotenoid Protein: Influences of OCP and phycobilisome structures

Summary of work

Cyanobacterial strains containing hemidiscoidal phycobilisomes with 2 (e.g. *Synechococcus elongatus* PCC 7942), 3 (e.g. *Synechocystis*) or 5 (e.g. *Anabaena variabilis*) APC cylinders per core naturally exist (reviewed in: McColl, 1998); some of them do not possess any OCP encoding gene (e.g. *Synechococcus elongatus*) (Boulay et al., 2008). After determining that OCP binds an APC_{660nm} subunit, we wondered how phycobilisome core architecture influences this attachment.

We then performed an in vitro assay aimed at evaluating the interactions between 4 phycobilisome types representative of the diversity described hereabove and 2 different OCPs. Protocols were developed allowing intact phycobilisome isolation. *Synechocystis* mutant strains overexpressing the *Synechocystis ocp* or *Arthrospira ocp* genes were constructed then the corresponding proteins purified. We tested the various OCP-phycobilisome combinations regarding fluorescence quenching induction in several buffer conditions, playing on phosphate concentration that seemed critical for OCP-phycobilisome complexes stabilization (Gwizdala et al., 2011).

Our results mainly suggested that 1) OCP with close aminoacid sequences and crystal structures can behave very differently in vitro regarding phycobilisome binding, 2) the number of APC cylinders in the core has no influence on OCP binding 3) other criteria concerning phycobilisome core architecture, like the distance between trimers, probably influence the ability of a given phycobilisome to interact with a given OCP.

Contribution to this work

I made all the molecular biology and most of the biochemistry/ the spectroscopy work described here; A.Thurotte participated in phycobilisomes isolation, characterization and OCP photoactivity study; R.L. Leverenz and C.A. Kerfeld helped for structural analyses.

This chapter is based on: Jallet D, Thurotte A, Leverenz RL, Perreau F, Kerfeld CA, Kirilovsky D (2013) Specificity of the cyanobacterial Orange Carotenoid Protein: Influences of OCP and phycobilisome structures. Plant Physiol pp.113.229997

Specificity of the cyanobacterial Orange Carotenoid Protein: Influences of OCP and phycobilisome structures

Denis Jallet [1,2], Adrien Thurotte[1,2], Ryan L. Leverenz[3] , François Perreau[4], Cheryl A. Kerfeld[3,5,6,7] and Diana Kirilovsky[1,2]

[1]Commissariat à l'Energie Atomique (CEA), Institut de Biologie et Technologies de Saclay (iBiTec-S), 91191 Gif sur Yvette, France

[2]Centre National de la Recherche Scientifique (CNRS), UMR 8221, 91191 Gif sur Yvette, France

[3]DOE-MSU Plant Research Laboratory, Michigan State University, East Lansing, Michigan 48824

[4]Institut Jean-Pierre Bourgin, UMR 1318 INRA-AgroParisTech, INRA Versailles-Grignon, Route de Saint Cyr, F-78026 Versailles, France

[5]Lawrence Berkeley National Laboratory, Berkeley, California 94720

[6]Department of Plant and Microbial Biology, University of California, Berkeley, California 94720

[7]Berkeley Synthetic Biology Institute, University of California, Berkeley 94720

Corresponding Author:

Diana Kirilovsky, iBiTec-S, Bât 532, CEA Saclay, 91191 Gif sur Yvette, FRANCE; Tel : 33-1-69089571; Fax : 33-1-69088717;

E-mail: diana.kirilovsky@cea.fr

ABSTRACT

Cyanobacteria have developed a photoprotective mechanism that decreases the energy arriving at the reaction centers by increasing thermal energy dissipation at the level of phycobilisome (PB), the extramembranous light harvesting antenna. This mechanism is triggered by the photoactive Orange Carotenoid Protein (OCP), which acts both as the photosensor and the energy quencher. The OCP binds the core of the PB. The structure of this core differs in diverse cyanobacterial strains. Here, using two isolated OCPs and four classes of PBs, we demonstrated that differences exist between OCPs related to PB binding, photoactivity and carotenoid binding. *Synechocystis* OCP, but not *Arthrospira* OCP, can attach echinenone in addition to hydroxyechinenone. *Arthrospira* OCP binds more strongly than *Synechocystis* OCP to all types of PBs. *Synechocystis* OCP can strongly bind only its own PB in 0.8 M potassium phosphate. However, if the *Synechocystis* OCP binds to the PB at very high phosphate concentrations (~1.4 M), it is able to quench the fluorescence of any type of PBs, even those isolated from strains that lack the OCP-mediated photoprotective mechanism. Thus, the determining step for induction of photoprotection is the binding of the OCP to PBs. Our results also indicated that the structure of PBs, at least *in vitro*, significantly influences OCP binding and the stabilization of OCP-PB complexes. Finally, the fact that the OCP induced large fluorescence quenching even in the two cylinder core of *Synechococcus elongatus* phycobilisomes strongly suggested that OCP binds to one of the basal APC cylinders.

INTRODUCTION

The cyanobacterial Orange Carotenoid Protein (OCP) is a photoactive soluble protein of 35 kDa which binds a ketocarotenoid, 3'hydroxyechinenone (hECN). It is present in the majority of phycobilisome-containing cyanobacterial strains (Kirilovsky and Kerfeld, 2012, 2013). The phycobilisomes (PBs) are light harvesting extramembrane complexes formed by a core from which rods radiate. The core and rods are constituted of water soluble blue and red phycobiliproteins, which covalently attach bilins (for reviews about phycobilisomes, see (Glazer, 1984; Grossman et al., 1993; MacColl, 1998; Tandeau de Marsac, 2003; Adir, 2005). The OCP was first described by Holt and Krogmann in 1981 (Holt and Krogmann, 1981) and its structure was determined in 2003 (Kerfeld et al., 2003). However, its function was discovered only in 2006 (Wilson et al., 2006) and its photoactivity in 2008 (Wilson et al., 2008). The OCP is essential in a photoprotective mechanism that decreases the energy arriving at the reaction centers under high irradiance. Strong light induces thermal dissipation of the energy absorbed by the PBs resulting in a decrease of PB fluorescence emission and of energy transfer from the PBs to the reaction centers (Wilson et al., 2006). This process, which is light intensity dependent, is induced by blue or green light but not by orange or red light (Rakhimberdieva et al., 2004; Wilson et al., 2006). The absorption of strong blue-green light by the OCP induces changes in the conformation of the carotenoid, converting the inactive orange dark form (OCP^o) into an active red form (OCP^r)(Wilson et al., 2008). In OCP^o, the hECN is in an all-trans-configuration (Kerfeld et al., 2003; Polivka et al., 2005). In OCP^r, the apparent conjugation length of the carotenoid increases, resulting in a less distorted, more planar structure (Wilson et al., 2008). FTIR spectra showed that conformational changes in the protein are also induced (Wilson et al., 2008) that are essential for the induction of the photoprotective mechanism. Only OCP^r is able to bind to the core of PBs and to induce thermal energy dissipation (Wilson et al., 2008; Punginelli et al., 2009; Gorbunov et al., 2011; Gwizdala et al., 2011). Since the photoactivation of the OCP has a very low quantum yield (0.03; (Wilson et al., 2008)), the concentration of activated protein is zero in darkness and very low under low light conditions (Wilson et al., 2008; Gorbunov et al., 2011). Thus, the photoprotective mechanism functions only under high light conditions.

The crystal structures of the *Arthrospira maxima* OCP and of the *Synechocystis* PCC 6803 (hereafter *Synechocystis*) OCP were solved in 2003 and 2010, respectively (Kerfeld et al., 2003; Wilson et al., 2010). These structures, assumed to correspond to the dark OCP^o form, are essentially identical. The OCP consists of an all α-helical N-terminal domain

(residues 1-165), unique to cyanobacteria, and an α/β C-terminal domain which is member of the nuclear transport factor 2 superfamily (residues 191-320, *Synechocystis* numbering). Both domains are joined by a linker (residues 166-190, *Synechocystis* numbering) that appears to be flexible. The hECN molecule spans the N- and C-terminal domains of the protein with its carbonyl end embedded in and hydrogen bonded to two absolutely conserved residues (Tyr201 and Trp288) in the C-terminal domain. The carotenoid is almost entirely buried; only 3.4% of the 3'-hECN is solvent exposed (Kerfeld et al., 2003). *Synechocystis* OCP can also bind with high affinity echinenone (ECN) and zeaxanthin. While the ECN OCP is photoactive, the zeaxanthin OCP is photoinactive (Punginelli et al., 2009), indicating the importance of the carotenoid carbonyl group for photoactivity. The largest interface through which the two domains interact and through which the carotenoid passes is stabilized by a small number hydrogen bonds, including one formed between Arg155 and Glu244 (Wilson et al., 2010). This salt bridge stabilizes the closed structure of OCP^{o}. Upon illumination, protein conformational changes cause the breakage of this bond and the opening of the protein (Wilson et al., 2012). Arg155, which becomes more exposed upon the separation of the two domains is essential for the OCP^{r} binding to the PBs (Wilson et al., 2012).

After exposure to high irradiance, when the light intensity decreases, recovery of full antenna capacity and fluorescence requires another protein, the Fluorescence Recovery Protein (FRP) (Boulay et al., 2010). The active form of this soluble 13 kDa protein is a dimer (Sutter et al., 2013). It interacts with the OCP^{r} C-terminal domain (Boulay et al., 2010; Sutter et al., 2013). This accelerates the red to orange OCP conversion and helps the OCP to detach from the PB (Boulay et al., 2010; Gwizdala et al., 2011).

Genes encoding the full length OCP are found in the vast majority of cyanobacteria but not in all; 90 of 127 genomes recently surveyed contain at least one gene for a full-length OCP (Kirilovsky and Kerfeld, 2013). The genomes of *Synechococcus elongatus* and *Thermosynechococcus elongatus*, two cyanobacterial strains used as model organisms in photosynthesis and stress studies, do not contain a full-length *ocp* gene. These strains also lack FRP and β-carotene ketolase (involved in ketocarotenoid synthesis). As a consequence, these strains lack the OCP-related photoprotective mechanism and they are more sensitive to fluctuating light intensities (Boulay et al., 2008).

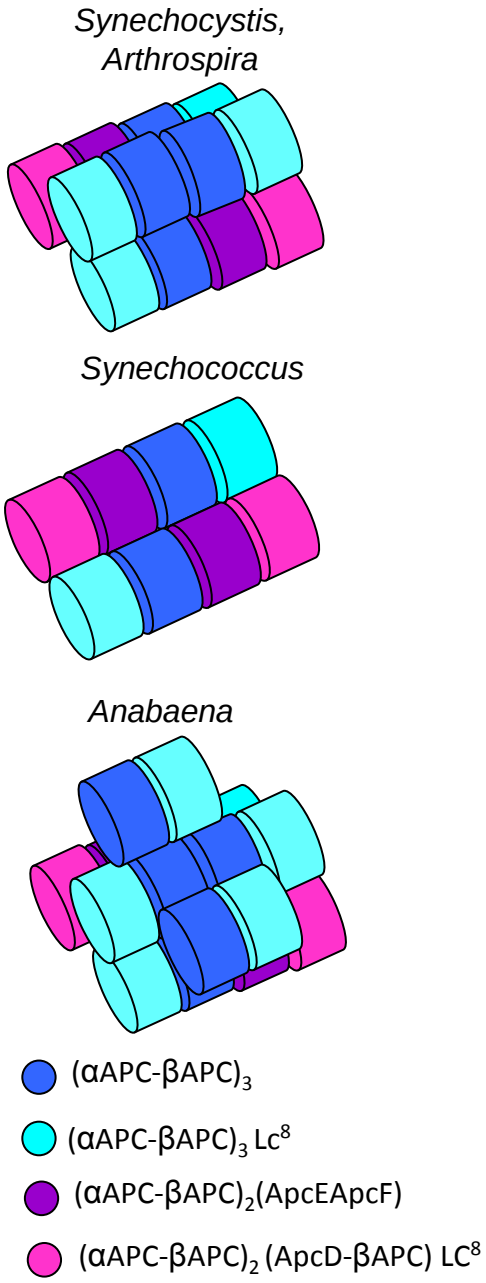

Figure 1. Schematic orthogonal projections of the various PB cores.
In the PBs containing three or five cylinders, the top complete cylinder is formed by four αAPC-βAPC trimers emitting at 660nm. Each of the basal cylinders of three type of PBs, contains two αAPC-βAPC trimers emitting at 660 nm and two trimers emitting at 683 nm. In one of them one αAPC is replaced by ApcD and in the other one αAPC-βAPC is replaced by the dimer ApcF-ApcE. In the 5 cylinder PBs, two additional semi-cylinders formed by two αAPC-βAPC trimers are present In all the cylinders, the 2 external trimers include a 8.7 kDa linker protein (ApcC).

The core of the hemidiscoidal PBs of *Synechocystis*, the model organism routinely used for the study of the OCP-related photoprotective mechanism, consists of 3 cylinders, each one formed by 4 trimers of allophycocyanin (APC) (Fig. 1) (for reviews about PBs: Glazer, 1984; Bryant, 1991; Grossman et al., 1993; MacColl, 1998; Adir, 2005). The APC trimers are predominantly assembled from a two-subunit heterodimer, αAPC-βAPC, which binds 2 phycocyanobilins, one in each subunit. Of the twelve total APC trimers in the PB core, eight are trimers of αAPC-βAPC. These trimers have a maximal emission at 660 nm (APC_{660}). The upper cylinder contains only APC_{660} trimers. In contrast, each basal cylinder contains only 2 APC_{660} trimers. Each basal cylinder also contains: 1.) a trimer in which one αAPC subunit is replaced by a special αAPC-like subunit called ApcD, and 2.) a trimer in which one β subunit is replaced by ApcF, a βAPC-like subunit, and one α subunit is replaced by the N-terminal domain of ApcE, an αAPC-like domain (Fig.1). The trimers containing one or two of these special subunits have a maximal emission at 680 nm (APC_{680}). In each cylinder the 2 external trimers are stabilized by an 8.7 kDa linker protein.

The C-terminal part of *Synechocystis* ApcE contains 3 interconnected repeated domains of about 120 residues (called Rep) which are similar to the conserved domains of rod linkers. Each Rep domain interacts with an APC trimer situated in different cylinders and thus this stabilizes the core of PB (Zhao et al., 1992; Shen et al., 1993; Ajlani et al., 1995; Ajlani and Vernotte, 1998). The ApcE protein also determines the number of APC cylinders that form the PB core (Capuano et al., 1991; Capuano et al., 1993). Indeed, there are PBs containing only the two basal cylinders, as in *Synechococcus elongatus* (ex *Synechococcus elongatus* PCC 7942) and *Synechococcus* PCC 6301. In these strains, the ~72 kDa ApcE posseses only 2 Rep domains. There also exists pentacylindrical cores in which in addition to the three cylinders existing in *Synechocystis* PBs , there are two other cylinders, each formed by two APC_{660} trimers, for example in *Anabaena variabilis*, *Anabaena* PCC 7120 and *Mastigocladus laminosus* (see (Glauser et al., 1992; Ducret et al., 1998)). In the pentacylindrical PBs, ApcE (~125 kDa) contains 4 Rep domains (Capuano et al., 1993). Finally, ApcE is also involved in the interaction between the PB and the thylakoids.

The bicylindric and tricylindric cores are surrounded by six rods formed generally by 3 hexamers of the blue phycocyanin (PC) or two PC hexamers and one hexamer containing phycoerythrin or phycoerythrincyanonin. The rods and the hexamers are stabilized by non-chromophorylated linker proteins. A linker protein, $L_{RC,}$ also stabilizes the binding of the rods to the core. The pentacylindric PBs can contain up to 8 rods. The quantity and length of rods

and the presence of phycoerythrin or phycoerythrocyanin at the periphery of the rods depends on environmental conditions like light intensity or quality (Kipe-Nolt et al., 1982; Glauser et al., 1992).

The OCP most probably binds to one of the APC_{660} trimers (Tian et al., 2011; Jallet et al., 2012; Tian et al., 2012) and the presence of the rods stabilizes this binding to *Synechocystis* PBs (Gwizdala et al., 2011). The different structures of PBs in other strains could affect the binding of the OCP. Thus, we undertook a study about the relationship between the structure of PBs and OCP binding in preparation for introducing the OCP-related photoprotective mechanism into *S. elongatus* using *Synechocystis* genes. In this study we used the *in vitro* reconstitution system developed by Gwizdala et al. (Gwizdala et al., 2011) with three different types of isolated phycobilisomes : *Arthrospira platensis* PCC7345 (hereafter called *Arthrospira*) PBs, having a tricylindrical core like *Synechocystis* PBs, *Anabaena variabilis* (hereafter called *Anabaena*) PBs having a pentacylindrical core and *Synechococcus elongatus* PCC 7942 (hereafter *Synechococcus*) PBs having a bicylindrical core. We also used two different OCPs, the *Synechocystis* OCP and the *Arthrospira* OCP. Each OCP was isolated from mutant *Synechocystis* cells overexpressing one or the other *ocp* genes with a C-terminal His-tag.

RESULTS

Phycobilisome isolation and characterization

To isolate PBs *Synechocystis, Arthrospira, Anabaena* and *Synechococcus* cells were broken in a highly concentrated K-Phosphate buffer (0.8 M to 1 M). Triton X100 was then used to solubilize membranes and release PBs in the aqueous phase. This phase was collected and deposited on sucrose gradients. After ultracentrifugation, fully assembled PBs concentrated in a well-defined dark blue band at the bottom 0.75 M sucrose layer (details in Materials and Methods).

The protein composition of the isolated PBs was analyzed by SDS-PAGE. The major phycobiliproteins, α/β subunits of phycocyanin (PC) or allophycocyanin (APC), appeared as intense bands in the region between 16 and 20 kDa (Fig.2A, B). Bands for ApcD and ApcF completely overlapped them. The rod-to-core and rod linkers (L^{RC}, L^{R}) were distributed from 27 to 35 kDa (Fig.2A,B). The molecular mass (MM) of these proteins slightly differed in the 4 strains as previously described in the literature (Lundell et al., 1981; Ducret et al., 1996;

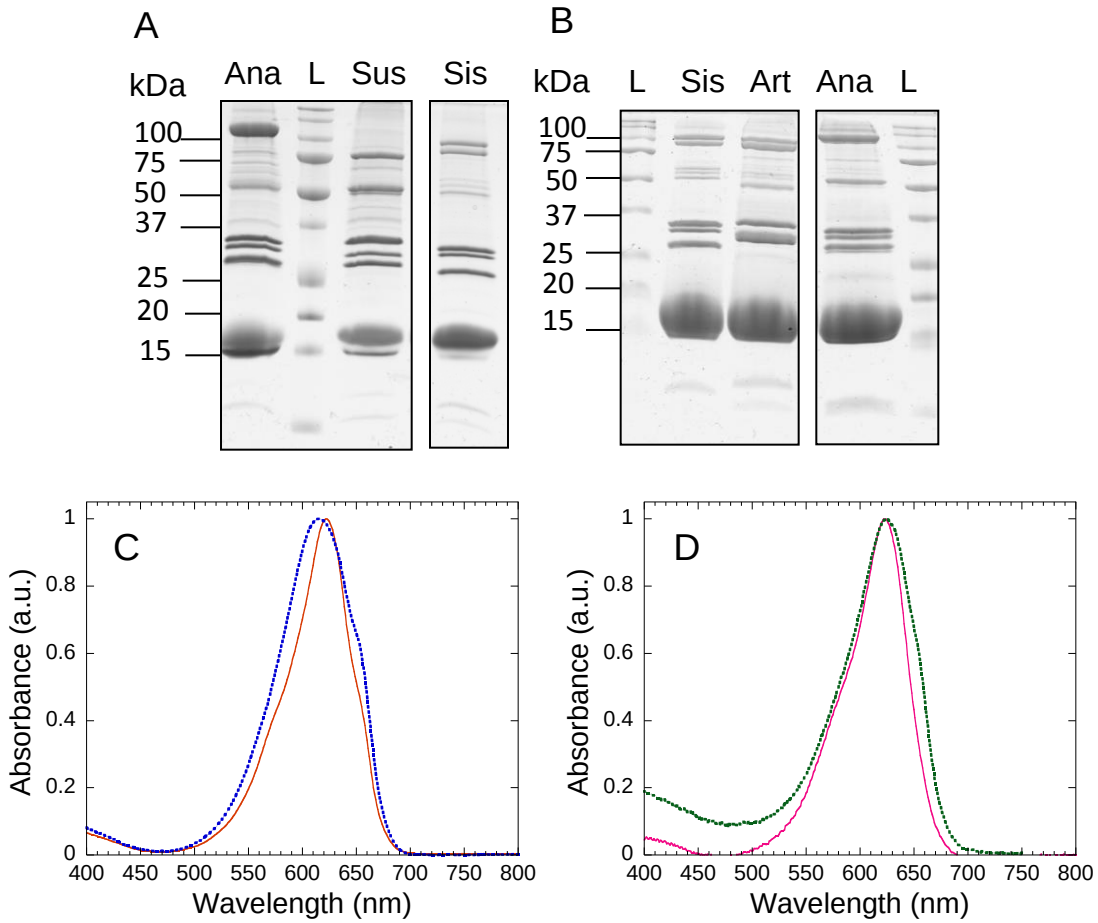

Figure 2. Composition analysis of the various PBs A) Polypeptide composition of the isolated *Anabaena* PBs (Ana), *Synechococcus* PBs (Sus) and *Synechocystis* PBs (Sis). L: Ladder B) Polypeptide composition of the isolated *Synechocystis* PBs (Sis), *Arthrospira* PBs (Art) and *Anabaena* PBs (Ana). L: Ladder C) and D) Room-temperature (RT) absorption spectra of the PBs isolated from C) *Synechocystis* (continuous orange line) and *Arthrospira* (dashed blue line) D) *Synechococcus* (continuous pink line) and *Anabaena* (dashed green line). Spectra are normalized at the maximum of absorbance around 620nm.

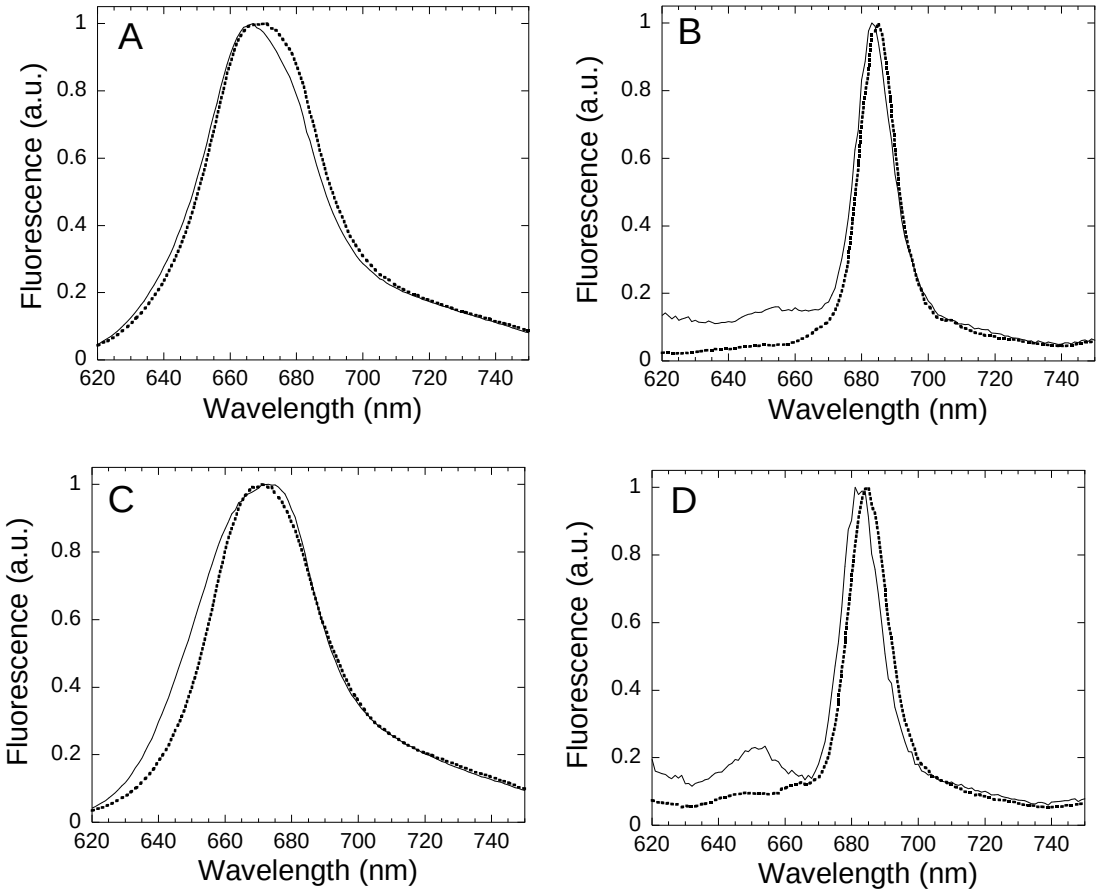

Figure 3. **Room temperature (A and C) and 77K (B and D) fluorescence emission spectra of the isolated PBs.** A) and B) *Synechocystis* PBs (continuous line) are compared to *Arthrospira* PBs (dashed line), C) and D) *Synechococcus* PBs (continuous line) are compared to *Anabaena* PBs (dashed line). Spectra are normalized to the maximum of emission. Excitation at 590nm.

Nomsawai et al., 1999; Piven et al., 2005) . ApcE (Lcm) had a higher MM, between 75 and 125 kDa, depending on PB architecture. In *Anabaena*, where PB cores contain 5 APC cylinders, the MM of ApcE was 120 kDa. The MM of ApcE was only 95 kDa in PBs containing 3 APC cylinders (*Synechocystis, Arthrospira*) and 75 kDa in PBs containing 2 APC cylinders (*Synechococcus*) (Fig.2A,B). The small rod (10 kDa) and core (8.7 kDa) linkers were barely detected in our SDS-PAGE gel.

Absorption spectra were recorded to obtain further insights into the relative quantities of PC and APC in the isolated PBs. PC, which is the most abundant phycobiliprotein in the PB, has a maximum of absorbance at 620 nm for *Synechocystis*, *Synechococcus* and *Anabaena* PBs (Fig.2 C, D). The absorbance band was larger and the maximum shifted to 615 nm in *Arthrospira* PBs (Fig.2C), owing to the fact that some α^{PC} subunits bind phycobiliviolin instead of phycocyanobilin (Babu et al., 1991). A more or less pronounced shoulder could be seen at 650 nm, related to APC absorbance. The PC to APC ratio was estimated by fitting the observed spectra to a combination of PC and APC absorbance spectra. As expected, the PC to APC ratio was higher in *Synechococcus* PBs (~4.6) and lower in *Anabaena* PBs (~1.3) than in *Synechocystis* PBs (~3). Such differences correlate well with the PB core architectures, *Synechococcus* containing less and *Anabaena* more APC cylinders than *Synechocystis*. *Arthrospira* PBs seemed to contain less PC than *Synechocystis* PBs. The ratio PC to APC in *Arthrospira* PBs was approximately 2 as already described in (Nomsawai et al., 1999). In *Anabaena* and *Arthrospira* phycobilisomes, the rods seemed to contain only two PC hexamers as observed in (Ducret et al., 1996; Nomsawai et al., 1999).

Fluorescence emission spectra were used to confirm functional energy transfer in the PBs. In intact PBs at room temperature, excitation flows from PC to APC which in turn equilibrates with terminal emitters (ApcD, ApcF, ApcE). That results in a fluorescence peak with maximum at around 670 nm (at room temperature) when the PC is preferentially excited (excitation light at 590 nm) (Fig3.A, C). At 77 °K, energy back-flow becomes less probable, so excitation arriving to the terminal emitters gets trapped. A fluorescence peak appeared at 683-684 nm for *Arthrospira, Anabaena* and *Synechocystis* PBs (Fig.3B, D), which was slightly blue-shifted in *Synechococcus* PBs (681 nm) (Fig.3D). Disconnected PC resulted in a small band at 645 nm especially in *Synechococcus* PBs (Fig.3C, D). Altogether, these data indicated that the isolated PBs were well assembled and functionally connected.

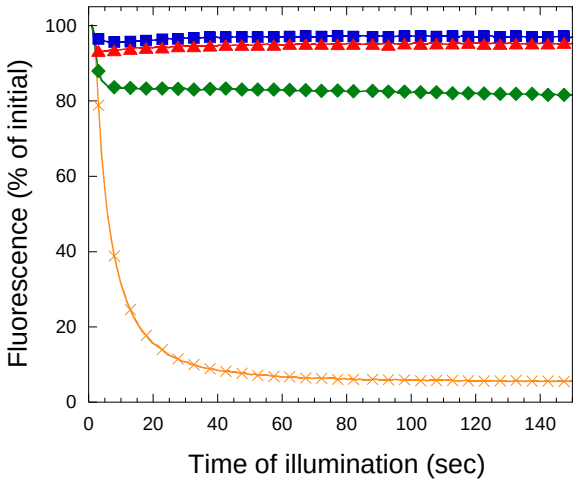

Figure 4. Fluorescence quenching induced by *Synechocystis* OCP in vitro. The PBs (0.012µM) were illuminated with blue-green light (900µmol.m^{-2}.s^{-1}) in the presence of an excess of pre-converted *Synechocystis* OCP^{r} (0.48µM; 40 per PB) at 23°C and 0.8M K-Phosphate. Fluorescence decrease was measured using a PAM fluorometer for *Synechocystis* PBs (orange crosses), *Arthrospira* PBs (blue squares), *Synechococcus* PBs (red triangles) and *Anabaena PBs* (green diamonds).

Quenching in vitro using *Synechocystis* OCP

To test whether *Synechocystis* OCP can interact with the different PBs and trigger their fluorescence quenching, an *in vitro* reconstitution system was employed (Gwizdala et al., 2011). *Synechocystis* OCP was isolated from a *Synechocystis* mutant strain overexpressing the *ocp* gene and lacking the β-carotene hydroxylase (CrtR). In this strain the OCP binds only echinenone (ECN) (neither zeaxanthin nor 3'-hECN). The ECN-binding OCP isolated from the ΔCrtR strain is photoactive and induces a large blue-light induced fluorescence quenching in cells (Punginelli et al., 2009; Wilson et al., 2011).

Reconstitution experiments require a minimum of 0.8 M phosphate to maintain PB integrity. However, it was already demonstrated that such high phosphate concentrations hinder OCP photoactivation (Gwizdala et al., 2011). In the experiments described here, the OCP was converted to the red form before being mixed with the PB solution. OCP conversion from its orange/inactive form (OCP^o) to its red/active one (OCP^r) was triggered with strong white light in Tris-HCl buffer at 4°C. OCP^r was then added to a PB solution in 0.8 M K-Phosphate buffer under continuous blue-green illumination (900 µmolphotons.m^{-2}.s^{-1}) and the fluorescence quenching was followed using a PAM fluorometer (Gwizdala et al., 2011). After *Synechocystis* OCP^r addition, the *Synechocystis* PBs fluorescence decreased strongly and rapidly (95% in 50s) (Fig.4). Almost no effect was observed on the other PBs. For *Anabaena* PBs only a slight quenching (20%) could be seen, which became even smaller for *Synechococcus* and *Arthrospira* PBs (~3%) (Fig.4). This indicates that *Synechocystis* OCP interacts poorly with PBs from other strains, or that it cannot trigger their fluorescence quenching under conditions in which it strongly interacts with *Synechocystis* PBs (0.8 M phosphate).

***Arthrospira* OCP purification**

The next question addressed was whether all OCPs are specific to their cognate PBs. Since *Arthrospira* OCP is also well characterized and its structure is known we selected it to test for OCP-PB specificity. No method is known that allows introducing modifications in the *Arthrospira* genome, precluding the production of His-tagged OCP in *Arthrospira* cells. Thus, a region containing the *Arthrospira ocp* and *frp* genes was cloned into the pPSBA2 plasmid (Lagarde et al., 2000). A sequence encoding for six histidine residues was added at the 3' end of the *Arthrospira ocp* gene, which was under control of the strong *psbA2* promoter.

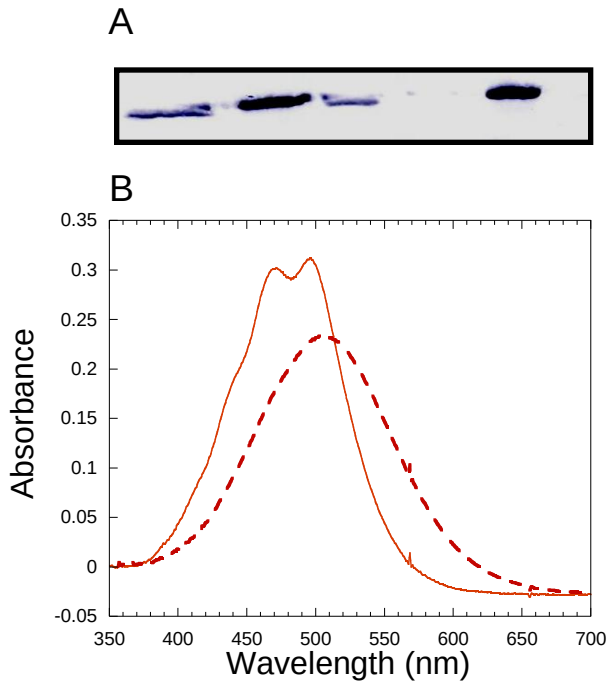

Figure 5. **Isolation of *Arthrospira* OCP**. A) Immunoblot detection using a primary antibody directed against *Arthrospira* OCP on whole cells extracts of WT (lane 1), oApOCPWT (lane 2), ΔCrtR (lane 3), oApOCPΔCrtR (lane 4) and oSynOCPΔCrtR cells (lane 5); 3µg Chlorophyll deposited per well. B) Absorbance spectra of the dark orange from (OCP^o; orange continuous line) and the photoactivated red form (OCP^r; red dashed line) of *Arthrospira* OCP isolated from oApOCPWT cells.

Synechocystis WT and ΔCrtR cells were then transformed using the resulting plasmid. In the mutants obtained, the endogenous *Synechocystis ocp* gene (*slr1963*) was interrupted by introduction of a Sp/Sm resistance cassette. This last step led to the oApOCPWT and oApOCPΔCrtR *Synechocystis* mutants, producing *Arthrospira* OCP. Additional details are described in Material and Methods.

Western blot analysis of cell extracts using a primary antibody directed against *Arthrospira maxima* OCP permitted estimation of the OCP content in mutant and WT *Synechocystis* cells (Fig.5A). The Western blot revealed a 35 kDa band corresponding to the OCP. The band was much stronger in oApOCPWT cells than in WT *Synechocystis* cells, indicating a large accumulation of *Arthrospira* OCP in this mutant. By contrast, almost no OCP was detected in the oApOCPΔCrtR strain. For comparison, it is shown that in oSynOCPΔCrtR (strain over-accumulating *Synechocystis* OCP), the *Synechocystis* OCP content was largely higher than in ΔCrtR. Thus, *Arthrospira* OCP is unable to accumulate in a strain lacking hECN while *Synechocystis* OCP is not affected by the lack of this carotenoid (see also (Wilson et al., 2011). *Arthrospira* OCP was purified from oApOCPWT cells, using a protocol similar to that developed for *Synechocystis* OCP isolation (Wilson et al., 2008) (Materials and Methods). In the dark, the absorbance spectrum of the isolated *Arthrospira* OCP showed peaks at 467 nm and 496 nm as well as a shoulder around 440 nm (Fig.5B). This spectrum is identical to those already published for *Arthrospira maxima* (Holt and Krogmann, 1981; Polivka et al., 2005) and *Synechocystis* OCP (Wilson et al., 2008). After illumination OCP^o converted to its red form. Its absorbance spectrum matched the one of *Synechocystis* OCP^r (Fig.5B). The carotenoid content of the isolated *Arthrospira* OCP was analyzed by High-Performance Liquid Chromatography. hECN was detected in 81% of OCPs, while the 19% remaining OCPs bound ECN (Fig.S1)).

Arthrospira OCP photoactivation kinetics were then studied. OCP^r accumulation under illumination results in an increase of the 550 nm absorbance (Fig.5B) that can be monitored over time. Fig.6A compares the photoactivation kinetics of hECN-*Arthrospira* and ECN-*Synechocystis* OCPs at 9 and 23°C. At both temperatures, *Arthrospira* OCP^o converted faster to OCP^r ($t_{1/2\sim}$37s and 10s respectively) than *Synechocystis* OCP^o ($t_{1/2\sim}$62s and 14s respectively). In addition, with recovery to the orange form being non-negligible at 23°C, only 62.9% of the *Arthrospira* OCP and 54.5% of the *Synechocystis* OCP were in the red form at equilibrium. A similar difference in the kinetics of photoconversion was observed when ECN-*Arthrospira* OCP was compared with the ECN-*Synechocystis* OCP (supplementary Fig.2), thus indicating that the differences in kinetics were not due to

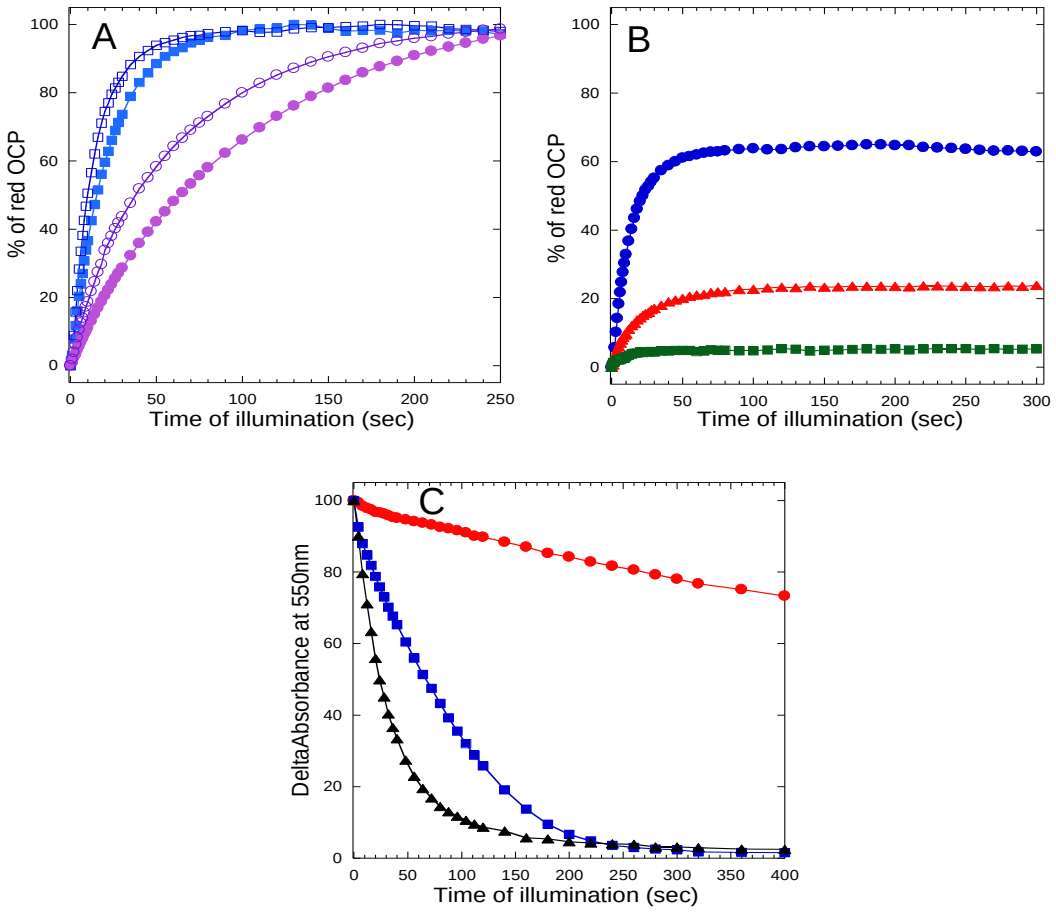

Figure 6. **Light driven photoconversion and dark recovery of *Arthrospira* OCP.** *Arthrospira* OCP^{o} (1.8µM) was illuminated using strong white light (5000µmol.m^{-2}.s^{-1}) and its A_{550nm} recorded over time. A) In Tris-HCl 40mM pH 8, comparing *Synechocystis* OCP (closed symbols) and *Arthrospira* OCP (opened symbols) at 23°C (squares) or 9°C (circles). Data normalized to the final % of red form in each condition. B) At 23°C, *Arthrospira* OCP being kept in Tris-HCl 40mM (blue circles), 0.8M K-Phosphate (red triangles) or 1.4M K-Phosphate (green squares) during its photoconversion. Data normalized to the final % of red form at 9°C. C) After *Arthrospira* OCP photoconversion, the light source was turned off and A_{550nm} evolution was followed at 9°C with (blue squares) or without (red circles) FRP addition (1 per 2 OCP). Recovery was also followed at 23°C (black triangles). Data normalized to the initial absorbance at 550nm.

differences in the bound carotenoid. These experiments were made in Tris-HCl 40mM and did not mimic the buffer conditions applied for quenching reconstitution, i.e. high phosphate concentration (Gwizdala et al., 2011). Indeed, high phosphate concentration also affected the accumulation of *Arthrospira* OCP^r as in the case of *Synechocystis* OCP^r (Gwizdala et al., 2011). Only 24% of *Arthrospira* OCP was converted to the red form at 0.8 M phosphate and 5.3 % at 1.4 M phosphate at 23°C (Fig. 6B).

Recovery from OCP^r to OCP^o was also studied (Fig.6C). At 9°C, in Tris-HCl 40 mM, *Arthrospira* OCP^r recovers very slowly while at 23°C it reverts to OCP^o rapidly ($t_{1/2\sim}$22s), similar to *Synechocystis* OCP (Wilson et al., 2008). Addition of the Fluorescence Recovery Protein (FRP) from *Synechocystis* largely accelerated the conversion of OCP^r to OCP^o at 9°C ($t_{1/2}$ from 15 min to 60 s, Fig 6C) indicating that *Arthrospira* OCP is able to interact with *Synechocystis* FRP.

Quenching in vitro using *Arthrospira* OCP

The decrease of fluorescence yield induced by strong blue-green light in WT, oApOCPWT, oApOCPΔCrtR and oSynOCPΔCrtR *Synechocystis* cells is compared in Fig 7A. As expected, due to the low concentration of the OCP in the oApOCPΔCrtR strain (Fig 5A), almost no fluorescence quenching was observed in this strain. In contrast, in the oApOCPWT strain, strong blue-green light induced a huge fluorescence quenching as in the oSynOCPΔCrtR strain (60% drop in about 50s). In vitro, when *Synechocystis* PBs were illuminated in the presence of *Arthrospira* OCP^r at 0.8 M phosphate, *Arthrospira* OCP rapidly quenched almost all PB fluorescence with kinetics similar to that of *Synechocystis* OCP (Fig.7B). Thus, *Arthrospira* OCP is able to interact with *Synechocystis* PBs *in vivo* and *in vitro* and to quench their fluorescence.

Fig.7C reveals that *Arthrospira* OCP^r was also able to induce a large quenching of *Synechococcus, Arthrospira* and *Anabaena* PBs fluorescence in 0.8 M K-Phosphate buffer; in contrast *Synechocystis* OCP^r was inactive (Fig.4). Illumination of PBs in the absence of OCP did not induce any fluorescence quenching (Fig 7C). In *Anabaena* PBs, a fast and large magnitude fluorescence decrease occurred (68% decrease in 10s) followed by a slow regain phase related to dislodging of the OCP from the PB and partial reconversion of OCP^r to OCP^o in the solution (9s to 300s, final quenching 57.2%). Similar profiles were observed with *Synechococcus* PBs (40.7% decrease after 8s, 17.7% at 300s) and *Arthrospira* PBs (40.8% after 34s, 22.75% at 300s). Thus, *Arthrospira* OCP seems to be less specific than

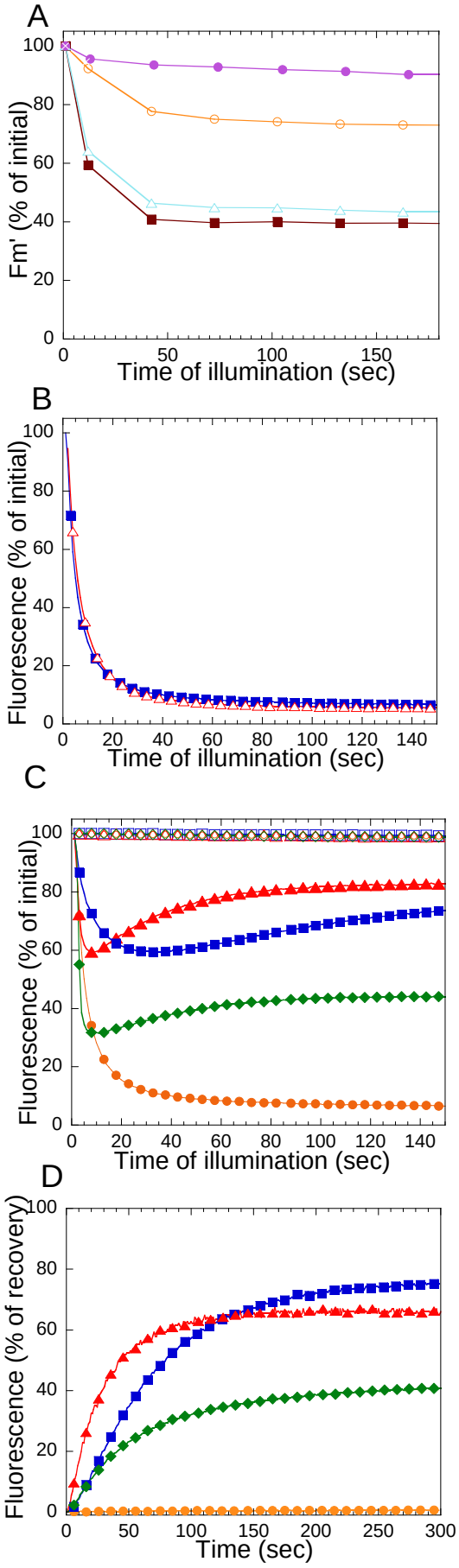

Figure 7. **Fluorescence quenching induced by Arthrospira OCP in vitro and in vivo**

A) Fluorescence quenching triggered by strong blue-green light (1400 µmol photons.m^{-2}.s^{-1}) in *Synechocystis* WT (orange open circles), oSynOCPΔCrtR (cyan open triangles), oApOCPWT (brown closed squares) and oApOCPΔCrtR cells (purple closed circles) at 33°C.

B) Isolated *Synechocystis* PBs were illuminated with blue-green light (900µmol.m^{-2}.s^{-1}) in the presence of an excess of preconverted *Synechocystis* OCP^{r} (orange triangles) or *Arthrospira* OCP^{r} (blue squares) (0.48µM: 40 per PB) at 0.8M K-Phosphate, 23°C.

C) Fluorescence quenching induced by strong blue-green light (900µmol.m^{-2}.s^{-1}) at 0.8 M K-Phosphate in the absence (open symbols) or in the presence of an excess of *Arthrospira* OCP^{r}

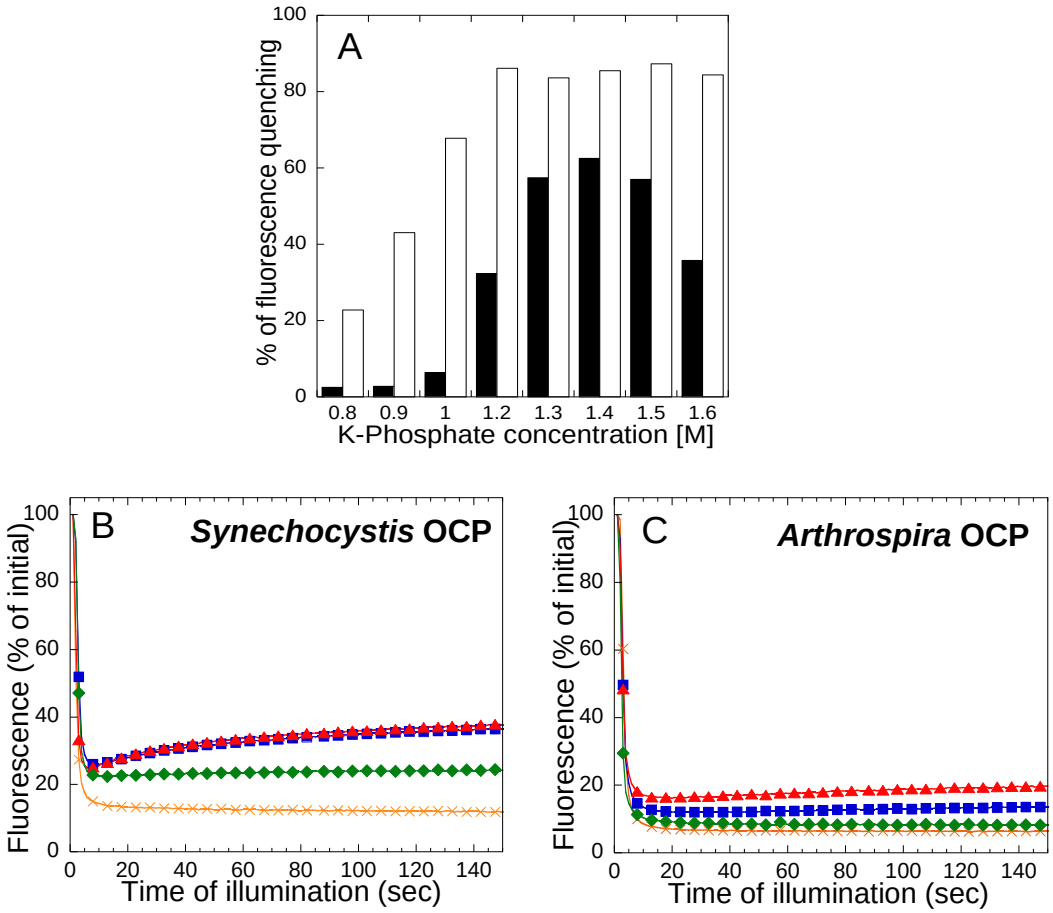

Figure 8. **Effect of K-phosphate concentration on PBs fluorescence quenching.** PBs (0.012µM) were illuminated with blue-green light (900µmol.m^{-2}.s^{-1}) in the presence of pre-converted OCP^{r} (0.48µM; 40 per PB) at 23°C. A) % of *Arthrospira* PB fluorescence quenching reached after 5 min illumination in the presence of *Synechocystis* OCP^{r} (black) or *Arthrospira* OCP^{r} (white) in increasing K-Phosphate concentration from 0.8M to 1.6M. B) Fluorescence decrease induced by *Synechocystis* OCP^{r} in *Synechocystis* PBs (orange crosses), *Arthrospira* PBs (blue squares), *Synechococcus* PBs (red triangles) and *Anabaena* PBs (green diamonds) at 1.4M K-Phosphate. C) Fluorescence decrease induced by *Arthrospira* OCP^{r} in *Synechocystis* PBs (orange crosses), *Arthrospira* PBs (blue squares), *Synechococcus* PBs (red triangles) or *Anabaena* PBs (green diamonds)

Synechocystis OCP. Moreover, it seems to interact more strongly with *Synechocystis* and *Anabaena* PBs than with *Arthrospira* PBs. This was also illustrated by the faster fluorescence recovery in the dark for *Synechococcus* and *Arthrospira* PBs than for *Anabaena* and *Synechocystis* PBs (Fig.7D).

The differences between *Arthrospira* and *Synechocystis* OCP are not due to the fact that one attaches hECN and the other ECN. Results similar to that shown in Fig.4 were obtained when hECN-*Synechocystis* OCP, isolated from WT *Synechocystis* cells, was used in the *in vitro* quenching experiments (Supplemental Fig.3A). A similar observation was made when employing ECN-*Arthrospira* OCP isolated from oApOCPΔCrtR instead of the 3'-hECN binding one from oApOCPWT cells (Supplemental Fig.3B). The observed differences in PB binding must be due to differences in the protein, not the pigment, of the two OCPs.

Effect of increasing phosphate concentration on induction of fluorescence quenching

Increasing phosphate concentration strengthens the *Synechocystis* OCP binding to *Synechocystis* whole PBs and PB cores (Gwizdala et al., 2011). The OCP is unable to induce fluorescence quenching of isolated cores of PBs at 0.5 M phosphate but it induces a large quenching at 0.8M phosphate (Gwizdala et al., 2011). Although at 0.5M phosphate, OCP is able to induce the total quenching of whole *Synechocystis* PBs, the rate of quenching increases with the concentration of phosphate (Fig.S4). We tested if *Synechocystis* OCP is able to bind to other PBs at concentrations higher than 0.8 M phosphate. Fig.8A shows the % of fluorescence quenching induced for *Arthrospira* PBs in K-Phosphate buffers from 0.8 M to 1.6 M. An optimum appeared at 1.4 M for *Arthrospira* PBs, where fluorescence yield dropped by 62.5% after 300s (instead of 2.5% at 0.8 M). Fig.8B compares the fluorescence quenching induced by *Synechocystis* OCP^r in *Arthrospira*, *Synechococcus* and *Anabaena* PBs at 1.4 M phosphate. At this concentration, *Synechocystis* OCP induced a large fluorescence quenching in *Anabaena* PBs (75.1%), *Arthrospira* PBs (60.9%) and *Synechococcus* PBs (59.3%). Nevertheless, the fluorescence quenching induced was still smaller than in *Synechocystis* PBs (88.6%) (Fig.8B), suggesting that *Synechocystis* OCP is still more specific for *Synechocystis* PBs even at 1.4 M phosphate. Note that for *Arthrospira* and *Synechococcus* PBs, a minimum fluorescence yield was reached after about 15s followed by a slow recovery even under illumination. Part of the OCP^r reverted spontaneously to OCP^o, and the binding strength to these PBs was not sufficient to compensate. Changing buffer concentration showed that *Synechocystis* OCP is able to trigger fluorescence quenching in *any* PB when the binding is

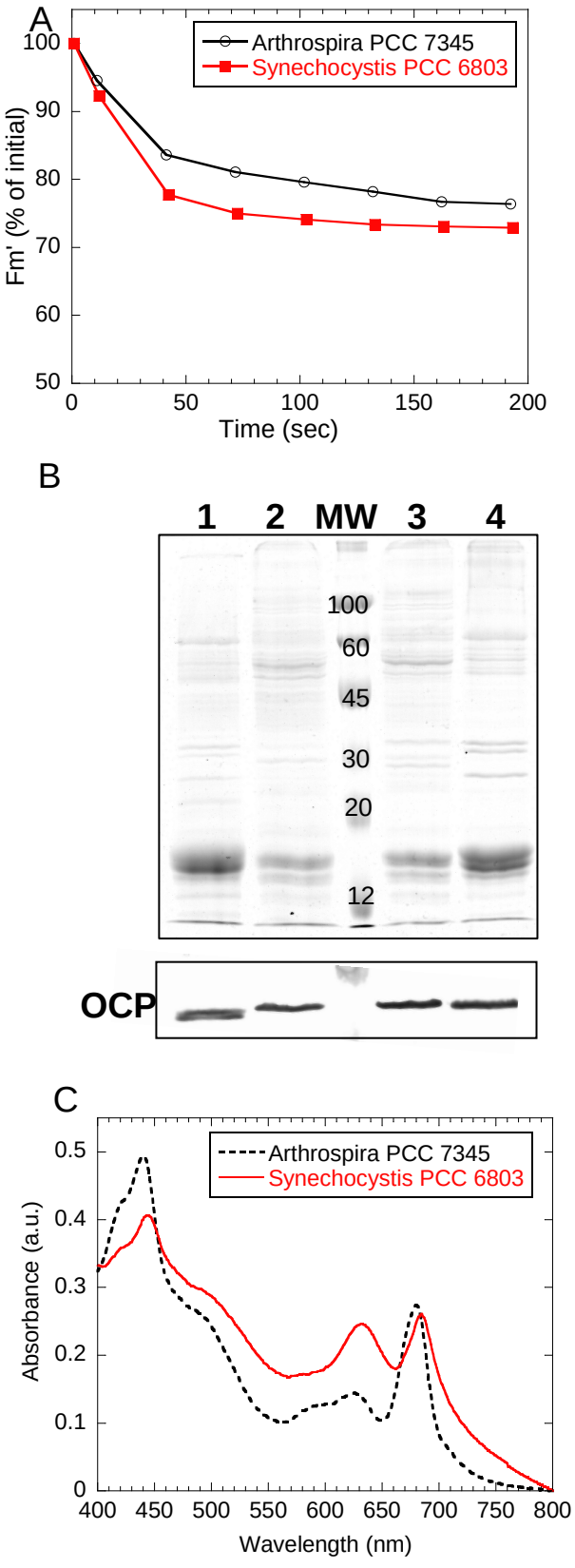

Figure 9. **Comparison of OCP-related fluorescence quenching in Arthrospira and Synechocystis cells.**
A) Fluorescence quenching triggered by strong blue-green light (1400 µmol photons.m^{-2}.s^{-1}) in Synechocystis WT (red close squares) and Arthrospira cells (black open circles) at 33°C.
B) Coomassie blue-stained gel electrophoresis (top) and immunoblot detection (bottom) of the OCP protein in Synechocystis WT cells (lane 1), Arthrospira cells (lane 2) and in membrane-phycobilisome fractions (MPs, prepared as described in (Wilson et al., 2006) obtained from Arthrospira (lane 3) or from Synechocystis (lane 4). Each lane contains 2 µg chlorophyll.
C) RT absorbance spectra of Synechocystis WT (continuous red line) and Arthrospira cells (dash black line). Cells diluted to 3µg Chl.mL^{-1}.

sufficiently strong.

Increasing phosphate concentration also strongly influenced *Arthrospira* PBs fluorescence quenching by *Arthrospira* OCP (Fig.8A, C). Between 0.8 and 1.2 M phosphate, a maximum fluorescence quenching was observed after 15-35 sec followed by a partial fluorescence recovery as shown in Fig.7C. At higher phosphate concentrations, the fluorescence quenching increased to 85.5% and the recovery phase almost disappeared suggesting an irreversible OCP binding. At 1.4 M phosphate *Arthrospira* OCP^r induced 94%, 78.5% and 92% fluorescence in *Synechocystis* PBs, *Synechococcus* PBs and *Anabaena* PBs respectively (Fig.8C).

Comparison of blue light induced fluorescence quenching in *Arthrospira* and *Synechocystis in vivo*.

Figure 9A shows that strong blue-green light induced a slightly faster and larger fluorescence quenching in *Synechocystis* cells than in *Arthrospira* cells. This can be ascribed to a lower concentration of OCP in *Arthrospira* cells or to a weaker interaction between the OCP and *Arthrospira* PBs *in vivo*. We first tested the quantity of OCP present in *Arthrospira* and *Synechocystis* cells and membrane bound phycobilisome complexes (MP) isolated from both strains. It was already shown that all the OCP present in the cells is attached to these complexes (Wilson et al., 2006). Western blot analysis showed that OCP is present in similar concentrations in both strains (Fig 9B) suggesting a weaker OCP interaction or a less effective induction of fluorescence quenching in *Arthrospira* PBs. On the other hand, absorbance spectra of whole cells presented a much larger Chl (abs 680nm) to phycobiliproteins (abs 615-655 nm) ratio in *Arthrospira* cells than in *Synechocystis* cells (Fig 9C). This indicated a lower PBs concentration in *Arthrospira* and as a consequence a higher OCP to PBs ratio. This is also suggested by the SDS-PAGE in which the bands in the 15-20 kDa region were stronger in *Synechocystis* than in *Arthrospira* cells and MPs (Fig 9B). Since the ratio of OCP to PBs is higher in *Arthrospira* cells than in *Synechocystis* cells a larger fluorescence quenching was expected in *Arthrospira* cells. This was not observed.

DISCUSSION

This study was aimed at determining whether the OCP isolated from a given cyanobacterial strain can bind to PBs from a different strain, including those that lack the OCP, and can induce their fluorescence quenching. Using an *in vitro* reconstitution system,

the combinations between various OCP^{r}s (from *Synechocystis* and *Arthrospira*) and PBs (from *Synechocystis*, *Arthrospira*, *Synechococcus* and *Anabaena*) were tested. The results obtained demonstrated that different OCPs are not equivalent in their capacity to induce PB fluorescence quenching or in their specificity. At 0.8 M phosphate, *Synechocystis* OCP induced a large fluorescence quenching only in *Synechocystis* PBs (Fig.4), *Arthrospira* OCP was able to induce a rather large quenching in all types of PBs (Fig.7C). At higher phosphate concentrations, *Synechocystis* OCP was able to induce fluorescence quenching of all PBs; however the amplitude of quenching was always smaller than that induced by the *Arthrospira* OCP (Fig.8A). It was previously shown that PB fluorescence quenching and OCP binding to PBs are correlated, and that the absence of fluorescence quenching is due to a lack of binding between OCP and PBs (Gwizdala et al., 2011). Thus, the results described in this work strongly suggest that *Arthrospira* OCP binds more strongly than *Synechocystis* OCP to all tested PBs. However, both strain's OCP are able to quench the fluorescence of all PBs once bound to them.

Influence of OCP primary structures on carotenoid binding

The other distinctive difference between the two OCPs resides in their capacity to bind ECN instead of hECN; *Synechocystis* OCP binds both carotenoids, but *Arthrospira* OCP cannot stabilize the ECN binding. The crystal structures of *Synechocystis* OCP^{o} (1.65Å resolution: (Wilson et al., 2010), and of *Arthrospira maxima* OCP^{o} (2.1 Å resolution, (Kerfeld et al., 2003) are known. The latter is 100% identical in primary structure to *Arthrospira platensis* OCP used in this study. The carotenoid structure and the secondary and tertiary protein structures of Synechocystis and Arthrospira OCPs are nearly identical (Wilson et al., 2010). The primary structures of the two OCPs investigated in this study are 83% identical. By analyzing the amino acids that differ between *Arthrospira* and *Synechocystis* OCPs we can develop hypotheses about the underlying basis of the differences observed in carotenoid binding and in their ability to induce fluorescence quenching (most probably due changes in PB binding specificity) in these two OCPs.

In WT cells, both *Synechocystis* and *Arthrospira* OCPs bind hECN. When the *Synechocystis ocp* gene is overexpressed in a *Synechocystis* mutant lacking zeaxanthin and hECN, cells contain a high concentration of OCP binding only echinenone (Punginelli et al., 2009; Wilson et al., 2010). In contrast, overexpression of the *Arthrospira ocp* gene in the same *Synechocystis* mutant results in cells in which almost no *Arthrospira* OCP is accumulated (Fig.5A). Likewise, in a WT background, the carotenoid preferentially bound

differs: *Synechocystis* OCP isolated from the overexpressing strain contained more echinenone (50 to 82% depending on the preparation) than hECN (11 to 32 %) (Punginelli et al., 2009; Wilson et al., 2010). This is most probably related to the higher concentration of ECN than that of hECN in cells. In contrast, *Arthrospira* OCP over-expressed in WT *Synechocystis* cells binds preferentially hECN over ECN (81% versus 19%, see Fig.S1) strongly suggesting that *Arthrospira* OCP is not able (or less able) to stably bind ECN . The interaction of the carotenoid hydroxyl group with the protein seems to be essential for the stabilization of carotenoid binding in *Arthrospira* OCP. We have demonstrated that in *Synechocystis* OCP the interaction of Tyr44 and Trp110 with the hydroxyl ring of the carotenoid are important for photoactivity (Wilson et al., 2010). In addition, the interaction between Trp110 and the carotenoid seems to be important to stabilize ECN binding. When Tyr44 was replaced by Ser, the OCP was present in high concentrations in the overexpressing Y44S-OCP cells and still bound 70% ECN, despite increased solvent accessibility of the carotenoid (Wilson et al., 2010). However when Trp 110 was replaced by Ser or Phe the mutated OCPs bound only 20% of ECN and the OCP concentration in the cells was reduced (Wilson et al., 2010). The replacement of Trp by Phe did not affect photoactivity but destabilized ECN binding, indicating that the interaction between Trp110 and the carotenoid is essential for carotenoid binding. Due to the high sequence identity among amino acids forming the carotenoid binding pocket and their similar orientation in the structures it is difficult to explain why *Arthrospira* OCP cannot stably bind ECN. We can hypothesize that small changes in the positions of amino acid side chains could disturb the interaction between Trp110 and the carotenoid ring. In *Arthrospira* OCP structure, a conserved water molecule (HOH 452) is hydrogen-bonded directly to the 3'-OH group of 3'-hECN (Kerfeld et al., 2003). It is possible that this bond is partially responsible for the stabilization 3'-hECN in *Arthrospira* OCP. We cannot discard that subtle differences in solvent accessibility and number of water molecules in the carotenoid pocket could also destabilize the pi-pi interactions between the carotenoid ring and Trp110 or other hydrophobic carotenoid-protein interactions rendering the ECN binding more or less favorable. Finally, nothing is known about the mechanism of carotenoid binding to the OCP and it is possible that non-conserved amino acids outside the carotenoid binding pocket of OCP^{o} could be involved in this process.

Comparison of OCP-PBs interactions of both OCPs

No significant differences in photoconversion kinetics or fluorescence quenching kinetics and amplitude were observed for hECN-OCP versus ECN-OCP from *Arthrospira*

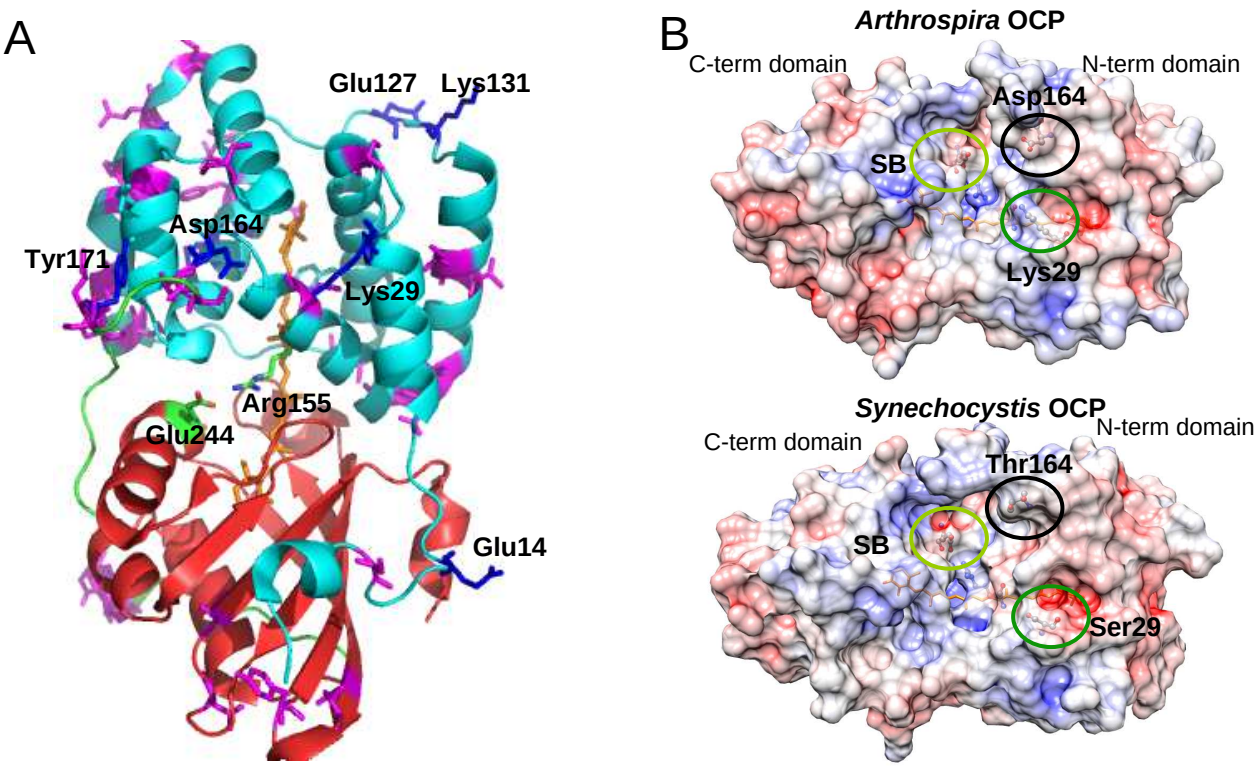

Figure 10. **Structural differences between *Arthrospira* OCP and *Synechocystis* OCP.**

A) Overview of the *Arthrospira maxima* OCP structure. Teal: N-terminal domain. Green: linker region. Red: C-terminal domain. 3'-hECN is shown in orange. The aminoacids changing between *Arthrospira* OCP and *Synechocystis* OCP are represented using purple sticks or blue stick for the ones bearing charges (and for Tyr171).

B) Electrostatic surface maps of *Arthrospira* and *Synechocystis* OCPs. See Materials and Methods for details. SB: salt-bridge between Arg155 and Glu244(246).

(Supplemental Figure S2 and S3). Thus, the differences observed in photoactivity and fluorescence quenching properties of ECN-OCP from *Synechocystis* versus hECN-OCP from *Arthrospira* most likely result from differences in protein structures between both OCPs. Many amino acid substitutions between *Synechocystis* OCP and *Arthrospira* OCP are localized on the outer surface of the N-terminal domain: several neutral amino acids in the N-terminal domain of *Synechocystis* OCP are replaced by charged amino acids in *Arthrospira* OCP (Figure 10A). These substitutions include N14E, S29K, Q72R, R112E, A127E, Q130K, and T164D. If the OCP-PB interaction has an important electrostatic component, the additional charged residues could strengthen the interactions between *Arthrospira* OCP and PBs. In addition, the replacement of a negative charge in *Synechocystis* OCP (Asp115) by a positive charge in *Arthrospira* OCP (Arg115) could also affect electrostatic interactions with the PBs. Differences in OCP binding strength to PBs are most probably the cause for differences in fluorescence quenching as previously demonstrated (Gwizdala et al., 2011).

The OCP's binding to the PB is known to involve a direct interaction between OCP's Arg155 residue and the APC protein (Wilson et al., 2012). Electrostatic surface plots of the region around Arg155 of *Arthrospira* and *Synechocystis* OCPs are shown in Fig.9B. In each structure, Arg155 (which forms a salt bridge with Glu244/246 in the non-quenching form of the OCP) is buried near the carotenoid chromophore in a large, centralized surface depression at the interface of the C-terminal and N-terminal domains of the protein. In this interface, most amino acids are identical or conservatively substituted (i.e. Asp146 versus Glu146 or Lys231 versus Arg233). However, we note two non-conservative substitutions at the entrance to this surface depression: Ser29 and Thr164 (*Synechocystis*) to Lys29 and Asp164 (*Arthrospira*). While residue 29 is not highly conserved among OCP orthologs (Wilson et al., 2010), the positively charged Lys29 of *Arthrospira* adds additional positive charge in the surface depression leading to Arg155. If the PB-OCP interaction involving Arg155 is electrostatic in nature, the addition of positive charge in this region could potentially enhance the binding interaction. The Thr164 residue of *Synechocystis* is likewise notable, since residue 164 is highly conserved across orthologs (Wilson et al., 2010) and is most often negatively charged (as is the case with Asp164 in *Arthrospira*). Given its proximity to Arg155, the nature of it's non-conservative substitution versus Asp164 of *Arthrospira*, and it's deviation from the majority of OCP sequences, we speculate that Thr164 might be at least partly responsible for the unique specificity of *Synechocystis* OCP to *Synechocystis* PBs.

Finally, the flexible linker region between the C- and N-terminal domains could also lead to differences in activity of both OCPs if this region is involved in light induced protein

conformational changes or PB binding. The flexible linker is the least conserved region of primary structure across OCP orthologs (Wilson et al., 2010), and possesses 59.5% identity in aminoacid sequences between the OCPs investigated in this work. It is shorter in *Synechocystsis* OCP, lacking two amino acids (Ser170, Tyr171), which could restrict the opening of the protein in the red form and subsequently affect the binding to APC trimers. These residue specific hypotheses await further testing. Additional interpretation is hindered by the fact that no structural data is yet available concerning OCP^r or OCP^r-PBs complexes.

Influence of PBs structure on OCP-PBs interaction

In addition to differences in amino acid sequence between the *Arthrospira* or *Synechocystis* OCP the PB structures also influenced the amplitude and kinetics of fluorescence quenching: a given OCP reacted differently with PBs isolated from different cyanobacterial strains. This is particularly true in 0.8 M phosphate, insufficient for a full stabilization of the OCP-PB complex when PBs other than *Synechocystis* PBs were used. In the past, this concentration of phosphate was considered optimal for in vitro fluorescence quenching induction (Gwizdala et al., 2011). Here, our results clearly demonstrated that *Synechocystis* PBs are quenched much more efficiently by both *Synechocystis* and *Arthrospira* OCPs than any other PB (Fig.4, 8). It could be assumed that OCP and PBs from the same cyanobacterial strain, having evolved concomitantly, developed a high affinity towards each other for an optimized response to high light. Considering the fact that *Arthrospira* PBs are only poorly quenched by *Arthrospira* OCP (Fig.7C) raises important questions. One possibility is that the *Arthrospira* PBs used here could have been partially disassembled or could have lost some components required for OCP binding during isolation. However, absorption spectra combined to 77K fluorescence emission spectra indicated they were assembled and functionally connected PBs (Fig.2, 3). No striking variations compared to *Synechocystis* PBs appeared in terms of peptide composition, as revealed by SDS-PAGE (Fig.2A). Nevertheless, Tian et al. showed that although the mechanism inducing fluorescence quenching was identical *in vivo* and *in vitro* and that the amounts of quenching were similar, the rate of quenching was slightly slower in the *in vitro* system than *in vivo* (Tian et al., 2011; Tian et al., 2012). This indicated that even in the case of *Synechocystis*, slight variations in PB structure, not detectable in fluorescence spectra, could affect OCP binding. In the case of *Arthrospira* PBs, perhaps changes in the core of the PB are induced that affect OCP binding but not energy transfer. A second interpretation can be formulated in which *Synechocystis* PBs are simply more prone to quenching than *Arthrospira* PBs even *in vivo*. Reasons could lie

in different overall structures between the PBs or more specific changes in the primary structure of one or more PB proteins. We showed that a similar concentration of OCP induced slightly slower and smaller fluorescence quenching in *Arthrospira* cells than in *Synechocystis* cells and that a larger OCP to PBs ratio in *Arthrospira* cells did not lead to a larger fluorescence quenching. Although our results suggest that *Arthrospira* PBs have a lower affinity for OCP than *Synechocystis* PBs *in vivo*, the effect seems to be much less pronounced than *in vitro* since the difference in the amplitude of fluorescence quenching was small between both strains

EM on isolated complexes showed that *Synechocystis, Arthrospira, Synechococcus* and *Anabaena* PBs have a common hemi-discoidal organization with PC rods radiating from an APC core (see reviews (MacColl, 1998; Adir, 2005). The number of APC cylinders differs from strain to strain. This could be a factor influencing OCP-PBs interactions as OCP binds to APC upon photoactivation (Tian et al., 2011; Jallet et al., 2012; Tian et al., 2012). However, our results did not confirm the hypothesis of a greater OCP binding in PBs with more APC trimers. *Synechococcus* PBs have only 2 APC cylinders but behaved like *Arthrospira* PBs (with 3 cylinders) in terms of fluorescence quenching *in vitro* (Fig.4, 7, 8). The missing upper cylinder, containing α/β subunits of APC plus a small linker polypeptide, seems not to be required for OCP attachment. *Anabaena* PBs were generally less quenched than *Synechocystis* PBs. Thus, the two extra APC cylinders present in these PBs seems not to result in an increased affinity for OCP. Our results strengthen the proposal that the OCP binds to a basal APC cylinder.

Many isolated phycobiliproteins in their trimeric or hexameric aggregation states have been crystallized and their X-ray structures determined (review (Adir, 2005)). However, a global picture of fully assembled PBs is still lacking. For example, it is not known how PC rods and APC cores are biochemically connected. PC rods stabilize OCP binding to PBs (Gwizdala et al., 2011) and species-specific changes of this connection could lead to different affinities for the OCP. It was recently shown that a more or less pronounced cavity exists between the APC trimers (Marx and Adir, 2012). This could influence PC rods binding or OCP attachment, but a systematic crystallographic study is needed for verification. We have already observed that OCP is able to induce less fluorescence quenching when mixed to "old" PBs preparations or to reconstituted PBs, in which energy transfer to the terminal emitters was slightly decreased, suggesting a weaker connection between APC trimers (Jallet and Kirilovsky, unpublished data). Thus, the interaction between APC trimers seems to be

important for OCP binding stabilization. This interaction could be modified in the PBs of the different cyanobacteria strains at least in the *in vitro* isolated preparations.

Finally, the OCP is thought to interact with α/β APC subunits emitting at 660 nm (Tian et al., 2011; Jallet et al., 2012; Tian et al., 2012) or with the ApcE core-membrane linker (Stadnichuk et al., 2012) or both (Kuzminov et al., 2012). α and β APCs are extremely well conserved, particularly within the group of cyanobacteria employed for this study (between 77% and 90% identity in primary structures compared to *Synechocystis*). ApcE is less conserved (Capuano et al., 1993) especially in the N-terminal phycobiliprotein part (60% to 64% identity in primary structures to *Synechocystis* within the group employed here), because it contains a very variable loop-region of unknown function. This could also influence OCP attachment. Once again, the lack of structural data on OCP^r-PB complexes makes any further interpretation merely speculative.

CONCLUSION

This study results in four important conclusions about the relationship between OCP and PBs : 1) Structurally distinct OCPs from different strains exhibit unique PB interaction properties. *Synechocystis* OCP manifests a high specificity for its own phycobilisomes. *Arthrospira* OCP has a stronger affinity for all PBs relative to that of *Synechocystis* OCP and therefore appears to be less specific. Our results suggest a role for electrostatics in the interaction; 2) The structure of the PBs, probably the interactions between APC trimers forming the core cylinders, could have a big influence on OCP binding and its stabilization; 3) The upper APC cylinder is not necessary for OCP interaction with PBs, strongly suggesting that OCP binds to one of the basal APC cylinders and 4) Once OCP binds to the PB, it is able to quench the fluorescence of any type of PBs, even those isolated from strains lacking OCP. This is true for both OCPs investigated here. We also conclude that *Arthrospira* OCP would be a better candidate to introduce the photoprotective mechanism in *Synechococcus elongatus* and *Thermosynechococcus elongatus* cells. These two cyanobacterial strains lack the OCP and are more sensitive to high light conditions (Boulay et al., 2008).

MATERIALS AND METHODS

Culture conditions

Synechocystis PCC 6803, *Synechococcus elongatus* PCC 7942 and *Anabaena variabilis* cells were grown photoautotrophically in a modified BG11 medium containing double amounts of sodium nitrate (Herdman et al., 1973). Cells were kept in a rotary shaker (120 rpm) at 30°C, under CO_2 enrichment, illuminated by fluorescence white lamps giving a total intensity of about 90 µmol photons.m^{-2}.s^{-1}. The *Arthrospira platensis* PCC 7345 culture conditions were identical, except for temperature. They were grown at 23°C. Cells were maintained in their logarithmic phase of growth.

oApOCP plasmid construction

A 1.7 kb DNA region containing the *ocp* and *frp* genes was amplified by PCR using genomic DNA of *Arthrospira platensis* PCC 7345 as template. Two synthesized oligonucleotides containing the sequences for creating NdeI and HpaI restriction sites were employed for that purpose: F_AP_OFNdeI (GACTTC**CATATG**CCATTCACCATTGACTCGGC) and R_AP_OFHpaI (GTAAGC**GTTAAC**AGTCCAACTACTCAACCCGC).

The resulting PCR product was cloned into pPSBA2 (Lagarde et al., 2000) into the *NdeI* and *HpaI* restriction sites of the plasmid. Nucleotides encoding for 6 His were added on the 3'side of *OCP* by site directed mutagenesis (Quickchange XL kit, Stratagene) using the mutagenic oligonucleotidesF_AP_OFHis (**CACCACCACCACCACCAC***TAG*AATAGAGTTCACCT AGAAATTATATAGG) and R_AP_OFHis (**GTGGTGGTGGTGGTGGTG**GCGCACCAA GTTCAACAACTCTTTGG). A 1.3kb kanamycin resistance cassette was finally inserted in the unique *HpaI* site, situated 48pb downstream of the *FRP* stop codon.

Transformation, selection, genetic analysis of mutants

The oApOCP plasmid construct was used to transform WT and ΔCrtR *Synechocystis* cells (lacking the β-carotene hydroxylase and unable to produce zeaxanthin or 3'-hECN), giving respectively the oApOCPWT and oApOCPΔCrtR mutants. Selection was made at 33°C, under dim light (30 µmol photons m^{-2} s^{-1}) on plates containing 40 µg.mL^{-1} kanamycin. The endogenous *slr1963* gene was then interrupted using the ΔOCP plasmid construct bearing a Spectinomycin/Streptomycin resistance cassette (Wilson et al., 2006). To confirm the complete segregation of the different mutants, PCR analysis and specific digestions by restriction enzymes were performed.

Isolation of phycobilisomes (PBs)

The protocol used derives from that described in (Ajlani et al., 1995). After reaching OD_{800nm}=1 cyanobacteria cells were harvested through centrifugation at 5400g, 23°C, for 6 min. They were washed twice using 0.8M K-Phosphate buffer pH 7.5, their chlorophyll concentration being then determined and adjusted to 1mg.ml^{-1}. Protease inhibitors were added (1mM EDTA, 1mM caproic acid, 1mM phenylmethylsulfonyl fluoride) as well as DNAse (50µg.mL^{-1}) prior to breaking. *Synechococchus, Anabaena* and *Arthrospira* cells were broken using a French Press system (800psi). *Synechocystis* cells were broken through vortexing in the presence of glass beads (diameter 200µm). The unbroken cells were removed by centrifugation at 2000g, 23°C, for 5 min. The supernatant was incubated in the presence of 2% (v/v) TritonX100 under dim stirring, at 23°C, during 2 hours. For *Synechocystis*, *Arthrospira* and *Synechococcus* PBs, the TritonX100 phase and debris were removed by centrifugation at 20000g, 23°C, for 20min and the dark blue supernatant was directly loaded onto a discontinuous Sucrose gradient. For *Anabaena* PBs, the Triton treated supernantant was centrifuged at 86000g, 23°C, for 1h. The dark-green supernatant was collected and PBs precipitated through centrifugation at 130000g, 23°C, for 1h. The dark blue pellet was resuspended using 1M K-Phosphate buffer pH 7.5 and deposited onto a Sucrose gradient. The sucrose gradient for isolation of all PBs contained 0.25, 0.5, 0.75 and 1.5M sucrose layers in 1M (final) K-Phosphate buffer pH 7.5. The gradient was spun at 150000g, 23°C, for 12h. The different layers were collected and their absorbance spectra recorded.

Calculation of PBs concentrations

The calculation of PBs concentrations was based on absorbance spectra. For *Synechocystis* PBs, 95% of the absorbance at 620nm comes from the absorption of PC (Yamanaka et al., 1978). The extinction coefficient of a PC hexamer is 2370 mM^{-1}.cm^{-1} (Glazer, 1984). We estimated that the extinction coefficient of *Synechocystis* PBs containing 18 hexamers of PC (six rods with three PC hexamers each) is 42660 mM^{-1}.cm^{-1}. We estimated that PC contributes to 85% of the absorbance at 620nm in *Arthrospira* PBs and in *Anabaena* PBs and 95% in *Synechococcus* PBs (Fig.S1). Taking into account the different architectures, this leads to an extinction coefficient of 39390 mM^{-1}.cm^{-1} for *Arthrospira* PBs, 30004 mM^{-1}.cm^{-1} for *Synechococcus* PBs and 52520 mM^{-1}.cm^{-1} for *Anabaena* PBs.

Purification of the *Arthrospira* and *Synechocystis* Orange Carotenoid Protein (OCP)

His-tagged *Arthrospira* OCP was purified from oApOCPWT or oApOCPΔCrtR *Synechocystis* mutants and *Synechocystis* OCP from oSynOCPΔCrtR as described in (Wilson et al., 2008) using a Ni-ProBond resin columm and a Whatman DE-52 column. The isolated OCP was dialyzed against 40mM Tris-HCl pH 8.0 and frozen at -80°C.

Protein separation and immunoblot analysis

Proteins were analyzed by SDS-PAGE on 12% polyacrylamide/2M Urea gels in a Tris-MES system (Kashino et al., 2001). PBs samples were concentrated by precipitation with 10% (v/v) trichloroacetic acid prior to loading (equal quantities in each lane). For whole cells extracts, 3µg Chlorophyll were deposited per well. The gels were stained by Coomassie Brilliant Blue. The OCP protein was detected using a polyclonal antibody directed against *Arthrospira maxima* OCP.

Absorbance measurements

The orange-to-red OCP conversion (and red-to-orange recovery) was monitored in a Specord S600 spectrophotometer (Analytikjena) and triggered using strong white light (5000µmol.m-^{2}.s-^{1}). PBs absorbance spectra were recorded in an Uvikon XL spectrophotometer (Secomam), at 23°C.

Fluorescence measurements

PAM fluoremeter

Fluorescence yield quenching was monitored using a pulse amplitude fluorometer (101/102/103-PAM; Walz). Measurements were made in 1 cm pathlength stirred cuvettes. Experiments carried on whole cells were performed at a chlorophyll concentration of 3µg/mL, at 33°C. In vitro reconstitutions were handled with a phycobilisome concentration of 0.012µM in K-Phosphate buffer (pH 7.5) concentrations ranging from 0.8 to 1.6M, at 23°C. Fluorescence quenching was induced *in vivo* by 1400µmol.m^{-2}.s^{-1} of blue-green light (Halogen white light filtered by a Corion cut-off 550nm filter; 400 to 550nm). *In vitro* blue-green light of 900 µmol.m^{-2}.s^{-1} was used for quenching.

Emission spectra

Fluorescence emission spectra were monitored in a CARY Eclipse spectrophotometer (Varian). For studies at room temperature, samples were placed in a 1 cm stirred cuvette. For

77K measurements, samples were collected in Pasteur pipettes then frozen by immersion in liquid nitrogen. Excitation was made at 590 nm.

OCP structural modeling and analysis

Prior to calculation of electrostatic surface potentials, missing residues in Synechocystis OCP were modeled using Coot, (Emsley and Cowtan, 2004) which allowed for placement of previously missing portions of the flexible linker and the sidechain of T164 in this structure. Electrostatic surface potentials of Chain A from 3MG1 and 1M98 were calculated using the Adaptive Possion-Boltzmann Solver plugin implemented in the PyMOL Molecular Graphics System (Version 1.6, Schrödinger, LLC).

Supplemental data

The following materials are available in the online version of this article

Supplemental Figure 1. HPLC analysis of carotenoids isolated from purified *Arthrospira* OCP (oApOCPWT mutant cells)

Supplemental Figure 2. Photoactivation kinetics of the 3'hECN or ECN binding *Arthrospira* OCP

Supplemental Figure 3. Effect of ECN or 3'hECN binding on phycobilisome fluorescence quenching induced by *Synechocystis* and *Arthrospira* OCP in vitro

Supplemental Figure 4. Effect of phosphate concentration on *Synechocystis* PBs fluorescence quenching by *Synechocystis* OCP^r

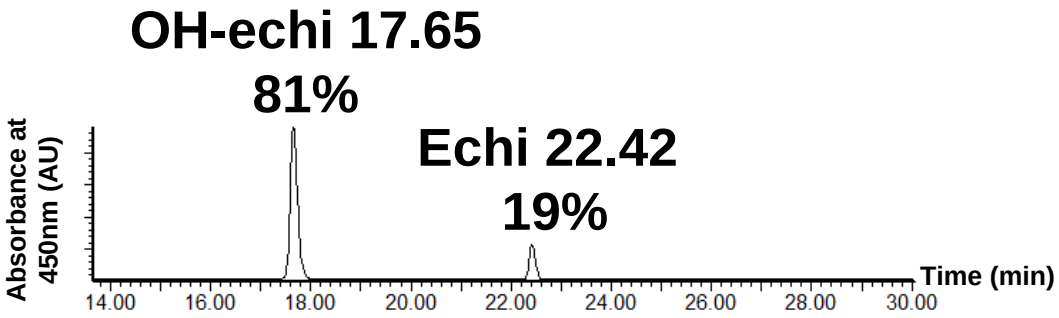

Fig.S1. HPLC analysis of carotenoids isolated from purified *Arthrospira* OCP (oApOCPWT mutant cells)

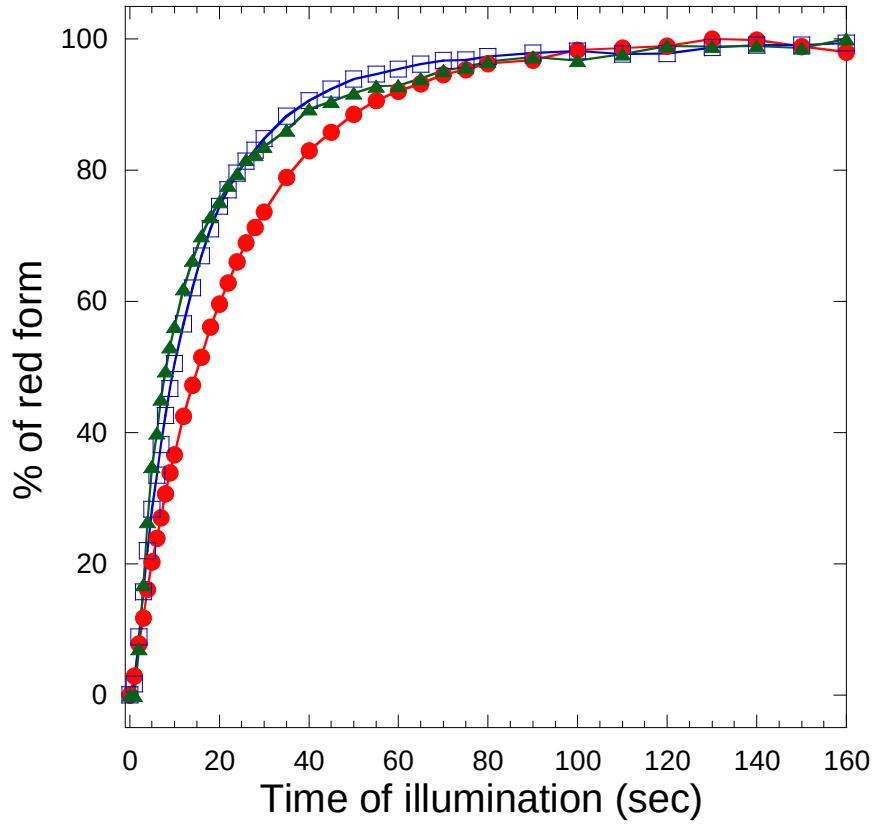

Figure S2. **Photoactivation kinetics of the 3'hECN or ECN binding *Arthrospira* OCP**

OCP^O (1.8µM) was illuminated using strong white light (5000µmol.m^{-2}.s^{-1}). The accumulation of OCPr was followed by measuring Δ A_{550nm} over time in TrisHCl 40mM pH 8, at 23°C; 3'hECN-binding *Arthrospira* OCP isolated from oApOCPWT cells (blue squares), ECN-binding *Arthrospira* OCP isolated from oApOCPΔCrtR cell (green triangles) and ECN-binding *Synechocystis* OCP isolated from oScOCPΔCrtR cells (red circles). Data are normalized to the maximal ΔA_{550nm} .corresponding to 100% OCP^r

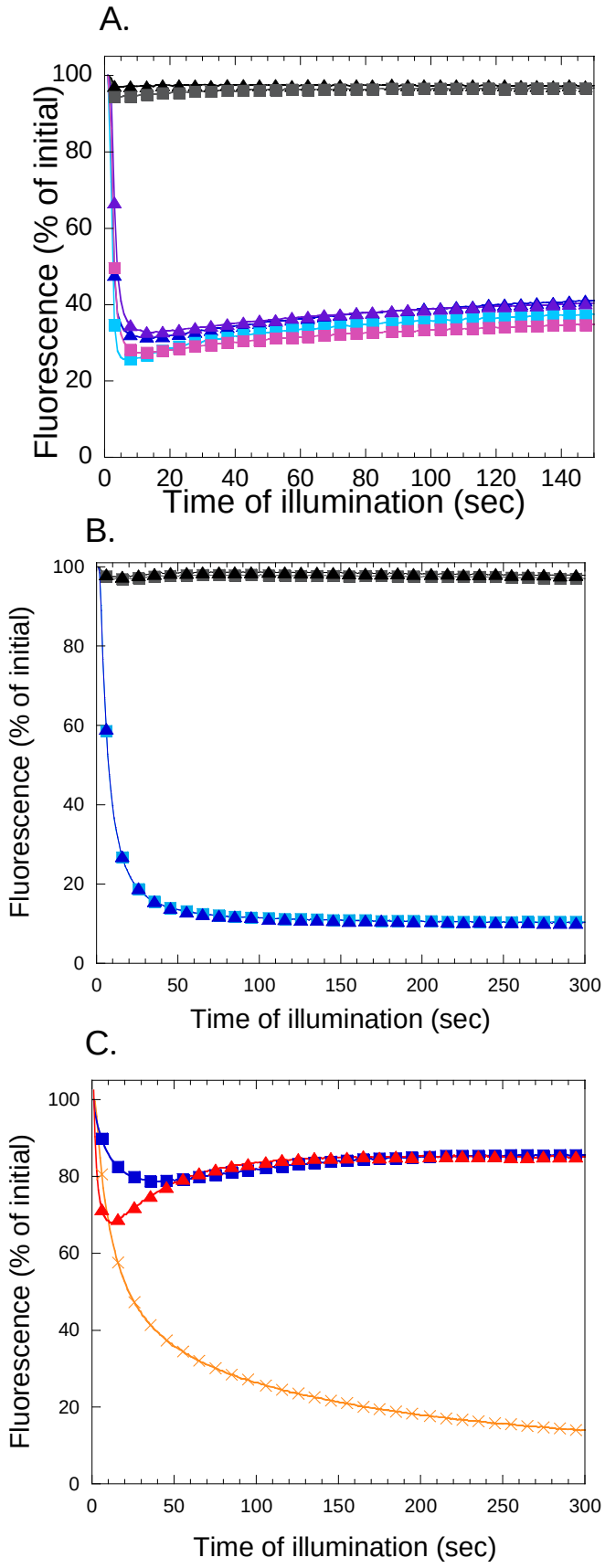

Figure S3. **Effect of ECN or 3'hECN binding on phycobilisome fluorescence quenching induced by Synechocystis and Arthrospira OCP in vitro.**
The isolated PBs were illuminated with blue-green light (900µmol.m^{-2}.s^{-1}) in the presence of an excess of preconverted OCP^{r} at 23°C.
A) Fluorescence quenching induced by adding 40 3'hECN-binding S*ynechocystis* OCP^{r} (isolated from WT, tagged cells; triangles) or 40 ECN-binding *Synechocystis* OCP^{r} (isolated from oOCP6803ΔCrtR; squares) under strong blue-green illumination (900 µmolphotons.m^{-2}.s^{-1}) to *Synechococcus* PBs at 0.8 MK-Phosphate (black/grey curves) and 1.4M K-Phosphate (blue curves) or to *Arthrospira* PBs at 1.4M K-Phosphate (purple/pink curves).
B) Fluorescence quenching induced by adding 40 3'hECN (triangles) or ECN (squares)-binding *Synechocystis* OCP^{r}, at 0.8M K-Phosphate under strong blue-green illumination, to *Arthrospira* PBs (black/grey curves) or *Synechocystis* PBs (blue curves)
C) Fluorescence quenching induced by adding 20 ECN-binding *Arthrospira* OCP^{r} (isolated from oApOCPΔCrtR cells) per *Arthrospira* PB (blue squares), *Synechococcus* PB (red triangles) and *Synechocystis* PB (orange crosses) in 0.8 M K-Phosphate. A ratio of 20 OCP per PB instead of 40 OCP per PB was used because of the extremely small amounts of *Arthrospira* OCP retrieved from the oApOCPΔCrtR cells. Due to the small quantities of ECN-*Arthrospira* OCP isolated from the ΔCrtR strain and the hECN-*Synechocystis* OCP isolated from WT cells we were unable to test all the different PBs.

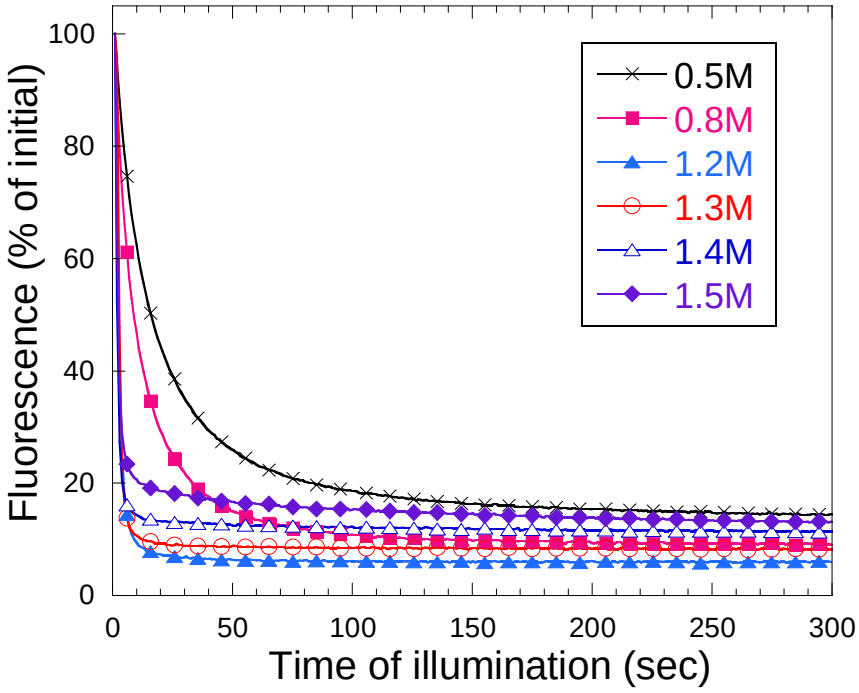

Figure S4. Effect of K-Phosphate concentration on *Synechocystis* PBs fluorescence quenching by *Synechocystis* OCP^{R}

Synechocystis PBs (0.012µM) were illuminated with blue-green light (900µmol.m^{-2}.s^{-1}) in the presence of pre-converted *Synechocystis* OCP^{r} (0.48µM; 40 per PB) at 23°C using various K-Phosphate buffer concentrations: 0.5M black crosses, 0.8M pink closed squars, 1.2M light blue closed triangles, 1.3M red open circles, 1.4M deep blue open triangles and 1.5M violet closed diamonds.

ACKNOWLEDGMENTS

We thank Sandrine Cot and Markus Sutter for technical assistance. We thank Adjélé Wilson for technical assistance in OCP preparation and discussions. We thank Dr.Ghada Ajlani for fruitful discussions.

REFERENCES

Adir N (2005) Elucidation of the molecular structures of components of the phycobilisome: reconstructing a giant. Photosynth Res **85:** 15-32

Adir N (2005) Elucidation of the molecular structures of components of the phycobilisome: reconstructing a giant. Photosynthesis Research **85:** 15-32

Ajlani G, Vernotte C (1998) Deletion of the PB-loop in the Lcm subunit does not affect phycobilisome assembly or energy transfer functions in the cyanobacterium *Synechocystis* sp. PCC6714. Eur J Biochem **257:** 154-159

Ajlani G, Vernotte C, Dimagno L, Haselkorn R (1995) Phycobilisome Core Mutants of *Synechocystis* PCC 6803. Biochim Biophys Acta **1231:** 189-196

Babu TS, Kumar1 A, Varma AK (1991) Effect of Light Quality on Phycobilisome Components of the Cyanobacterium *Spirulina platensis*. Plant Physiol. **95:** 492-497.

Boulay C, Abasova L, Six C, Vass I, Kirilovsky D (2008) Occurrence and function of the orange carotenoid protein in photoprotective mechanisms in various cyanobacteria. Biochim Biophys Acta **1777:** 1344-1354

Boulay C, Wilson A, D'Haene S, Kirilovsky D (2010) Identification of a protein required for recovery of full antenna capacity in OCP-related photoprotective mechanism in cyanobacteria. Proc Natl Acad Sci U S A **107:** 11620-11625

Bryant DA (1991) Cyanobacterial phycobilisomes: progress towards a complete structural and functional analysis via molecular genetics. *In* L Bogorad, IK Vasil, eds, The molecular biology of plastids and mitochondria. Academic Press, New York, pp 257-300

Capuano V, Braux AS, Tandeau de Marsac N, Houmard J (1991) The "anchor polypeptide" of cyanobacterial phycobilisomes. Molecular characterization of the *Synechococcus* sp. PCC 6301 apce gene. J Biol Chem **266:** 7239-7247

Capuano V, Thomas JC, Tandeau de Marsac N, Houmard J (1993) An *in vivo* approach to define the role of the L_{CM}, the key polypeptide of cyanobacterial phycobilisomes. J Biol Chem **268:** 8277-8283

Ducret A, Muller SA, Goldie KN, Hefti A, Sidler WA, Zuber H, Engel A (1998) Reconstitution, characterisation and mass analysis of the pentacylindrical allophycocyanin core complex from the cyanobacterium *Anabaena* sp. PCC 7120. J Mol Biol **278:** 369-388

Ducret A, Sidler W, Wehrli E, Frank G, Zuber H (1996) Isolation, characterization and electron microscopy analysis of a hemidiscoidal phycobilisome type from the cyanobacterium *Anabaena* sp. PCC 7120. Eur J Biochem **236:** 1010-1024

Emsley P, Cowtan K (2004) Coot: model-building tools for molecular graphics. Acta Crystallogr D Biol Crystallogr **60:** 2126-2132

Glauser M, Sidler WA, Graham KW, Bryant DA, Frank G, Wehrli E, Zuber H (1992) Three C-phycoerythrin-associated linker polypeptides in the phycobilisome of green-light-grown Calothrix sp. PCC 7601 (cyanobacteria). FEBS Lett **297:** 19-23

Glazer AN (1984) Phycobilisome - a macromolecular complex optimized for light energy-transfer. Biochim Biophys Acta **768:** 29-51

Gorbunov MY, Kuzminov FI, Fadeev VV, Kim JD, Falkowski PG (2011) A kinetic model of non-photochemical quenching in cyanobacteria. Biochim Biophys Acta **1807:** 1591-1599

Grossman AR, Schaefer MR, Chiang GG, Collier JL (1993) The phycobilisome, a light-harvesting complex responsive to environmental-conditions. Microbiol. Rev. **57:** 725-749

Gwizdala M, Wilson A, Kirilovsky D (2011) *In vitro* reconstitution of the cyanobacterial photoprotective mechanism mediated by the Orange Carotenoid Protein in *Synechocystis* PCC 6803. Plant Cell **23:** 2631-2643

Herdman M, Delaney SF, Carr NG (1973) A new medium for the isolation and growth of auxotrophic mutants of the blue-green alga *Anacystis nidulans*. J. Gen. Microbiol. **79:** 233-237

Holt TK, Krogmann DW (1981) A carotenoid-protein from cyanobacteria. Biochim. Biophys. Acta. **637:** 408-414

Jallet D, Gwizdala M, Kirilovsky D (2012) ApcD, ApcF and ApcE are not required for the Orange Carotenoid Protein related phycobilisome fluorescence quenching in the cyanobacterium *Synechocystis* PCC 6803. Biochim Biophys Acta **1817:** 1418-1427

Kashino Y, Koike H, Satoh K (2001) An improved sodium dodecyl sulfate-polyacrylamide gel electrophoresis system for the analysis of membrane protein complexes. Electrophoresis **22:** 1004-1007

Kerfeld CA, Sawaya MR, Brahmandam V, Cascio D, Ho KK, Trevithick-Sutton CC, Krogmann DW, Yeates TO (2003) The crystal structure of a cyanobacterial water-soluble carotenoid binding protein. Structure **11:** 55-65

Kipe-Nolt JA, Stevens SE, Bryant DA (1982) Growth and chromatic adaptation of *Nostoc* sp. Strain MAC and the pigment mutant R-MAC. Plant Physiol **70:** 1549-1553

Kirilovsky D, Kerfeld CA (2012) The orange carotenoid protein in photoprotection of photosystem II in cyanobacteria. Biochim Biophys Acta **1817:** 158-166

Kirilovsky D, Kerfeld CA (2013) The Orange Carotenoid Protein: a blue-green light photoactive protein. Photochem Photobiol Sci **12:** 1135-1143

Kuzminov FI, Karapetyan NV, Rakhimberdieva MG, Elanskaya IV, Gorbunov MY, Fadeev VV (2012) Investigation of OCP-triggered dissipation of excitation energy in PSI/PSII-less *Synechocystis* sp. PCC 6803 mutant using non-linear laser fluorimetry. Biochim Biophys Acta **1817:** 1012-1021

Lagarde D, Beuf L, Vermaas W (2000) Increased production of zeaxanthin and other pigments by application of genetic engineering techniques to *Synechocystis* sp. strain PCC 6803. Appl Environ Microbiol **66:** 64-72

Lundell DJ, Williams RC, Glazer AN (1981) Molecular architecture of a light-harvesting antenna. In vitro assembly of the rod substructures of *Synechococcus* 6301 phycobilisomes. J Biol Chem **256:** 3580-3592

MacColl R (1998) Cyanobacterial phycobilisomes. J Struct Biol **124:** 311-334

Marx A, Adir N (2012) Allophycocyanin and phycocyanin crystal structures reveal facets of phycobilisome assembly. Biochim Biophys Acta **1827:** 311-318

Nomsawai P, Tandeau-de-Marsac N, Thomas J-C, Tanticharoen M, Cheevadhanarak S (1999) Light Regulation of Phycobilisome Structure and Gene Expression in *Spirulina platensis* Cl (*Arthrospira* sp. PCC 9438). Plant Cell Physiol **40:** 1194-1202

Piven I, Ajlani G, Sokolenko A (2005) Phycobilisome linker proteins are phosphorylated in *Synechocystis* sp. PCC 6803. J Biol Chem **280:** 21667-21672

Polivka T, Kerfeld CA, Pascher T, Sundström V (2005) Spectroscopic properties of the carotenoid 3'-hydroxyechinenone in the orange carotenoid protein from the cyanobacterium *Arthrospira maxima*. Biochemistry **44:** 3994-4003

Punginelli C, Wilson A, Routaboul JM, Kirilovsky D (2009) Influence of zeaxanthin and echinenone binding on the activity of the Orange Carotenoid Protein. Biochim Biophys Acta **1787:** 280-288

Rakhimberdieva MG, Stadnichuk IN, Elanskaya IV, Karapetyan NV (2004) Carotenoid-induced quenching of the phycobilisome fluorescence in photosystem II-deficient mutant of *Synechocystis* sp. FEBS Lett. **574:** 85-88

Shen G, Boussiba S, Vermaas WF (1993) *Synechocystis* sp PCC 6803 strains lacking photosystem I and phycobilisome function. Plant Cell **5:** 1853-1863

Stadnichuk IN, Yanyushin MF, Maksimov EG, Lukashev EP, Zharmukhamedov SK, Elanskaya IV, Paschenko VZ (2012) Site of non-photochemical quenching of the phycobilisome by orange carotenoid protein in the cyanobacterium *Synechocystis* sp. PCC 6803. Biochim Biophys Acta **1917:** 1436-1445

Sutter M, Wilson A, Leverenz RL, Lopez-Igual R, Thurotte A, Salmeen AE, Kirilovsky D, Kerfeld CA (2013) Crystal structure of the FRP and identification of the active site for modulation of OCP-mediated photoprotection in cyanobacteria. Proc Natl Acad Sci U S A **110:** 10022-10027

Tandeau de Marsac N (2003) Phycobiliproteins and phycobilisomes: the early observations. Photosynth. Res. **76:** 197-205

Tian L, Gwizdala M, van Stokkum IH, Koehorst RB, Kirilovsky D, van Amerongen H (2012) Picosecond kinetics of light harvesting and photoprotective quenching in wild-type and mutant phycobilisomes isolated from the cyanobacterium Synechocystis PCC 6803. Biophys J **102:** 1692-1700

Tian L, van Stokkum IH, Koehorst RB, Jongerius A, Kirilovsky D, van Amerongen H (2011) Site, rate, and mechanism of photoprotective quenching in cyanobacteria. J Am Chem Soc **133:** 18304-18311

Wilson A, Ajlani G, Verbavatz JM, Vass I, Kerfeld CA, Kirilovsky D (2006) A soluble carotenoid protein involved in phycobilisome-related energy dissipation in cyanobacteria. Plant Cell **18:** 992-1007

Wilson A, Gwizdala M, Mezzetti A, Alexandre M, Kerfeld CA, Kirilovsky D (2012) The essential role of the N-terminal domain of the orange carotenoid protein in cyanobacterial photoprotection: importance of a positive charge for phycobilisome binding. Plant Cell **24:** 1972-1983

Wilson A, Kinney JN, Zwart PH, Punginelli C, D'Haene S, Perreau F, Klein MG, Kirilovsky D, Kerfeld CA (2010) Structural determinants underlying photoprotection

in the photoactive orange carotenoid protein of cyanobacteria. J Biol Chem **285:** 18364-18375

Wilson A, Punginelli C, Couturier M, Perrau F, Kirilovsky D (2011) Essential role of two tyrosines and two tryptophans on photoprotection activity of the Orange Carotenoid Protein. Biochim Biophys Acta **1807:** 293-301

Wilson A, Punginelli C, Gall A, Bonetti C, Alexandre M, Routaboul JM, Kerfeld CA, van Grondelle R, Robert B, Kennis JT, Kirilovsky D (2008) A photoactive carotenoid protein acting as light intensity sensor. Proc. Natl. Acad. Sci. U. S. A. **105:** 12075-12080

Yamanaka G, Glazer AN, Williams RC (1978) Cyanobacterial phycobilisomes. Characterization of the phycobilisomes of Synechococcus sp. 6301. J Biol Chem **253:** 8303-8310

Zhao JD, Zhou JH, Bryant DA (1992) Energy transfer processes in phycobilisomes as deduced from mutational analyses. Photosynth. Res. **34:** 83-83

Chapter 3

Structural and Functional Modularity of the Orange Carotenoid Protein: Distinct Roles for the N- and C-terminal Domains in Cyanobacterial Photoprotection

Summary of work

It was recently demonstrated in our laboratory that while OCP^o has a "closed" conformation stabilized by the salt bridge between Arg155 and Glu244, OCP^r has an open conformation in which this bridge got disrupted (Wilson et al., 2012). Moreover, Arg155 appeared as absolutely required for OCP^r binding to phycobilisomes (Wilson et al., 2012).

To test the roles of the N- and C- terminal domains in OCP binding to phycobilisomes, Ryan Leverenz performed a tryptic digestion of *Arthrospira* OCP then purified 2 proteolytic fragments. One of them was red and identified as the isolated N-terminal domain with bound 3'-hECN; it was named Red Carotenoid Protein (RCP). The other one was colorless and identified as the C-terminal domain. Absorbance and Raman spectra suggested that the conformation of the carotenoid in OCP^r and RCP were similar.

RCP's capacity to bind phycobilisomes and trigger fluorescence quenching in vitro was tested. OCP needs to be photoactivated and opened to attach the phycobilisome. RCP did not require any photoactivation. In addition, it could induce a huge and rapid quenching of phycobilisome fluorescence. Thus while the N-terminal domain is a constitutive quencher of phycobilisome fluorescence, the C-terminal domain is the regulator of this activity. In darkness and low light, by interacting with the N-terminal domain, the C-terminal domain avoids exposure of Arg155 and surrounding aminoacids then inhibiting the binding of OCP to phycobilisomes.

Contribution to this work

In this work, I performed all the fluorescence measurements required for assessing RCP's capacity to bind phycobilisomes and induce their quenching.

This chapter is based on:

Leverenz RL, Jallet D, Li MD, Mathies RA, Kirilovsky D and Kerfeld CA, Plant Cell, in press.

Structural and Functional Modularity of the Orange Carotenoid Protein: Distinct Roles for the N- and C-terminal Domains in Cyanobacterial Photoprotection

Ryan L. Leverenz[a,1], Denis Jallet[b,c], Ming-De Li[d,2], Richard A. Mathies[d], Diana Kirilovsky[b,c] and Cheryl A. Kerfeld[a,e,f,1,3]

[a]Department of Plant and Microbial Biology, University of California, Berkeley, California 94720

[b]Commissariat à l'Energie Atomique (CEA), Institut de Biologie et Technologies de Saclay, 91191 Gif sur Yvette, France

[c]Centre National de la Recherche Scientifique, Unite Mixte de Recherche 8221, 91191 Gif sur Yvette, France

[d]Department of Chemistry, University of California, Berkeley, California 94720, USA

[e]U.S. Department of Energy Joint Genome Institute, Walnut Creek, California 94598

[f]Berkeley Synthetic Biology Institute, University of California, Berkeley 94720

[1]Current address: MSU-Department of Energy Plant Research Laboratory, Michigan State University, East Lansing, Michigan 48824

[2]Current address: Department of Chemistry, The University of Hong Kong, Pokfulam Road, Hong Kong S.A.R., People's Republic of China

Corresponding author:

Cheryl A. Kerfeld, MSU-Department of Energy Plant Research Laboratory, Michigan State University, East Lansing, Michigan 48824;

Email: ckerfeld@lbl.gov

ABSTRACT

The Orange Carotenoid Protein (OCP) serves as a sensor of light intensity and an effector of phycobilisome (PB) associated photoprotection in cyanobacteria. Structurally, the OCP is composed of two distinct domains spanned by a single carotenoid chromophore. Functionally, in response to high light, the OCP converts from a dark stable orange form, OCP^O, to an active red form, OCP^R. The C-terminal domain of the OCP has been implicated in the dynamic response to light intensity and plays a role in switching off the OCP's photoprotective response through its interaction with the Fluorescence Recovery Protein (FRP). The function of the N-terminal domain, which is uniquely found in cyanobacteria, is unclear. To investigate its function, we isolated the N-terminal domain *in vitro* using limited proteolysis of native OCP. The N-terminal domain retains the carotenoid chromophore; this Red Carotenoid Protein (RCP) has constitutive PB fluorescence quenching activity comparable in magnitude to that of active, full-length OCP^R. A comparison of the spectroscopic properties of the RCP with OCP^R indicates that critical protein-chromophore interactions within the C-terminal domain are weakened in the OCP^R form. These results suggest that the C-terminal domain dynamically regulates the photoprotective activity of an otherwise constitutively active carotenoid-binding N-terminal domain.

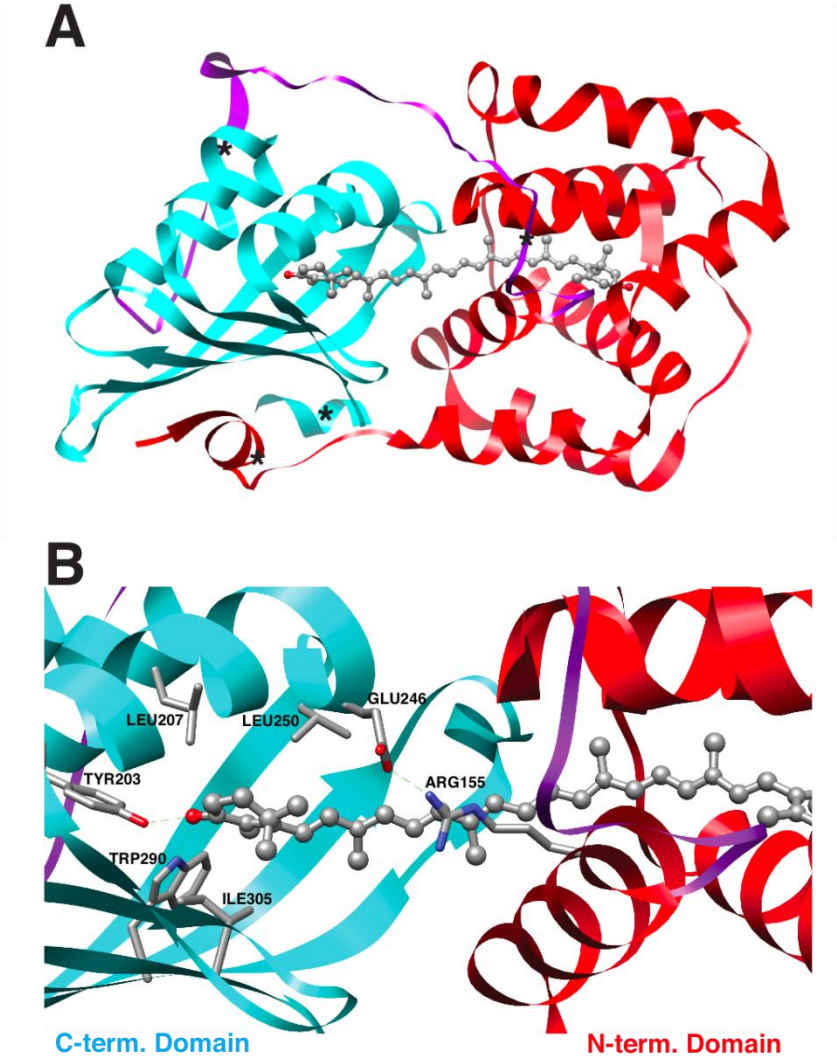

Figure 1. Structure of the OCP from *Arthrospira maxima* (PDB ID: 1M98). (A) The OCP monomer in the OCP^O state. The C-terminal domain (residues 197-315, cyan) is connected to the N-terminal domain (residues 1-160, red) via a long flexible linker (residues 161-196, purple). Preferential trypsin cleavage sites of native OCP (R9, K167, R187, K312) are marked (*). The carotenoid, 3'-hydroxyechineone, is shown in ball and sticks. (B) Close-up view of protein-chromophore interactions in the C-terminal domain and the interface between the N- and C-terminal domains. Tyr203 and Trp290 residues (sticks) H-bond to the 4-keto group of 3'-hECN. Residues Leu207, Leu250, and Ile305 in the C-terminal domain are proposed to sterically constrain the carotenoid in the twisted conformation characteristic of OCP^O (see discussion). The inter-domain salt-bridge between Glu246 and Arg155, known to be disrupted upon photoactivation, is also shown. Figures prepared with the UCSF Chimera package (Pettersen et al., 2004).

INTRODUCTION

The water-soluble Orange Carotenoid Protein (OCP) is a photoactive carotenoid binding protein found in nearly all cyanobacteria (Kirilovsky and Kerfeld, 2013). The OCP plays an important role in regulating energy transfer from the light harvesting phycobilisome (PB) antennae of these organisms by participating in a light-activated, photoprotective non-photochemical quenching mechanism (Scott et al., 2006; Wilson et al., 2006). The photoactivity of the OCP is directly linked to its role as the inducer of photoprotection. Absorption of blue-green light by the single 3'-hydroxyechinenone (3'-hECN) chromophore of the OCP causes a conversion from OCP's dark stable form, OCP^O, to its light activated form, OCP^R (Wilson et al., 2008). Conformational changes in both the carotenoid and the protein (Wilson et al., 2008, 2012) accompany the formation of the OCP^R photoproduct, which binds to PBs and acts as a direct quencher of excess energy and PB fluorescence (Wilson et al., 2008; Gwizdala et al., 2011) The OCP^O state is thus active photochemically (i.e. it is a photoswitch), while the OCP^R photoproduct is active in photoprotection. The structural bases for these diverse functions of the OCP remain largely uncharacterized.

The crystal structure of the OCP^O form has been solved to 2.1 Å for *Arthrospira maxima* OCP (Kerfeld et al., 2003) and, more recently, to 1.65 Å for *Synechocystis* PCC6803 OCP (Wilson et al., 2010). The OCP structure (Figure 1A) includes a mixed α/β C-terminal domain (belonging to the Nuclear Transport Factor-2 [NTF-2] fold; Pfam 02136) and an additional all-helical N-terminal domain unique to cyanobacteria (Pfam 09150). The two domains are connected via a long, flexible linker (residues 160 to 196 in *Arthrospira*). The 3'-hECN chromophore of the OCP is buried in the interior of the protein and spans both domains. Figure 1B shows a detailed view of the protein-chromophore interactions in the C-terminal domain, where absolutely conserved residues Tyr203 and Trp290 (*Arthrospira* numbering; Tyr201 and Trp288 in *Synechocystis*) simultaneously hydrogen bond to the carbonyl group of 3'-hECN in a geometry evocative of the active site of the enzyme ketosteroid isomerase (also a NTF-2 fold) (Cho et al., 1999) or the hydrogen-bonding environment of the p-coumeric acid chromophore in photoactive yellow protein (Borgstahl et al., 1995).

The structural modularity of the OCP, combined with the observation that a large number of cyanobacterial genomes encode multiple copies of genes for the N- and C-terminal domains (often in addition to one or more full-length OCPs)[(Kirilovsky and Kerfeld, 2013)], hints that the N-terminal and C-terminal domains may function independently or perhaps "mix and match" with carotenoids to assemble functionally diverse full length OCPs (Kerfeld et al., 2003). Modular assembly is a recurring theme in many plant and cyanobacterial photoreceptor proteins (Möglich et al., 2010). But do OCP's structurally modular domains perform distinct functions in the context of photoactivity and/or photoprotection?

The first clue to the importance of the OCP's N-terminal structural domain in phycobilisome binding and quenching was recently established by Wilson, et al (2012). Specifically, a positively charged residue, Arg155, in the N-terminal domain was shown to be critical to PB binding and quenching activity in full-length OCP. Isolation of pigmented N-terminal domain fragments during lengthy native source purifications of OCP (Holt and Krogmann, 1981; Wu and Krogmann, 1997; Wilson et al., 2006) suggested a preferential and stable binding of 3'-hECN to the N-terminal domain. These fragments, referred to as "Red Carotenoid Proteins" (RCPs) were presumed to be proteolytic degradation products of the full-length OCP. The absence of genes encoding only the N-terminal domain in *Arthrospira* genomes verifies that these RCPs are the products of proteolysis. Wu and Krogmann determined that one particular 16.7 kDa RCP from *Arthrospira maxima* possessed a mass and primary structure consistent with OCP's N-terminal domain minus the first 15 residues (Wu and Krogmann, 1997). While RCP is not photoactive, it still possesses the molecular characteristics currently known to be required for quenching activity: a 3'-hECN chromophore and a positively charged residue Arg155.

Here, we produced and characterized a homogeneous carotenoid binding N-terminal domain (RCP) fragment obtained via limited proteolysis of native OCP. Using an *in vitro* phycobilisome fluorescence quenching assay (Gwizdala et al., 2011), we show that this RCP is comparable to OCP^R as an active quencher of PB fluorescence *in vitro*. Furthermore, a striking similarity in the electronic and molecular structure of 3'-hECN in RCP and full-length OCP^R (as determined by UV-Visible and Raman spectroscopy)

suggests that the C-terminal domain minimally interacts with 3'-hECN in full-length OCP^R. We propose a model in which protein-chromophore interactions prime photochemistry in OCP^O, but are weakened or absent in the vicinity of the C-terminal domain following formation of OCP^R. These changes are responsible for regulating the activity of the carotenoid binding N-terminal domain. Furthermore, in the absence of the C-terminal domain, the resulting RCP is constitutively active. Collectively, our data identifies distinct functional roles for each structural domain of the OCP in photochemistry and photoprotection.

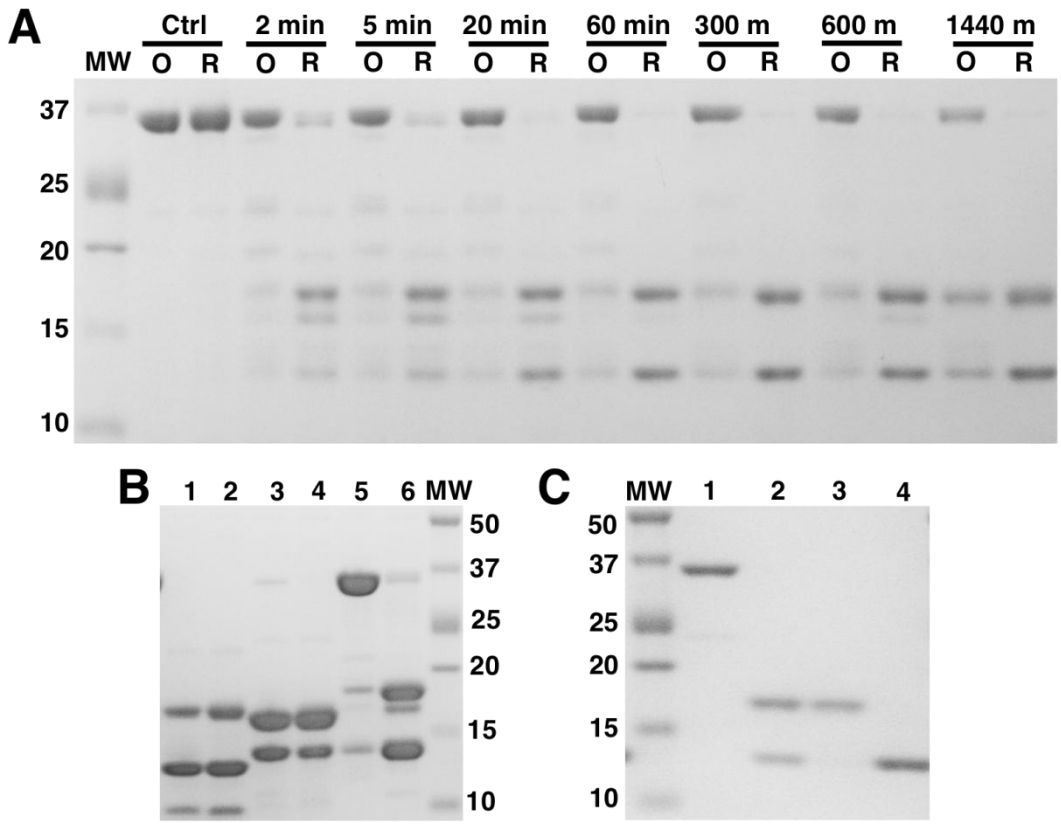

Figure 2. SDS-PAGE of protease products formed by protease digestion of OCP^O and OCP^R. (A) Time-course of native proteolytic digestion of OCP^O and OCP^R by trypsin. Digestions of OCP^O (O) and OCP^R (R) were stopped at times indicated on the horizontal axis. No trypsin was added to control (Ctrl) samples. (B), chymotrypsin (Lanes 3, 4), and glu-c protease (Lanes 5, 6) after 72 hours. (C) Products of an OCP (Lane 1) digest by immobilized trypsin (Lane 2) and the purified 17.5 kDa (Lane 3) and 14.1 kDa (Lane 4) fragments isolated by ion-exchange-chromatography.

RESULTS

Limited Proteolysis of Native OCP

Arthrospira RCP isolated by the method of Holt and Krogmann (1981) was found to be inhomogeneous even after extensive attempts to purify the protein using high resolution ion-exchange chromatography (IEC) and size-exclusion chromatography (SEC). Coomassie-stained SDS-PAGE of the most highly purified fractions exhibited one or two diffuse bands at approximately 15-17 kDa, and in some cases an additional weak band at 12-14 kDa (Supplemental Figure 1). These RCP samples exhibited broad visible absorption spectra with a maximum at 505-507 nm and A_{max}/A_{280} values ranging from 1.88 to 2.28 (Supplemental Figure 1B). In contrast, no 15-17 kDa RCP fragments were observed at any point during the rapid OCP purification from *A. plantensis* described in this work. Instead, this OCP purification resulted in a largely homogeneous 35 kDa OCP as visualized by SDS-PAGE (Figure 2A, Ctrl samples). The A_{max}/A_{280} ratio of OCP purified by this method was >1.8.

Results of SDS-PAGE analysis of limited digestions of OCP^O and OCP^R at different timepoints during a 24-hour digest by trypsin are shown in Figure 2A. Hydrolysis of OCP^O and OCP^R occurred at significantly different rates, with OCP^R exhibiting relatively accelerated degradation to 17 kDa and 14 kDa digestion products. In fact, while OCP^R was completely digested in less than 60 min, more than 50% of full-length OCP was still present after 10 hours of digestion of the OCP^O form. Additional proteolytic digests performed with chymotrypsin and glu-C protease also exhibited a substantial enhancement in the rate of proteolysis of the OCP^R form (Supplemental Figure 2 online). Extended (72 hour) digestions performed with each type of serine protease also produced two dominant protease-resistant fragments (Figure 2B). The observation that two large polypeptide fragments appear regardless of protease substrate specificity strongly suggests that these two large segments of the OCP are inherently resistant to proteolysis (i.e. they form stable, well-folded domains in both OCP^O and OCP^R).

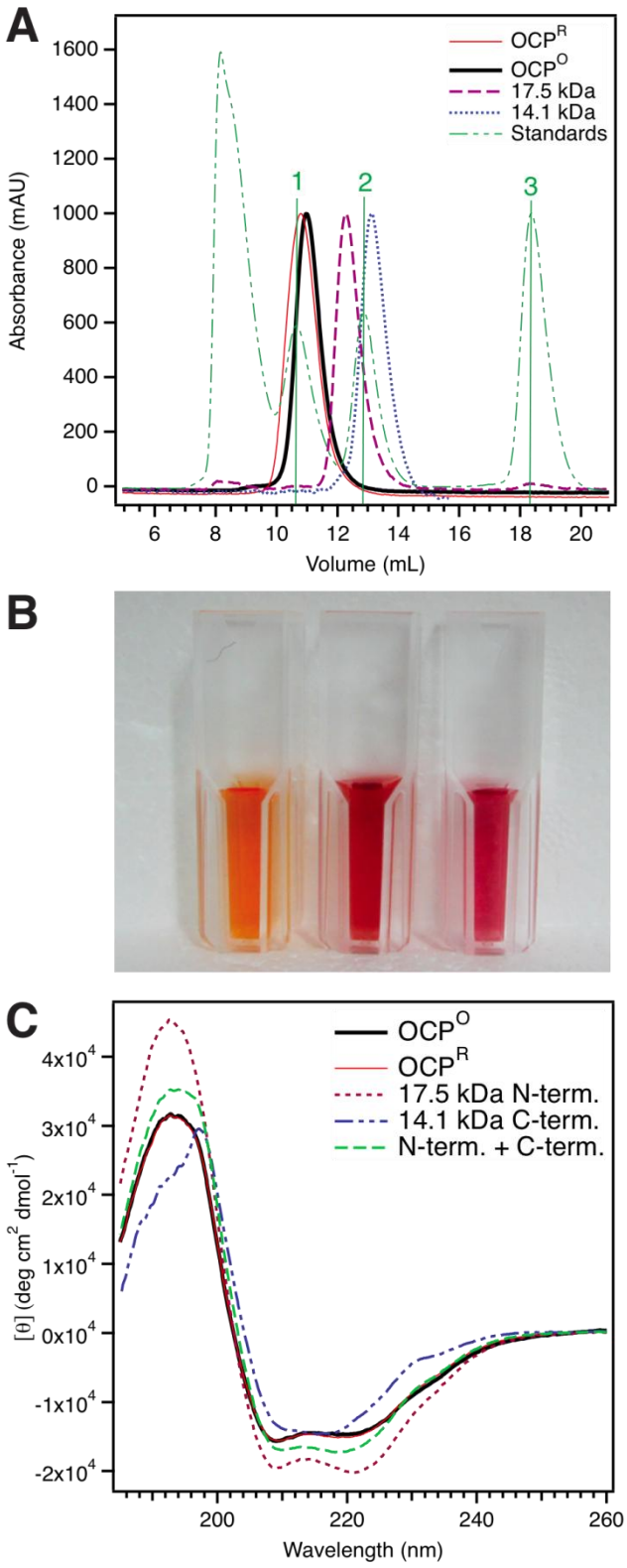

Figure 3. Characterization of the OCP and its isolated domains. (A) Size-exclusion chromatography of gel-filtration standards (dot-dashed green), OCP^R (solid red), OCP^O (solid black), and the 17.5 kDa (dashed purple) and 14.1 kDa (dotted blue) fragments from trypsin digestion of the OCP. For clarity, all absorbance maxima have been normalized to 1000 mAU with exception of the gel-filtration standards. MW markers are labeled with vertical lines as follows: (1) 44 kDa, (2) 17 kDa, and (3) 1.35 kDa (B) OCP^O (left), OCP^R (center), and 17.5 kDa RCP (right) in a 1 cm pathlength cuvette. (C) Far-UV circular dichroism spectra of the isolated 17.5 kDa N-terminal domain (dotted purple), 14.1 kDa C-terminal domain (dot-dashed blue), OCP^O (solid black), and OCP^R (solid red). The sum of the N-terminal and C-terminal domain CD spectra is also shown (dashed green).

Isolation and Identification of the N- and C-terminal Domains of the OCP

Preparative-scale digests of native *Arthrospira* OCP with immobilized trypsin yielded similar degradation fragments to those observed with trypsin in solution (Figure 2C). The primary structure of each fragment was determined by a combination of N-terminal sequencing and matrix assisted laser desorption/ionization time-of-flight (MALDI-TOF) mass spectrometry. From the N-terminal sequence and the MALDI molecular weight (MW) we obtained for each fragment we could identify the cleavage site for trypsin (C-terminal to Lys in both cases). The mass of the larger protein produced during digestion by immobilized trypsin was determined to be 17.46 kDa by MALDI-TOF MS and the N-terminal sequence determined to be Ser-Ile-Phe-Pro-Glu-Thr-Leu-Ala by Edman degradation. This MW and N-terminus corresponds to Residues S10-K167 of the N-terminal domain of *Arthrospira* OCP. The MW of the smaller fragment was determined to be 14.11 kDa by MALDI-TOF MS with an N-terminal sequence of Thr-Lys-Val-Gln-Ile-Glu-Gly-Val, which corresponds to residues T188-K312 of the C-terminal domain. These preferential sites of proteolysis by trypsin are indicated in Figure 1A and the results indicate that trypsinization of native OCP preferentially digests the flexible linker but leaves the structural domains largely intact.

The 17.5 and 14.1 kDa protein fragments were separated by subsequent IEC and SEC purification. Both the 17.5 kDa and 14.1 kDa fragments eluted as single peaks during final SEC (Figure 3A). The 17.5 kDa N-terminal domain from preparative trypsin digests was found to elute at an apparent MW of 22 kDa by analytical SEC, while the C-terminal domain fragment eluted at an apparent MW of 15 kDa. On the same analytical SEC column, full-length OCP^O (in darkness) eluted with an apparent molecular weight (MW) of 41 kDa, while illuminated OCP (enriched in the OCP^R form) was observed to elute at a higher apparent MW (43 kDa) with a significantly broadened elution profile as compared to OCP^O (see also Figure 3A). No clearly resolved peaks suggestive of multiple stable oligomeric states were observed during the OCP^O or OCP^R size exclusion runs. The isolated 17.5 kDa fragment was visibly red in appearance (Figure 3B), whereas the purified 14.1 kDa fragment was colorless. Collectively, these data show that the OCP can

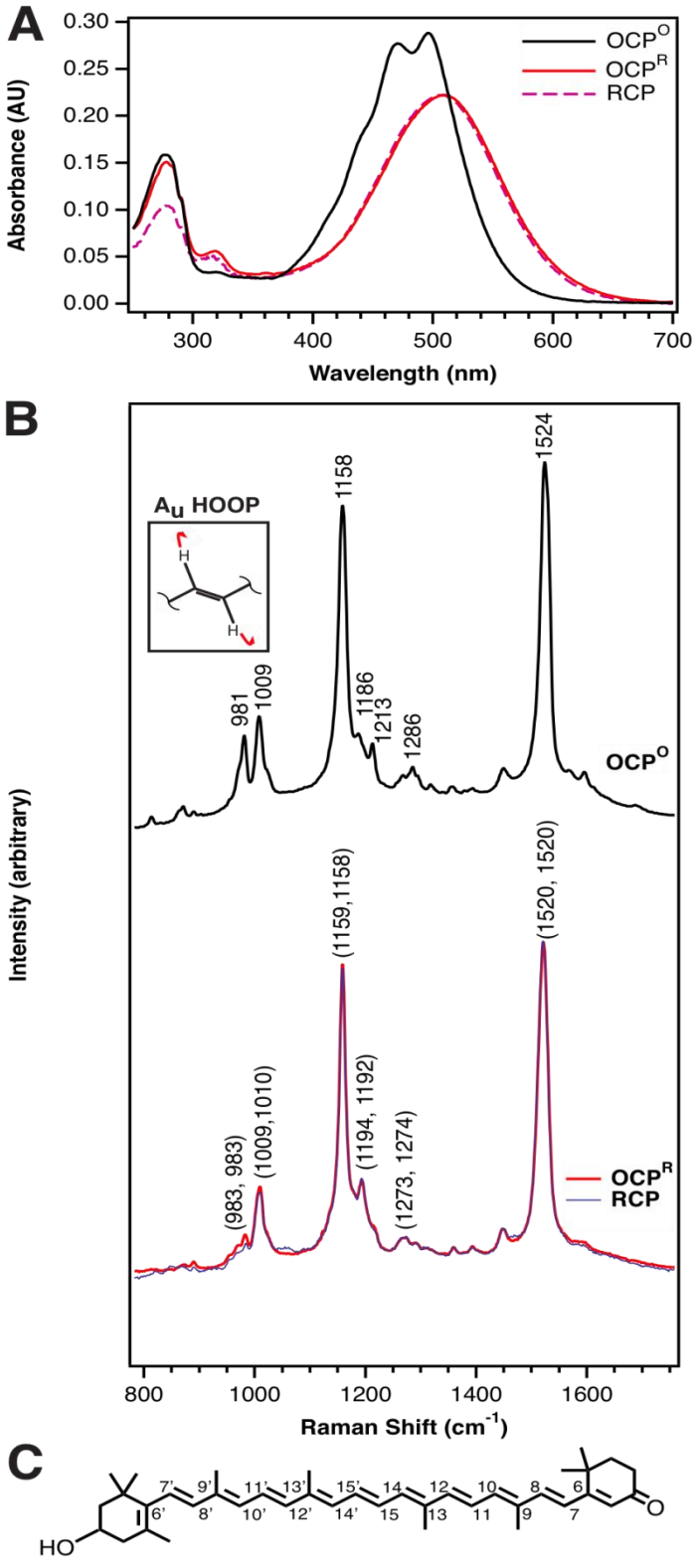

Figure 4. Spectroscopic characterization of 3'-hECN in OCP and RCP. (A) UV-Visible absorption spectra of *A. platensis* OCP^O (black), OCP^R (red), and 17.5 kDa RCP (dotted purple). The inset shows OCP^O, OCP^R, and RCP each in a 1 cm pathlength cuvette. (B) Resonance Raman spectra of OCP^O (black), OCP^R (red), and RCP (blue). The frequencies (1,2) noted in parenthesis correspond to the (1) OCP^R and (2) RCP spectra respectively. The inset depicts the ~980 cm^{-1} in-phase HOOP wagging mode. (C) Structure and C atom numbering of 3'-hECN in the C_6–C_7 *s-trans* configuration.

be reproducibly cleaved into its two structural domains, with the N-terminal domain retaining the carotenoid, forming a 17.5 kDa RCP.

Spectroscopic Characterization of OCP^O, OCP^R, and RCP

The presence of well-ordered secondary structure in each domain isolated by proteolytic digestion of the OCP was confirmed by measuring the far-UV circular dichroism (CD) spectra of the domains (Figure 3C). The N-terminal Domain (RCP) CD spectrum is characterized by a large positive band at 193 nm and negative bands at 209 and 222 nm; consistent with helical secondary structure content (Kelly et al., 2005; Greenfield, 2007). The C-terminal domain CD spectrum is characterized by a positive band 197 nm and negative band at 215 nm; this spectrum is consistent with a mixture of anti-parallel beta-sheet and helix (Greenfield 2006). The sum of the N-terminal and C-terminal domain CD spectra approximate the full-length OCP spectra, and the few observed differences can be attributed to the presence of the flexible linker which contributes additional disordered secondary structure (expected to have a negative band at 195 nm and a small positive band at 210-230 nm [Greenfield 2006]) to full-length OCP^O or OCP^R. These results are entirely consistent with removal of the OCP's disordered flexible linker by trypsin, resulting in separated, but structurally intact N- and C-terminal domains.

The 17.5 kDa N-terminal domain RCP produced by trypsin digestion of highly purified *A. platensis* OCP represents the first *homogeneous* RCP described to date. In order to further characterize the protein and chromophore structure of this RCP, steady-state spectroscopic characterization was performed in parallel with a similar characterization of full-length *A. platensis* OCP^O and OCP^R. The UV-Visible absorption spectra of *A. platensis* OCP^O, OCP^R, and of the RCP are shown in Figure 4A. The absorption spectrum of RCP described here differs in some ways from those previously reported (Holt and Krogmann, 1981; Chábera et al., 2011). Significantly less vibronic structure is observed in the $S_0 \rightarrow S_2$ transition of the carotenoid in the visible region of the spectrum. Pronounced vibronic structure in the OCP^O spectrum results from the constrained, C_6–C_7 *s-trans* conformation of 3'-hECN observed in the OCP^O crystal

structure (see Figure 4C for C atom numbering in the 3'-hECN structure). In previous studies, vibronic structure in the RCP spectrum is readily apparent in the form of distinct shoulders at 410 and 470 nm, with the shoulder at 410 nm being attributed to RCP aggregates (Chábera et al., 2011). The visible absorption spectra of RCP isolated in this work is nearly identical to that of the full-length OCP^R photoproduct (Fig 4A). That is, while the OCP^O spectrum possesses clear vibronic structure, the RCP and OCP^R spectra are almost identically broadened and red-shifted (with maximum absorbance at 510 nm for OCP^R and 507 nm for RCP) with a striking absence of any vibronic features. The broadening and red-shifting of the 3'-hECN chromophore in the OCP and RCP, attributed to conformational heterogeneity of 3'-hECN in these proteins, as well as orientation and local environment of the carbonyl oxygen, has been discussed in detail elsewhere (Polívka et al., 2005; Chábera et al., 2011; Berera et al., 2012). Similar effects are observed in the absorption spectra for other carotenoids with conjugated carbonyl groups when dissolved in polar solvents (Bautista et al., 1999; Frank et al., 2000). The reduced A_{280} in the RCP spectrum is consistent with the loss of aromatic amino acids associated with the C-terminal domain. Furthermore, as compared to the OCP^O spectrum, both the RCP and OCP^R absorbance spectra exhibit significantly increased intensity in a near-UV band at 318 nm.

The molecular structure of the RCP's 3'-hECN chromophore was further characterized by resonance Raman spectroscopy. Resonance Raman spectra of the RCP, as well as *Arthrospira* OCP^R and OCP^O, are shown in Figure 4B. The OCP^R and RCP spectra exhibit nearly identical frequencies and relative intensities for all vibrational modes observed. However, a comparison of these spectra to that of OCP^O reveals a number of differences. First, a blue shift of the intense C=C stretching mode of OCP^O, from 1520 cm^{-1} to 1524 cm^{-1}, is observed. This suggests a larger effective conjugation length in the 3'-hECN chromophore of RCP/OCP^R: an observation previously proposed to result from a more planar *s-trans* conformation of the 4-keto-β-ionylidene ring in OCP^R (Wilson et al., 2008). Additionally, while no large differences were observed for the intense methyl rocking and C–C stretching modes observed at ~1008 cm^{-1} and ~1157 cm^{-1} respectively, there are still some notable differences in the 1100 cm^{-1} to 1400 cm^{-1} fingerprint region of the spectrum. Two distinct peaks at 1186 and 1213 cm^{-1} in the OCP^O

spectrum are replaced by a single, dominant, 1193 cm^{-1} peak in the OCP^R/RCP spectrum. A moderately intense peak at 1286 cm^{-1} is also unique to the OCP^O spectrum. While the OCP^R and RCP fingerprint spectra are in excellent qualitative agreement with that of trans β-carotene in solution (Koyama et al., 1988), the fingerprint region of the OCP^O spectrum is rather unusual for an all-trans C40 carotenoid. However, this is perhaps unsurprising given the unique protein environment of OCP^O and the twisted and bowed conformation of 3'-hECN observed in the crystal structure.

The most striking feature distinguishing the Raman spectra of RCP/OCP^R from that of OCP^O, however, is the extremely large intensity difference observed for a ~980 cm^{-1} hydrogen-out-of-plane (HOOP) wagging mode. The relatively high frequency of this particular HOOP vibration is most consistent with a combination A_u type HOOP mode resulting from the in-phase wagging of two hydrogens across an unsubstituted double bond in the all-trans polyene chain (see Figure 4B, inset).This assignment is supported by the 955-965 cm^{-1} frequency calculated for these modes by normal-coordinate analysis of all-trans beta-carotene (Saito and Tasumi, 1983). HOOP modes can serve as direct reporters of out-of-plane distortions, since the intensity of these modes are typically quite low for a planar polyene, but increase if local symmetry in the vicinity of the bond is broken (Eyring et al., 1980). Thus, we expect the intensity of this mode in OCP^O to originate from torsional distortions to the polyene chain enhancing one or more of the A_u type CH=CH HOOP modes. The observation of the reduced HOOP mode intensity in *Arthrospira* OCP^R is consistent with the Raman data presented for *Synechocystis* PCC 6803 OCP of Wilson et al. (2008) and their proposal of a twisted-to planar conformational change for 3'-hECN in the $OCP^O \rightarrow OCP^R$ transition (Wilson et al., 2008). The interpretation of the Raman spectrum of the RCP is consistent with that of OCP^R: even in the absence of the C-terminal domain, the 3'-hECN polyene of RCP is in a relatively planar, and likely *all-trans* configuration (based on the similarity of the OCP^R/RCP spectra to that of trans β-carotene in solution (Koyama et al., 1988)). This observation further underscores the specific effect of the C-terminal domain protein environment on the carotenoid structure in OCP^O. Furthermore, the RCP Raman results suggest that the ~980 cm^{-1} HOOP intensity observed in the OCP^O spectrum can be assigned to one or more of the torsionally distorted $C_7H=C_8H$, $C_{11}H=C_{12}H$, or

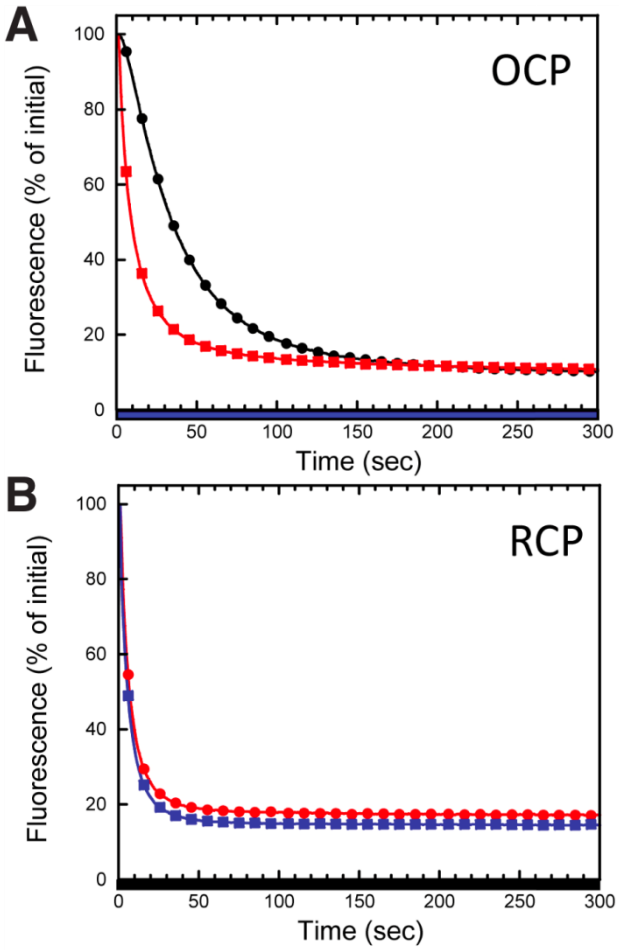

Figure 5. Quenching of phycobilisome fluorescence induced by the OCP (A) and the RCP (B). (A) Isolated *Synechocystis* phycobilisomes were illuminated in the presence of OCP^O (black, circles) or in the presence of OCP^R (red, squares). OCP^O was preconverted to OCP^R by illumination with strong white light. (B) Isolated *Synechocystis* phycobilisomes were incubated in darkness with RCP (red circles) or a mixture of unfractionated proteolytic products from trypsin digestion of OCP (blue, squares).

$C_{15}H{=}C_{15'}H$ combination HOOP wagging modes localized in the vicinity of the C-terminal domain of OCP^O. The striking similarity of the electronic absorption and Raman spectra of 3'-hECN in RCP and OCP^R together suggests that 3'-hECN chromophore is in a similar local environment in RCP and OCP^R; an environment distinctly different than that of 3'-hECN in OCP^O.

Phycobilisome Fluorescence Quenching Assays

Next, we investigated whether the RCP could bind to PBs and trigger quenching of their fluorescence. An *in vitro* reconstitution system allowed measuring the changes in the fluorescence of isolated *Synechocystis* PBs following addition of *Arthrospira* OCP or RCP (Gwizdala et al., 2011). Figure 5A reveals that *Arthrospira* OCP^O induced a rapid fluorescence decrease (83% in 100s) when mixed with *Synechocystis* PBs under continuous blue-green illumination. This process was accelerated by pre-converting OCP^O to OCP^R prior to mixing (83% in 50s). Similar experiments carried out using *Synechocystis* OCP instead of *Arthrospira* OCP gave identical traces (see Fig.5 in Gwizdala et al., 2011), showing that both OCPs have a strong affinity for *Synechocystis* PBs.

The quenching activity of the *Arthrospira* 17.5kDa RCP, as well as that of the unfractionated proteolytic products from immobilized trypsin digests of the OCP (i.e. a 1:1 mix of the 17.5 kDa N- and 14.1 kDa C-terminal fragments) was then assayed. Both samples were found to induce a fast fluorescence quenching similar to that induced by full-length *Arthrospira* OCP^R. *Synechocystis* PB fluorescence decreased by 80-83% in only 50s (Figure 5B). Thus, the 17.5 kDa RCP strongly induced PB fluorescence quenching comparable to that of OCP^R (Figure 5A). PB fluorescence quenching by the RCP occurred in darkness and no additional quenching was observed upon the addition of actinic light. Since quenching of PB fluorescence by the RCP did not require photoactivation and was not affected by the presence of the 14.1 kDa C-terminal fragment, this indicates that quenching is the function of the constitutively active N-terminal domain alone.

DISCUSSION

Formation of RCP by Native Proteolysis: a Probe of OCP Structural Change *in vitro*

Comparative proteolysis of native OCP^O and OCP^R were used to probe for structural differences between the two forms of full-length OCP, as well as to optimize conditions for preparative digests of native OCP to produce RCP. Comparison of the OCP^R and OCP^O digestions shows a remarkably enhanced susceptibility of OCP^R to proteolysis into its two component domains using a variety of serine proteases. The enhanced protease susceptibility of OCP^R provides clear evidence for structural rearrangement of the OCP holoprotein following light absorption.

The results of our proteolytic assays are also consistent with the results of analytical gel-filtration of OCP^R, in which a higher apparent MW (as compared to OCP^O) suggests an increase in the Stokes radius of the protein. This change can be attributed to a change in overall tertiary protein structure following photoconversion. Proteolysis results in two intact domains and each, as demonstrated by CD, largely retains its native secondary structure. This, and the observation that the linker joining them is preferentially digested in OCP^R, suggests that the major changes to the protein structure result in an increased accessibility of the linker to protease. Together, these data suggest that photoactivation minimally alters secondary structure, but that the global tertiary structure and linker accessibility of the OCP changes significantly in the photoprotective OCP^R form. This is consistent with our previous proposal of an "open" form of OCP^R: a dissociation of the N- and C-terminal domains results in increased solvent exposure of the N-terminal domain surface containing R155 and the carotenoid. Importantly, far-UV CD spectra collected on OCP^O and OCP^R (Figure 3C) are consistent with the proteolysis results; no major changes to secondary structure are observed between the two forms of full-length OCP. The enhanced rate of proteolysis in the OCP^R form is more likely due to a change in global tertiary structure affecting accessibility to the linker.

The OCP is a Modular Protein With Specific Functional Roles for its Structural Domains.

The results of PB fluorescence quenching induced *in vitro* by the RCP clearly shows that this protein, which contains only 3'-hECN and the OCP N-terminal domain, is an active quencher of PB fluorescence comparable to full-length OCP^R. This result suggests that the C-terminal domain of the OCP is not absolutely required for either OCP-phycobilisome binding or quenching.. While it is certainly possible that protein-protein interactions between the C-terminal domain and the PB core make minor contributions to the binding/affinity between full-length OCP and the PB, such interactions must be comparatively weaker. We conclude that the RCP, the carotenoid binding N-terminal domain of the OCP, is a constitutively active quencher of phycobilisome fluorescence.

The preferential retention of 3'-hECN by the N-terminal domain also suggests a relatively high affinity for this hydrophobic molecule; accordingly, the RCP is a remarkably compact soluble carotenoid binding protein. And while select N-terminal domain residues (i.e. Y44, W110) in the chromophore binding pocket have been shown to be critical for photosensory response (Wilson et al., 2010, 2011), the molecular basis for this relationship has yet to be explained. To our knowledge, there is no current evidence localizing structural dynamics during the photocycle to the N-terminal domain.

The function of the C-terminal domain is partly identified by our spectroscopic characterization of RCP and OCP; it appears that the C-terminal domain minimally interacts, sterically or electrostatically, with 3'-hECN in full-length OCP^R. The observed differences in the steady-state spectroscopic properties that distinguish OCP^O and RCP/OCP^R are modulated primarily by the C-terminal domain. This is a provocative result, since nearly all data pertaining to structural dynamics in the OCP photocycle have also been localized to possible changes in this domain. Specific proposals for structural changes implicating C-terminal domain dynamics include; (1) H-bonding changes in the Y203/Y290 H-bonds to the 3'-hECN carbonyl oxygen (Wilson et al., 2011); (2) proline isomerization at a loop in the C-terminal domain β-beta sheet (Gorbunov et al., 2011); and (3) breaking of the Arg155:Glu244 salt bridge to form an "open" OCP (Wilson et al., 2012). Furthermore, the general requirement for a conjugated carbonyl group at the C_4

position of the carotenoid (Punginelli et al., 2009) and the absolute requirement of residues Y203 and Y290 for photoactivity (Wilson et al., 2011) also suggest the critical nature of this domain in photosensing. At the same time, the C-terminal domain appears to function in the deactivation of the OCP's quenching activity: recent structural modeling and co-immunoprecipitation results with Fluorescence Recovery Protein (FRP), a protein responsible for a catalyzing the OCP^R to OCP^O dark reaction (Boulay et al., 2010), have clearly identified the C-terminal domain as the site of OCP:FRP interaction (Sutter et al., 2013). These data collectively imply a regulatory role (through responses to light and to the FRP) for the C-terminal domain.

In addition to the dynamic protein structural changes listed previously, the C-terminal domain is also responsible for dynamic changes in the structure of the carotenoid. Removal of the C-terminal domain from the OCP^O structure (Figure 1A), to form RCP must result in the solvent exposure of the 4-keto-β-ionylidene ring of 3'-hECN. Of course, since the C-terminal domain is entirely absent in RCP, the H-bonds to Y203 and W288 must also be broken. Our data suggest that the chromophore binding pocket in the C-terminal domain of OCP^R must be loosened substantially or the chromophore is entirely unbound from the domain. Either picture is consistent with the broadening of the OCP^R/RCP absorption spectra, which can be attributed increased conformational heterogeneity (i.e. unrestricted rotation around C_6-C_7 and other single bonds), as well as potential solvent polarity induced effects resulting from H-bonding between the carbonyl group of the carotenoid and water. This is in stark contrast to the carotenoid-protein interactions in OCP^O, where Tyr203 and Trp290 are hydrogen bonded to 3'-hECN's carbonyl oxygen and carotenoid-protein interactions are largely responsible for locking the carotenoid in a twisted conformation (Kerfeld et al.; 2003). This twisted conformation is apparent in the crystal structure (Figure 1B), where the 4-keto-β-ionylidene ring of 3'-hECN appears to adopt an unusually out-of-plane conformation to enable its H-bonding with Tyr203 and Trp290. This locked and twisted chromophore structure is further evidenced by the well-defined vibronic structure in the electronic absorption spectrum and the large ~980 cm^{-1} HOOP mode intensity in the Raman spectrum of OCP^O.

It appears that interactions between 3'-hECN and the C-terminal domain in OCP^O are responsible for the out of plane distortions giving rise to the observed ~980 cm^{-1} HOOP intensity in the OCP^O Raman spectrum, which we propose to result from distortion around the C_7=C_8 region of the chromophore. While the unique hydrogen-bonding environment of the 3'-hECN's carbonyl group in the C-terminal domain is known to be required for carotenoid binding and photoactivity, it is also appears that three highly conserved bulky residues, Leu207, Leu250, and Ile305, form a bulky "hydrophobic clamp" which may additionally contribute to the out-of-plane twisting of the chromophore's 4-keto-β-ionylidene ring in the OCP^O form.

We suggest that distortions resulting from protein-chromophore interactions in the C-terminal domain may prime an isomerization about the C_7=C_8 bond and that a C_7=C_8 trans-cis isomerization is a distinct possibility for primary photochemistry. While this result might seem to contradict the likely all-trans chromophore structure observed in the OCP^R Raman spectrum (Figure 4B), we note that a re-isomerization to an all-trans structure may occur as a thermal/dark reaction on a faster timescale than slow protein structural changes implicated in the formation of the final OCP^R form. This proposal is thus consistent with both the OCP^O chromophore structure observed by x-ray crystallography, as well our spectroscopic data. Importantly, we would expect a cis C_7=C_8 chromophore to introduce a large amount of strain to the confined C-terminal domain chromophore binding pocket; an effect which would be expected to drive further structural changes in this domain. Protein structural changes driven through the relaxation of strained protein-chromophore intermediates are known to play a signaling role in other blue light photosensors, such as PYP (Ihee et al., 2005).

A Revised Model for OCP Function

The emerging picture of the OCP as a modular protein with distinct structural and functional domains significantly advances the mechanistic understanding of the OCP's photoprotective function. Given the constitutive quenching activity of the N-terminal domain RCP isolated and characterized here, we suggest that the primary role of OCP's C-terminal domain is to regulate the accessibility, and hence activity, of the PB binding

N-terminal domain. This occurs via a mechanism that effectively exposes the inter-domain interface of the N-terminal domain containing Arg155 following photochemical activation. Without such regulation, it seems that OCP's carotenoid-binding N-terminal domain could bind to the phycobilisome even in dim light or darkness. The PB-binding interface of the N-terminal domain and the carotenoid are shielded by the C-terminal domain in OCP^O until required for photoprotection. FRP restores the ground state OCP^O structure by catalyzing the rate-limiting step of the OCP^R to OCP^O reaction through an interaction with the C-terminal domain, thus reforming the quenching inactive OCP^O state.

The identification of the RCP as a constitutively active quencher of phycobilisome fluorescence raises the question as to the role of genes encoding N-terminal domain homologues in many cyanobacterial genomes; do they play an OCP-like photoprotective role *in vivo*? Furthermore, the specialized functions of OCP's discrete domains demonstrated in this work are also consistent with the speculation of modular assembly of homologs to the N- and C-terminal domains to form full length OCPs with unique photosensory and photoprotective properties. This type modular assembly is known for other photosensory proteins, in which blue-light sensing BLUF and LOV domains are fused to various output modules (Crosson et al., 2003).

Finally, we note that the modular structure and function of the OCP differs from those of other photosensory proteins in that each domain of the OCP absolutely requires the 3'-hECN chromophore to perform its function. The C-terminal domain cannot function as a photosensor without a light absorbing chromophore. The N-terminal effector domain, once bound to the phycobilisome, requires 3'-hECN to directly dissipate energy in the OCP induced photoprotective mechanism (Tian et al., 2011, 2012). The OCP thus represents a remarkably minimized system in which sensor and effector domains share a single chromophore that is critical to both photosensory and photoprotective function.

Methods

Purification of Orange Carotenoid Protein from *Arthrospira platensis*

Frozen cells of *A. platensis* were a generous gift of the Cyanotech Corporation and were stored as a wet paste at -80 °C until needed. All purification steps were carried out at 0-4°C in dim light or darkness. Cells were lysed by thawing wet cell paste in 100 mM Tris-HCl pH 8.0 (4°C), 100 mM NaCl, 5% glycerol, 4 mM PMSF, 4 mM EDTA, 2 mM EGTA (1 g wet cells / 1 mL buffer). The cells were broken in 200 mL batches by beating with 0.1 mm glass beads for 15 seconds × 8 cycles. Following lysis, the cellular extract was centrifuged at 10 000 × g to remove insoluble material. A saturated $(NH_4)_2SO_4$ solution was then slowly added to the decanted supernatant until the $(NH_4)_2SO_4$ concentration of the extract reached 1.5 M. The extract was centrifuged at 40 000 × g to pellet remaining thylakoids and a small amount of precipitated phycobiliproteins. The supernatant was decanted and filtered (0.45 um) prior to column chromatography.

A rapid separation of the OCP from the clarified soluble extract was performed using hydrophobic interaction chromatography (HIC). A detailed summary of HIC parameters can be found in Supplemental Table 1 online. HIC effectively separated the OCP from phycobiliproteins in the lysate. Visibly orange fractions containing OCP were reserved and desalted on a 2.5 cm diameter, 60 cm high column of Superdex G-25 (GE Health Sciences) using 20 mM Tris-HCl pH 8.5, 1 mM EDTA as an elution buffer. Intermediate purification of the desalted OCP was performed using anion exchange chromatography (AEC, details in Supplemental Table 1). Following initial AEC, OCP containing fractions with $A_{496}/A_{280} > 1.5$ were pooled and concentrated to approximately OD_{496} = 50/cm using Amicon 15 Spin Concentrators (Millipore). These fractions were desalted and further polished using a Mono-Q HR 16/10 IEC column (GE Health Sciences). Following final size exclusion chromatography (SEC, details in Supplemental Table S1), the purity of the OCP was checked by absorption spectroscopy and SDS-PAGE. Absorption spectra of the OCP fractions reserved for further analysis all exhibited $A_{496}/A_{280} >= 1.8$. SDS-PAGE was performed using 12% Bis-Tris Gels (Criterion XT, Bio-Rad) and MOPS or MES running buffer. Protein bands were stained with Coomassie G-250 (Thermo GelCode Blue).

Limited Proteolysis of Orange Carotenoid Protein

Proteolytic digests of OCP^O and OCP^R were performed using trypsin, chymotrypsin, and glu-C protease (Promega). Each digest was performed at 4°C with a protease:protein ratio of 1:100. For OCP^R digests, OCP^O was converted to OCP^R using strong, blue LED illumination (~470 nm λ_{max}, Philips Lumileds LXML-PB01-0030). Illumination was maintained throughout the duration of the digest following addition of protease to OCP^R sample. The OCP concentration was 0.3 mg/mL for all digests. Following addition of protease, aliquots were removed at specified time points and the reaction stopped via addition of protease inhibitor (PMSF for trypsin and chymotrypsin) followed by freezing on dry ice. Digestions with glu-C were stopped by flash freezing alone. Control samples of OCP^O and OCP^R (with no protease added) were incubated for the full time course and treated identically to protease containing samples. After flash freezing, each sample was immediately transferred to -80°C for storage. Samples were quickly thawed in warm SDS buffer prior to analysis by SDS-PAGE. SDS-PAGE was performed as described previously using MES running buffer.

Preparative Isolation of Red Carotenoid Protein

RCP was initially isolated as a degradation product of OCP produced during purifications by a method similar to that of Holt and Krogmann (1981) with isoelectric focusing omitted. RCP produced by this method was initially separated from OCP during size exclusion chromatography and protein isolated by this method was found to be inhomogeneous as indicated by SDS-PAGE (Supplemental Figure 1 online). Thus, a more homogeneous N-terminal domain OCP fragment was produced by controlled proteolytic digestion of *A. platensis* OCP with immobilized trypsin (Pierce). Trypsin gel (washed and suspended according to the manufacturer's instructions) was added to 0.6 mg/mL *A. platensis* OCP in 50 mM Tris-HCl pH 7.4, 200 mM NaCl at a ratio of 3:1 (v:v) of OCP:gel. The mixture was incubated with mixing for 24 hours under blue light at 4°C. Trypsin gel was then removed by centrifugation, followed by 0.22 um filtration of the supernatant. The native digestion products produced by this method were separated by IEC on a Mono-Q 5/50 GL column (GE Healthcare) or HiLoad 16/10 Q-sepharose HP

column (GE Healthcare) using a linear gradient of 0 to 100 mM NaCl in 20 mM Tris-HCl pH 7.5, followed by final SEC as described previously. The purity of the isolated RCP was checked by absorption spectroscopy and SDS-PAGE.

Analytical Size Exclusion Chromatography

Analytical size exclusion chromatography was performed on a Superdex 75 GL 10/300 gel filtration column (GE) with 50 mM Tris-HCl pH 7.4, 200 mM NaCl as the running buffer. Bio-Rad molecular weight (MW) standards were used for calibration of the column. OCP^O was run in darkness, while OCP^R was run following 10 minutes of actinic illumination from a blue LED. All samples (including standards) were run in triplicate and the average retention time was used for MW estimation. Apparent MWs were determined for proteins of interest by fitting the partition coefficent (K_{av}) of the analyte to a linear fit of K_{av} vs log(MW) for the fractionated standards.

MALDI and N-terminal Sequencing

MALDI mass determination of unfractionated fragments produced by trypsin digestion was performed at the Stanford Protein and Nucleic Acid (PAN) facility using an ABI Voyager DE-RP mass spectrometer. N-terminal sequencing of digest fragments was performed on solution-state samples (purified by IEC/SEC as described previously) using an ABI 494-HT Procise Edman Sequencer at the UC Davis Genome Center Proteomics Core facility. A single, unambiguous sequence was detected during N-terminal sequencing of both N-terminal and C-terminal OCP domain fragments produced during trypsin digests.

Circular Dichroism Spectroscopy

All protein samples were dialyzed into 20 mM potassium phosphate, 100 mM NaF prior to far-UV CD measurements. Far-UV CD spectra were acquired in 1 mm path-length quartz cuvette using a Jasco J-815 spectropolarimeter with 1 nm bandwidth, 1 s time constant, 50 nm/min scan speed, and 8-16 averages per spectrum. OCP^R spectra were collected following 5 minutes of blue LED illumation prior to each individual scan. A buffer blank was subtracted from each CD spectrum and no smoothing of the averaged

data was performed. Protein concentrations were determined by quantitative Amino Acid Analysis using a Hitachi L-8800 amino acid analyzer (UC Davis Proteomics Core Facility) and the mean residue ellipticity, [θ], for each sample was calculated using the formula: [θ] = (raw data in millidegrees × MRW) / (path length [in mm] × concentration [in mg/mL]), where the mean residue weight, MRW, of the protein is given by MRW = molecular weight / number of backbone amides (Greenfield, 2006).

UV-Visible Spectroscopy

Samples were buffer exchanged into 50 mM Tris-HCl, pH 7.4, 200 mM prior to spectroscopic measurements. The UV-Visible absorption spectrum of OCP^R was collected using an Agilent 8453 spectrophotometer following 10 minutes of 470 nm LED illumination at 0°C. The OCP^O spectrum was collected identically without actinic illumination. All other UV-Visible absorbance spectra reported were collected on a Varian Cary Bio 100 spectrophotometer at room temperature.

Raman Spectroscopy

Raman spectra of OCP^O, OCP^R, and RCP in 50 mM Tris-HCl pH 7.4, 200 mM NaCl were collected using the 514.5 emission line of an Ar^+ Laser (Spectra Physics Model 2020). The laser power was < 2 mW for all measurements. The beam was spherically focused on a 0.8 mm ID glass capillary and perpendicular Raman scattering collected and subsequently imaged using a double subtractive spectrograph and LN_2 cooled CCD. Protein concentrations were 0.10 – 0.30 mg/mL for all measured samples and samples were flowed through the capillary using a peristaltic pump. OCP^Ospectra were collected under rapid-flow conditions (50 mL/min) in order to minimize the effect of photolysis on the measured spectrum. The OCP^R spectrum was collected under identical conditions, except with continuous blue LED illumination of the sample reservoir 10 minutes prior to beginning the measurement and throughout data acquisition. RCP spectra were collected in darkness with capillary flow techniques, or (for volume limited samples) using a spinning cell in a backscattering geometry. All spectra were measured in triplicate using protein from three independent preparations and the reported frequencies, calibrated using a cyclohexane external standard, are accurate +/- 2 cm^{-1}.

Phycobilisome Fluorescence Quenching Assays

Phycobilisomes isolation from *Synechocystis* cells followed the protocol described in Gwizdala et al. (2011). At the beginning of every measurement, OCP or RCP was added to the isolated PBs (0.012µM) kept in 0.8 M potassium-phosphate buffer (pH 7.5) giving an OCP or RCP-to-PB ratio of 40 or 20. Fluorescence was recorded at 23°C, using a PAM fluorometer (101-102-103-PAM; Walz). Concerning actinic treatment, samples were illuminated by blue-green light (Halogen white light filtered with a Corion cut-off 550-nm filter; 400 to 550nm, 900 µmol photons m^{-2} s^{-1}) (Figure 5A) or kept in the dark for 300 s prior to illumination (Figure 5B).

Supplemental Table

Method	Resin	Bed Height × Diameter	Buffer A	Buffer B	Gradient Slope (total CV)	Flow Rate (mL/ min)
HIC	Tosoh Bioscience Toyopearl Super-Q HIC Phenyl 650-M	5 × 20 cm	50 mM Tris-HCl, pH 7.5, 1.5 M $(NH_4)_2SO_4$, 2 mM PMSF, 2 mM EDTA	50 mM Tris-HCL, pH 7.5, 0 M $(NH_4)_2SO_4$, 2 mM PMSF, 2 mM EDTA	10 CV	10
QAE	Tosoh Toyopearl Super-Q QAE 650-M	2.5 x 25 cm	20 mM Tris-HCl pH 7.5	Buffer A + 400 mM NaCl	20 CV	5
QAE	GE Healthcare Mono-Q 5/50	5 x 50 mm	20 mM Tris-HCl pH 7.5	Buffer A + 250 mM NaCl	20 CV	0.5
SEC	GE Healthcare Hi Load 16/60 Superdex 75	16 mm x 60 cm	50 mM Tris-HCl pH 7.5, 200 mM NaCl, 10% glycerol	None	NA	0.5

Table S1. Parameters used for column chromatography during native source purifications of the OCP from *Arthrospira.*

Supplemental Figures

S1

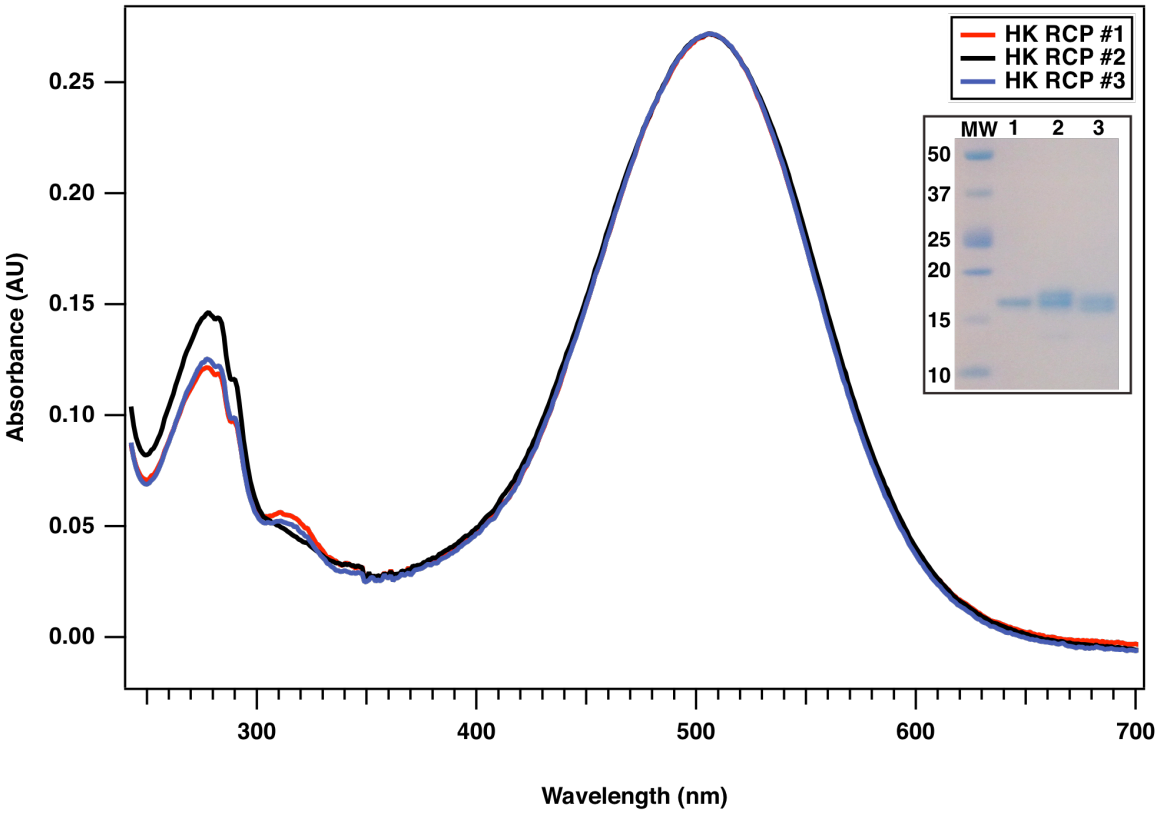

Supplemental Figure 1. UV-Visible spectra and SDS-PAGE of RCP isolated from native source OCP purifications performed by a method similar to that of Holt and Krogmann (1981). UV-Vis spectra of RCP samples from three independent protein purifications are shown. Corresponding SDS-PAGE analysis of these samples is shown in the inset.

S2

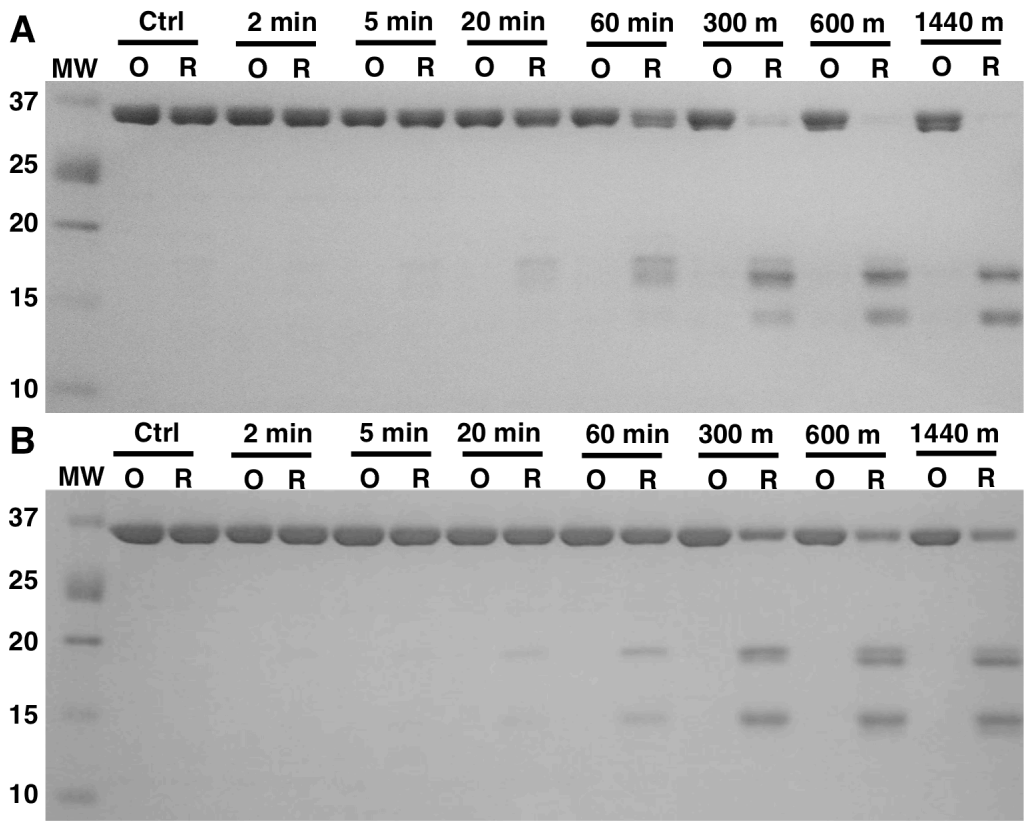

Supplemental Figure 2. SDS-PAGE of additional time-dependent OCP^O and OCP^R digestions by additional serine proteases. **(A)** digestion of native OCP by chymotrypsin **(B)** digestion by glu-c protease. Digestions of OCP^O (O) and OCP^R (R) were stopped at times indicated on the horizontal axis. No protease was added to control (Ctrl) samples.

ACKNOWLEDGMENTS

CAK and RLL acknowledge the support of the NSF (MCB 0851094 and MCB1160614). The research of DK and DJ was supported by grants from the Agence Nationale de la Recherche (ANR, project CYANOPROTECT), the Centre National de la Recherche Scientifique (CNRS), the Commissariat à l'Energie Atomique (CEA) and HARVEST EU FP7 Marie Curie Research Training Network. DJ has a fellowship of the University Paris XI. RLL, ML, and RAM acknowledge financial support from the Mathies Royalty Fund.

AUTHOR CONTRIBUTIONS

R.L.L. designed and performed the research, analyzed and interpreted data, and wrote the article. C.A.K. designed the research, interpreted the data and wrote the article. D.J., M.L. R.A.M., and D.K performed research and contributed to the analysis and interpretation of the data.

REFERENCES

Bautista, J.A., Connors, R.E., Raju, B.B., Hiller, R.G., Sharples, F.P., Gosztola, D., Wasielewski, M.R., and Frank, H.A. (1999). Excited State Properties of Peridinin: Observation of a Solvent Dependence of the Lowest Excited Singlet State Lifetime and Spectral Behavior Unique among Carotenoids. J. Phys. Chem. B **103**: 8751-8758.

Berera, R., van Stokkum, I.H.M., Gwizdala, M., Wilson, A., Kirilovsky, D., and van Grondelle, R. (2012). The Photophysics of the Orange Carotenoid Protein, a Light-Powered Molecular Switch. J. Phys. Chem. B **116**: 2568-2574.

Borgstahl, G.E.O., Williams, D.R., and Getzoff, E.D. (1995). 1.4 .ANG. Structure of Photoactive Yellow Protein, a Cytosolic Photoreceptor: Unusual Fold, Active Site, and Chromophore. Biochemistry **34**: 6278-6287.

Boulay, C., Wilson, A., D'Haene, S., and Kirilovsky, D. (2010). Identification of a protein required for recovery of full antenna capacity in OCP-related

photoprotective mechanism in cyanobacteria. Proc. Natl. Acad. Sci. U.S.A. **107**: 11620 -11625.

Chábera, P., Durchan, M., Shih, P.M., Kerfeld, C.A., and Polívka, T. (2011). Excited-state properties of the 16 kDa red carotenoid protein from *Arthrospira maxima*. Biochim. Biophys. Acta **1807**: 30-35.

Cho, H.-S., Ha, N.-C., Choi, G., Kim, H.-J., Lee, D., Oh, K.S., Kim, K.S., Lee, W., Choi, K.Y., and Oh, B.-H. (1999). Crystal Structure of Δ5-3-Ketosteroid Isomerase from Pseudomonas testosteroni in Complex with Equilenin Settles the Correct Hydrogen Bonding Scheme for Transition State Stabilization. J. Biol. Chem. **274**: 32863-32868.

Crosson, S., Rajagopal, S., and Moffat, K. (2003). The LOV Domain Family: Photoresponsive Signaling Modules Coupled to Diverse Output Domains†. Biochemistry **42**: 2-10.

Eyring, G., Curry, B., Mathies, R., Fransen, R., Palings, I., and Lugtenburg, J. (1980). Interpretation of the resonance Raman spectrum of bathorhodopsin based on visual pigment analogs. Biochemistry **19**: 2410-2418.

Frank, H.A., Bautista, J.A., Josue, J., Pendon, Z., Hiller, R.G., Sharples, F.P., Gosztola, D., and Wasielewski, M.R. (2000). Effect of the Solvent Environment on the Spectroscopic Properties and Dynamics of the Lowest Excited States of Carotenoids. J. Phys. Chem. B **104**: 4569-4577.

Gorbunov, M.Y., Kuzminov, F.I., Fadeev, V.V., Kim, J.D., and Falkowski, P.G. (2011). A kinetic model of non-photochemical quenching in cyanobacteria. Biochim. Biophys. Acta **1807**: 1591-1599.

Greenfield, N.J. (2007). Using circular dichroism spectra to estimate protein secondary structure. Nat. Protocols **1**: 2876-2890.

Gwizdala, M., Wilson, A., and Kirilovsky, D. (2011). In Vitro Reconstitution of the Cyanobacterial Photoprotective Mechanism Mediated by the Orange Carotenoid Protein in *Synechocystis* PCC 6803. Plant Cell **23**: 2631 -2643.

Ihee, H., Rajagopal, S., Šrajer, V., Pahl, R., Anderson, S., Schmidt, M., Schotte, F., Anfinrud, P.A., Wulff, M., and Moffat, K. (2005). Visualizing reaction pathways in photoactive yellow protein from nanoseconds to seconds. Proc. Natl. Acad. Sci. U.S.A. **102**: 7145-7150.

Holt, T. and Krogmann, D.W. (1981). A carotenoid-protein from cyanobacteria. Biochim. Biophys. Acta **637**: 408-414.

Kelly, S.M., Jess, T.J., and Price, N.C. (2005). How to study proteins by circular dichroism. BBA Proteins Proteom. **1751**: 119-139.

Kerfeld, C., Sawaya, M., Brahmandam, V., Cascio, D., Ho, K., Trevithicksutton, C., Krogmann, D., and Yeates, T. (2003). The Crystal Structure of a Cyanobacterial Water-Soluble Carotenoid Binding Protein. Structure **11**: 55-65.

Kirilovsky, D. and Kerfeld, C.A. (2013). The Orange Carotenoid Protein: a blue-green light photoactive protein. Photochem. Photobiol. Sci. **12**: 1135-1143.

Koyama, Y., Takatsuka, I., Nakata, M., and Tasumi, M. (1988). Raman and infrared spectra of the all-trans, 7-cis, 9-cis, 13-cis and 15-cis isomers of β-carotene: Key bands distinguishing stretched or terminal-bent configurations form central-bent configurations. J. Raman Spectrosc. **19**: 37–49.

Möglich, A., Yang, X., Ayers, R.A., and Moffat, K. (2010). Structure and Function of Plant Photoreceptors. Annu. Rev. Plant Biol. **61**: 21-47.

Pettersen, E.F., Goddard, T.D., Huang, C.C., Couch, G.S., Greenblatt, D.M., Meng, E.C., and Ferrin, T.E. (2004). UCSF Chimera—A visualization system for exploratory research and analysis. J. Comput. Chem. **25**: 1605–1612.

Polívka, T., Kerfeld, C.A., Pascher, T., and Sundström, V. (2005). Spectroscopic Properties of the Carotenoid 3‘-Hydroxyechinenone in the Orange Carotenoid Protein from the Cyanobacterium *Arthrospira maxima*†. Biochemistry **44**: 3994-4003.

Punginelli, C., Wilson, A., Routaboul, J.-M., and Kirilovsky, D. (2009). Influence of zeaxanthin and echinenone binding on the activity of the Orange Carotenoid Protein. Biochim. Biophys. Acta **1787**: 280-288.

Saito, S. and Tasumi, M. (1983). Normal-coordinate analysis of β-carotene isomers and assignments of the Raman and infrared bands. J. Raman Spectrosc. **14**: 310-321.

Scott, M., McCollum, C., Vasil’ev, S., Crozier, C., Espie, G.S., Krol, M., Huner, N.P.A., and Bruce, D. (2006). Mechanism of the Down Regulation of Photosynthesis by Blue Light in the Cyanobacterium *Synechocystis* sp. PCC 6803†. Biochemistry **45**: 8952-8958.

Sutter, M., Wilson, A., Leverenz, R.L., Lopez-Igual, R., Thurotte, A., Salmeen, A.E., Kirilovsky, D., and Kerfeld, C.A. (2013). Crystal structure of the FRP and identification of the active site for modulation of OCP-mediated photoprotection in cyanobacteria. Proc. Natl. Acad. Sci. U.S.A. **110**: 10022-10027.

Wilson, A., Ajlani, G., Verbavatz, J.-M., Vass, I., Kerfeld, C.A., and Kirilovsky, D. (2006). A Soluble Carotenoid Protein Involved in Phycobilisome-Related Energy Dissipation in Cyanobacteria. Plant Cell **18**: 992-1007.

Wilson, A., Gwizdala, M., Mezzetti, A., Alexandre, M., Kerfeld, C.A., and Kirilovsky, D. (2012). The Essential Role of the N-Terminal Domain of the Orange Carotenoid Protein in Cyanobacterial Photoprotection: Importance of a Positive Charge for Phycobilisome Binding. Plant Cell **24**: 1972-1983.

Wilson, A., Kinney, J.N., Zwart, P.H., Punginelli, C., D’Haene, S., Perreau, F., Klein, M.G., Kirilovsky, D., and Kerfeld, C.A. (2010). Structural Determinants

Underlying Photoprotection in the Photoactive Orange Carotenoid Protein of Cyanobacteria. J. Biol. Chem. **285**: 18364 -18375.

Wilson, A., Punginelli, C., Couturier, M., Perreau, F., and Kirilovsky, D. (2011). Essential role of two tyrosines and two tryptophans on the photoprotection activity of the Orange Carotenoid Protein. Biochim. Biophys. Acta **1807**: 293-301.

Wilson, A., Punginelli, C., Gall, A., Bonetti, C., Alexandre, M., Routaboul, J.-M., Kerfeld, C.A., van Grondelle, R., Robert, B., Kennis, J.T.M., and Kirilovsky, D. (2008). A photoactive carotenoid protein acting as light intensity sensor. Proc. Natl. Acad. Sci. U.S.A. **105**: 12075-12080.

Wu, Y.P. and Krogmann, D.W. (1997). The orange carotenoid protein of *Synechocystis* PCC 6803. Biochim. Biophys. Acta **1322**: 1-7.

Conclusion and perspectives

Conclusion

Although when this project began, an overall picture of OCP's role in cyanobacterial photoprotection was already drawn, several aspects of the underlying mechanism remained unclear. Particularly, no data was available about the protein-protein contacts allowing OCP-phycobilisome complex formation/stabilization. Also, the phycobilisome (PB) subunit responsible for OCP attachment was not clearly identified at that moment. Finally, the process leading to heat dissipation after OCP's binding was totally unknown. My work consequently focused on characterizing deeper the interactions between OCP and PBs, to get a more detailed view of OCP's function. I got involved in 3 different studies, presented in chapters 1 to 3 of the present manuscript. Based on these works I was able to answer to the following three important questions:

Question 1: What is the binding site for OCP in PBs?

Several preliminary results were obtained by Gwizdala and coworkers thanks to an in vitro reconstitution system of the OCP-related photoprotective mechanism. It was found that, following photoactivation, OCP^r directly binds PBs; this triggers fluorescence quenching (Gwizdala et al., 2011). OCP^r attaches to the allophycocyanin (APC) core but not to the phycocyanin (PC) rods (Gwizdala et al., 2011). Eventually, 1 to 2 OCP^r are present in the quenched OCP-PB complex (Gwizdala et al., 2011). Considering such data, the existence of a specific binding site for OCP in PB cores appeared likely. There are 2 types of APC forms in the core: major ones – emitting fluorescence mainly at 660nm (α^{APC}/β^{APC}; noted APC_{660nm}) – and minor ones, called terminal emitters because of their red-shifted fluorescence emission (ApcD/ApcF/ApcE; noted APC_{680nm}). My first aim consisted in **determining whether OCP^r can interact with APC_{660nm}, APC_{680nm} or both**.

To answer this question I created *Synechocystis* mutant strains with either suppressed or modified APC_{680nm} (ΔApcD, ΔApcF, ΔApcDF and ApcEC190S strains; see chapter 1). Using fluorescence spectroscopy, I showed that strong blue-green light induced identical quenching in the WT and mutant cells. Moreover, the WT and mutated PBs displayed similar affinity for *Synechocystis* OCP in vitro. This study thus proved that neither ApcD nor ApcF are required for OCP attachment. It also revealed that the ApcE-bound bilin is not essential for the OCP-related photoprotective mechanism onset. However, as I could not work on a ΔApcE strain – that would have disassembled PBs – the possibility that some ApcE aminoacids participate in OCP fixation remains open. **My results strongly suggested that OCP binds**

PBs and induces fluorescence quenching at the level of APC_{660nm} (see chapter 1; adapted from Jallet et al., 2012).

This conclusion was rapidly confirmed thanks to our collaboration with H. van Amerongen's group (VU University, Amsterdam). Spectrally resolved picosecond fluorescence spectroscopy was performed in vivo, comparing WT, OCP-deficient and OCP-overaccumulating *Synechocystis s*trains (Tian et al., 2011). Measurements were performed on cells kept either under dark conditions or illuminated with strong blue-green light to trigger the OCP-related photoprotective mechanism (Tian et al., 2011). A model placing the various photosynthetic pigment pools into separated compartments was built then completed through data target analysis, i.e. Species Associated Spectra establishment, permitting to estimate the energy transfer rates between each compartment (Tian et al., 2011). The OCP-associated trapping was integrated as an additional dissipation route and its position iteratively changed, giving satisfying fits only when placed in the APC_{660nm} pool (Tian et al., 2011). Thus, **the OCP-associated mechanism dissipates well away energy from PBs at the level of APC_{660nm}.** Similar conclusion was drawn from another series of measurements made in vitro, on isolated OCP-PB complexes (Tian et al., 2012).

Additionally, some other research groups released data about the OCP binding site in PBs. Submitting PSI/PSII-deficient *Synechocystis* mutant cells to non-linear laser fluorometry, Kuzminov and coworkers retrieved parameters associated with the various phycobiliproteins – including relaxation times, effective excitation cross-sections – in a quenched versus non quenched state (Kuzminov et al., 2012). They concluded that energy losses directly happen at the level of APC_{660nm} (Kuzminov et al., 2012). They also suggested that part of the dissipation process potentially implies APC_{680nm} but could not quantify the contribution from this possible alternative route in vivo. Tian and coworkers had obtained very poor fits of their data when hypothesizing that OCP interacts with an APC_{680nm} trimer (Tian et al., 2011); thus, **the main pathway for energy dissipation implies APC_{660nm} trimers**. Finally, Stadnichuk and coworkers isolated ApcE from *Synechocystis* PBs and tested its interaction with OCP in vitro. They showed a small fluorescence decrease when ApcE was illuminated in the presence of OCP (Stadnichuk et al., 2012; Stadnichuk et al., 2013). However, the very acidic solution employed for ApcE solubilization plus the addition of urea did not mimic physiological conditions. In this buffer, OCP was partly denaturated as revealed by its modified absorbance spectra (both for OCP^o and OCP^r; see Fig.1 in Stadnichuk et al., 2012).Thus, whether the quenching observed would also occur in vivo seems extremely questionable.

To summarize, my work demonstrated that no terminal emitter (APC_{680nm}) is absolutely required for the OCP-related photoprotective mechanism (chapter 1; derived from Jallet et al., 2012). This was confirmed by other laboratories using different techniques. The most probable scenario right now is that OCP interacts with some aminoacids from an APC_{660nm} trimer and/or from ApcE. Once the OCP-PB complex is formed, the OCP-bound carotenoid gets in close vicinity to a 660nm emitting phycocyanobilin and heat dissipation starts.

After reaching this point, I started working on another model cyanobacterium called *Synechococcus elongatus* PCC 7942 (hereafter referred to as *Synechococcus*). It possesses hemidiscoidal PBs with similar architecture to the *Synechocystis* ones, except that they include only 2 APC cylinders instead of 3 (the upper cylinder is missing). Interestingly, *Synechococcus* does not have any OCP encoding gene; strong blue-green light fails triggering a reversible fluorescence quenching in vivo (see Boulay et al., 2008). My initial aim was to assess whether the absence of the upper cylinder in *Synechococcus* PBs could possibly impact OCP binding. I then decided to isolate PBs from this strain and to test their interaction with *Synechocystis* OCP in vitro, using our reconstitution system.

Question 2: What is the influence of PB core structure on OCP attachment?

To broaden the study, PBs from 4 different cyanobacterial strains were purified (see chapter 2; from Jallet et al., 2013). The number of APC cylinders varied from 2 (*Synechococcus*) to 3 (*Synechocystis*, *Arthrospira platensis* PCC 7345) or even 5 (*Anabaena variabilis*). I then showed that – under standard conditions (0.8M K-Phosphate buffer) – *Synechocystis* OCP induced a fast and strong fluorescence quenching only when mixed to *Synechocystis* PBs. Increasing phosphate concentration in the assays tends stabilizing OCP-PB complexes, as previously described (Gwizdala et al., 2011). Very high phosphate molarities (1.2M to 1.4M) stabilized the binding of *Synechocystis* OCP to other PBs and resulted in important fluorescence decreases. Thus, once the binding strengthened, *Synechocystis* OCP could interact with the PB core no matter how many APC cylinders it contains.

From these results, it appeared that the upper cylinder absent in *Synechococcus* is not required for OCP-PB complex formation. This strongly suggests that **the OCP binding site is an APC_{660nm} trimer situated on the basal cylinders**. Moreover, the 2 extra cylinders present

in *Anabaena variabilis* PBs did not lead to an increased affinity for OCP as one could expect if they comprised additional binding sites.

The question why at 0.8M K-Phosphate only *Synechocystis* PBs can attach *Synechocystis* OCP remains opened. No structural data about fully assembled PBs is available at the moment which hinders comparisons across species. However, a recent study revealed that the distance between APC trimers in each core cylinder may vary according to the strain considered based on APC hexamer crystal structures (Marx and Adir, 2013). A bigger space could ease OCP insertion and increase the area of contact but this remains purely speculative. Even though APC subunits are well conserved in term of primary structures, it is also possible that specific aminoacids present in *Synechocystis* but absent in other species are responsible for such a high affinity.

Given the fact that *Synechocystis* OCP shows some specificity for *Synechocystis* PBs in vitro, another question arises: which kinds of interaction underlie the OCP-PB complex formation? Does the OCP retrieved from a given cyanobacterium always bind stronger its cognate PBs? To answer it, I purified *Arthrospira platensis* PCC 7345 (hereafter *Arthrospira*) OCP.

Question 3: Which kinds of interaction underlie the OCP-PB complex formation?

Since it is not known how to genetically engineer *Arthrospira* cells, to obtain *Arthrospira* OCP, I constructed a *Synechocystis* mutant strain overaccumulating its tagged form (see chapter 2; from Jallet et al., 2013). The purified *Arthrospira* OCP displayed similar optical properties and photoactivity as *Synechocystis* OCP. I employed it in the reconstitution system, testing its ability to induce fluorescence quenching of *Synechocystis*, *Synechococcus*, *Arthrospira* and *Anabaena variabilis* PBs. *Arthrospira* OCP triggered an important fluorescence decrease in all PB types already at 0.8M K-Phosphate, contrary to *Synechocystis* OCP; the difference was still visible at 1.4M K-Phosphate. *Arthrospira* OCP did not show any specificity for *Arthrospira* PBs.

Looking at *Synechocystis* OCP (PDB file 3MG1: Wislon et al., 2010) and *Arthrospira* OCP (PDB file 1M98: Kerfeld et al., 2003) structures, I found possible explanations for the opposite behaviors observed. Even though both OCPs share 83% of their aminoacids, *Arthrospira* OCP has clearly more charged residues exposed on its N-terminal domain surface. The absolutely conserved Arg155 – also located in the N-terminal domain – was recently

identified by our group as essential for PBs binding (Wilson et al., 2012). This suggests that **hydrogen bonds/salt bridges underlie the OCP-PB complex appearance and stabilization**. The additional charged aminoacids present in *Arthrospira* OCP, particularly Lys29 and Asp164 because of their close vicinity to Arg155, could participate in establishing such kind of interaction. This could potentially ease OCP binding to PBs and/or strengthen its attachment.

Arg155 (N-terminal domain) forms a salt bridge with Glu244 (C-terminal domain) in OCP^o (Wilson et al., 2012). This bridge gets disrupted upon photoactivation; OCP^r appears as a more "opened" conformation, where Arg155 exposure allows PB binding (Wilson et al., 2012). It was then proposed that **OCP's N-terminal domain contains residues important for OCP-PB complex formation** (like Arg155 and potentially Lys29 or Asp164 in *Arthrospira* OCP) whereas **OCP's C-terminal domain plays a key role in controlling the N-terminal domain activity**. Recent finding that the Fluorescence Recovery Protein – fastening OCP^r reconversion to OCP^o – interacts specifically with OCP's C-terminal domain goes into that direction (Sutter et al., 2013). During the last months of my thesis, I worked in collaboration with C.Kerfeld's group (Michigan State University) to study the ability of isolated OCP N-terminal or C-terminal domains for PB fluorescence quenching (see chapter 3; from Leverenz et al., in press).

Thanks to proteolytic treatments, *Arthrospira* OCP N-terminal (residues 10 to 167) and C-terminal domains (residues 188 to 310) were separated. The N-terminal one appeared red in solution because retaining a bound carotenoid; it was then called Red Carotenoid Protein (RCP). Absorption spectroscopy combined to Raman spectroscopy revealed similar conformations for the carotenoid in OCP^r and RCP. I performed quenching assays proving that RCP induced a very fast/important PB fluorescence quenching even without any photoactivation process (Leverenz et al., in press). On the contrary, the isolated C-terminal domain was colorless and induced no fluorescence decrease in the reconstitution system. Thus, **OCP N-terminal domain alone can constitutively bind PBs and induce the dissipation process**. **The C-terminal domain**, for example by establishing salt bridges with some residues required for PB attachment, **blocks this activity in OCP^o**.

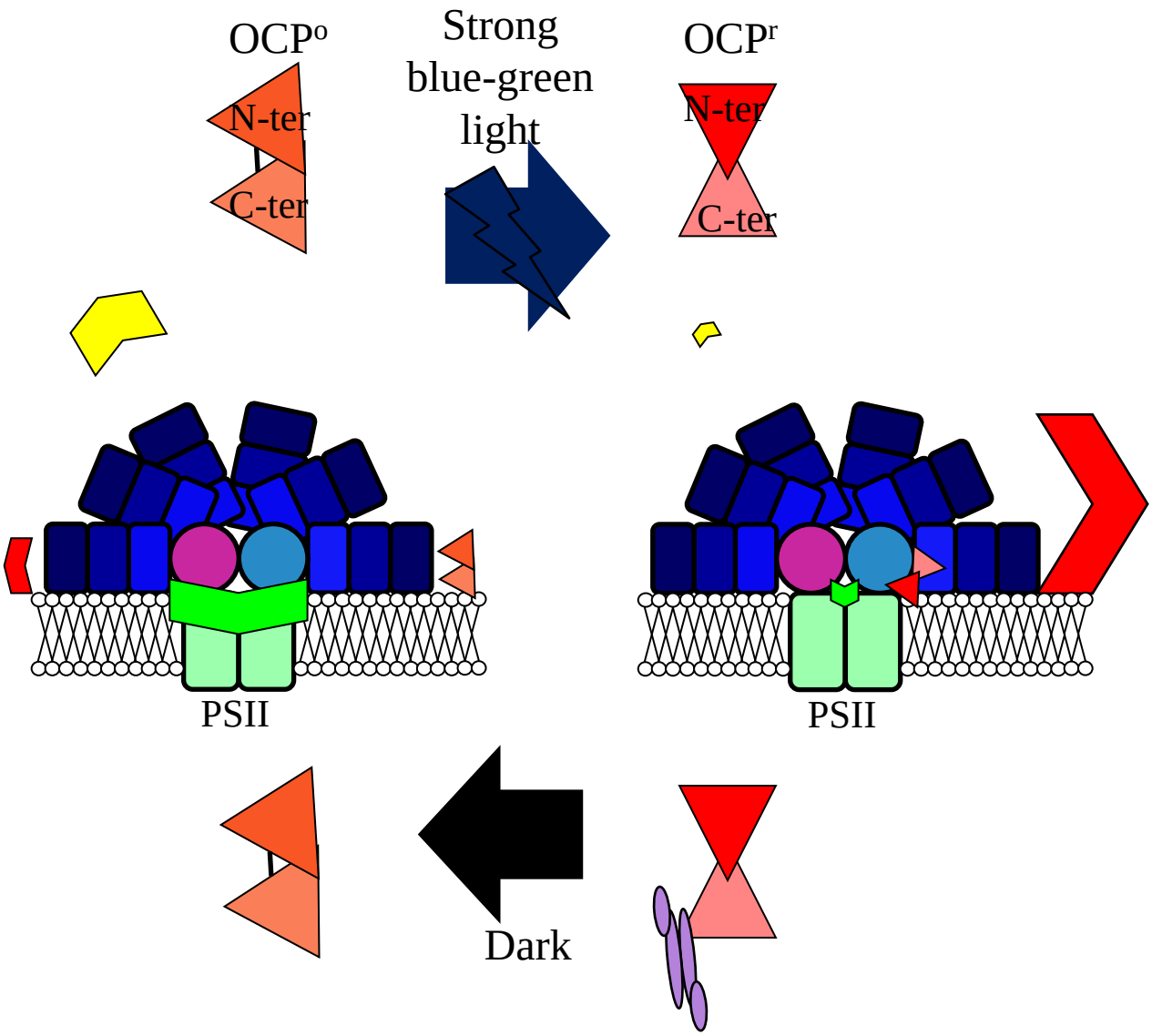

Figure C1. Current model of the OCP-related photoprotective mechanism. OCP^o is a closed form displaying salt bridges at the N- to C-terminal domains interface, particularly between Arg155 and Glu244 (*Synechocystis* numeration, shown as a black line; Wilson et al., 2012). Upon photoactivation, these bridges disappear and the protein opens which leads to OCP^r apparition. OCP^r establishes electrostatic contacts with an APC subunit in phycobilisome cores, through its N-terminal domain (Leverenz et al., in press). Particularly, Arg155 plays an important role for binding (Wilson et al., 2012) as well as other charged residues exposed on OCP N-terminal domain surface (Jallet et al., submitted). Once attached, OCP^r directly triggers the photoprotective mechanism leading to energy quenching (Gwizdala et al., 2011), at the level of APC_{660nm} mainly (Tian et al., 2011; Jallet et al., 2012). In the dark, FRP functions as a dimer to bind the C-terminal domain of OCP^r and to allow reconversion to OCP^o: the system returns to its original state (Sutter et al., 2013).

An improved model for the OCP-related photoprotective mechanism

In introduction, Fig.16 (p.40) summarized our understanding of the OCP-related photoprotective mechanism when this PhD project started. The studies presented here, completed by other works performed in our group and in collaboration with several laboratories, allow us to propose a more complete model nowadays: 1) OCP^r induces heat dissipation at the level of an APC_{660nm} trimer (Jallet et al., 2012; Tian et al., 2011; Tian et al., 2012) 2); this APC_{660nm} trimer must be situated in one of the basal PB cylinders (Jallet et al., 2013) 3) additional APC cylinders do not lead to an increased capacity for OCP binding (Jallet et al., 2013) 4) different PBs show different affinities for a given OCP, probably because of the distance between the APC trimers in core cylinders (Jallet et al., 2013) 5) Salt-bridges and/or hydrogen bonds are implied in the OCP-PB complex formation (Wilson et al., 2012; Jallet et al., 2013) 6) OCPs from different strains may show more or less affinity for PBs, probably depending on the exposed charges of their N-terminal domain (Jallet et al., 2013) 7) the N-terminal domain of OCP can bind PBs and induce fluorescence quenching (Wilson et al., 2012; Leverenz et al., in press) and 8) the C-terminal domain of OCP has a regulatory role, making sure that the N-terminal domain triggers energy dissipation only under high blue-green light conditions. These findings are summarized in Fig. C1.

Perspectives

Short-term perspectives: for a better characterization of the OCP-PB interactions

So far, the only structural data available about OCP concerns the orange form, both in *Arthrospira* (PDB file 1M98: Kerfeld et al., 2003) and *Synechocystis* (PDB file 3MG1: Wilson et al., 2010). Even if some assumptions can be made regarding OCP's opening following photoactivation, nobody managed to crystallize OCP^r at this point. This is probably due to the meta-stability of OCP^r at room-temperature or a higher degree of flexibility compared to OCP^o. Recently, some mutant OCPs (e.g. R155E or E244L; Wilson et al., 2012) with a stabilized red form have been described; they could be used for crystallization trials. Concerning the OCP-PB complex, absolutely no structural information has been retrieved yet. PBs are gigantic complexes, extremely difficult to handle when it comes to defining proper

crystallization conditions (N. Adir, personal communication). One solution could rely in cross-linking OCP to its binding site and then work on this "simplified" OCP-APC_{660nm} complex. Attempts are still ongoing regarding these aspects thanks to collaborations with C. Kerfeld's group and N. Adir's group (Technion University, Israel).

Alternative methods can help describing the OCP-PB interactions. Comparing *Arthrospira* and *Synechocystis* OCPs' ability to induce fluorescence quenching in vitro, we identified several aminoacids possibly important for PB binding (see chapter 2; from Jallet et al., 2013). Purifying OCPs from other cyanobacterial strains and testing them in the reconstitution system would help retrieving more candidate residues. Also, it would allow making 2 classes according to whether the considered OCP behaves similarly to *Synechocystis* OCP (better binding to the cognate PBs) or *Arthrospira* OCP (binding to all tested PBs). Looking at the common points in term of primary structure within each class could permit to determine what makes an OCP "specific" or not. Finally, the targeted mutagenesis approach in *Synechocystis* already led to understand Arg155's role; working on some yet-unstudied conserved residues may potentially give similar discoveries.

Mid-term perspectives: What happens in the strains naturally lacking OCP?

As said before, certain cyanobacteria – such as *Synechococcus* – naturally lack an *ocp* gene. It was shown that strong white light induces more photoinhibition (visible as a non-reversible fluorescence quenching) in these strains than in the OCP containing ones (see Fig.8 in Boulay et al., 2008). Several questions arise: Have the OCP-deficient strains developed alternative photoprotective strategies to cope with excess light? Do they normally live in environments where they never face photoinhibitory conditions?

For example, *Thermosynechococcus elongatus* (hereafter *Thermosynechococcus*) does not possess any full-length OCP encoding gene (Boulay et al., 2008). This cyanobacterium was collected from a volcanic lake, quite deep under water surface (Yamaoka et al., 1978). It probably rarely faces saturating light conditions. In 2013, dozens of cyanobacterial genomes were released (Shih et al., 2013); it would be interesting to see how the OCP-deficient cyanobacteria are distributed, both from a taxonomical and ecological point of view.

The existence of alternative photoprotective strategies (besides the ones described in introduction) seems likely too. It was observed that prolonged iron depletion leads to a very rapid PB disassembly and degradation (faster than for photosystems) in *Synechococcus* or *Thermosynechococcus* while in the OCP-containing strains the degradation of PBs is slower

than that of photosystems (see Fig.7 in Boulay et al., 2008). More work is required to understand the underlying mechanism.

Another interesting project would be to insert the *ocp* gene (and the *crto* one for ketocarotenoids synthesis plus the *frp* one) in a normally deficient strain, such as *Synechococcus*. We could then make sure that these 3 elements are sufficient to re-create the blue-green light triggered PB fluorescence quenching. Also, we could evaluate how the transformed cells respond to photoinhibitory conditions compared to the WT ones. Finally, it would be a good way to confirm the in vitro results presented in chapter 2 and to see whether *Arthrospira* OCP binds better PBs than *Synechocystis* OCP in vivo.

Additional perspectives: How does FRP allows reconversion from OCP^r to OCP^o?

In 2013, *Synechocystis* FRP crystal structure was released (PDB file 4JDX: Sutter et al., 2013). We were able to identify the FRP active site – a patch of exposed aminoacids at the monomer-monomer interface (Sutter et al., 2013). Co-immuno precipitation experiments revealed that FRP interacts only with the C-terminal domain of OCP (Sutter et al., 2013). Nothing is known yet about which OCP aminoacids participate in FRP binding, even though a docking model gave good fits and candidate residues for targeted mutagenesis (Sutter et al., 2013). Once a good picture of the OCP-FRP complex drawn, we will be able to describe the OCP residues important for conformational changes from OCP^o to OCP^r.

Boulay C, Abasova L, Six C, Vass I, Kirilovsky D (2008) Occurrence and function of the orange carotenoid protein in photoprotective mechanisms in various cyanobacteria. Biochim Biophys Acta BBA - Bioenerg **1777**: 1344–1354

Gwizdala M, Wilson A, Kirilovsky D (2011) In Vitro Reconstitution of the Cyanobacterial Photoprotective Mechanism Mediated by the Orange Carotenoid Protein in Synechocystis PCC 6803. Plant Cell Online **23**: 2631–2643

Jallet D, Gwizdala M, Kirilovsky D (2012) ApcD, ApcF and ApcE are not required for the Orange Carotenoid Protein related phycobilisome fluorescence quenching in the cyanobacterium Synechocystis PCC 6803. Biochim Biophys Acta **1817**: 1418–1427

Jallet D, Thurotte A, Leverenz RL, Perreau F, Kerfeld CA, Kirilovsky D (2013) Specificity of the cyanobacterial Orange Carotenoid Protein: Influences of OCP and phycobilisome structures. Plant Physiol pp.113.229997

Kerfeld CA, Sawaya MR, Brahmandam V, Cascio D, Ho KK, Trevithick-Sutton CC, Krogmann DW, Yeates TO (2003) The Crystal Structure of a Cyanobacterial Water-Soluble Carotenoid Binding Protein. Structure **11**: 55–65

Kuzminov FI, Karapetyan NV, Rakhimberdieva MG, Elanskaya IV, Gorbunov MY, Fadeev VV (2012) Investigation of OCP-triggered dissipation of excitation energy in PSI/PSII-less Synechocystis sp. PCC 6803 mutant using non-linear laser fluorimetry. Biochim Biophys Acta BBA - Bioenerg **1817**: 1012–1021

Marx A, Adir N (2013) Allophycocyanin and phycocyanin crystal structures reveal facets of phycobilisome assembly. Biochim Biophys Acta BBA - Bioenerg **1827**: 311–318

Shih PM, Wu D, Latifi A, Axen SD, Fewer DP, Talla E, Calteau A, Cai F, Tandeau de Marsac N, Rippka R, et al (2013) Improving the coverage of the cyanobacterial phylum using diversity-driven genome sequencing. Proc Natl Acad Sci U S A **110**: 1053–1058

Stadnichuk IN, Yanyushin MF, Bernát G, Zlenko DV, Krasilnikov PM, Lukashev EP, Maksimov EG, Paschenko VZ (2013) Fluorescence quenching of the phycobilisome terminal emitter LCM from the cyanobacterium Synechocystis sp. PCC 6803 detected in vivo and in vitro. J Photochem Photobiol B **125**: 137–145

Stadnichuk IN, Yanyushin MF, Maksimov EG, Lukashev EP, Zharmukhamedov SK, Elanskaya IV, Paschenko VZ (2012) Site of non-photochemical quenching of the phycobilisome by orange carotenoid protein in the cyanobacterium Synechocystis sp. PCC 6803. Biochim Biophys Acta BBA - Bioenerg **1817**: 1436–1445

Sutter M, Wilson A, Leverenz RL, Lopez-Igual R, Thurotte A, Salmeen AE, Kirilovsky D, Kerfeld CA (2013) Crystal structure of the FRP and identification of the active site for modulation of OCP-mediated photoprotection in cyanobacteria. Proc Natl Acad Sci **110**: 10022–10027

Tian L, Gwizdala M, van Stokkum IHM, Koehorst RBM, Kirilovsky D, van Amerongen H (2012) Picosecond Kinetics of Light Harvesting and Photoprotective Quenching in Wild-Type and Mutant Phycobilisomes Isolated from the Cyanobacterium Synechocystis PCC 6803. Biophys J **102**: 1692–1700

Tian L, van Stokkum IHM, Koehorst RBM, Jongerius A, Kirilovsky D, van Amerongen H (2011) Site, Rate, and Mechanism of Photoprotective Quenching in Cyanobacteria. J Am Chem Soc **133**: 18304–18311

Wilson A, Gwizdala M, Mezzetti A, Alexandre M, Kerfeld CA, Kirilovsky D (2012) The Essential Role of the N-Terminal Domain of the Orange Carotenoid Protein in Cyanobacterial Photoprotection: Importance of a Positive Charge for Phycobilisome Binding. Plant Cell Online **24**: 1972–1983

Wilson A, Kinney JN, Zwart PH, Punginelli C, D'Haene S, Perreau F, Klein MG, Kirilovsky D, Kerfeld CA (2010) Structural Determinants Underlying Photoprotection in the Photoactive Orange Carotenoid Protein of Cyanobacteria. J Biol Chem **285**: 18364–18375

Yamaoka T, Satoh K, Katoh S (1978) Photosynthetic activities of a thermophilic blue-green alga. Plant Cell Physiol **19**: 943–954

Interactions entre l'Orange Carotenoid Protein et les phycobilisomes dans un mécanisme de photoprotection chez les cyanobactéries

Un excès d'énergie lumineuse peut être délétère pour les organismes photosynthétiques ; en effet, il en résulte la formation d'espèces réactives de l'oxygène au sein des centres réactionnels. Les cyanobactéries ont adopté divers mécanismes de photoprotection afin de contrer ce phénomène. L'un d'eux repose sur l'activité de l'Orange Carotenoid Protein (OCP), protéine soluble qui attache un kéto-caroténoïde (hydroxy-echinenone). Subissant de fortes intensités de lumière bleu-verte, l'OCP se convertit d'une forme inactive/orange vers sa forme active/rouge. L'OCP ainsi photoactivée possède la faculté d'interagir avec les phycobilisomes - principales antennes collectrices de lumière - induisant la dissipation de l'énergie collectée par ces gigantesques complexes sous forme de chaleur. La pression d'excitation au niveau des centres réactionnels ainsi que la fluorescence du système décroissent alors.

L'OCP photoactivée se fixe au cœur des phycobilisomes qui sont majoritairement constitués de protéines chromophorylées de la famille des allophycocyanines (APC). J'ai construit différentes souches mutantes de *Synechocystis* PCC 6803 en modifiant ou supprimant les sous-unités mineures d'APC (ApcD, ApcF et ApcE). Ces sous-unités jouent le rôle essentiel d'émetteurs terminaux des phycobilisomes, véhiculant l'énergie qu'elles reçoivent à la Chlorophylle *a*. J'ai aussi démontré que le mécanisme photoprotectif associé à l'OCP chez ces mutants restait inchangé, aussi bien in vivo que in vitro. Ces résultats suggèrent qu'aucun émetteur terminal n'est nécessairement requis pour l'attachement de l'OCP aux phycobilisomes et sous-entendent que l'OCP interagit probablement avec une sous-unité majeure d'APC.

Divers phycobilisomes, contenant 2, 3 ou 5 cylindres d'APC dans leur cœur, ont été isolés à partir de cyanobactéries variées. Les OCPs de *Synechocytis* et d'*Arthrospira* ont été purifiées à partir de souches mutantes de *Synechocystis*. J'ai alors mené une étude in vitro des interactions entre ces OCPs et les phycobilisomes. Le nombre de cylindres d'APC présents au sein des phycobilisomes n'affecte en rien la diminution de fluorescence. De plus, j'ai constaté que l'OCP de *Synechocystis* est spécifique pour ses propres phycobilisomes alors que l'OCP d'*Arthrospira* interagit avec tous les phycobilisomes employés ici. Des hypothèses, fondées sur les structures disponibles, ont été formulées pour élucider ces différences.

Les domaines N- et C-terminaux de l'OCP d'*Arthrospira* ont été dissociés par protéolyse. Le domaine N-terminal isolé conserve le caroténoïde attaché, ayant une conformation similaire à celle observée lorsque l'OCP est photoactivée. Ce domaine N-terminal est aussi capable d'induire une importante diminution de la fluorescence des phycobilisomes. A l'inverse, le domaine C-terminal isolé est incolore et n'a aucun effet sur la fluorescence des phycobilisomes. Ces résultats suggèrent que seul le domaine N-terminal de l'OCP est impliqué dans l'interaction avec les phycobilisomes. Le domaine C-terminal quant à lui module son activité.

Interactions between the Orange Carotenoid Protein and the phycobilisomes in cyanobacterial photoprotection

Too much light can be lethal for photosynthetic organisms. Under such conditions harmful reactive oxygen species are generated at the reaction center level. Cyanobacteria have developed photoprotective mechanisms to avoid this. One of them relies on the soluble Orange Carotenoid Protein (OCP) that binds a ketocarotenoid (hydroxyechinenone, hECN). Under strong blue-green illumination, OCP gets photoconverted from an orange inactive form (OCP^o) to a red active one (OCP^r). OCP^r interacts with phycobilisomes, the major cyanobacterial light harvesting antennae, and triggers heat dissipation of the excess light energy collected by these gigantic pigment-protein complexes. Consequently, excitation pressure on reaction centers and fluorescence emission decrease.

OCP^r binds to phycobilisome cores, containing mainly chromophorylated proteins of the allophycocyanin (APC) family. I constructed *Synechocystis* PCC 6803 mutants affected in some minor APC forms (ApcD, ApcF and ApcE). These special APCs play the role of terminal emitters, i.e. funnel light energy to Chlorophyll *a*. Strong-blue green illumination triggered normal OCP-related fluorescence quenching in all mutant cells. The fluorescence decrease induced by *Synechocystis* OCP in vitro was similar when using phycobilisomes isolated from wild-type or mutant cells. These results demonstrated that the terminal emitters are not needed for interaction with the OCP and they strongly suggested that OCP^r interacts with one of the major APC forms of the phycobilisome core.

Phycobilisomes containing 2, 3 or 5 APC cylinders per core were isolated from different cyanobacterial strains. *Synechocystis* and *Arthrospira* OCPs were purified from over-expressing *Synechocystis* mutant strains. I then performed in vitro OCP/phycobilisome interaction studies. The number of APC cylinders per core had no clear influence on the amount of fluorescence quenching. Both OCPs behaved very differently, one appearing much more species-specific than the other. Structure-based hypotheses were emitted to explain such dissimilarity.

Arthrospira OCP N-terminal and C-terminal domains were separated through proteolysis. The isolated N-terminal domain retained a bound carotenoid, which displayed similar conformation than in OCP^r. This isolated N-terminal domain triggered important phycobilisome fluorescence quenching even under dark conditions. In contrast, the isolated C-terminal domain attached no pigment and had no visible effect on phycobilisome emission. It was then proposed that only the N-terminal domain of OCP is implied in interactions with phycobilisomes. The C-terminal domain modulates its activity.